An Initial Investigation into the Sources and Transport of Particulate Organic Matter in the Nelson River System, Manitoba

by

Tassia M. Stainton

A Thesis submitted to the Faculty of Graduate Studies of

The University of Manitoba

in partial fulfilment of the requirements of the degree of

Master of Science

Department of Geological Sciences

University of Manitoba

Winnipeg, Canada

Abstract

The Nelson River, a subarctic river in north-central Manitoba, is the largest river discharging to Hudson Bay and its watershed has seen extensive land-modification in the upper reaches, permafrost thaw in the lower reaches, and hydroelectric development throughout. To characterize sources of sediment and particulate organic matter (OM) in the Nelson River system, and to identify processes influencing its transport to Hudson Bay, water quality parameters, Compound-Specific Stable Isotope (CSSI) fingerprinting, and Bayesian unmixing models were employed on terrestrial and instream samples. Distinct regional, longitudinal, and temporal differences in water quality parameters and particulate OM sources were observed among all three regions of the Nelson River system (upper Nelson River, Rat-Burntwood River, lower Nelson River). The application of CSSI fingerprinting and unmixing models showed that the dominant sources of OM to suspended sediment in the lower reaches of the Nelson River are proximally derived and comprise soils, upstream suspended sediment, river bed sediment, and tributary suspended sediment.

Acknowledgements

I would first like to thank my supervisor Dr. Zou Zou Kuzyk. Her enthusiasm for field-based science is boundless, and I am thankful for her support, encouragement, and mentorship. Her positivity motivated me though the most challenging aspects of this work, and I consider myself very fortunate to have learned from her on both a professional and personal level. Thanks are also extended to my committee members, Dr. Greg McCullough and Dr. Nancy Chow. Greg, I consider myself privileged for the opportunity to pick your brain on years of science on the Nelson River system, and you were truly instrumental in the compilation and preservation of historical data on this project. Nancy, I have the utmost personal and professional respect for you, and I am very fortunate to have had your meticulous and well thought out input applied to this work.

I am grateful for the support of Manitoba Hydro BaySys team leaders Sarah Wakelin, Allison Zacharias, and Michael Morris for their assistance with planning field work. For their logistical support, I thank Emmelia Wiley, Michelle Kamula and David Binne. Thanks are also extended to Brendan Brooks, Ashley Soloway, Julie DePauw, Jiang Liu, Sam Huyghe, Skye Kushner for their assistance during field work.

Special thanks to Dominic Reiffarth, Paul Martin, Patricia Ramlal, Allison MacHutchon, and Eva Slavicek for their efforts in sample analysis, and to Claire Herbert and Alessia Guzzi for their assistance in providing analytical method protocols and sample preparation. Sincere thanks are due to the whole of BaySys Team 5, specifically Dr. Kathleen Munson, Masoud Goharrokhi, James Singer, Dr. David Lobb, Dr. Feiyue Wang, Dr. Ellen Pettricrew, and Dr. Phil Owens.

I thank my family and friends for their endless support. Thanks are especially extended to my father Michael Stainton, who provided advice and explanation on freshwater analytical methods over the course of this thesis. Special thanks are also extended to my fellow

graduate students for their camaraderie and enthusiasm for geoscience.

Finally, I thank Ian Deniset for his unwavering love and support. It has been nearly ten years since we started our undergraduate degrees together in the Wallace building, and I can't think of a better person with whom to embark upon the scheme to quit our jobs, move home, and pursue graduate degrees.

Financial support for this work was provided by BaySys, NSERC, CERC, ArcticNet, and the Centre for Earth Observation Science (CEOS).

Contents

List of Figures

List of Tables

List of Abbreviations

BaySys	Hudson Bay System Study	iii, iv, vi, viii–x, xii, 4, 27, 34–36, 40–46, 50, 52–54, 56, 59, 60, 62, 63, 67, 69, 77, 136, A2
CAMP	Coordinated Aquatic Monitoring Program	v, 3, 22, 36, 39
CRD	Churchill River Diversion	v, 18, 20, 22, 24, 31, 37, 64, 70, 84, 124, 125
CS	Control Structure	21, 48, 63
CSSI	Compound-Specific Stable Isotope	ii, v, vii–x, xii, xiii, 8–10, 26, 80, 83, 85–87, 91, 93–95, 103, 120, 121, 126–131, 133, 135, B13
DFO	Department of Fisheries and Oceans	36–39

FA	fatty acid	vii, ix, x, xiii, 6, 8–10, 83, 92, 93, 95, 96, 99–103, 107, 108, 111, 112, 114, 115, 121–124, 129, 133–135, B19
FAME	fatty acid methyl esters	92
FEMP	Federal Ecological Monitoring Program	v, 22, 23, 37, 70
GS	Generating Station	v, 18, 20, 24, 25, 37, 38, 44–48, 53, 56, 59, 60, 62–64, 68, 78, 125, 129, A4
LNR	lower Nelson River	ii, viii–x, 10, 11, 14–17, 20–22, 24, 31, 32, 41, 44–47, 49, 51, 53, 54, 56–60, 65–79, 83, 84, 86–88, 96, 98, 99, 103–106, 112, 114–116, 118, 120–122, 124–127, 129, 130, 132–137, A4, B23
LWR	Lake Winnipeg Regulation	v, 18, 20, 22, 37, 62

MCMC	Markov Chain Monte Carlo	93, 114, 115, 118
MEMP	Manitoba Ecological Monitoring Program	23, 37, 70
OC	organic carbon	vi, vii, 1–7, 25, 28, 29, 38, 39, 69, 80–82, 91, 95–99, 120, 122, 123, 126, 127, 129, 133, 135–137, A2
OM	organic matter	ii, v, vii, 1–9, 26–29, 31, 43, 48, 51, 59, 60, 62, 63, 68, 70, 76–83, 86, 95–97, 103, 104, 120–137
RBR	Rat-Burntwood River	ii, ix, x, 10, 11, 14–17, 21, 23, 31, 32, 37, 41, 44, 46, 48, 49, 51, 54, 56, 58–60, 63–67, 69–72, 74–77, 79, 83, 84, 87, 96, 98, 99, 104–106, 112, 114–116, 122, 123, 126, 127, 130, 132–134, A2, B23
SIL	Southern Indian Lake	18, 21, 24, 63

SOM	soil organic matter	ix, xi, 3, 5, 7, 8, 28, 29, 47–49, 56, 59, 60, 63, 64, 67–69, 77, 78, 80, 81, 121, 126, 133–135
SuspN	total suspended nitrogen	vi, 35, 38, 51, 52, 132
SuspOC	suspended organic carbon	vi, ix, x, 35, 38, 40–42, 44–64, 67–70, 72–79, 132, 133
TSS	total suspended solids	vi, ix, x, 25, 35, 38–40, 42, 43, 45–53, 56–64, 67–70, 72–79, 132, 133, A2
UNR	upper Nelson River	ii, ix, x, 10, 11, 14–17, 20, 26, 31, 32, 37, 41, 42, 44, 45, 47, 49, 51, 53, 54, 56, 57, 59, 60, 62–64, 66, 70–79, 83, 84, 86, 87, 96, 98, 99, 104–106, 112, 114–116, 122, 123, 126–130, 132–136, A2, B23

Chapter 1

General Introduction

1.1 Preamble

Rivers are important transporters of mineral sediment and terrestrial organic matter (OM) (Battin et al., 2008; Aufdenkampe et al., 2011; Bianchi, 2011) and deliver an estimated 0.4 Gt of total organic carbon (OC) to oceans each year (Hedges et al., 1997; Schlesinger & Melack, 2016). The fate of terrestrial OC (in dissolved and particulate form) delivered from rivers as it cycles through the coastal carbon cycle can be envisioned as in Figure 1.1. In the coastal zone, terrestrial OC can undergo burial and thereafter be preserved or mineralized to dissolved inorganic carbon by microorganisms. If terrestrial OC remains in surface waters, it can be mineralized by microorganisms or photo-oxidized. Changes to the sources and chemical composition of OM affect its degradability. Modifying the quantity of OC mineralized to dissolved inorganic carbon could affect the pH and trophic status of coastal waters and ultimately how the coastal ocean behaves as a sink for CO_2 or as a source of CO_2 to the atmosphere. Estuarine zones and continental shelves have been shown to be new sources of CO_2 to the atmosphere (Cole et al., 2007; Cai, 2011), although Arctic

Ocean waters are still generally considered a sink with disproportionally high OC burial rates when compared to the whole ocean worldwide (Stein & Macdonald, 2004).

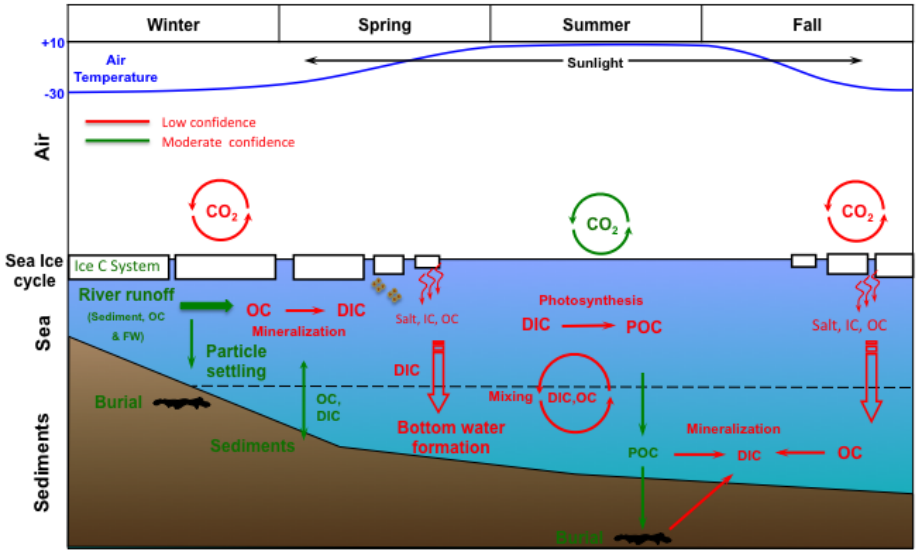

Fig. 1.1: Schematic showing the annual cycle of carbon transport and transformation processes in the coastal zone (Tim Papakyriakou, personal communication, April 28, 2017). FW: fresh water, OC: organic carbon; IC: inorganic carbon; DIC: dissolved organic carbon; POC: particulate organic carbon

Terrestrial OM in fluvial systems comprises dissolved and particulate fractions of carbon-based compounds (Hedges et al., 1997). It is often associated with or bound to the silt and clay particle fraction (<63 µm); therefore the transport and storage of mineral sediment and OM in riverine systems are closely linked (McConnachie & Petticrew, 2006). Fluvial sediment delivery from continental land masses to the coastal zone is controlled by the tectonic setting, bedrock geology, geomorphology, climate, and hydrology of drainage basins, and also by anthropogenic activities occurring there within (Syvitski & Milliman, 2007). A number of factors simultaneously affect the quantity and characteristics of mineral sediment and terrestrial OM transported within drainage basins. Activities such as agriculture, deforestation, and mining intensify the rate of soil erosion which in turn increases the amount of sediment available for transport, whereas processes such as channel bank hardening, water diversion, and hydroelectric reservoir storage limit the amount of sediment

transport to coastal zones (Syvitski, Vorosmarty, Kettner, & Green, 2005). These activities and processes can also affect the storage, release and total quantities of OC exported, and the elemental, isotopic, and molecular composition of OM mobilized within drainage basins.

Subarctic river basins have typically sequestered OC over millennia in extensive peatlands. Increasing temperatures in subarctic drainage basins (Arctic Climate Impact Assessment, 2005) and altered hydrology due to consequent thawing and erosion of permafrost (Romanovsky et al., 2017) could mobilize previously stored OC associated with soil organic matter (SOM) into rivers (Guo et al., 2007; Gustafsson et al., 2011; Vonk et al., 2013; Vonk & Gustafsson, 2013) and increase amounts of OC transferred to the coastal carbon cycle (Figure 1.1).

The Nelson River is a subarctic river of Canada and the single largest river discharging to Hudson Bay, with a mean annual rate (1987-2017) of $110\,km^3yr^{-1}$ (Environment and Climate Change Canada, 2018d, 2018e, 2018f). Its drainage basin comprises a diverse mix of cropland, grassland, wetland, and forest, and covers four ecozones that vary in climate, precipitation, and permafrost cover. The Nelson River supplies over 40% ($895\,Gg\ yr^{-1}$) of the total terrestrial OC delivered from all rivers draining into Hudson Bay, of which $53\,Gg\ yr^{-1}$ are in the particulate phase (Godin et al., 2017). The Nelson River basin has seen extensive land-modification in its upper reaches, possible permafrost thaw in its lower reaches, and hydroelectric development throughout.

Bulk quantities and fluxes of terrestrial OC from the Nelson River into Hudson Bay have been estimated (Godin et al., 2017), and the concentration of OC (total and dissolved) is regularly measured at various instream locations by the Coordinated Aquatic Monitoring Program (CAMP). However, little work has been done to characterize the sources of sediment and associated particulate OM within the Nelson River system or to identify the

processes influencing their transport to the coast of Hudson Bay.

This study focuses on the particulate fraction of terrigenous OM, which is often thought to be non-labile (or recalcitrant). However, recent work shows that particulate terrigenous OM is more degradable in the coastal system than previously thought, and hence may be available for biogeochemical cycling (Sánchez-García et al., 2007; Vonk et al., 2008). The pan-Arctic tundra and taiga region contains about 50 % of the reported global OC pool in soils or shallow permafrost (Tarnocai et al., 2009). Particulate OC is a major component of thaw-released permafrost carbon in fluvial systems (Guo & Macdonald, 2006; Guo et al., 2007) and therefore is of interest since changes to climate and hydrological conditions in these regions make the below-ground OC pool vulnerable to re-enter the modern carbon cycle (Gustafsson et al., 2011). The relative ease with which large volumes of particulate matter can be collected allows detailed geochemical analysis and is helpful in characterizing source particulate matter in suspension that can ultimately be transported through the watershed into the coastal zone (Ittekkot & Laane, 1991; Hedges et al., 1997). By investigating particulate OM sources in the Nelson River system, insight will be gained into natural and anthropogenic watershed processes that may affect the quantity and quality of OC transported to the coastal zone. These findings will contribute to the Hudson Bay System Study (BaySys) project, a collaborative effort of university researchers and Manitoba Hydro, which is investigating the relative impacts of hydroelectric activity and climate change on the freshwater-marine coupling in Hudson Bay (Barber, 2015).

1.1.1 Organic matter sources and transport in large fluvial systems

Large river systems, like the Nelson River, exhibit longitudinal complexity as waters flow through river channels, flood plain areas, and lake basins. Morphological differences between waterbodies affect both OM composition itself and processes acting on OM. Main-

stem rivers also receive OM from subcatchments in the watershed via tributary rivers and streams that could be compositionally distinct, presenting a potentially complex mixture of OM sources within the river system.

When investigating OM transport by rivers, it is important to consider the entire particulate fraction (both mineral sediment and organic matter operationally defined in this study as material >1.0 µm) because a large fraction of OM in fluvial systems is typically associated with or bound to the silt and clay particle fraction (McConnachie & Petticrew, 2006). Particulate OM in rivers and lakes is typically classifed as being derived from allochthonous OM sources (e.g. soil organic matter and plant debris) or autochthonous sources (e.g. instream production of macrophytes, benthic algae, and phytoplankton). It may also be produced in-situ by physico-chemical and biological processes acting on dissolved OM (Ittekkot & Laane, 1991). In rivers, Allochthonous sources typically dominate (Kendall, Silva, & Kelly, 2001), with OM either bound to inorganic particles (as biofilms or through ion exchange) or present as independent suspended particles.

Soil organic matter is primarily contributed to watersheds by erosive processes and is a primary source of particulate OC in suspension within river systems and in lacustrine sediments. Floodplains of rivers can act as sites of active OM transformation and store sediment within drainage basins, but can also act as sources of OC by processes such as floodplain drainage and channel bank erosion (Goñi et al., 2014).

In lacustrine environments, OM is supplied by a similar combination of autochthonous primary production and allochthonous loading of OM from the watershed; the dominance of either process varies depending on factors such as lake size, water residence time, algal productivity, and concentration of suspended matter (Cole et al., 2002). In watersheds, lake basins are sites of carbon transformation and can facilitate processes such as heterotrophic decomposition by bacteria and remineralization of OM during sedimentation (Meyers &

Ishiwatari, 1993), both of which decrease the transport of OM downstream.

1.1.2 Effects of hydroelectric development on fluvial systems

Hydroelectric development in the form of cross-watershed diversion or reservoir creation causes large areas of previously unflooded land to be impounded by water, changing waterbody morphology (Egré & Milewski, 2002). Impoundments as a result of dam construction convert waterbodies from riverine to lacustrine systems, imparting changes to water residence times, autochthonous primary production, shoreline erosion, sediment transport, sedimentation, hydraulic regime seasonality, and biogeochemical cycles (Friedl & Wuest, 2002). In boreal river systems, impoundments result in an influx of terrestrial OM into the flooded system since adjacent lands are typically forested or comprised of organic-rich wetlands (Rosenberg et al., 1997). Dams also affect the transport of sediment and particulate matter in river systems by disrupting longitudinal continuity. Reservoirs reduce the water velocity and competence of a river by expanding the cross-sectional area available for flow, promoting sediment deposition. This stored water, when released from the dam, has higher energy, a comparatively low sediment load, and the ability to cause enhanced downstream erosion when compared to river water unaffected by damming (Kondolf, 1997).

1.1.3 Characterizing particulate organic matter

Sources of terrestrial OM in watersheds can be characterized by their unique biochemical properties which can be used to trace the extent of downstream transport. Waterborne particulate OC (i.e. suspended sediment), soil, river bank material, and lake sediment can be analyzed to determine the "bulk" composition of OM as elemental (C, N) amounts, and molar C/N ratios and stable carbon isotope signal (δ^{13}C). These samples can also be analyzed for "biomarkers" such as fatty acids that are more specific tracers of OM

classes.

Bulk organic matter composition Molar C/N ratios can define sources of particulate OM in fluvial systems fairly easily through the collection of relatively small water samples and measurement of standard chemical water quality parameters (particulate OC and particulate N concentrations). Molar C/N ratios calculated from these measurements identify OM composition by comparison to typical ratio ranges of OM in terrestrial sources. Ratio ranges for OM composition are well documented in the literature for lacustrine algae (4 - 10), soil organic matter (8 - 15), and plant matter from terrestrial land plants (15 - >40) (Meyers & Ishiwatari, 1993; Meyers, 1994; Meyers & Teranes, 2001; Kendall et al., 2001; McConnachie & Petticrew, 2006). These ranges have been used to characterize sources to OM suspended in river, lake and tributary waters (Figure 1.2).

Stable carbon isotope ratios of OC can provide bulk isotopic compositions of OM in riverine systems. Carbon isotopic composition within plant and algal tissue is primarily affected by isotope fractionation during CO_2 uptake, and depends on the type of environment (terrestrial vs. aquatic) in which it occurs (O'Leary, 1988; Chikaraishi, 2014). Carbon isotopic signatures (δ^{13}C in ‰) are calculated for natural organic materials using Equation 1.1 where R is the ratio of $^{13}CO_2/^{12}CO_2$ measured on a mass spectrometer for both the sample and V-PDB standard (carbon dioxide from the Pee Dee Formation Belemnite limestone) (Coplen, 1994).

$$\delta^{13}C = \left[\frac{R(sample)}{R(standard)} - 1\right] \times 1000 \tag{1.1}$$

Over 90% of plant species use the Calvin-Benson (C_3) photosynthetic pathway including trees, shrubs, and cool climate grasses; C_4 plants (using the Hatch-Slack pathway) encompass most of the remaining 10% of plant species including agricultural crops such as corn (Glaser, 2005; Mackenzie & Lerman, 2006). The isotopic signatures (δ^{13}C) of C_3 plants range between -32 ‰ and -22 ‰; δ^{13}C values of C_4 plants typically range between -20 ‰

and $-9\,‰$, and lacustrine algae exhibit $\delta^{13}C$ values between $-35\,‰$ and $-24\,‰$ (Figure 1.2) (Badeck et al., 2005). Elemental and isotopic parameters can be used in conjunction with one another to characterize and classify terrestrial OM and distinguish between allochthonous and autochthonous sources (Figure 1.2). However, these methods only inform upon bulk OM composition, and therefore do not provide definitive source information for OM mixtures.

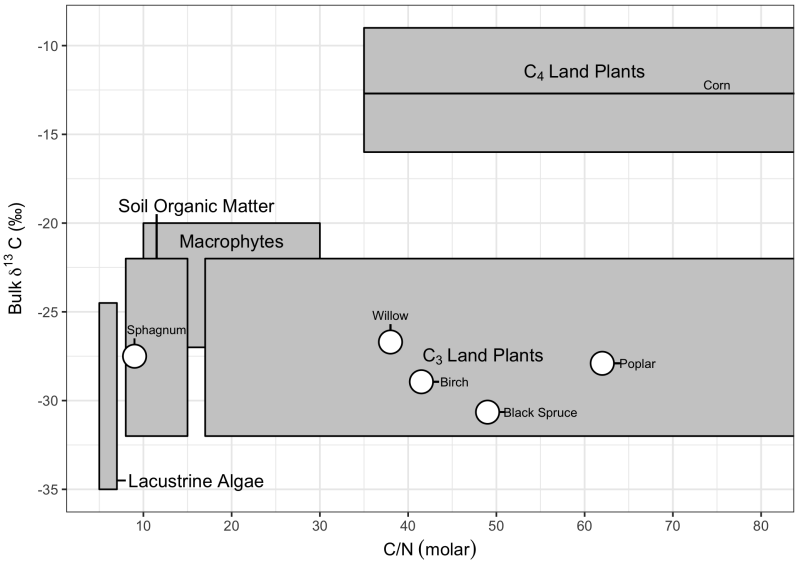

Fig. 1.2: Typical elemental and carbon isotopic compositions of lacustrine algae, soil organic matter, C3 plants, C4 plants, and macrophytes determined by Meyers and Ishiwatari (1993) and summarized by Kendall et al. (2001). Typical values for plants present in the study area are shown by labeled white circles or horizontal lines (Meyers, 1994; Meyers et al., 1995; Chikaraishi & Naraoka, 2003; Moingt et al., 2016).

Biomarkers as tracers and CSSI organic matter fingerprinting Fatty acids (FA) are chain-structure lipids synthesized by marine and terrestrial plants that contain a varying number of carbon atoms (Sikes et al., 2009), and can be used as biomarkers. Long FA chain lengths (C_{25}-C_{35}) are typically found in epicuticular waxes in higher plants (Eglinton & Hamilton, 1967), whereas shorter chain FAs typically originate from energy storage in algae or phytoplankton (Meyers & Ishiwatari, 1993). Compound Specific Stable Isotope (CSSI)

analysis is an emerging method that utilizes $\delta^{13}C$ values of individual FA chain lengths to differentiate between types of OM contributed to river systems (Figure 1.3) (Gibbs, 2008; Blake et al., 2012; Hancock & Revill, 2012, 2012; Upadhayay, Smith, et al., 2018). Workers employing CSSI analysis of FAs as sediment fingerprints typically sample upstream terrestrial "source" material, and downstream "mixtures" of suspended sediment (Reiffarth et al., 2016). As a biochemical tracer, CSSIs of FAs are robust because carbon skeletons of long chain FAs persist in soil and remain intact during diagenetic processes (Meyers & Teranes, 2001). CSSI fingerprinting draws on the principles defined by sediment fingerprinting in general whereby a set of properties is chosen to distinguish between sources contributing to downstream suspended sediment. Unique properties, comprising the fingerprint, are then measured in both source and sediment materials to estimate the contribution of sediment from each source to a downstream suspended sediment mixture (Koiter et al., 2013). Detailed descriptions of the sediment fingerprinting concept are reported by Gellis and Walling (2011), Walling (2013), and Koiter et al. (2013).

Bayesian statistical unmixing models, such as those created using the open-source R package MixSIAR, can then be used to determine the relative proportional contribution of a particular source to downstream suspended sediment (Reiffarth et al., 2016; Blake et al., 2018). Bayesian unmixing models offer advantages over linear mixing models because they allow for representation of inherent variability in source and mixture tracer data caused by environmental processes; they also allow for "prior" probability distributions based on existing knowledge to be combined with tracer data (Blake et al., 2018). This modelling method has successfully differentiated between vegetation types and estimated the proportions of source contribution downstream in small river systems (Alewell et al., 2016). A list of recent studies that have applied CSSI analysis and fingerprinting to OM in river systems is provided in Table B.1 and reviews of CSSI applications and methodologies are outlined by Reiffarth et al. (2016) and Upadhayay et al. (2017).

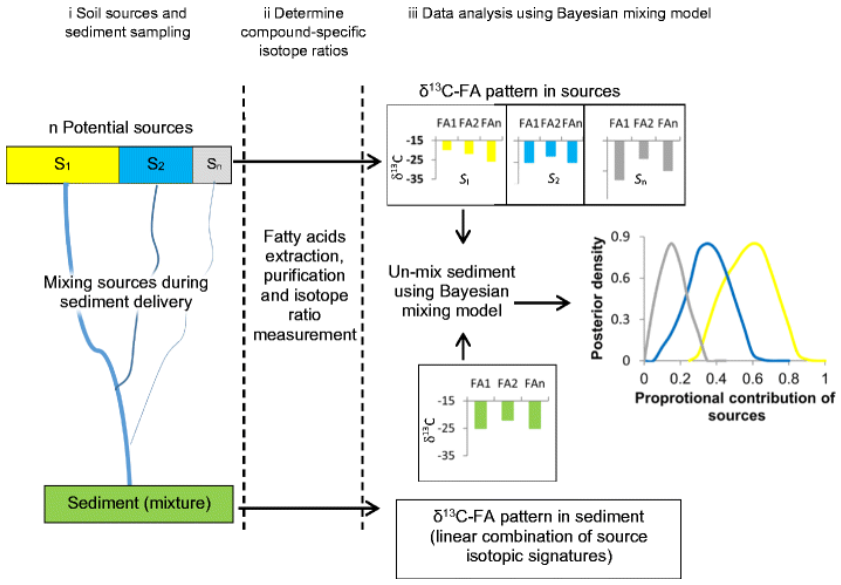

Fig. 1.3: Organic matter fingerprinting concept using CSSI analysis on fatty acids as tracers. Used with permission from Upadhayay et al. (2017).

1.2 Study Area

1.2.1 Location, hydrology and topography

The Nelson River watershed north of Lake Winnipeg extends over 91 000 km^2 in north central Manitoba to the southwest of Hudson Bay, and its >1 000 000 km^2 drainage basin ranges as far as Minnesota and South Dakota in the south, Alberta in the west, and Ontario in the east (Figure 1.4).

Due to the extensive history of hydrological regulation for hydroelectric power development, the lower Nelson River (LNR) between Split Lake and Hudson Bay receives water primarily from two catchments, each with distinct physical characteristics. The Rat-Burntwood River (RBR) system transports diverted Churchill River waters at Southern Indian Lake and supplies ∼25% of the total flow to the LNR from the primarily Precambrian Shield landscape of the Churchill River Drainage Basin (Figure 1.4 and 1.5). The upper Nelson River (UNR), which flows between Lake Winnipeg and Split Lake, contributes

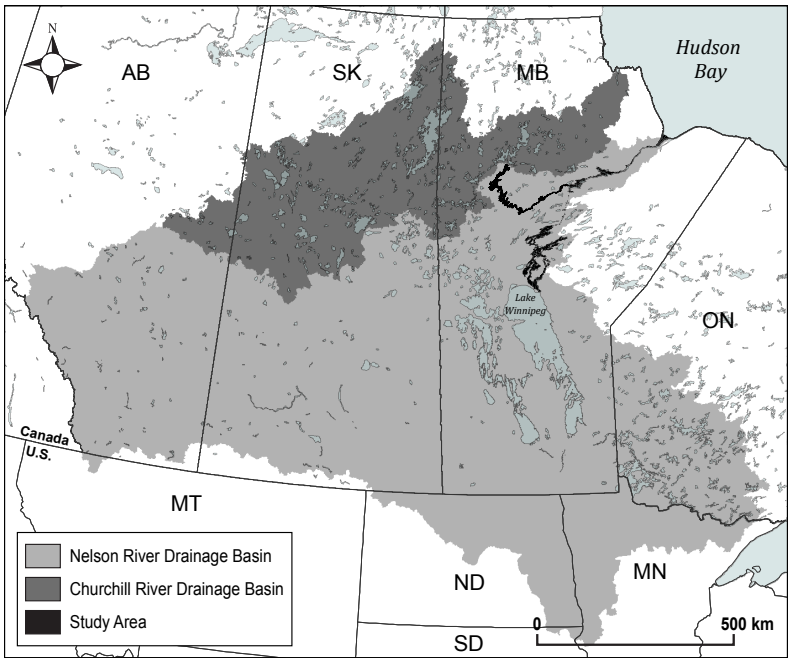

Fig. 1.4: Map showing the extent of the Nelson and Churchill River Drainage Basins in central Canada and northern United States. Study area water bodies are outlined in black.

$\sim$75% of the total flow to the LNR and drains the predominantly agriculturally-developed prairie landscape upstream of Lake Winnipeg (Figure 1.5). The study area encompasses all three of these regions (UNR, RBR, and LNR) and a select number of their associated sub-basins and tributaries (Figure 1.5).

Relief in the study area ranges from 0 $-$350 m above sea level and generally decreases to the northeast. Topographic highs consist of outcropping bedrock ridges, and incised Quaternary sediments. Topographic lows include coastal lowlands and poorly drained wetlands. River gradient in the study area is generally shallow; water levels range from 217 m elevation at the Lake Winnipeg outlet and 257 m in the South Bay diversion channel (at Southern Indian Lake), to 166 m in Split Lake. River channels in the Nelson system incise glacial cover or are bound by bedrock and expand to flow through a complex series of lakes. A mix of natural and controlled lakes occur in the UNR and RBR but the largest waterbodies present downstream of Split Lake in the LNR are hydroelectric reservoirs.

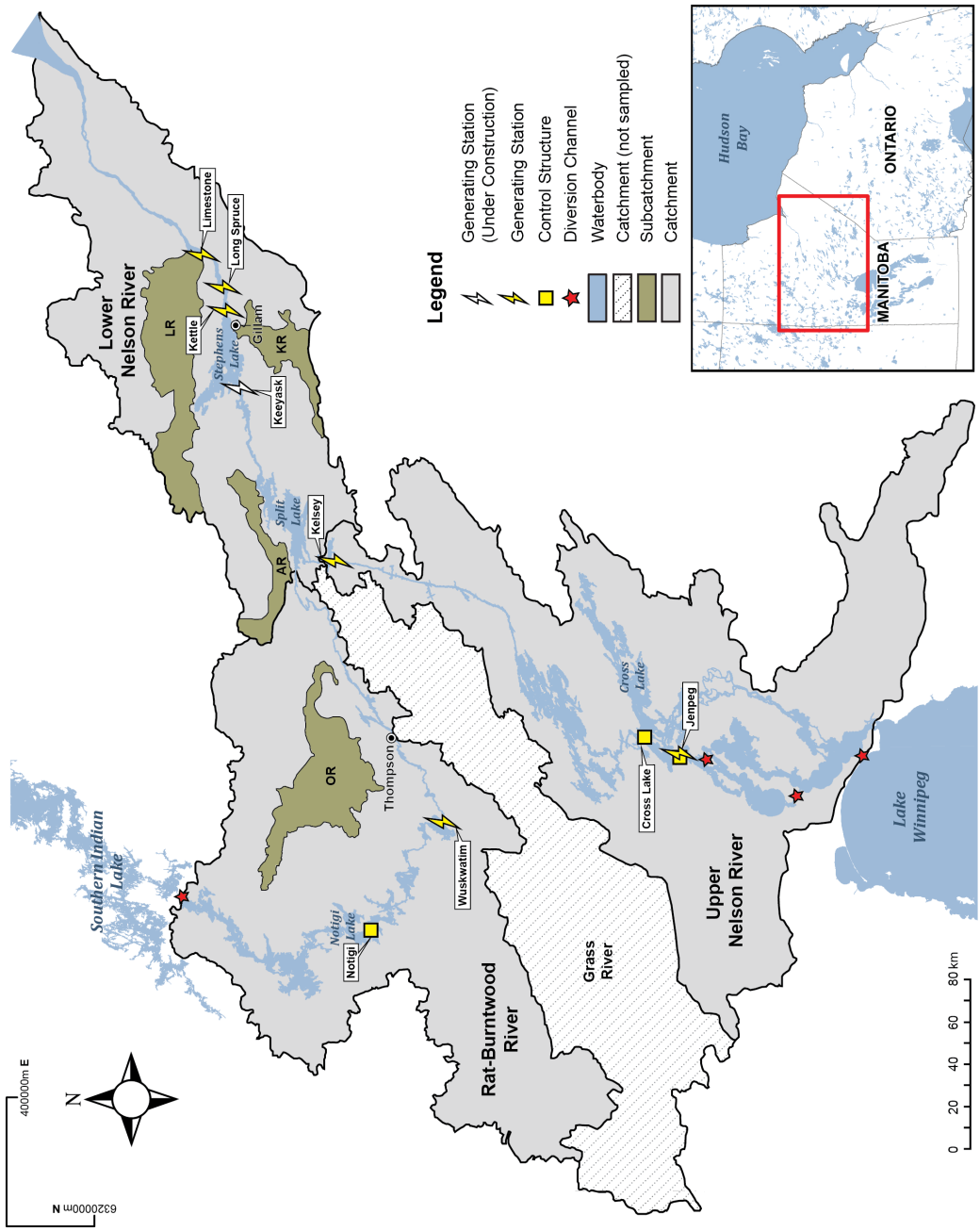

Fig. 1.5: Map of catchments within the Nelson River watershed in north-central Manitoba (Manitoba Water Stewardship, 2005; Natural Resources Canada, 2013). Hydroelectric power structures and diversion channels within the study area are shown by symbols indicated in the map legend. OR: Odei River, AR: Assean River, KR: Kettle River, LR: Limestone River

1.2.2 Geological setting

Precambrian bedrock underlies the majority of the study area and is comprised of Archean granites and gneisses of the Superior Province in the southeast and Proterozoic granites and gneisses of the Trans-Hudson Orogen in the northwest (Figure 1.6a) (GIS Map Gallery, 2006). In two regions of the study area, Precambrian rocks are overlain by two Phanerozoic sedimentary basins: the Western Canadian Sedimentary Basin in the southwest and the Hudson Bay Basin in the northeast (Corkery, 1996). The last glaciation event in northern Manitoba that caused advancement of the Laurentide ice sheet ended ∼8,000 years ago. The retreat of the glacial ice margin developed Lake Agassiz, a large proglacial lake (Teller & Yang, 2015). The study area is thus blanketed by glacial till that is overlain by post-glacial alluvial deposits and Lake Agassiz clays; Tyrrell Sea marine waters inundated the isostatically depressed surface of the Hudson Bay Plain following deglaciation, capping the northeastern part of the study area with marine sediments (Figure 1.6b) (GIS Map Gallery, 2006).

Post glacial isostatic adjustment in the study area occurs more rapidly in areas subjected to thicker ice cover. Because ice was thickest at the lower end of the watershed, landscape gradient is shallowing over time. Present day uplift rates of $\sim$1 cm yr^{-1} are observed near Hudson Bay with rates decreasing with distance from Hudson Bay to 0.6 cm yr^{-1} upstream at Lake Winnipeg, and to 0.7 cm yr^{-1} upstream at Southern Indian Lake (Sella et al., 2007; Simon et al., 2017).

1.2.3 Climate and vegetation

Climate in the study area includes wide variation in temperatures between summer and winter seasons and exhibits a south-to-north cooling gradient. Environment Canada climate normals (1981-2010) from four stations in the study area indicate that the average daily

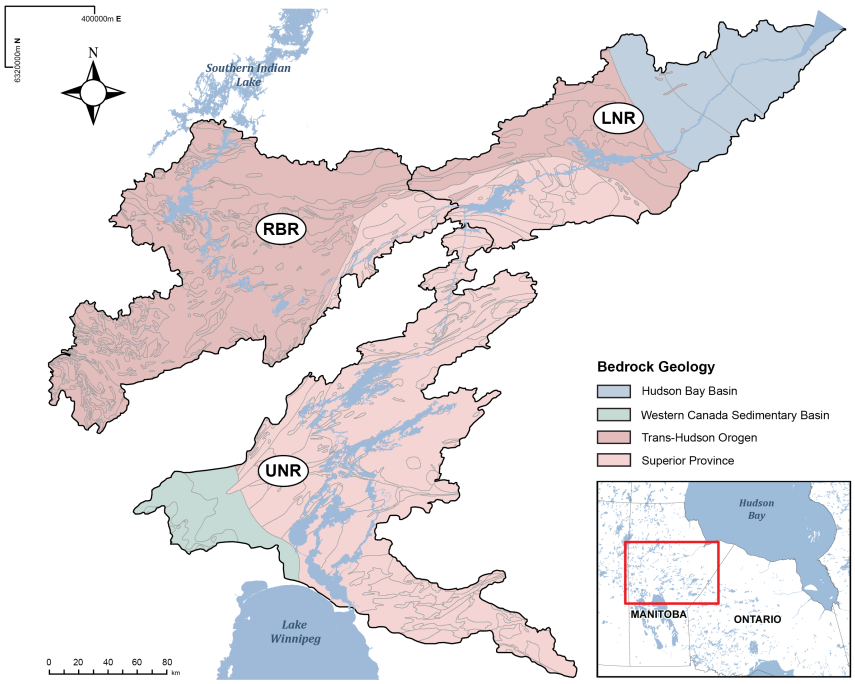

(a)

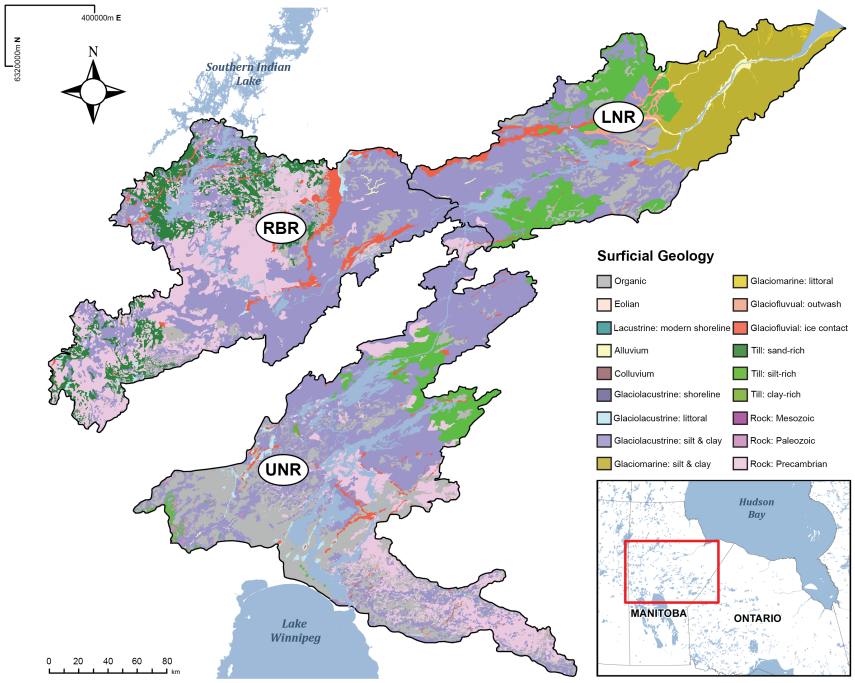

(b)

Fig. 1.6: Geological and geographical environment of the study area. **1.6a**: Simplified bedrock geology. **1.6b**: Surficial geology. **1.6c**: Ecozones. **1.6d**: Permafrost. UNR: upper Nelson River, LNR: lower Nelson River, RBR: Rat-Burntwood River (GIS Map Gallery, 2006).

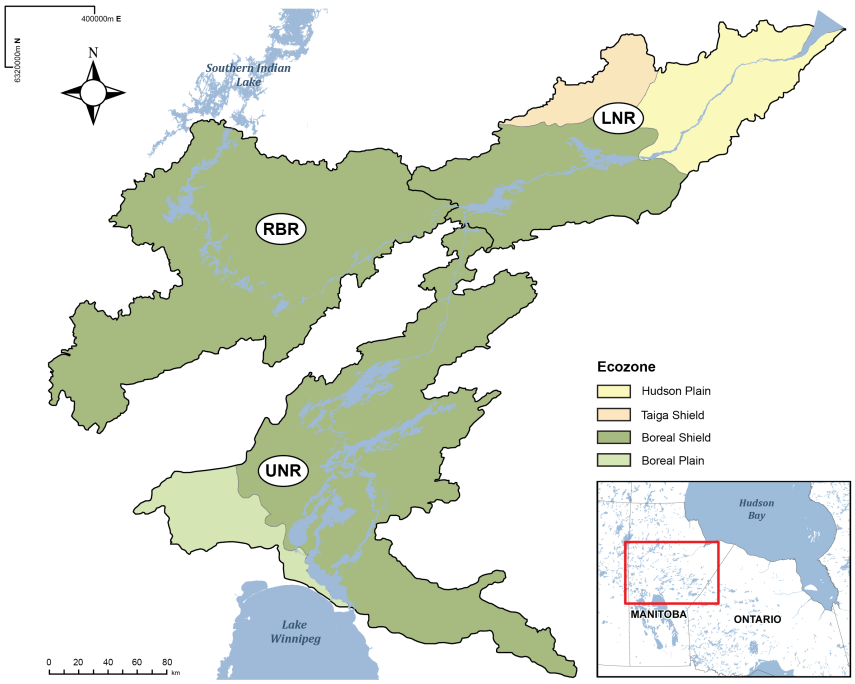

(c)

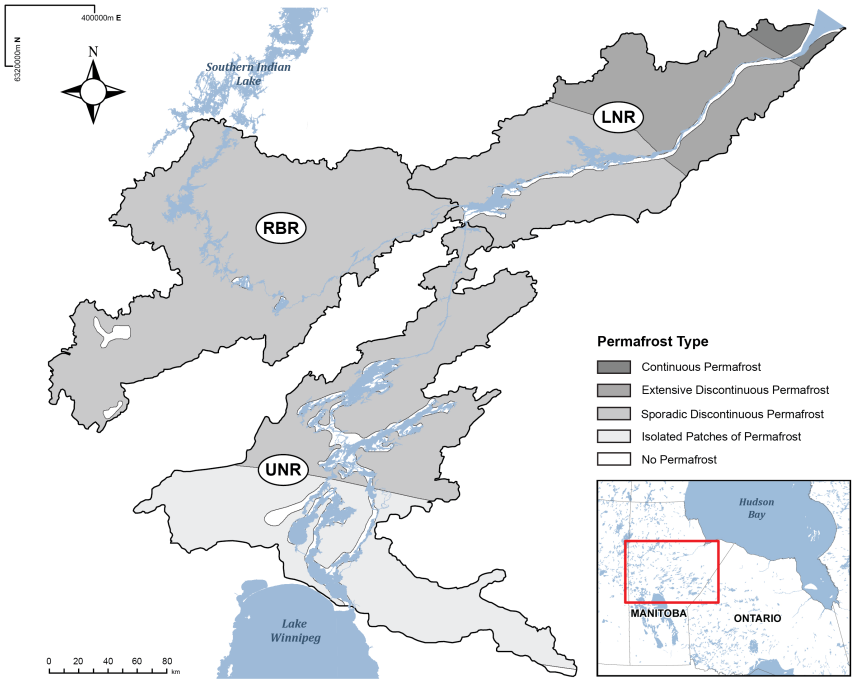

(d)

Fig. 1.6: Geological and geographical environment of the study area. **1.6a**: Simplified bedrock geology. **1.6b**: Surficial geology (GIS Map Gallery, 2006). **1.6c**: Ecozones. **1.6d**: Permafrost. UNR: upper Nelson River, LNR: lower Nelson River, RBR: Rat-Burntwood River (GIS Map Gallery, 2006).

temperature and average yearly precipitation range from $-24.3\,^{\circ}\mathrm{C}$ in January to $17.6\,^{\circ}\mathrm{C}$ in July, and from 477.9 mm to 532.3 mm respectively (Environment and Climate Change Canada, 2017).

Four terrestrial ecozones intersect at the study area: Boreal Plain, Boreal Shield, Hudson Plain, and Taiga Shield. They are distinguished by different soil, vegetation, wetland, and permafrost types. Although variation occurs between ecozones, dominant forest species throughout the study area consist of black spruce, jack pine, aspen, sphagnum, and willows (Rosenberg et al., 2005) (Figure 1.6c). Permafrost in the study area ranges from non-existent in the southwest, to continuous in the northeast (Figure 1.6d), and underlies peatlands classified as bogs, which have low surface water temperatures (Halsey et al., 1997), or wetlands and upland forests covered sufficient overburden. In the UNR, wooded-to-forested permafrost bogs (peat plateaus) cover between $0.1-10\,\%$ of the land surface, whereas in the RBR this increases to $20-30\,\%$ (Halsey et al., 1997). In the LNR, peat plateaus cover between $20-80\,\%$ of the landscape whereas open permafrost bogs dominate the landscape north of the Nelson River near the western coast of Hudson Bay (Halsey et al., 1997).

1.2.4 Land use and ecological change

Landscape and land use in the study area differ dramatically between the two catchments supplying water to the LNR, and are described in detail by Rosenberg et al. (2005). Key features are summarized in this section. The portion of Churchill River that is diverted to the LNR through the RBR system, drains a $281\,300\,\mathrm{km}^2$ catchment and flows mainly through Precambrian Shield with Boreal Forest/Taiga habitats in northern Saskatchewan and Manitoba (Figure 1.4 and 1.6). Instream water use dominates in this catchment where activities such as subsistence hunting, fishing, and trapping are widely pursued. Waters

contributing to the RBR system flow through bedrock and shallow soils in heavily forested regions which efficiently uptake and store nitrogen and phosphorus.

The UNR originates at the outlet of Lake Winnipeg, which collects water from the predominantly Grasslands/Savanna/Shrub habitats of the Saskatchewan, Red-Assiniboine, and Winnipeg River subcatchments that comprise ∼50% agricultural lands (Figure 1.4 and 1.6). Offstream water use for irrigation, municipal water supplies, and industrial use is prevalent in these subcatchments but instream use such as commercial fishing is also prevalent in Lakes Winnipeg, Manitoba, and Winnipegosis. Waters contributing to the UNR become increasingly rich in nitrogen and phosphorus due to nutrient input from naturally fertile soils and anthropogenic sources such as agricultural fertilizer application, municipal wastewater discharge, and industrial activities.

Key issues concerning ecological change in the study area differ between regions. In the UNR, the large land drainage to lake surface area ratio of Lake Winnipeg makes the lake susceptible to loading of nutrients, contaminants, and sediments at levels far above the lake's natural processing capacity (Lake Winnipeg Stewardship Board, 2007). An increase in both water discharge and anthropogenic loading (specifically associated with waste water discharge, agricultural development and animal husbandry) over time has caused a doubling of total phosphorus and plankton biomass in Lake Winnipeg and a shift to a cyanobacteria-dominated plankton population since the late-1990s (McCullough et al., 2012).

Permafrost degradation is an issue for all regions of the study area, but especially in the northern, subarctic reaches of the RBR and in tributary catchments of the LNR. Thawing of permafrost peatlands has been occurring across north-central Manitoba due to increases in temperature and precipitation in the last century (Umbanhowar et al., 2013; Vitt & Halsey, 1994). Continued warming (based on the ∼0.4 °C per decade modelled trend in the Arctic) will affect the carbon storage and wetland drainage control provided

by peat plateaus as these are degraded through thawing, subsidence, and collapse, and subsequently converted to fens (Arctic Climate Impact Assessment, 2005; Dyke & Sladen, 2010). The presence of permafrost in shoreline substrates also has implications for the potential increase in erosional processes if banks are exposed to increased water level or wave activity. Permafrost degradation of shoreline materials has been observed in the study area at Southern Indian Lake (SIL) where shoreline erosion has been hastened by the cyclic process of melting, undercutting/fracturing, and shoreline failure/removal, a process that has been ongoing for the for more than 40 years (Newbury & McCullough, 1984).

Hydroelectric power development has affected land use and imparted significant physical and ecological changes within the study area, and is described in detail in the following section.

1.2.5 Hydroelectric development

Hydroelectric power development in the study area began in 1958 and is ongoing. Four diversion channels and two control structures regulate flow through six hydroelectric generating stations along the Nelson and Rat-Burntwood River systems with the total capacity of 4181 MW, and produce daily and seasonal fluctuations in discharge rates and water levels (Manitoba Hydro, 2015). Brief descriptions and timelines of all major projects are outlined in Table 1.1. Three of these in the study area, Lake Winnipeg Regulation (LWR), Churchill River Diversion (CRD), and the Kettle Generating Station (GS), are of special consideration to this research due to their significant impact on the morphology, hydrology and suspended sediment regime of affected waterbodies.

Table 1.1: History of hydroelectric power development in the study area summarized from Manitoba Hydro (2015). Year(s) indicate construction time periods. (GS: Generating Station, CS: Control Structure)

Year(s)	Hydroelectric Development	Description
1958-1961	Kelsey Generating Station	Constructed on the upper Nelson River, upstream of Split Lake.
1966-1974	Kettle Generating Station	Constructed on the lower Nelson River, downstream of Stephens Lake.
1970-1976	Lake Winnipeg Regulation	Construction of the Jenpeg GS and CS was completed to regulate water levels in Lake Winnipeg through the western channel of the upper Nelson River. Three diversion channels (2-mile channel, 8-mile channel, and the Ominawin bypass channel), a control structure at Kiskitto Lake, and a weir at Cross Lake were constructed to increase outflow capacity, minimize backwater effects, and reduce water level ranges, respectively.
1973-1976	Churchill River Diversion	Waters from the Churchill River were diverted through Southern Indian Lake (SIL) into the Rat-Burntwood River system by construction of the Missi Falls Control Structure at the northeast outflow of SIL, the South Bay Diversion Channel between SIL and Isset Lake, and the Notigi CS at the outflow of Notigi Lake.
1971-1979	Long Spruce Generating Station	Constructed on lower Nelson River downstream of Kettle GS.
1976-1992	Limestone Generating Station	Constructed on the lower Nelson River downstream of Long Spruce GS, upstream of the Limestone River.
1990-2014	Conwapa Generation Project	Planned to be constructed on the lower Nelson River, downstream of Limestone GS. Following a series of feasibility studies, it was ultimately terminated.
2006-2012	Wuskwatim Generating Station	Developed as a partnership between the Nisichawayasihk Cree Nation and Manitoba Hydro. Constructed on the Burntwood River system between Nelson House and Thompson.

continued ...

. . . continued

Year(s)	Hydroelectric Development	Description
2012-2019	Keeyask Generation Project	Currently under development, and is being constructed on the lower Nelson River above the inflow to Stephens Lake.

Kettle GS construction and the Stephens Lake reservoir The Kettle GS in the lower Nelson River began operation in December of 1970 (Figure 1.5). Prior to construction, waterbody morphology upstream of the Kettle GS site comprised the riverine channel of the LNR and a lake known to local Cree as Moose Nose Lake (Split Lake Cree and Manitoba Hydro, 1996). Damming at Kettle GS flooded over 220 km^2 of land and created the reservoir now known as Stephens Lake with water levels ∼31.5 m higher than natural conditions (North/South Consultants Inc., 2012).

Lake Winnipeg Regulation (LWR) Lake Winnipeg Regulation works were completed between 1970 and 1976 and primarily affected the outlet lakes region[1] of the UNR. A number of hydrological control structures (described in Table 1.1) were constructed to regulate levels and store water in Lake Winnipeg, and supply larger water volumes during the winter peak demand period to the newly constructed Jenpeg GS (Manitoba Hydro, 2015). Post-regulation, water levels in Lake Winnipeg are maintained between 216.7 m and 218.5 m above sea level; in the outlet lakes region, total lake area increased by 78 km^2 from natural conditions and altogether 64 km^2 of land was flooded (Environment Canada and Department of Fisheries and Oceans, 1992a).

Churchill River Diversion (CRD) In 1973, Manitoba Hydro began development of the Churchill River Diversion project that involved diverting 75% of flow from the Churchill

[1]Outlet Lakes Region Waterbodies: Playgreen Lake, Little Playgreen Lake, Kiskittogisu Lake, Kiskitto Lake, and the Nelson River above Jenpeg GS

River into the RBR system to augment flows to hydroelectric generating stations constructed on the lower Nelson River (Environment Canada and Department of Fisheries and Oceans, 1992a). This large-scale watershed diversion was accomplished by damming the natural outlet of Southern Indian Lake (SIL), constructing a diversion channel in the southernmost region of SIL across the natural drainage divide of the Churchill and Nelson river basins, and constructing a control structure at the outflow of Notigi Lake (Newbury et al., 1984). Post-impoundment, water level in SIL was raised by $\sim$3 m and lake area increased in SIL and other affected downstream lakes by 295 km^2 (Environment Canada and Department of Fisheries and Oceans, 1992a). The Notigi CS and the Burntwood River in Thompson saw mean discharge rates of 825 $m^3 s^{-1}$ and 888 $m^3 s^{-1}$ in the following decade, compared to estimated natural flow rates of 31 $m^3 s^{-1}$ and 93 $m^3 s^{-1}$ respectively (Environment Canada and Department of Fisheries and Oceans, 1992a). The widespread presence of permafrost in the uplands and lack of bedrock-bound shoreline post-impoundment left SIL susceptible to severe erosion of backshore deposits and created a longstanding period of shoreline instability (Newbury et al., 1984). Although 90 % of the eroded material remained in SIL, the majority of suspended load produced by the abrasion of erosion-generated clay aggregates is transported out of the lake downstream to the RBR system (Hecky & McCullough, 1984).

1.3 Previous Work

Since the inception of hydroelectric power development in Manitoba, efforts in various fields have monitored, investigated, and researched the Nelson River system to further our understanding of the impacts of hydroelectric power development on hydrology, water quality and contaminants, fisheries, erosion and sedimentation, and local communities. Due to the immense body of work conducted by government organizations, industry, consultants,

and academic institutions, only key programs and research pertaining directly to the study area and to the goals of this M.Sc. thesis will be highlighted in this section.

1.3.1 Monitoring programs

Following LWR and CRD, two notable government-partnered aquatic monitoring programs have occurred in the study area: the Federal Ecological Monitoring Program (FEMP) between 1985 and 1989, and the Coordinated Aquatic Monitoring Program (CAMP) from 2008 to present.

FEMP The Federal Ecological Monitoring Program began in 1985 as a result of a legal challenge by the Northern Flood Committee to contractual obligations of Manitoba Hydro and the governments of Canada and Manitoba pertaining to the 1977 Northern Flood Agreement (Environment Canada and Department of Fisheries and Oceans, 1992c). FEMP's mandate, outlined fully in a report by Environment Canada and Department of Fisheries and Oceans (1992c), was to determine the environmental impacts of LWR, CRD and the construction of dams on the lower Nelson River as evidenced by impacts to water quantity and quality, sediment and shoreline morphology, mercury levels, fisheries and aquatic life, waterfowl, and resource harvesting. Full results, conclusions and recommendations from FEMP are outlined in Environment Canada and Department of Fisheries and Oceans (1992a, 1992b, 1992c).

CAMP The Coordinated Aquatic Monitoring Program, initiated by a coordinated effort between the Government of Manitoba and Manitoba Hydro, began as a pilot program in 2008 to implement long-term aquatic monitoring in Manitoba's hydroelectric power system (Coordinated Aquatic Monitoring Program, 2014). Modelled on existing monitoring programs in Manitoba and Canada, CAMP monitors the following components of the aquatic

environment: hydrometrics, aquatic habitat, water quality, sediment quality, phytoplankton, benthic microinvertebrates, fish communities, and mercury levels in fish. Full details of the monitoring plan, study areas, and results from each component are given in Coordinated Aquatic Monitoring Program (2014).

1.3.2 Industry investigations

A vast amount of work and reporting has been conducted in the study area by private consultants since the inception of hydroelectric development in the late 1950s including but not limited to: environmental assessments, dam feasibility studies, hydraulic monitoring and modelling, water quality monitoring, and erosion/sedimentation studies. For the purposes of this Master's research, only work pertaining to the goals of this study will be described in this section.

A four-year monitoring program funded under the Federal Ecological Monitoring Program was designed and executed by North/South Consultants Inc. between 1986 and 1989 to determine the effects of hydroelectric development on the water quality of the Nelson River system (Strange, 1990). This work is of special consideration to the goals of this thesis since it is one of the only water quality monitoring programs conducted in the study area that sampled riverine sites and included raw data in the report appendix; these data are utilized in Chapter 2 of this thesis.

During the same time period as FEMP, the Manitoba Department of Natural Resources Fisheries Branch began a similar ecological monitoring program in the Rat-Burntwood River and Nelson River systems, colloquially referred to in consultant literature as the Manitoba Ecological Monitoring Program (MEMP) (Green, 1990). Predominantly lacustrine sites were chosen in this program, but, of special interest to this thesis, biweekly water samples were collected between 1985 and 1989 at riverine sites in each region of the study

area including the Thompson Water Treatment plant, Jenpeg GS, Kelsey GS, and Kettle GS.

A comprehensive synthesis of all data collected and reported during all Limestone GS monitoring programs was completed by North/South Consultants Inc. (2012). This work compiled results from over 80 consultant reports (some of which include data sets used in this thesis) with the goal of understanding the long-term effects of the Limestone GS on the LNR. Sedimentary processes in the Nelson River estuary are described by RSW-Environment Illimite Inc. (2014) with results obtained from an oceanographic monitoring program that occurred between 2005 and 2009. Although the main focus of RSW-Environment Illimite Inc. (2014) was on the estuarine environment, their investigations aid this Master's research by presenting information on particulate matter concentrations and fluxes at the Nelson River mouth.

Recently, Manitoba Hydro (2015) described the effects of previous and current hydroelectric development on environmental and socioeconomic change over time in the whole of Manitoba Hydro's hydroelectric power system.

1.3.3 Academic research

Research in various disciplines related to this Master's work has been pursued in the study area both prior to and following major hydroelectric development projects.

In a series of publications, workers from the Freshwater Institute of the Department of Fisheries and Oceans outlined their work in the late 1970s during which they described the SIL impoundment and CRD hydroelectric development project and conducted a series of pre- and post-impoundment studies to monitor the effects of the changing hydraulic regime in SIL. Newbury et al. (1984) gave a comprehensive summary of the physical environment of SIL and other affected waterbodies both pre- and post-impoundment and diversion.

Subsequent work by Newbury and McCullough (1984) and Hecky and McCullough (1984) looked at changes to physical processes such as erosion, sedimentation and sediment budgets in the affected waterbodies.

Many of the investigations into carbon delivery to Hudson Bay from the Nelson River (in particulate and dissolved phases) were based on samples collected at the river mouth. However, exports of dissolved organic carbon (2003-2006) from the Nelson River calculated by Kirk and St. Louis (2009) were based on water sampled at the Limestone GS, ∼120 km from the river mouth. Suspended particulate matter properties from the Nelson River were studied by Kuzyk et al. (2009) as part of the construction of a preliminary sediment and OC budget for Hudson Bay; samples collected primarily in 2005 yielded molar C/N ratios of suspended particulate matter ranging between 16.3 in October and 24.1 in July whereas δ^{13}C composition of particulate OC ranged between -27.65 ‰ in October and -28.15 ‰ in July. Godin et al. (2017) investigated the concentration, fluxes, and isotopic properties of dissolved and particulate OC in the Nelson River from water and sediment samples collected ∼35 km upstream of the river mouth and reported total suspended solids (TSS), particulate OC, dissolved OC and total OC concentrations of $39\,\mathrm{mg\,L^{-1}}$, $0.56\,\mathrm{mg\,L^{-1}}$, $8.95\,\mathrm{mg\,L^{-1}}$, and $9.5\,\mathrm{mg\,L^{-1}}$ respectively. Particulate, dissolved and total OC fluxes were calculated using discharge data averaged from 1964-2000 yielding rates of $53\,\mathrm{Gg\ yr^{-1}}$, $842\,\mathrm{Gg\ yr^{-1}}$ and $895\,\mathrm{Gg\ yr^{-1}}$ respectively (Godin, 2014).

Déry et al. (2005) and Duboc et al. (2017) reported on the effects of damming by exploring the changes to river discharge over time and to hydrology and sedimentary regimes, respectively. Déry et al. (2005) studied trends and characteristics of river discharge into Hudson Bay between 1964 and 2000 and determined that the Nelson River contributes upwards of 34 % of the daily freshwater discharge for the entire Hudson Bay system during winter months, but this amount decreases during the spring and summer. The influence of damming on the sedimentary regime and hydrology of the Nelson River was investigated

by Duboc et al. (2017) using physical and chemical analyses on gravity cores sampled at the Nelson River mouth. Dam construction in the 1960s may have changed downstream sediment dynamics by controlling floods produced by ice-jamming during the spring freshet, which reduces downstream transport of ice and related hyperpycnal flows that would occur under natural river conditions (Duboc et al., 2017).

Sediment fingerprinting has not been widely used in the Nelson River system, but Theroux (2017) applied Cs-137 and colour property reflectance spectra sediment fingerprinting, along with Bayesian statistical modelling using MixSIAR, an open-source R package, to suspended sediment samples in the UNR to investigate and differentiate the sources of sediment to the Jack River, the drinking water source for the Norway House Cree Nation.

Although many of these studies inform upon important processes occurring in the Nelson River system that relate to this Master's research, significant gaps exist with respect to identifying particulate matter sources within the watershed and determining the extent of their transport throughout the Nelson River system.

1.4 Research objectives and anticipated significance

To investigate the source contributions and transport of terrestrial OM within the Nelson River system, the specific research objectives of this M.Sc. thesis were to:

1. Examine historical and newly collected summer-season physical and chemical water quality data from riverine stations in the Nelson River system to characterize particulate sources (organic matter and mineral sediment) in each region of the study area and investigate longitudinal and temporal changes to this particulate matter.

2. Utilize biochemical tracers, Compound-Specific Stable Isotope (CSSI) fingerprinting

techniques, and Bayesian statistical unmixing models to identify and characterize terrestrial OM sources in the Nelson River system, and quantify the relative contributions of these sources to terrestrial OM in downstream suspended sediments.

This work contributes to the broader goals of the BaySys project by identifying and characterizing the sources of particulate matter and terrestrial OM in the largest river system contributing to Hudson Bay. It is also the first application of CSSI fingerprinting to waterbodies within the Nelson River watershed and will aid in determining the extent to which sources of particulate matter and terrestrial OM can be traced as they are transported and transformed throughout the Nelson River system.

1.5 Thesis structure

Fieldwork was completed over two summer seasons (2016 and 2017) during which water, soil, and sediment samples were collected to produce two independent data sets that each relate to specific research objectives of this study. Following the general introduction in this chapter, each objective will be described and expanded upon in "sandwich thesis" style in its own chapter that includes sections on introduction, methods, results, discussion and conclusions. Chapter 2 will elaborate on Objective 1 by utilizing physical and chemical data from surface water samples to investigate particulate matter sources in the Nelson River system. Chapter 3 will build upon the findings of Chapter 2 by employing more sophisticated compositional and biochemical tracer analysis to soil and sediment samples and Bayesian statistical unmixing models to quantify the relative contributions of spatial- and substrate-related sources to downstream suspended sediment. The last chapter will synthesize the previous chapters, review significant findings in the data, and offer recommendations for future work in the Nelson River system. References for all chapters are listed following the final synthesis.

Chapter 2

Sources and characteristics of particulate matter in the Nelson River system

2.1 Introduction

Rivers are important transporters of sediment and organic matter (OM) from the continental land mass to the coastal zone (Battin et al., 2008; Aufdenkampe et al., 2011; Bianchi, 2011). In rivers, particulate OM is derived from allochthonous OM sources (e.g. soil organic matter (SOM) and plant debris) and autochthonous in-stream OM sources (e.g. macrophytes, algae, and phytoplankton), or produced in-situ by physio-chemical and biological processes acting on dissolved OM (Ittekkot & Laane, 1991). Carbon is a major constituent of OM and the quantity and form of organic carbon (OC) discharged by rivers can influence its fate in coastal waters. In the coastal zone, OC can undergo burial or be mineralized to dissolved inorganic carbon, affecting the pH and trophic status of coastal

waters and whether the coastal ocean as a whole behaves as a sink for CO_2 or as a source of CO_2 to the atmosphere. Since estuarine zones and continental shelves have been shown to be new sources of CO_2 to the atmosphere (Cole et al., 2007; Cai, 2011), it is prudent to study OM sources in the watersheds that contribute terrestrial OC to the coastal zone as well as watershed processes that may affect the form and magnitude in which OC is delivered to the ocean.

Subarctic river basins have typically sequestered OC in permafrost and areas of extensive peatlands and are particularly susceptible to processes that alter delivery of OC to the coastal ocean. Increasing temperatures in subarctic drainage basins (Arctic Climate Impact Assessment, 2005) and the resultant thawing and erosion of permafrost will mobilize previously stored OC associated with SOM into rivers (Guo et al., 2007; Gustafsson et al., 2011; Vonk et al., 2013; Vonk & Gustafsson, 2013) and therefore increase loading of OC to the coastal carbon cycle.

The Nelson River in Manitoba, Canada is a subarctic river with an expansive watershed and is the largest river flowing to Hudson Bay (Figure 2.1). It is a major source of both dissolved and particulate terrestrial OC to the coastal zone (Godin et al., 2017) and its watershed contains physically distinct subcatchments that are all affected by hydroelectric development as well as other anthropogenic impacts including climatic change. The mainstem of the river exhibits longitudinal complexity as waters flow through river channels, lake basins, and hydroelectric reservoirs.

The Nelson River system has been studied extensively by monitoring programs lead by industry, government agencies, and academic institutions since the inception of hydroelectric development in the region (Newbury et al., 1984; Newbury & McCullough, 1984; Hecky & McCullough, 1984; Strange, 1990; Green, 1990; Environment Canada and Department of Fisheries and Oceans, 1992a, 1992c, 1992b; Split Lake Cree and Manitoba Hydro, 1996;

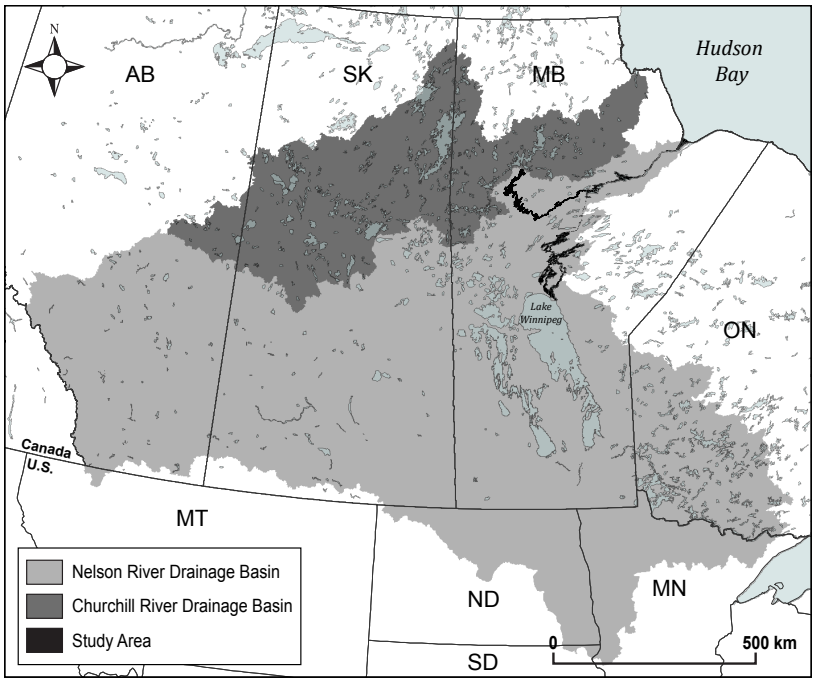

Fig. 2.1: Map showing the extent of the Nelson and Churchill River Drainage Basins in central Canada and northern United States. Study area water bodies are outlined in black.

Déry et al., 2005; Kirk & St. Louis, 2009; Kuzyk et al., 2009; North/South Consultants Inc., 2012; Coordinated Aquatic Monitoring Program, 2014; RSW-Environment Illimite Inc., 2014; Manitoba Hydro, 2015; Theroux, 2017; Duboc et al., 2017; Godin et al., 2017). Although particular focus was paid to physical and chemical water quality, many of these programs measured parameters related to particulate matter (both organic and mineral) within the Nelson River system, and workers like Godin (2014) and RSW-Environment Illimite Inc. (2014) have calculated particulate flux contributions from the Nelson River to Hudson Bay. Little work, however, has been done to explore particulate matter sources within the watershed as well as processes in the watershed that may affect the extent of their downstream transport.

In this work, physical and chemical water quality data are used to characterize particulate sources in each region of the Nelson River system and investigate longitudinal and

temporal changes to the sources of particulate matter (organic matter and mineral sediment). Particulate water quality data obtained in 2016-2017 and previously collected water quality data sets are used to explore distributions of sources and sinks, and shifts (both spatial and temporal) in the contributions of allochthonous and autochthonous OM in relation to morphological variation and erosional processes. Spanning three decades, the results also provide insight into the persistence of effects of river modification and natural hydrologic variability.

2.1.1 Study area description

The Nelson River in Manitoba is the single largest river discharging to Hudson Bay at a mean annual rate (1987-2017) of 110 km^3yr^{-1} (Environment and Climate Change Canada, 2018d, 2018e, 2018f). Its watershed extends over 91 000 km^2 in north central Manitoba to the southwest of Hudson Bay, and its >1 000 000 km^2 drainage basin ranges as far as Minnesota and South Dakota in the south, the Alberta in the west, and Ontario near Lake Superior in the east (Figure 2.1).

As a result of hydrological alteration for hydroelectric power development, the lower Nelson River (LNR) between Split Lake and Hudson Bay receives water primarily from two physically distinct catchments: 1) the upper Nelson River (UNR), which is the natural upstream portion of the Nelson River and 2) the Rat-Burntwood River (RBR) system, where discharge has been augmented by cross-watershed diversion. The study area encompasses the main stem waterbodies of these three regions and four associated tributaries (Figure 2.2). Since the inception of the Churchill River Diversion (CRD) project in the 1970s, the RBR system (from Southern Indian Lake to Split Lake) transports diverted Churchill River waters supplying ∼25% of total flow to the LNR, an approximate 10-fold increase from pre-development levels. The remaining ∼75% of total flow to the LNR is supplied by the UNR

between the outflow of Lake Winnipeg and Split Lake. These catchments differ in their physical characteristics: the RBR being a predominantly Precambrian Shield landscape whereas the UNR drains the vast, agriculturally-developed prairie landscape of the Lake Winnipeg watershed. River channels in all regions are either bounded by bedrock or incised into glacial cover. In the UNR and RBR, river channels expand to flow through several natural and controlled lakes whereas in the LNR, the largest reservoirs downstream of Split Lake (Stephens Lake and generating station forebays) occur as a result of hydroelectric development.

Four terrestrial ecozones intersect in the study area: Boreal Plain, Boreal Shield, Hudson Plain, and Taiga Shield. They are distinguished by different soil, vegetation, wetland, and permafrost types. Although variation occurs between ecozones, forest species throughout the study area primarily consists of black spruce, jack pine, aspen, sphagnum, and willows (Rosenberg et al., 2005). Permafrost in the study area underlies wetlands and upland forest with sufficient overburden and becomes more prevalent towards Hudson Bay. In the UNR, peat plateaus cover between $0.1-10\,\%$ of the land surface whereas in the RBR this range increases to between $20-30\,\%$; in the LNR peat plateaus cover between $20-80\,\%$ of the landscape whereas permafrost-dominated open permafrost bogs dominate the landscape north of the Nelson River in the LNR near the western coast of Hudson Bay (Halsey et al., 1997).

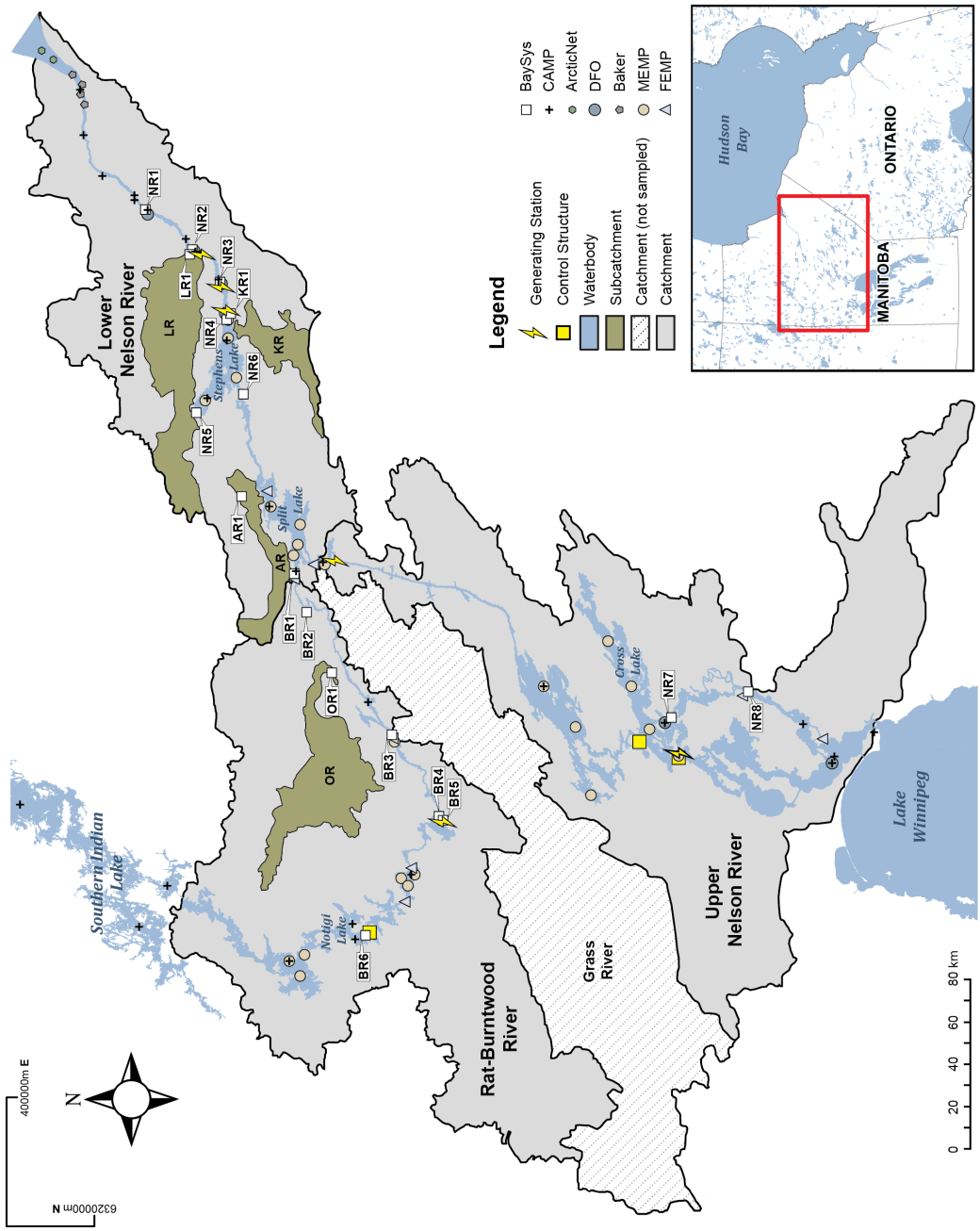

Fig. 2.2: Map showing study area and location of water quality sites sampled in the study area from 1985 to 2017, symbolized by monitoring program (abbreviations described in Table 2.1). Tributary watersheds are shown in green. OR: Odei River, AR: Assean River, KR: Kettle River, LR: Limestone River

2.2 Methods

2.2.1 Sample collection and data compilation

Water samples were collected for this project during field work in July and August of 2016 and 2017 as part of the Hudson Bay System Study (BaySys) (hereon known as the BaySys data set). Particulate data from ongoing and historical water quality sampling programs supplemented the BaySys data set to improve site density along the run of the river and provide perspective on the parameters of interest in the Nelson River system over time. Supplementary data was selected based on the use of the same sampling and analytical methods as the BaySys program. Duration, analytical methods, and water quality parameters of interest from each monitoring program are summarized in Table 2.1. Data collection methods for all sampling programs are described in this section.

2.2.1.1 Hudson Bay System Study (BaySys)

Eighteen sampling sites were selected based on their accessibility by truck, and their proximity to either pre-existing water quality sites or Water Survey of Canada hydrometric stations. Surface water samples (< 0.5 m depth) were collected from shoreline or bridges in late July or early August of 2016 and 2017. At shoreline sites, water samples were collected by wading as far as possible into flowing water and hand-dipping 1 L amber Nalgene bottles. At bridge sites, samples were collected by lowering a weighted bridge sampler equipped with a 2 L amber Nalgene bottle into surface water. All Nalgene bottles were pre-washed with 10 % HCl, rinsed Milli-Q water, and rinsed three times with sample water in the field prior to collection. Sample sites were predominantly riverine, but samples were also collected from lakes proximal to the shoreline when channels in the area were not accessible by truck. To test whether shoreline water samples represented particulate conditions at each site, a water sample and CTD (conductivity, temperature, and depth measurement instrument)

Table 2.1: Duration, relevant water quality parameters, and analytical methods used by monitoring programs in the study area between 1987 and 2017. (TSS: total suspended solids, SuspOC: suspended organic carbon, SuspC: suspended carbon, SuspN: suspended nitrogen, DFO: Department of Fisheries and Oceans, ALS: ALS Environmental Laboratory)

Data Source	Year(s)	Water Quality Parameter(s)	Analytical Method
BaySys[1]	2016 to 2017	TSS, SuspOC, SuspN	DFO
CAMP[2]	2008 to 2017	TSS	ALS
ArcticNet[3]	2005 to 2007	TSS, SuspOC, SuspN	DFO
DFO[4]	1990 to 1993	TSS, SuspC*, SuspN	DFO
Baker[5]	1989	TSS, SuspC*, SuspN	DFO
FEMP[6]	1985 to 1989	TSS, SuspOC, SuspN	DFO
MEMP[7]	1985 to 1989	TSS, SuspC*, SuspN	DFO

* Converted to SuspOC using area-specific conversion factor
[1] Hudson Bay System Study (BaySys)
[2] Coordinated Aquatic Monitoring Program (Coordinated Aquatic Monitoring Program, 2014)
[3] ArcticNet Nelson River estuary study (Greg McCullough, personal communication, February 2018)
[4] Department of Fisheries and Oceans archive (Michael Stainton, personal communication, June 2017)
[5] Nelson River estuary study (Baker, 1989)
[6] Federal Ecological Monitoring Program (Environment Canada and Department of Fisheries and Oceans, 1992b), (Strange, 1990)
[7] Manitoba Ecological Monitoring Program (Green, 1990)

transect was completed at the Kichi Sipi bridge over the Nelson River (site NR7) upstream from the community of Cross Lake (described in Section 2.2.4).

Water samples were kept cold in coolers until each field survey was complete and delivered to the Department of Fisheries and Oceans (DFO) Water Chemistry Laboratory in Winnipeg, Manitoba for filtration and analysis.

2.2.1.2 Other monitoring programs (1987-2017)

Supplementary data sets used in conjunction with BaySys data are listed in Table 2.1 and include data from monitoring programs in which water was sampled from both lake and river sites throughout the study area. A brief background description of each of these programs and their sampling methods is outlined below.

The Coordinated Aquatic Monitoring Program (CAMP) began in 2008 as a long-term aquatic monitoring program centred on Manitoba's hydroelectric power waterways (Coordinated Aquatic Monitoring Program, 2014). As a coordinated effort between the Government of Manitoba and Manitoba Hydro, CAMP investigates many components of the aquatic environment of both on- and off-system waterbodies. Multi-seasonal water quality sampling is performed by CAMP on river and lake sites within the study area. Near-surface (< 30 cm) water samples are hand-dipped and stored in coolers prior to analysis at ALS Environmental Laboratory in Winnipeg, Manitoba (Coordinated Aquatic Monitoring Program, 2014).

Opportunistic sampling in the lower reaches of the Nelson River was undertaken as part of the ArcticNet Nelson River estuary study during the summer and fall seasons between 2005 and 2007 (Greg McCullough, personal communication, February 2018).

Unpublished analytical results for samples collected from generating stations between

1990 and 1993 were acquired from the DFO Freshwater Institute Water Chemistry Laboratory archive (Michael Stainton, personal communication, June 2017). Water samples were collected from a raw river water intake tap within each of the generating stations, stored in coolers, and shipped to DFO for analysis.

Water quality samples were collected by Baker (1989) near the Nelson River mouth as part of a study to collect baseline information on the physical and biological environment of the Nelson River estuary following the construction of the Limestone Generating Station (GS). Surface water samples were hand-dipped into bottles and refrigerated until analyzed.

The Federal Ecological Monitoring Program (FEMP) was a 5-year federally run monitoring program that began in 1986 to assess the environmental impacts of the CRD and Lake Winnipeg Regulation (LWR) on the Nelson River system (Environment Canada and Department of Fisheries and Oceans, 1992a, 1992b). Although this program encompassed a variety of scientific investigations to meet these assessment goals, of specific interest to this thesis is a sampling program funded by FEMP that aimed to assess the effects of hydroelectric development on water quality in the region. Strange (1990) collected monthly water samples from 11 riverine sites in the UNR, RBR, and Split Lake regions between 1986 and 1989. Sites were accessed by helicopter, float plane or boat (depending on the season). Samples were collected by either hand dipping bottles or by weighted sampler, stored in coolers, and filtered on site in a mobile field lab.

The Manitoba Ecological Monitoring Program (MEMP) was a monitoring program run by the Manitoba Department of Natural Resources Fisheries Branch in the study area from 1985 to 1989 with the goal of evaluating the impacts of hydroelectric development on water quality in the area as a result of the CRD and LWR (Green, 1990). Although its goals were similar to those of FEMP, this monitoring program focused on sampling water from lake

sites, Generating Stations, and the city of Thompson water treatment plant. Lake surface water samples were collected into bottles by hand. Samples were collected from the raw water supply intake line at generating stations, and from the aqueduct in the treatment plant station house in Thompson. All samples were stored refrigerated and shipped for analysis at the DFO Water Chemistry Laboratory.

2.2.2 Laboratory analysis

2.2.2.1 Total suspended solids (TSS)

Water samples collected for this thesis were analyzed for TSS concentration (in $\mathrm{mg\,L^{-1}}$) at the DFO Water Chemistry Laboratory using standard methods and procedures developed by Stainton et al. (1977). Water samples were agitated by hand and vacuum filtered through pre-weighed, 1.2 µm nominal pore size, 4.25 cm wide Whatman GF/C filters that were pre-combusted at 500 °C. At least 100 mL of water was filtered for each sample, but exact volumes were recorded. Filters were then dried at 104 °C for one hour and the filter plus particulate material was re-weighed multiple times to demonstrate accurate tare and final weight.

All other monitoring programs selected for inclusion in this thesis used either the same laboratory facility or one using the same methodology and filter pore size to measure TSS concentration in fresh water.

2.2.2.2 Suspended organic carbon (SuspOC) and suspended nitrogen (SuspN)

Water samples collected for this study were analyzed for suspended carbon, nitrogen, and OC concentrations (in $\mathrm{\mu g\,L^{-1}}$) at the DFO Water Chemistry Laboratory as per methods and procedures described by Stainton et al. (1977). Water samples were agitated by hand

and vacuum filtered through pre-weighed, 1.2 µm nominal pore size, 4.25 cm wide Whatman GF/C filters that were pre-combusted at 550 °C for 16 hours. Using a CE-440 Elemental Analyzer (Exeter Analytical, Inc.), particulate material was combusted to measure total carbon and nitrogen. Particulate OC was measured by the same instrument but filters containing suspended carbon sample were pre-treated with 10 mL of 1.2 mol HCl until no effervescence was observed, rinsed with 50 mL of Milli-Q water, and desiccated prior to combustion.

All other monitoring programs selected for inclusion in this thesis used the same laboratory facility or one using the same methodology to measure suspended carbon, nitrogen, and organic carbon concentrations, except the CAMP program that used ALS laboratories. Particulate carbon and nitrogen concentrations from CAMP could not be utilized by this thesis because the methods used by ALS to measure these parameters differ too greatly from the DFO lab method[1], and therefore results are not considered by the author to be comparable.

2.2.3 Data analysis

All statistical analysis described in this section, as well as graphical methods used to produce plots, were undertaken using R software (version 3.3.2, R Core Team, 2016) using the following packages in the library: tidyverse (Wickham, 2017), gridextra (Auguie, 2017), and ggplot2 (Wickham, 2016).

Statistical tests were performed using the built-in R stats package in R software (R Core Team, 2013). Shapiro-Wilks normality tests were performed using the **shapiro.test()** func-

[1]The filter nominal pore size used by ALS to measure particulate carbon, OC, and nitrogen is smaller than that used to measure TSS (0.45 µm versus 1.2 µm), so they are effectively measuring different particle fractions. Particulate organic carbon concentration at ALS Laboratory is also determined by measuring total and dissolved carbon and calculating the difference whereas the DFO method measures particulate carbon concentration directly.

tion, analysis of variance (ANOVA) was calculated using the **aov()** function, and Tukey's HSD (Honest Significant Difference) test was performed using the **TukeyHSD()** function.

2.2.3.1 Hudson Bay System Study (BaySys)

Statistical analysis in R (R Core Team, 2013) was performed on the BaySys data set to test for normal data distributions for each measured water quality parameter. The Shapiro-Wilk normality test and graphical tests such as histograms, and the **qqnorm()** and **qqline()** functions showed that not all parameters exhibit a normal data distribution. Due to the overall size of the data set, number of samples collected per site, and the fact that outliers could inform upon processes occurring within the region from which samples were collected, no outliers were trimmed from the data set and therefore all data visualizations are shown using medians and quartile ranges.

The proportion of SuspOC of TSS (% SuspOC of TSS) and molar carbon to nitrogen ratios (C/N) were calculated from measured concentrations.

2.2.3.2 Compiled data set (1987-2017)

All supplementary monitoring program data sets were cleaned and subjected to a series of statistical tests prior to the creation of the compiled data set. Stations sampled during the BaySys program, the bulk of which are within main-stem channels of the Nelson River system, were collected during the summer months. Therefore, all other data sets were filtered to include only riverine sites sampled from June to August. Obvious outliers and non-detect concentrations were removed from each data set. As a results of these steps, all individual monitoring program data sets except ArcticNet (Greg McCullough, personal communication, February 2018) and Baker (1989) exhibited a normal distribution for each

measured and calculated parameter when tested using the Shapiro-Wilk normality test and graphical tests such as histograms, and the **qqnorm()** and **qqline()** functions.

Three monitoring programs (MEMP, Baker, and DFO) used analytical methods described in Section 2.2.2, but limited their sample analysis to total suspended carbon (SuspC), and did not proceed to analyze for suspended organic carbon (SuspOC). To include these programs into the compiled data set, SuspC concentrations were converted to SuspOC using regional conversion factors. A Tukey HSD test performed on the BaySys data set revealed a statistically significant difference in the proportion of SuspOC in SuspC concentrations between the UNR and each other region ($p < 0.001$, $n = 46$), but no significant difference was observed between the LNR and RBR ($p = 0.14$, $n = 38$). Therefore, a conversion factor of 0.89 was calculated using the mean of SuspOC in SuspC in all UNR samples. The same method was applied for remaining samples in the RBR and LNR yielding a conversion factor of 0.71 (Figure 2.3a and 2.3b). Total SuspC measurements were converted to SuspOC for each region using Equations 2.1, 2.2, and 2.3.

$$SuspOC_{(UNR)} = SuspC_{(UNR)} \times 0.89 \tag{2.1}$$

$$SuspOC_{(RBR)} = SuspC_{(RBR)} \times 0.71 \tag{2.2}$$

$$SuspOC_{(LNR)} = SuspC_{(LNR)} \times 0.71 \tag{2.3}$$

Prior to merging all data sets, water quality parameters from each monitoring program were first standardized using Equation 2.4 where x_i is the parameter value, μ and σ are the mean and standard deviation of each parameter in the whole data set, and z_i is the standardized value.

$$z_i = \frac{(x_i - \mu)}{\sigma} \tag{2.4}$$

This was done so water quality parameters from all monitoring programs could be evaluated

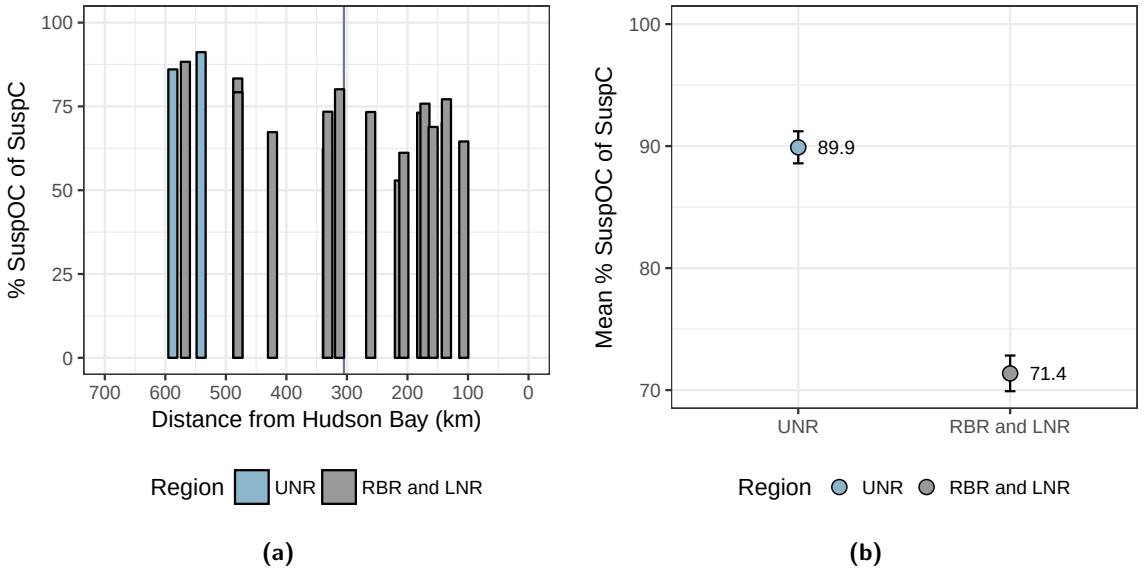

Fig. 2.3: BaySys SuspOC conversion factors. **2.3a**: % SuspOC of SuspC in each region of the study area. Vertical line represents location of Split Lake. **2.3b**: Mean % SuspOC of SuspC by region of the study area.

longitudinally even though sampling was conducted over the period of many years under different climatic and discharge conditions. The compiled data set exhibited a normal distribution for each measured and calculated parameter when tested using the Shapiro-Wilk normality test ($p < 0.05$, $n = 282$) and graphical tests such as histograms, and the **qqnorm()** and **qqline()** functions.

2.2.4 Water sampling method evaluation

A water sampling and CTD transect was preformed at site NR7 (Figure 2.2) in the UNR to evaluate the validity of shoreline sampling in riverine systems. Water was collected from the Kichi Sipi bridge by lowering a weighted 2 L amber Nalgene bottle at each point into surface water (<0.5 m). A continuous transect was collected between points NR7-e and NR7-a by walking the rope-suspended CTD north across the bridge (Figure 2.4). Between transect points, lab-based TSS concentrations range from $7\,mg\,L^{-1}$ to $9\,mg\,L^{-1}$.

The laboratory method for measuring TSS concentration estimates a precision error of $\pm 0.5\,\mathrm{mg\,L^{-1}}$ (Stainton et al., 1977). Nearshore samples indicate median cross-section values $\pm 1\,\mathrm{mg\,L^{-1}}$ (i.e. the uncertainty is about two times the lab uncertainty of $\pm 0.5\,\mathrm{mg\,L^{-1}}$). Turbidity measurements also support this since most measurements across the channel show uniform values (<50 NTU).

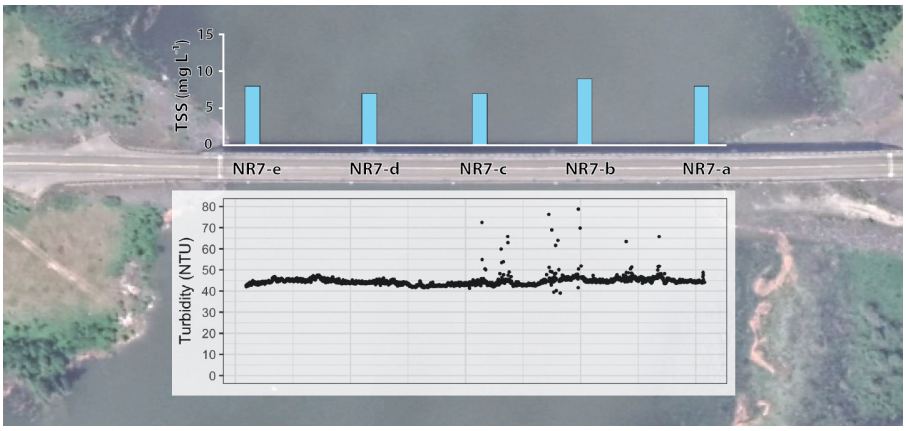

Fig. 2.4: Map showing water sampling and CTD transect across the Nelson River at the Kichi Sipi Bridge south of the community of Cross Lake. Blue bars indicate point TSS concentration at sample points and inset plot shows continuous turbidity (in NTU) measured by CTD between sites NR7-e and NR7-a. Satellite image sourced from Google Earth on August 18, 2018.

2.3 Results

In this section, water quality results from all sites sampled during the BaySys will first be presented alone in Section 2.3.1, and then alongside data from other monitoring programs as a part of the compiled data set in Section 2.3.2.

2.3.1 Hudson Bay System Study (BaySys)

To evaluate the characteristics and distribution of each water quality parameter and OM source in each region, results from the BaySys program (Table 2.2) are displayed

longitudinally in this section. For ease of data visualization, each upstream region (UNR and RBR) and the LNR is treated as a separate continuous river system (Figures 2.5a and 2.6a) and water quality parameters are displayed longitudinally by station distance in kilometres from Hudson Bay (Figure 2.5b and 2.6b) for each corresponding river region.

Table 2.2: Water quality results from the BaySys study. "Site km" column indicates distance upstream from Hudson Bay. Water quality results are listed as median values with interquartile range (25-75 percentile) in brackets.

Region	Site km	Site	n	TSS ($mg\,L^{-1}$)	% SuspOC	C/N (molar)
UNR	540.9	NR7	6	8.0 (7.3 - 8.8)	9.4 (9.0 - 9.7)	8.0 (7.7 - 8.1)
	587.6	NR8	1	15.0 (n/a)	17.3 (n/a)	5.5 (n/a)
RBR	312.1	BR1	2	27.0 (23.0 - 31.0)	2.5 (2.2 - 2.8)	7.5 (7.5 - 7.6)
	331.6	BR2	2	26.5 (22.8 - 30.3)	3.0 (2.5 - 3.4)	7.6 (7.4 - 7.8)
	332.3	OR1	2	29.0 (27.5 - 30.5)	2.8 (2.8 - 2.9)	8.5 (8.3 - 8.7)
	423.0	BR3	7	24.0 (23.0 - 25.0)	2.4 (2.3 - 2.4)	9.4 (7.4 - 9.9)
	480.1	BR4	2	26.5 (23.3 - 29.8)	2.4 (2.3 - 2.5)	7.8 (7.3 - 8.4)
	480.4	BR5	2	19.0 (18.5 - 19.5)	2.8 (2.8 - 2.8)	7.5 (7.1 - 7.9)
	566.9	BR6	2	8.5 (7.3 - 9.8)	5.3 (4.6 - 6.1)	9.3 (9.1 - 9.6)
LNR	107.0	NR1	2	22.0 (20.5 - 23.5)	3.3 (3.0 - 3.6)	6.7 (6.2-7.1)
	135.6	LR1	2	3.5 (3.3 - 3.8)	15.6 (14.6 - 16.5)	9.9 (9.7-10.2)
	135.8	NR2	2	21.0 (20.0 - 22.0)	3.3 (3.1 - 3.5)	7.3 (7.3-7.4)
	157.6	NR3	2	14.5 (9.3 - 19.8)	7.6 (5.2 - 9.9)	8.8 (8.3-9.2)
	171.1	KR1	2	6.5 (6.3 - 6.8)	11.2 (10.8 - 11.7)	9.0 (8.9-9.2)
	176.5	NR4	2	19.0 (19.0 - 31.5)	3.3 (3.3 - 4.1)	6.9 (6.9-9.0)
	206.0	NR5	2	15.5 (15.3 - 15.8)	3.3 (3.3 - 3.4)	8.5 (8.1-8.9)
	213.4	NR6	2	37.0 (32.5 - 41.5)	2.5 (2.4 - 2.7)	8.5 (7.9-9.1)
	260.8	AR1	2	9.0 (8.5 - 9.5)	7.8 (7.2 - 8.5)	8.3 (8.2-8.4)

2.3.1.1 Upper Nelson River - lower Nelson River

Total suspended solids concentration at sites in the UNR between the outflow of Lake Winnipeg and Jenpeg GS is low compared to other regions with median (interquartile range) values between $8\,mg\,L^{-1}$ ($7.3\,mg\,L^{-1}$ to $8.8\,mg\,L^{-1}$) and $15\,mg\,L^{-1}$ (Figure 2.5b top

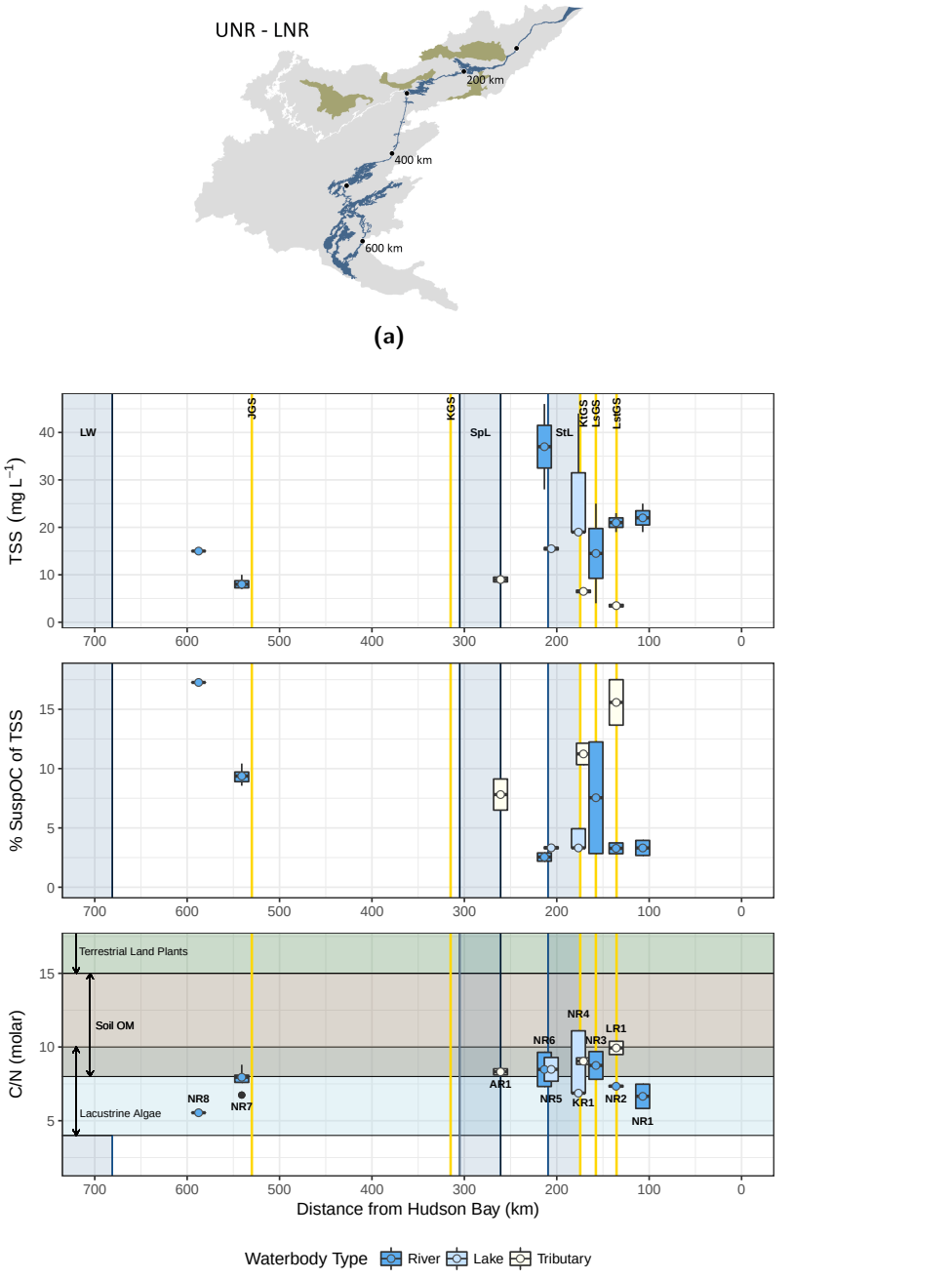

Fig. 2.5: 2.5a: Map showing distance (km) on x-axis in Figure 2.5b; tributary watersheds shown in green. **2.5b**: TSS ($\mathrm{mg\,L^{-1}}$), % SuspOC of TSS and molar C/N ratios in the UNR and LNR from the BaySys program arranged longitudinally. Key hydraulic features labeled. Box and whisker plots show median as line and open circle, upper and lower hinges are 75% and 25% quartile, upper and lower whiskers are ymin and ymax, and black dots are outliers. LW: Lake Winnipeg, JGS: Jenpeg GS, KGS: Kelsey GS, SpL: Split Lake, StL: Stephens Lake, KtGS: Kettle GS, LsGS: Long Spruce GS, LstGS: Limestone GS

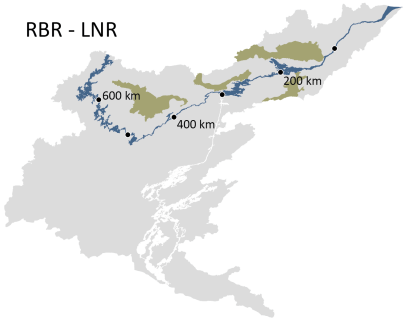

(a)

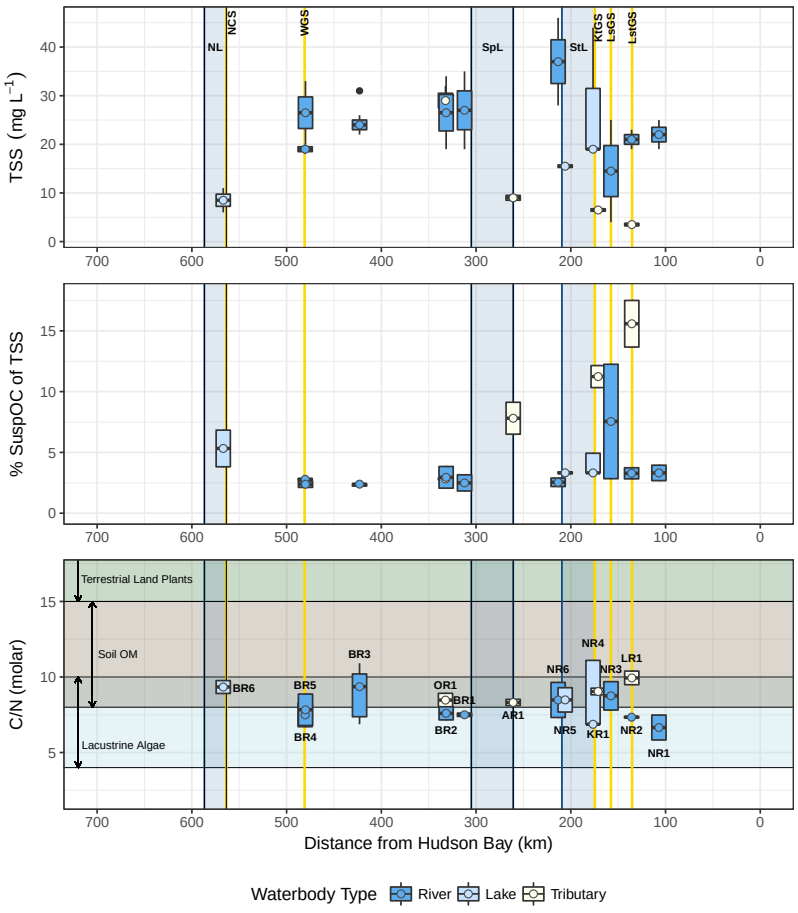

(b)

Fig. 2.6: **2.6a**: Map showing distance (km) on x-axis in Figure 2.6b; tributary watersheds shown in green. **2.6b**: TSS ($\mathrm{mg\,L^{-1}}$), % SuspOC of TSS and molar C/N ratios in the RBR and LNR from the BaySys program arranged longitudinally. Key hydraulic features are labeled. NL: Notigi Lake, NCS: Notigi CS, WGS: Wuskwatim GS, SpL: Split Lake, StL: Stephens Lake, KtGS: Kettle GS, LsGS: Long Spruce GS, LstGS: Limestone GS

panel). In the LNR, site NR6 upstream of Stephens Lake has a median TSS concentration of 37 mg L^{-1} (32.5 mg L^{-1} to 41.5 mg L^{-1}). Downstream of the inflow to Stephens Lake, median TSS concentrations at sites on the main stem Nelson River range between 14.5 mg L^{-1} (9.3 mg L^{-1} to 19.8 mg L^{-1}) and 22.0 mg L^{-1} (20.5 mg L^{-1} to 23.5 mg L^{-1}). Tributaries flowing into the LNR, such as the Assean River (AR1), the Kettle River (KR1), and the Limestone River (LR1), all have median TSS concentrations below 10 mg L^{-1}.

The proportion of SuspOC in total suspended solids (% SuspOC of TSS) at sites in the UNR between the outflow of Lake Winnipeg and Jenpeg GS is generally high compared to other regions with median values between 9.4 % (9.0 % to 9.7 %) and 17.3 % (Figure 2.5b middle panel). In the LNR, % SuspOC of TSS at main stem Nelson River sites downstream of Split Lake ranges between 2.5 % (2.4 % to 2.7 %) and 7.6 % (5.2 % to 9.9 %). Tributaries in the LNR region show a higher proportion of % SuspOC in TSS than main stem Nelson River sites with median values of 7.8 % (7.2 % to 8.5 %) in the Assean River, 11.2 % (10.8 % to 11.7 %) in the Kettle River and 15.6 % (14.6 % to 16.5 %) in the Limestone River.

In the UNR, molar C/N ratios fall within the lacustrine algae source range (4 - 10) (Meyers & Ishiwatari, 1993; Meyers, 1994; Meyers & Teranes, 2001; Kendall et al., 2001; McConnachie & Petticrew, 2006) with median ratios of 5.5 at site NR8 and 8.0 (7.7 to 8.1) at site NR7 (Figure 2.5b bottom panel). In the LNR, molar C/N ratios lay within lacustrine algae source range at sites NR4, NR2, and NR1 with median ratios of 6.9 (6.9 to 9.0), 7.3 (7.3 to 7.4), and 6.7 (6.2 to 7.1) respectively. Median molar C/N ratios of 8.5 (7.9 to 9.1) at site NR6, 8.5 (8.1 to 8.9) at site NR5, and 8.8 (8.3 to 9.2) at site NR3 fall within the source ranges of both SOM (8 - 15) and lacustrine algae (Meyers & Ishiwatari, 1993; Meyers, 1994; Meyers & Teranes, 2001; Kendall et al., 2001; McConnachie & Petticrew, 2006). Tributaries flowing into the LNR exhibit C/N ratios that fall within the SOM source range with median ratios at sites AR1, KR1, and LR1 of 8.3 (8.2 to 8.4), 9.0 (8.9 to 9.2), and 9.9 (9.7 to 10.2) respectively.

2.3.1.2 Rat-Burntwood River

In the RBR, TSS is low upstream of the Notigi CS at site BR6 with a median (interquartile range) concentration of 8.5 mg L^{-1} (7.3 mg L^{-1} to 9.8 mg L^{-1}) (Figure 2.6b top panel). However, TSS concentration downstream of the Wuskwatim GS to the inflow of Split Lake is high compared to other regions with median values between 19.0 mg L^{-1} (18.5 mg L^{-1} to 19.5 mg L^{-1}) and 27.0 mg L^{-1} (23.0 mg L^{-1} to 31.0 mg L^{-1}). The Odei River, a tributary flowing into the RBR, also exhibits high TSS with a median concentration of 29.0 mg L^{-1}.

Percent SuspOC of TSS in the upper reaches of the RBR is high in relation to downstream sites that exhibit some of the lowest proportions of SuspOC in the study area (Figure 2.6b middle panel). At site BR6, upstream of the Notigi CS, median % SuspOC of TSS is 5.3 % (4.6 % to 6.1 %). From Wuskwatim GS to the inflow of Split Lake, median values range between 2.4 % (2.3 % to 2.4 %) and 3.0 % (2.5 % to 3.4 %). The Odei River also exhibits low % SuspOC of TSS with a median value of 2.8 %.

Molar C/N ratios in the RBR lie within both the lacustrine algae source range (4 - 10) and the SOM source range (8 - 15) (Figure 2.6b bottom panel). Sites BR5, BR2, and BR1 show C/N ratios within the lacustrine algae source range with median ratios of 7.5 (7.1 to 7.9), 7.6 (7.4 to 7.8), and 7.5 (7.5 to 7.6) respectively. Soil organic matter sources dominate sites BR6, BR4, and BR3 with median C/N ratios of 9.3 (9.1 to 9.6), 7.8 (7.3 to 8.4), and 8.5 (8.3 to 8.7) respectively. A median molar C/N ratio of 8.5 (8.3 to 8.7) at RBR tributary site OR1 falls within the SOM range.

2.3.1.3 Regional analysis

The LNR shows variation in water quality parameter characteristics where the natural river channel is dammed by several hydroelectric generating stations creating flooded reservoirs and forebays. However, marked regional and longitudinal differences are observed between the UNR and RBR when compared to each other and the LNR.

Comparing each parameter by region, median (interquartile range) TSS concentration is highest in the RBR at $23.0\,\mathrm{mg\,L^{-1}}$ ($19.5\,\mathrm{mg\,L^{-1}}$ to $28.5\,\mathrm{mg\,L^{-1}}$) and lowest in the UNR at $8.5\,\mathrm{mg\,L^{-1}}$ ($7.8\,\mathrm{mg\,L^{-1}}$ to $11.3\,\mathrm{mg\,L^{-1}}$) (Figure 2.7a). Median TSS concentration in the LNR is $19.0\,\mathrm{mg\,L^{-1}}$ ($7.5\,\mathrm{mg\,L^{-1}}$ to $24.0\,\mathrm{mg\,L^{-1}}$), and is much more variable depending on location within the region. An ANOVA test was used to determine statistical significance of differences in TSS concentration between regions and revealed that the TSS concentration in the UNR is significantly lower ($p < 0.05$, $n = 27$) than in the RBR, and nearly significantly different ($p = 0.12$, $n = 27$) from the LNR. No statistical difference was observed in TSS concentration between the RBR and LNR regions.

The UNR shows the highest median % SuspOC of TSS compared to other regions at 9.7 % (9.1 % to 12.1 %) whereas the RBR region has the lowest at 2.4 % (2.3 % to 2.9 %) (Figure 2.7b). Similar to TSS concentration, the LNR shows variation in % SuspOC of TSS but median values are generally low at 3.7 % (3.1 % to 9.7 %). An ANOVA test showed a statistically significant difference ($p < 0.05$, $n = 27$) in % SuspOC of TSS between the UNR and the other two regions, but as with TSS, no significant difference was observed between the RBR and LNR.

Molar C/N ratios are lowest in the UNR with a median value of 7.71 (6.4 to 8.1), and fall within the lacustrine algae source range (Figure 2.7c). Molar C/N ratios in the RBR and LNR border both lacustrine algae and SOM source ranges with median values of 8.0 (7.4 to 9.1) and 8.1 (7.4 to 9.4) respectively. No significant difference was observed between C/N

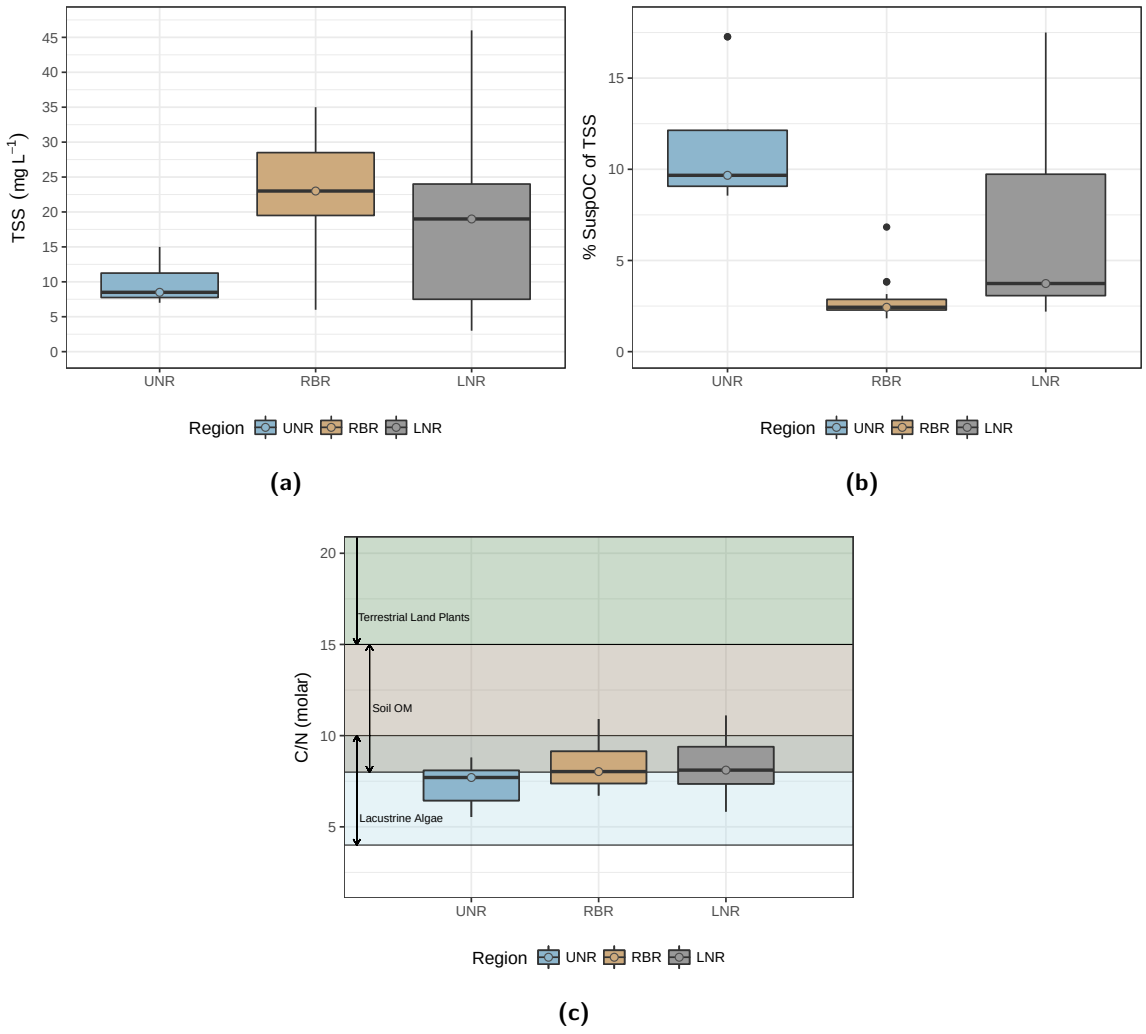

Fig. 2.7: Regional median and quartile summary boxplots of water quality parameters sampled during the BaySys program. **2.7a**: TSS concentration ($\mathrm{mg\,L^{-1}}$) by study area region. **2.7b**: % SuspOC of TSS by study area region. **2.7c**: Molar C/N ratios by study area region.

ratios in the RBR and LNR. An ANOVA showed a near-statistically significant difference ($p < 0.15$, $n = 27$) between of C/N ratios between the UNR and the other two regions.

Along with the regional comparison of particulate water quality parameters, investigation of relationships between water quality parameters themselves is warranted. The following relationships were explored within each region using the **lm()** function in R software to calculate linear model regression: TSS versus SuspOC, SuspN versus SuspOC, and N/C ratios versus SuspOC. No significant relationship is observed between TSS and SuspOC in either the RBR or LNR ($R^2 < 0.5$, $p > 0.05$, $n = 19$), but a linear model regression indicates a significant relationship between these parameters in the UNR ($R^2 = 0.79$, $p = 0.01$, $n = 6$) (Figure 2.8a). Molar concentrations of SuspOC and SuspN were plotted and a linear model regression line was calculated, indicating a positive correlation between these two parameters ($R^2 = 0.70$, $p < 0.05$, $n = 46$)(Figure 2.8b). The slope of this linear relationship (5.05) represents the average C/N ratio for all regions. A positive SuspOC intercept when SuspN is zero indicates the likelihood of a high carbon, nitrogen-depleted source of particulate OM in the system such as woody plants that have C/N ratios from 40 to >200 (Meyers & Ishiwatari, 1993). No significant relationship was observed between SuspOC and N/C ratios in the RBR and LNR (Figure 2.8c). A near-significant correlation exists between these parameters in the UNR ($R^2 = 0.3$, $p = 0.14$, $n = 6$) and when compared to other regions, both N/C ratios and SuspOC concentrations are higher in the UNR.

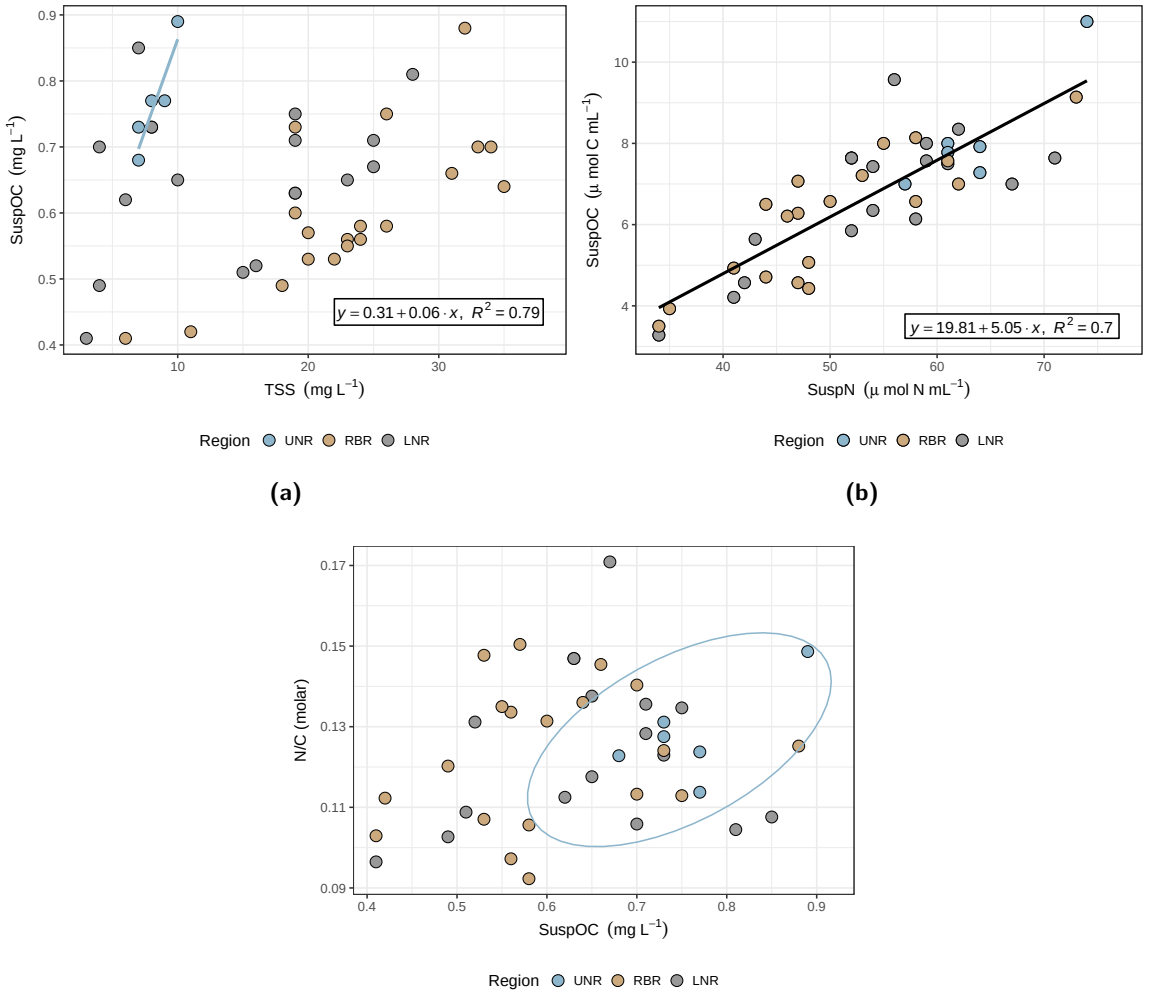

Fig. 2.8: BaySys water quality parameter relationships. **2.8a**: TSS versus SuspOC concentration ($\mathrm{mg\,L^{-1}}$). **2.8b**: SuspN versus SuspOC concentration ($\mu\mathrm{mol\,mL^{-1}}$). **2.8c**: Molar N/C ratio versus SuspOC concentration ($\mathrm{mg\,L^{-1}}$).

2.3.2 Monitoring programs (1987-2017)

Results from the BaySys program were supplemented by water quality data from six other monitoring programs (Table 2.1). All water quality results included in the compiled data set were measured from riverine sites and are summarized from raw data in Table 2.3, but in order to compare visually results between monitoring programs while accounting for variation in discharge and climate over the time span of all programs, water quality parameter measurements within each data set were standardized using Formula 2.4. As in Section 2.3.1, water quality parameters (standardized TSS, standardized % SuspOC of TSS, and molar C/N ratios) from riverine sites sampled in the summer season are displayed longitudinally by station distance in kilometres from Hudson Bay with corresponding river regions (Figure 2.9a and 2.10a). The standardized data displayed in Figures 2.9b and 2.10b no longer represent physical measurements, and therefore will be described as longitudinal increases or decreases in each parameter.

2.3.2.1 Upper Nelson River - lower Nelson River

When compared to the BaySys results in Section 2.3.1.1, the compiled data set also shows low median TSS concentration between the outflow of Lake Winnipeg and Jenpeg GS in the UNR compared to other regions (Figure 2.9b top panel). Sites in the lower reaches of the UNR show slightly elevated TSS concentration upstream of Kelsey GS compared to the upstream portion of this region. In the LNR, TSS concentration is higher upstream of Stephens Lake, and is lower between Stephens Lake and Limestone GS, where all generating stations in the LNR are located. A slight step-wise increase in TSS occurs downstream of Limestone GS and the confluence of the Angling River, a tributary ∼100 km upstream of the Nelson River mouth. The lower reaches of the LNR show another step-wise increase in TSS concentration in the length of river ∼60 km upstream of the Nelson River mouth.

Table 2.3: Water quality results at river sites from all supplementary monitoring programs. Median values with interquartile range (25-75 percentile) in brackets. Note that this table contains results summarized from raw data reported in physical units, whereas Figures 2.9 and 2.10 were produced using standardized water quality parameters.

Region	Program	Site km	Site	n	TSS ($mg\,L^{-1}$)	% SuspOC	C/N (molar)
UNR	BaySys	540.9	NR7	6	8.0 (7.3 - 8.8)	9.4 (9.0 - 9.7)	8.0 (7.7 - 8.1)
		587.6	NR8	1	15.0 (n/a)	17.3 (n/a)	5.5 (n/a)
	CAMP	313.4	UFS017	4	16.4 (14.1 - 18.8)	–	–
		668.4	UBS010	10	5.6 (4.8 - 7.0)	–	–
	MEMP	314.9	Kelsey GS	19	7.0 (3.0 - 14.5)	7.3 (4.9 - 9.4)	10.8 (9.3 - 11.8)
		544.0	Jenpeg GS	17	10.0 (9.0 - 13.0)	4.9 (4.2 - 6.8)	8.1 (7.4 - 8.6)
	FEMP	309.7	UF0005	16	6.0 (5.0 - 7.3)	5.4 (4.1 - 6.2)	7.7 (7.1 - 8.7)
		589.2	UB0006	9	10.0 (6.0 - 10.0)	5.8 (5.1 - 5.9)	8.0 (7.8 - 8.9)
		633.0	UB0013	9	7.0 (6.0 - 10.0)	6.0 (5.3 - 7.2)	7.7 (7.4 - 9.4)
RBR	BaySys	312.2	BR1	2	27.0 (23.0 - 31.0)	2.5 (2.2 - 2.8)	7.5 (7.5 - 7.6)
		331.6	BR2	2	26.5 (22.8 - 30.3)	3.0 (2.5 - 3.4)	7.6 (7.4 - 7.8)
		423.0	BR3	7	24.0 (23.0 - 25.0)	2.4 (2.3 - 2.4)	9.4 (7.4 - 9.9)
		480.1	BR4	2	26.5 (23.3 - 29.8)	2.4 (2.3 - 2.5)	7.8 (7.3 - 8.4)
		480.4	BR5	2	19.0 (18.5 - 19.5)	2.8 (2.8 - 2.8)	7.5 (7.1 - 7.9)
	CAMP	309.8	TGS015	14	16.8 (13.5 - 23.2)	–	–
		401.7	TGS014	2	11.6 (10.2 - 13.0)	–	–
	MEMP	424.8	Thompson	15	19.0 (17.5 - 24.0)	2.3 (2.2 - 2.7)	9.4 (8.8 - 10.8)
	FEMP	313.5	TG0003	16	23.5 (20.0 - 24.5)	2.8 (2.4 - 3.0)	11.4 (10.5 - 12.4)
		419.4	TG0001	15	19.0 (17.0 - 20.0)	2.6 (2.2 - 3.4)	10.7 (8.0 - 14.0)
		514.9	TF0004	16	10.0 (8.0 - 11.0)	3.4 (3.1 - 3.8)	7.7 (6.9 - 8.7)
		532.0	TF0001	16	8.5 (6.8 - 10.3)	3.4 (3.0 - 4.6)	7.8 (7.2 - 8.5)
LNR	BaySys	107.0	NR1	2	22.0 (20.5 - 23.5)	3.3 (3.0 - 3.6)	6.7 (6.2 - 7.1)

continued . . .

... continued

Region	Program	Site km	Site	n	TSS (mg L^{-1})	% SuspOC	C/N (molar)
		135.8	NR2	2	21.0 (20.0 - 22.0)	3.3 (3.1 - 3.5)	7.3 (7.3 - 7.4)
		157.6	NR3	2	14.5 (9.3 - 19.8)	7.6 (5.2 - 9.9)	8.8 (8.3 - 9.2)
		213.4	NR6	2	37.0 (32.5 - 41.5)	2.5 (2.4 - 2.7)	8.5 (7.9 - 9.1)
	CAMP	33.9	NR-8	3	20.8 (16.6 - 38.2)	–	–
		55.1	NR-7	3	19.6 (17.6 - 36.6)	–	–
		95.9	NR-6	6	13.8 (9.4 - 14.6)	–	–
		97.4	UHS002	20	14.8 (12.0 - 16.9)	–	–
		106.8	NR-5	6	16.8 (9.5 - 20.5)	–	–
		129.3	UHS003	1	11.0 (n/a)	–	–
		137.2	NR-4	4	11.8 (9.6 - 13.6)	–	–
		138.2	UHS004	8	11.5 (9.2 - 13.3)	–	–
		158.6	NR-3	10	13.7 (11.7 - 14.6)	–	–
	ArcticNet	8.8	B5	2	72.0 (58.5 - 85.5)	1.1 (1.0 - 1.2)	5.8 (5.8 - 5.8)
		13.9	B4	1	29.0 (n/a)	3.0 (n/a)	7.0 (n/a)
	DFO	107.0	Conwapa	18	11.5 (9.5 - 16.5)	4.4 (3.6 - 5.0)	8.5 (7.8 - 9.7)
		126.5	Limestone	19	11.0 (9.0 - 13.0)	4.0 (3.6 - 4.9)	7.4 (6.7 - 8.3)
		159.5	Long Spruce	19	10.0 (9.5 - 11.0)	4.6 (4.0 - 4.6)	7.3 (6.5 - 7.9)
		184.0	Kettle	19	10.0 (9.0 - 12.0)	4.6 (3.8 - 5.1)	6.7 (6.2 - 8.23)
	Baker	29.3	4	1	9.0 (n/a)	5.6 (n/a)	8.3 (n/a)
		34.6	2	1	8.0 (n/a)	6.0 (n/a)	8.0 (n/a)
		35.1	3	1	10.0 (n/a)	5.6 (n/a)	9.3 (n/a)
		42.1	1	1	12.0 (n/a)	6.6 (n/a)	11.1 (n/a)
	MEMP	174.6	Kettle GS	19	9.0 (7.5 - 9.5)	5.7 (4.5 - 7.0)	7.1 (6.2 - 7.4)

As observed in BaySys results, the compiled data set shows a high proportion of SuspOC in TSS in the UNR between the outflow of Lake Winnipeg and Jenpeg GS (Figure 2.9b middle panel). Sites near Kelsey GS in the lower reaches of the UNR also exhibit high % SuspOC of TSS. In the LNR, % SuspOC of TSS is generally low and only increases at point locations near the Limestone GS and in the lower reaches within the length of river ∼60 km upstream of the Nelson River mouth.

When compared to BaySys results, the compiled data set also shows molar C/N ratios in the UNR predominantly in the lacustrine algae source range (4 - 10) (Figure 2.9b bottom panel). Median (interquartile range) ratios range between 5.5 and 8.1 (7.4 to 8.6) at sites except Kelsey GS, at which C/N values fall within the SOM range with a median (interquartile range) ratio of 10.8 (9.3 to 11.8). In the LNR, molar C/N ratios at most sites are within the lacustrine algae source range. Point locations upstream of Stephens Lake, downstream of the Limestone GS, and in the lower reaches of the Nelson River exhibit molar C/N ratios typical of both SOM and lacustrine algae source ranges.

2.3.2.2 Rat-Burntwood River

Similar to BaySys results in the Section 2.3.1.2, TSS concentration is low in the RBR between Notigi Lake and Wuskwatim GS (Figure 2.10b top panel). The compiled data set also shows a large step-wise increase in TSS between Wuskwatim GS and the inflow of Split Lake, with concentrations comparatively higher than all other regions of the study area.

The compiled data set shows a higher % SuspOC of TSS in the upper reaches of the RBR compared to the length of river between Wuskwatim GS and the inflow of Split Lake (Figure 2.10b middle panel). These step-wise changes are also observed in the BaySys data.

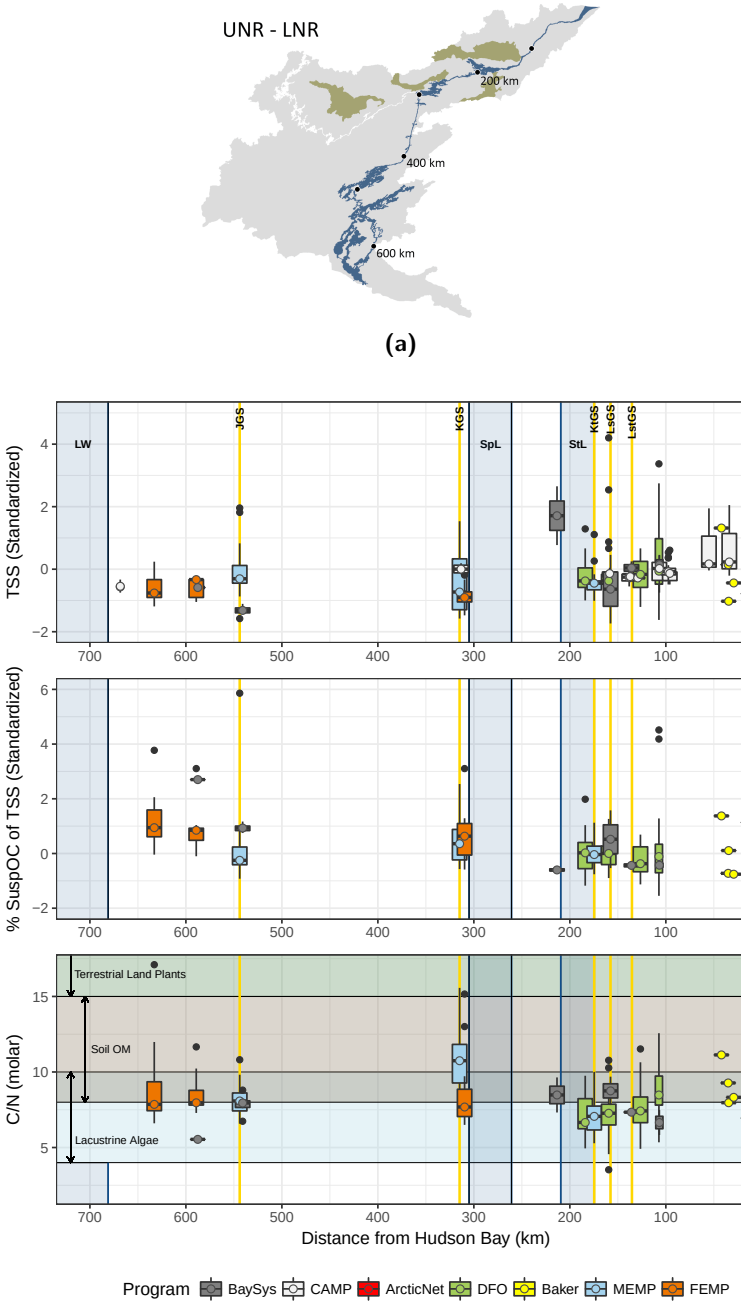

Fig. 2.9: **2.9a**: Map showing distance (km) on x-axis in Figure 2.9b; tributary watersheds shown in green. **2.9b**: Standardized TSS concentration and % SuspOC of TSS, and molar C/N ratios in the UNR and LNR from all sampling programs arranged longitudinally. Key hydraulic features are labeled. LW: Lake Winnipeg, JGS: Jenpeg GS, KGS: Kettle GS, SpL: Split Lake, StL: Stephens Lake, KtGS: Kettle GS, LsGS: Long Spruce GS, LstGS: Limestone GS

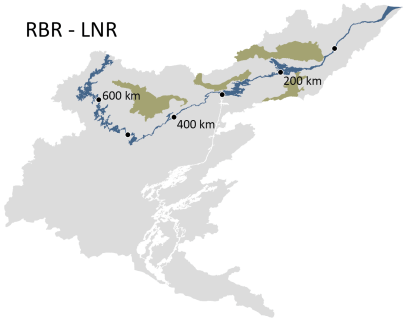

(a)

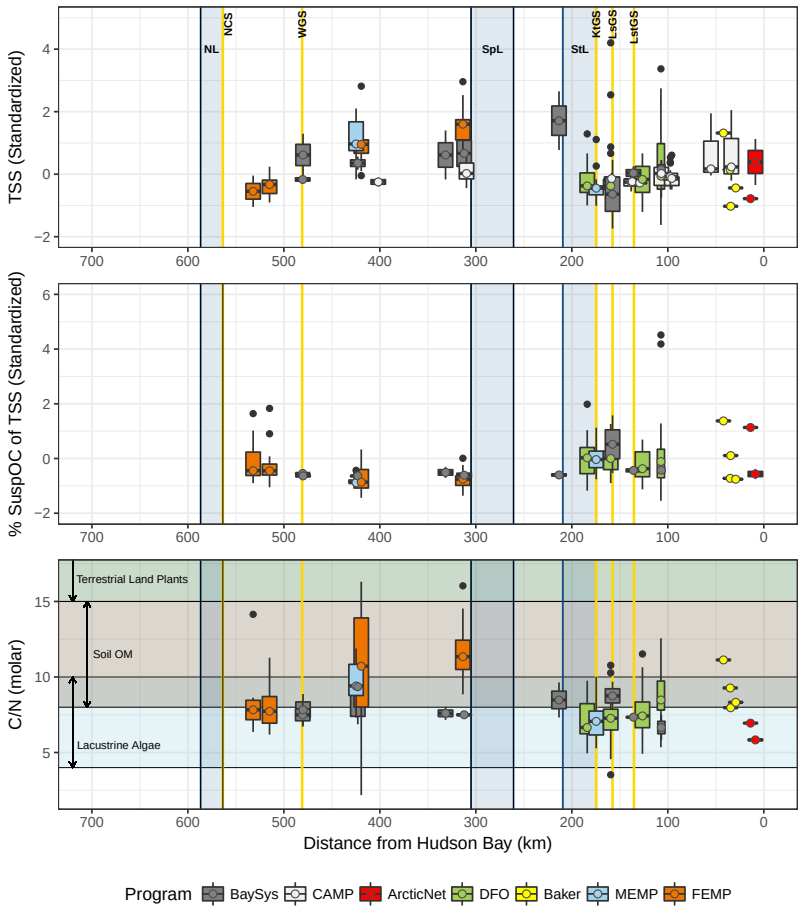

(b)

Fig. 2.10: 2.10a: Map showing river length on x-axis in Figure 2.10b; tributary watersheds shown in green. **2.10b**: Standardized TSS concentration and % SuspOC of TSS, and molar C/N ratios in the RBR and LNR from all sampling programs arranged longitudinally. Key hydraulic features are labeled. NCS: Notigi CS, WGS: Wuskwatim GS, SpL: Split Lake, StL: Stephens Lake, KtGS: Kettle GS, LsGS: Long Spruce GS, LstGS: Limestone GS.

In the RBR, molar C/N ratios are within both the lacustrine algae source (4 - 10) and SOM source (8 - 15) ranges (Figure 2.10b bottom panel). Upstream and immediately downstream of Wuskwatim GS, median (interquartile range) ratios range between 7.5 (7.1 to 7.9) and 7.8 (7.2 to 8.5), indicative of lacustrine algae sources. Between the city of Thompson and the inflow to Split Lake, most sites fall within the SOM source range with median ratios range between 9.4 (7.4 to 9.9) and 11.4 (10.5 to 12.4).

2.3.2.3 Regional analysis

Results from the BaySys program show a distinct regional and longitudinal difference in water quality parameters and particulate OM sources among the three regions of the Nelson River system. Sample site density is greatly improved with addition of results from other monitoring programs, and therefore a comparison is made in this section using the compiled data set to see if results observed from the BaySys program are supported by the addition of data from other monitoring programs. Because each program occurred over the course of many years under different climatic and discharge conditions, regional analysis of the compiled data set will only include standardized values of each water quality parameter. Therefore, differences or similarities between or within regions are based on visual plots instead of quantitative values. To address the time span over which of monitoring programs operated in the study area, the temporal analysis of water quality parameters is explored in Section 2.4.2.

When comparing each parameter by region using the compiled data set, the results are similar to those from the BaySys program. TSS concentration is highest in the RBR, lowest in the UNR, and at a mid range between the two contributing catchments in the LNR (Figure 2.11a). The UNR exhibits the highest % SuspOC of TSS compared to all other regions, whereas the % SuspOC of TSS is lowest in the RBR. Similar to TSS concentration,

the LNR varies in % SuspOC of TSS with values at a mid-range between the upstream catchments. Molar C/N ratios in each region are similar to those defined in the BaySys program but have shifted slightly due to the addition of key sites that show variation in OM sources compared to the rest of the region. Particulate OM in the UNR is dominantly sourced from lacustrine algae with a median (interquartile range) regional ratio of 8.09 (7.43 to 9.92). However, molar C/N ratios in the BaySys results are lower that those from the compiled data set in the UNR due to the addition of samples from the Kelsey GS, which contained OM sourced from SOM (Figure 2.10b bottom panel). The RBR exhibits a median molar C/N ratio of 8.79 (7.42 to 10.83), indicating a dominant SOM source. Notably lower C/N ratios are observed in the LNR with a regional C/N ratio of 7.39 (6.49 to 8.50) indicative of a dominantly lacustrine algae source. This region exhibits outliers with much higher ratios (in the range of SOM and terrestrial land plants) and since many of the samples from the LNR in the compiled data set were collected at generating stations using reservoir water from intake lines, it is likely these samples contain OM sourced from algal activity in the reservoir, lowering the median regional C/N ratio.

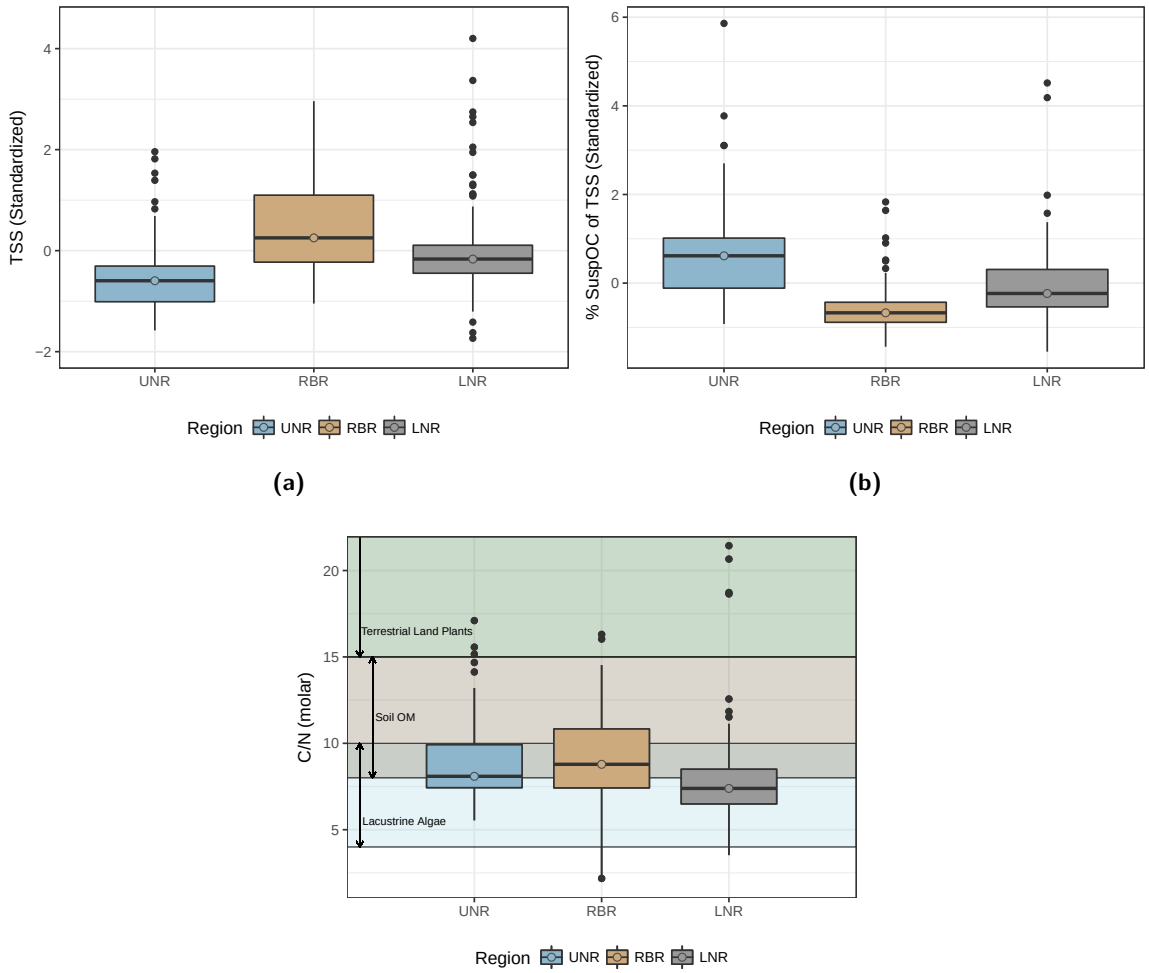

Fig. 2.11: Regional median and quartile summary boxplots of water quality parameters for all monitoring programs. **2.11a**: Standardized TSS concentration in $\mathrm{mg\,L^{-1}}$ by study area region. **2.11b**: Standardized % SuspOC of TSS by study area region. **2.11c**: Molar C/N ratios by study area region.

2.4 Discussion

2.4.1 Drivers of longitudinal variability in the Nelson River system

Results from the BaySys program, supplemented by compiled results from other monitoring programs, show distinct regional and longitudinal differences in water quality parameters and particulate OM sources between all three regions of the Nelson River system. These can be explained by past or ongoing physical and chemical processes occurring within each region of the study area.

2.4.1.1 Upper Nelson River

Among the three regions examined, the UNR stands out as having the lowest TSS concentration, highest proportion of SuspOC in TSS, and C/N ratios within the lacustrine algae source range (Figure 2.5b). Based on this bulk characterization and the location of BaySys sites, it is likely that particulate OM in sampled riverine waters of the UNR is heavily influenced by algal activity in Lake Winnipeg (∼150 km upstream), which has seen increased algal productivity in the lake as a whole since the 1990s (McCullough et al., 2012; Lake Winnipeg Stewardship Board, 2007). The upper reaches of the UNR has also seen increased bank instability, slumping, and erosion in the outlet lakes region[2] of Lake Winnipeg (e.g. on the north shore of Lake Winnipeg, in the newly constructed outlet channels, and in Playgreen Lake). This comes as a result of Lake Winnipeg Regulation from 1970-1976 (Baker & Davies, 1989, 1991; Environment Canada and Department of Fisheries and Oceans, 1992c). Although banks in these regions are still actively contributing suspended sediment to the system, a recent sediment fingerprinting study investigating water quality at Norway House determined that most of the total suspended sediment in

[2]Outlet Lakes Region Waterbodies: Playgreen Lake, Little Playgreen Lake, Kiskittogisu Lake, Kiskitto Lake, and the Nelson River above Jenpeg GS

the main-stem Nelson River downstream of Lake Winnipeg is sourced from the natural outlet (Theroux, 2017). The relatively low TSS concentrations, as well as high % SuspOC of TSS and C/N ratios that lie within the lacustrine algae range at BaySys UNR sites, align well with these findings and suggest that suspended sediment generated by erosive processes in the outlet lakes region of the UNR is deposited relatively proximal to its source.

Samples from other monitoring programs provide improved coverage of various lengths of the UNR, particularly at and just upstream of the Kelsey GS. These sites show low TSS concentration and high % SuspOC of TSS similar to the BaySys sites, but higher C/N ratios (in the SOM source range) compared to the upper reaches of the UNR where ratios are dominantly in the lacustrine algae source range.

2.4.1.2 Rat-Burntwood River

Within areas of the RBR sampled during the BaySys program, the influence of several sources and processes is observed. In the upper reaches of the RBR at Notigi Lake (site BR6), TSS concentration is low, % SuspOC in TSS is high, and C/N ratios are typical of SOM sources (Figure 2.6b). Conditions in this section of the RBR are very different from those downstream. Notigi Lake was transformed into a hydroelectric reservoir and major sediment sink for diverted Churchill River waters from Southern Indian Lake in 1976 (Northwest Hydraulic Consultants Ltd., 1987). The construction of the Notigi CS expanded the lake from 15.1 km^2 to 584 km^2 and in the process flooded upstream wetlands (Newbury et al., 1984; Environment Canada and Department of Fisheries and Oceans, 1992b). Based on water quality results and wave-driven shoreline erosion observed during field investigations in 2016, Notigi Lake acts as a sink for sediments. TSS concentrations are low, and, based on % SuspOC and C/N ratios, the lake is subjected to the ongoing addition of terrestrial OM sources since the reservoir was created.

Between Wuskwatim GS and Split Lake, TSS concentration is high whereas % SuspOC in TSS is low and nearly the same at all sites. Therefore, it is likely any change to TSS concentration in this portion of the RBR is due to an increased input of mineral sediment. As a result of the Churchill River Diversion, increased discharge (10 times natural discharge rates) to the RBR had a generally destabilizing effect on lake shores and river banks in the region as a whole (Northwest Hydraulic Consultants Ltd., 1988). Kellerhals Engineering Services Ltd. (1987), Kellerhals Engineering Services Ltd. (1988), Northwest Hydraulic Consultants Ltd. (1988), and Manitoba Hydro (1991) all reported numerous sites of increased bank erosion in the RBR between Thompson and Split Lake, especially at bedrock-bound rapids. Recent air photo and erosion monitoring studies also indicate that shoreline erosion continues to persist throughout the region (Manitoba Hydro, 2015). At First Rapids on the RBR, upstream of the confluence of the Odei River, river banks have been eroded due to ongoing permafrost degradation (Manitoba Hydro, 1991). Although this section of river was not visited during 2016/2017 field investigations or sampled during this study, bank erosion in some capacity (sloughing, slumping, wave action, or complete bank failure) was observed at all other RBR sites (Figure 2.12a and 2.12b). Based on TSS concentration in this section of the RBR, it is reasonable to conclude that river bank erosion is an ongoing issue. The high suspended sediment load in the RBR is notably different from that of the UNR, and is easily visible in aerial images (Figure 2.13a) where a light brown-coloured plume extends from the RBR mouth along the northern margins of Split Lake. Furthermore, C/N ratios in this section of the RBR predominantly fall within the SOM source range. This aligns well with processes such as bank slumping or failure that would allow for the addition of SOM which were observed both during field investigations in 2016/2017, and reported on by workers (Kellerhals Engineering Services Ltd., 1987, 1988; Northwest Hydraulic Consultants Ltd., 1988; Manitoba Hydro, 1991).

Destabilization of banks due to permafrost degradation has been observed in many

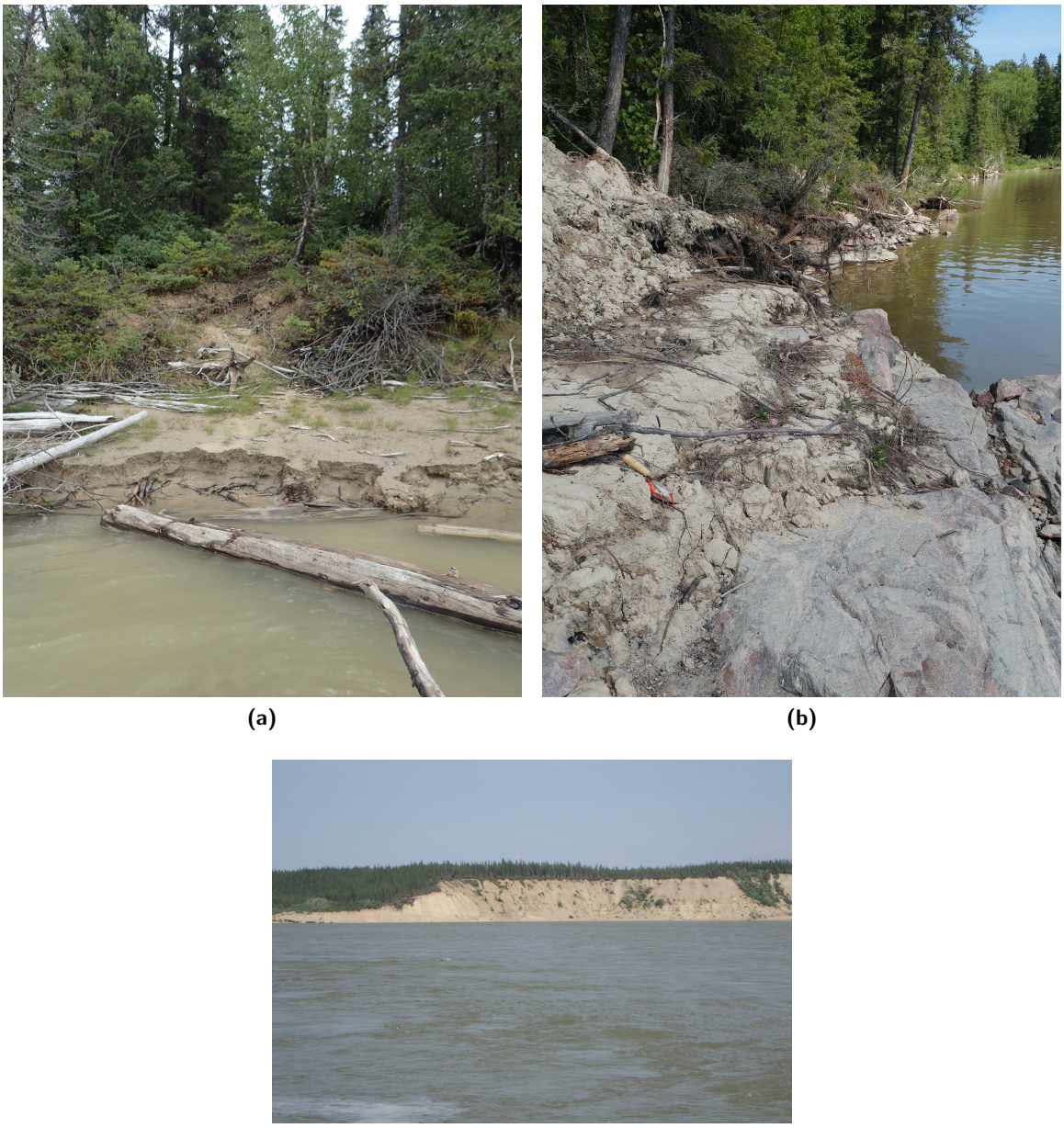

(a) **(b)**

(c)

Fig. 2.12: Field images of river bank morphology in the RBR and LNR. **2.12a**: Scalloped erosion of fine sand- to silt/clay-sized overbank deposits at site BR1. **2.12b**: Erosion (sloughing and bank failure) of river bank comprised of vegetated till deposits on top of bedrock at Site BR2. **2.12c**: South bank of the LNR at site NR1 showing terrestrial material falling from the top of ∼25 m high bluffs (incised glacial deposits). Erosion site locations are shown in Figure 2.2.

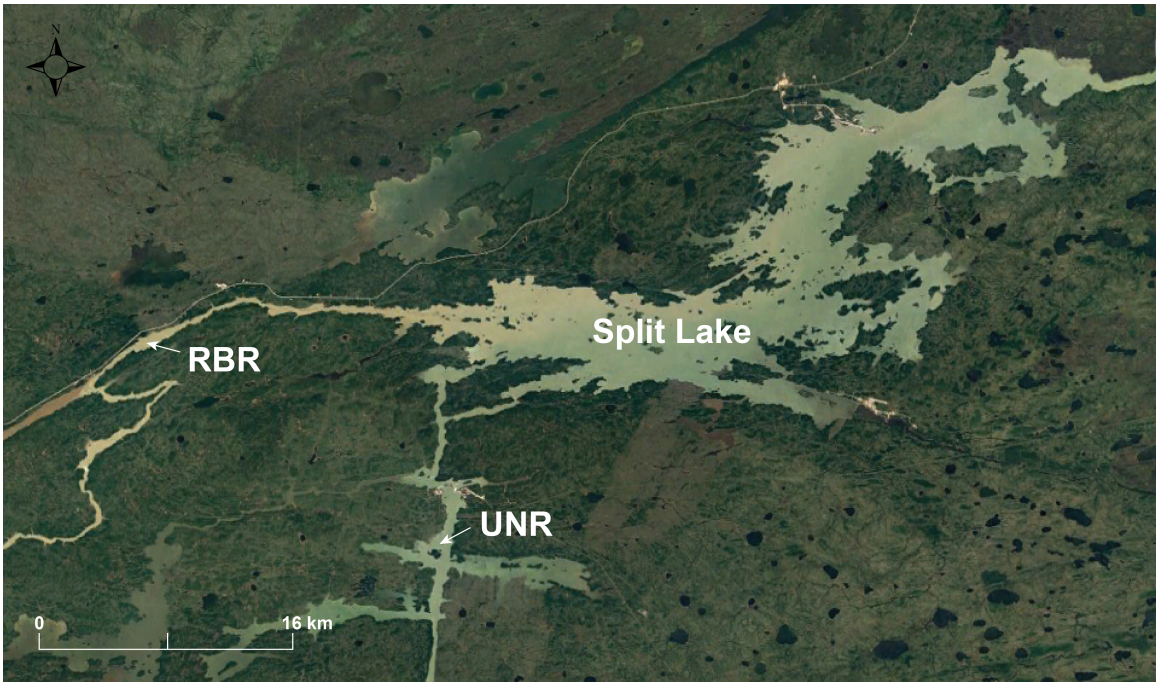

(a)

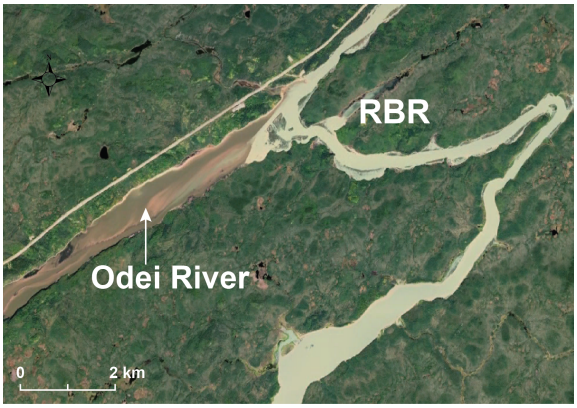

(b)

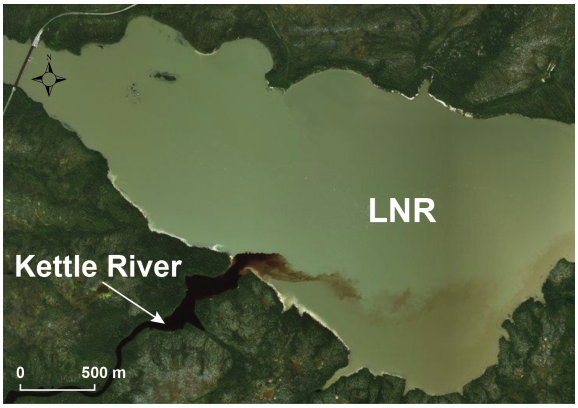

(c)

Fig. 2.13: Aerial images (sourced from Google Earth on September 15, 2018) from the study area showing contrasts in suspended load between water bodies. **2.13a**: Aerial image showing the convergence of the RBR and UNR into Split Lake. Turbid water from the RBR is light brown, whereas water from the UNR is light green-blue. **2.13b**: Confluence of the Odei River into the RBR. **2.13c**: Kettle River flowing into the LNR.

localities in the RBR (Greg McCullough, personal communication, September 2018). Due to the prevalence of permafrost-affected glacial till surrounding many waterbodies in the Nelson River system, shorelines of waterbodies altered by hydroelectric development can take years to restabilize (Newbury & McCullough, 1984). Workers have observed visible lenses of ice in clay banks at both Southern Indian Lake and Wuskwatim Lake that form soupy, readily erodible material at their margins (Greg McCullough, personal communication, September 2018). Tributaries flowing to this region, such as the Odei River, notably exhibit high particulate loads with dominantly SOM sources compared to tributaries in the LNR. This suggests that permafrost degradation also affects water bodies unaffected by hydrological alteration in the region, and therefore is likely exacerbated by processes related to both anthropogenic and climatic changes to the river system, working in a positive feedback loop.

Increased site density from the compiled data set confirms BaySys results throughout the RBR in general, where TSS is high, % SuspOC of TSS is low, and molar C/N ratios mainly in the SOM source range (Figure 2.10b).

2.4.1.3 Lower Nelson River

In the LNR, TSS concentration is very high upstream of Stephens Lake at site NR6 compared to the rest of the region (Figure 2.5b). Low % SuspOC in TSS, and a C/N ratio typical of SOM at this site indicates that higher TSS concentration upstream of Stephens Lake is due to either increased upstream or local mineral sediment sources. This could be linked to several natural rapids that are present in this stretch of the river, since as seen in the RBR, these sites are particularly susceptible to bank destabilization.

Downstream of the inflow of Stephens Lake, TSS concentration and % SuspOC in TSS remain relatively uniform, but sources of carbon vary in composition in relation to water-

body morphology. This section of the LNR contains three hydroelectric dams separated by an expansive reservoir, and lengths of river that have been impounded into dam forebays. Natural river banks are present downstream of the Limestone GS. In Stephens Lake, the range in molar C/N ratios can be explained by its current and historical morphology. Stephens Lake was created by flooding over 220 km^2 of land upstream of the Kettle GS to form a hydroelectric power reservoir with water levels ~31.5 m higher than natural conditions (North/South Consultants Inc., 2012). Particulate OM in Stephens Lake is sourced from both lacustrine algae and SOM. As a large reservoir, it supports algal growth and activity but due to its history as an impounded waterbody, it also receives terrestrial OM as a result of shoreline erosion and peatland disintegration. Cosford et al. (2013) and J.D. Mollard and Associated (2010) Limited (2009) characterized nearshore sedimentation processes in Stephens Lake since its impoundment and described a complex sedimentation history that typically occurs in three phases: 1) erosion and deposition of poorly sorted detrital organic material such as peat, soil, and forest floor, 2) erosion and deposition of both organic- and mineral-rich sediment, and 3) erosion and deposition of predominantly mineral sediment. Although slowed, many of these processes still occur at Stephens Lake. Banks on the south shore of Stephens Lake containing buried layers of organic soil were seen slumping and sloughing into the water during 2016/2017 fieldwork, transferring both mineral sediment and organic material from the banks into the waterbody.

Downstream of Stephens Lake, particulate matter at all sites exhibits near uniform characteristics, except site NR3, which is similar to tributaries flowing into the LNR. Samples at NR3 were collected on the Nelson River downstream of a tributary confluence, and are evidently influenced by tributary waters based on TSS concentration, % SuspOC and C/N ratio. C/N ratios at sites NR2 and NR1 are lower than what would be expected for riverine sites, but could be explained by increased algal productivity in the Limestone GS forebay.

The compiled data set from previous programs adds many sites in the lower reaches of the LNR, downstream of BaySys sites. In the lower ∼100 km of the LNR, water quality parameter characteristics are variable. TSS concentration and % SuspOC of TSS fluctuate depending on the site. These parameters were explored as part of a Nelson River estuary study by Baker et al. (1993) which determined that TSS concentration showed a step-wise increase to Port Nelson, whereas particulate carbon generally decreased over the same area. This aligns somewhat with the results of the compiled data set since TSS in this portion of the river is generally higher than near the generating stations. Variation in % SuspOC of TSS within this region could be correlated either to changes to SuspOC concentration or to the mineral component of suspended sediment at these sites. Which one it is remains unclear since this region was not sampled during this study. High bluffs (up to ∼ 30 m) of glacial material were observed in the lower reaches of the LNR (Figure 2.12c), therefore changes to particulate concentrations and C/N ratios could result from slumping or failure of banks comprised of large volumes of inorganic sediment, or those associated with peatland degradation. Relict OC sources from glaciomarine sediments are another potential source in this region. Molar C/N ratios in the lower reaches of the LNR fall within the SOM source range, which could be linked to tributaries flowing from peatlands in the LNR catchment. Proximal to the river mouth, particulate matter shows algal source ratios that could be influenced by algal productivity in the Nelson River estuary.

2.4.1.4 Tributaries

Particulate matter characteristics in tributaries in the study area vary depending on the region through which they flow. The Odei River in the RBR has much higher TSS and much lower % SuspOC of TSS than tributaries flowing into the LNR (Figure 2.6b, 2.13b, 2.13c). Since all tributaries have molar C/N ratios typical of SOM sources, it is likely that low % SuspOC of TSS observed in the Odei River is not due to a lack of particulate OC

but instead a surplus of suspended mineral sediment (Figure 2.13b); potential causes of this surplus in particulate matter are discussed in Section 2.4.1.2. The Assean, Kettle, and Limestone rivers in the LNR region all have low TSS concentration and high % SuspOC of TSS, probably because they drain vast areas of peatlands (Figure 2.13c).

2.4.2 Temporal analysis of suspended particulate matter in the Nelson River system

Although longitudinal changes to water quality parameters exist and particulate OM sources can be distinguished between regions of the study area, sampling programs included in the compiled data set span ∼30 years and therefore provide an opportunity to investigate temporal changes within the study area. Over this time period, there have been significant changes in mean annual discharge in the some regions (Figure 2.14a). In the UNR and LNR, there is a distinct change in the range of annual discharge rate from $\sim 1200 - 3000\,\mathrm{m^3\,s^{-1}}$ in the mid 1990s to $\sim 2300 - 5000\,\mathrm{m^3\,s^{-1}}$ in the early 2000s (Environment and Climate Change Canada, 2018e, 2018d). The RBR in contrast has had a near constant discharge rate, around $1000\,\mathrm{m^3\,s^{-1}}$ since the Churchill River Diversion in the late 1970s (Environment and Climate Change Canada, 2018f). Mean annual temperature in all regions is low ($-2.66\,^{\circ}\mathrm{C}$) in the time period during which FEMP, MEMP and the Baker monitoring programs were implemented (1987 to 1993), and relatively higher ($-1.72\,^{\circ}\mathrm{C}$) in the time period of the remaining monitoring programs (2005 to 2017) (Figure 2.14b) (Environment and Climate Change Canada, 2018a, 2018b, 2018c).

Even though discharge typically affects fluxes and transport of particulate matter, linear regression models between daily mean discharge and instantaneous TSS and SuspOC concentration at each hydrometric station are not significantly correlated (Figures 2.15a and 2.15b). No statistical relationship exists between these parameters that can be used

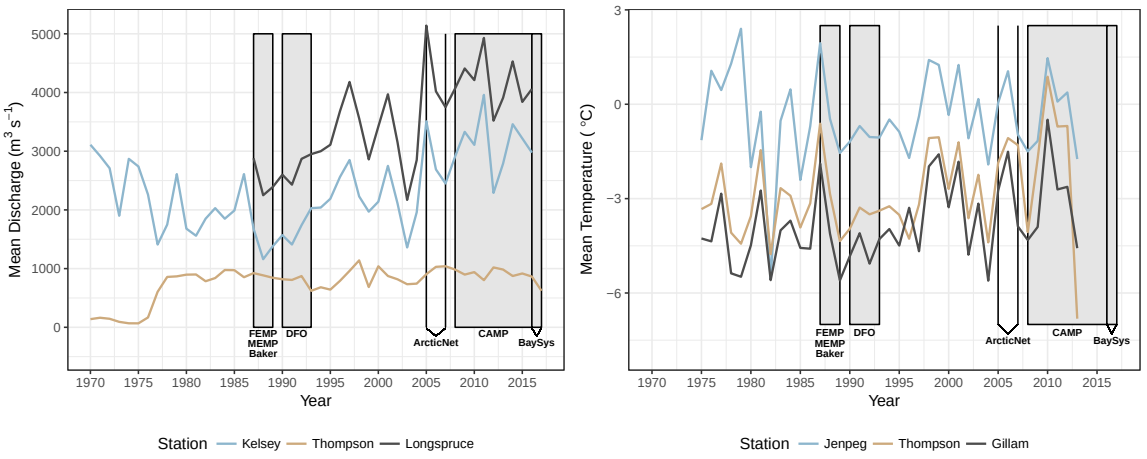

(a) **(b)**

Fig. 2.14: Annual mean discharge and temperature by region of the study area and time periods of each sampling program (Kelsey: UNR, Thompson: RBR, Long Spruce: LNR). **2.14a**: Annual mean discharge since 1961 (Environment and Climate Change Canada, 2018d, 2018e, 2018f). **2.14b**: Annual mean temperature since 1975 (Environment and Climate Change Canada, 2018a, 2018b, 2018c).

to adjust for the influence of discharge on parameter concentrations over the sampling period. Therefore, the effect of discharge on concentration will only be discussed from the perspective of other processes associated with higher or lower discharge rates.

To investigate and summarize temporal variability using raw data from the compiled data set, "dry/cool" (1987 to 1993) and "wet/warm" (2005 to 2017) time periods were designated and compared for all three regions (UNR, RBR, and LNR). Data from the UNR and LNR are graphically summarized by climate period. Parameters from the RBR were plotted year by year because there were generally fewer samples collected between climate periods and discharge in this region varies less compared to the UNR and LNR. ANOVA tests were applied to a log-normalized version of the compiled data set to see if statistically significant differences between each parameter arise between climate periods.

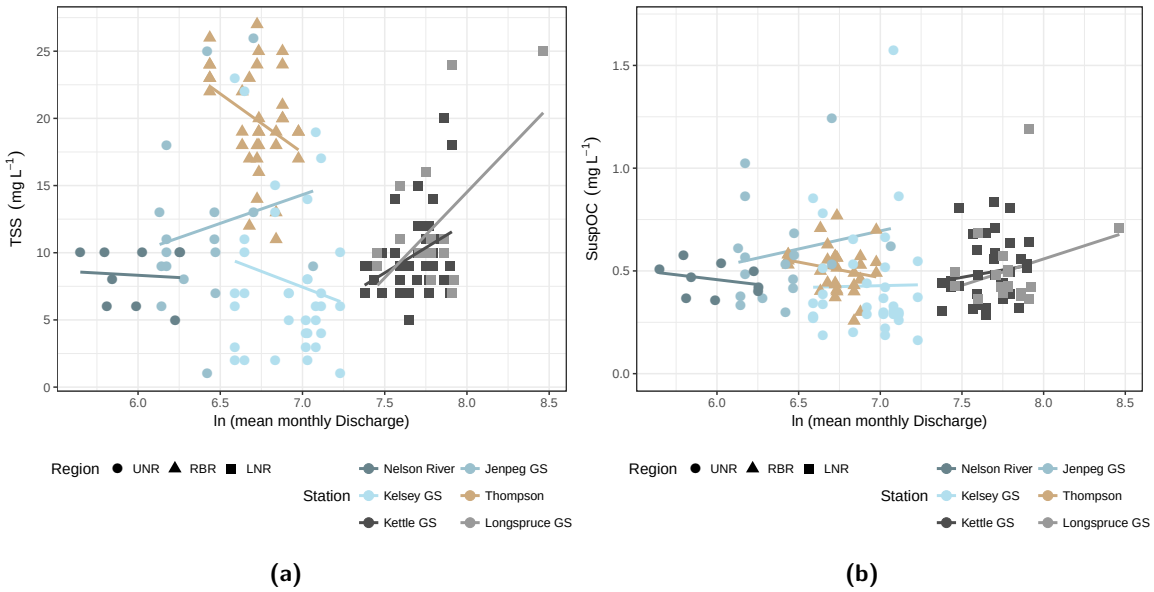

Fig. 2.15: Relationship between discharge and water quality parameters, lines show general trends for each station, but are not statistically significant relationships. **2.15a**: Relationship between the natural log of mean monthly discharge ($\mathrm{m^3\,s^{-1}}$) and TSS concentration ($\mathrm{mg\,L^{-1}}$). **2.15b**: Relationship between the natural log of mean monthly discharge ($\mathrm{m^3\,s^{-1}}$) and SuspOC concentration ($\mathrm{mg\,L^{-1}}$).

2.4.2.1 Temporal changes to particulate matter in all regions

All regions varied in mean summer discharge rates between climate periods, but some changes in discharge are considerably larger than others. In the UNR and LNR, median discharge approximately doubled between the dry/cool and wet/warm time periods increasing from $1190\,\mathrm{m^3\,s^{-1}}$ to $3410\,\mathrm{m^3\,s^{-1}}$ and from $2280\,\mathrm{m^3\,s^{-1}}$ to $4440\,\mathrm{m^3\,s^{-1}}$ respectively (Figure 2.16a). Mean summer discharge in the RBR generally decreased over time within a range between $548\,\mathrm{m^3\,s^{-1}}$ and $1090\,\mathrm{m^3\,s^{-1}}$ but did not change as drastically as in the UNR and LNR (Figure 2.17a).

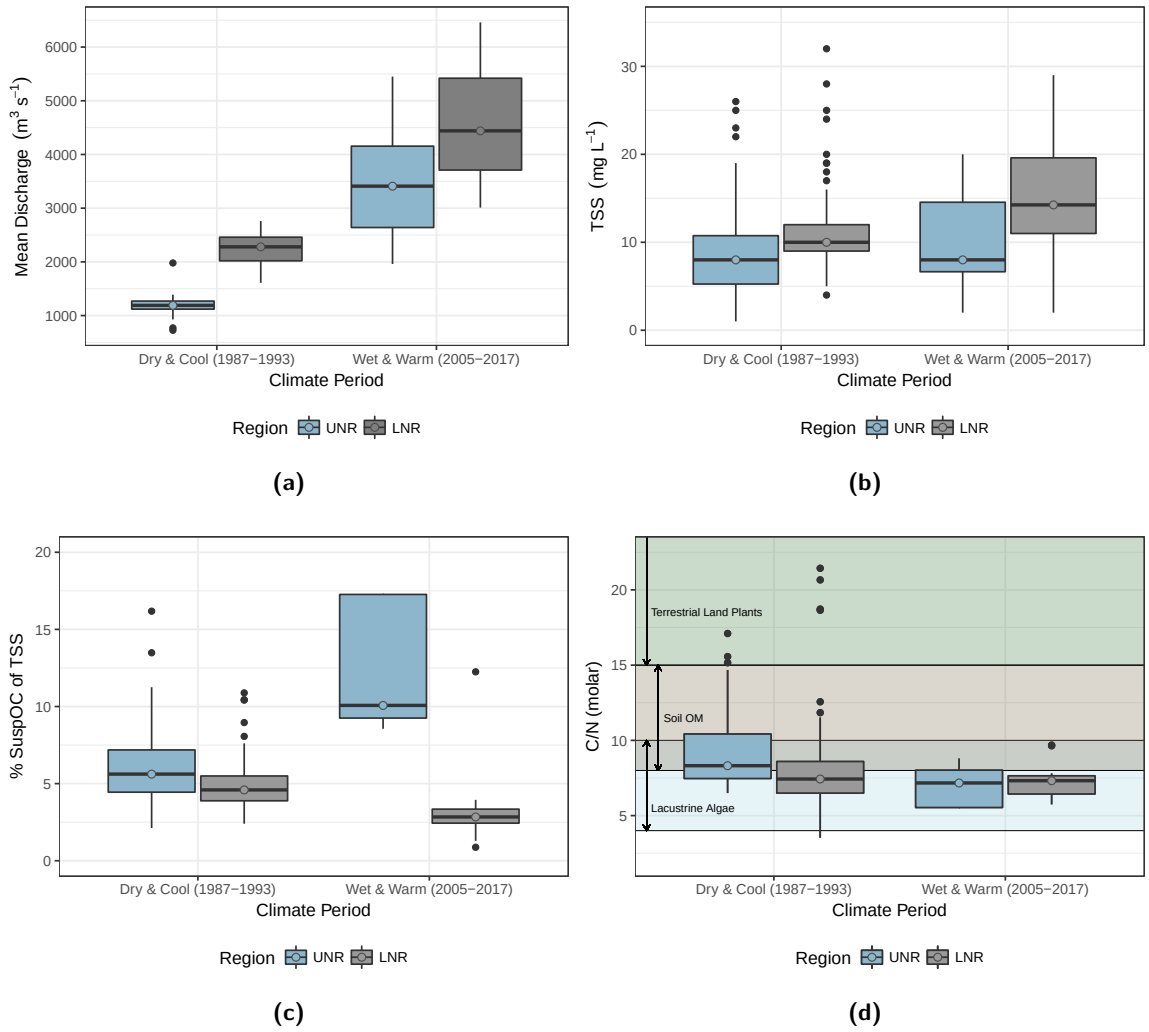

Fig. 2.16: Median and quartile boxplots summarizing discharge and water quality parameters from all sampling programs in the UNR and LNR between climate periods. **2.16a**: Mean summer season discharge ($\mathrm{m^3\,s^{-1}}$). **2.16b**: TSS concentration ($\mathrm{mg\,L^{-1}}$). **2.16c**: % SuspOC of TSS. **2.16d**: Molar C/N.

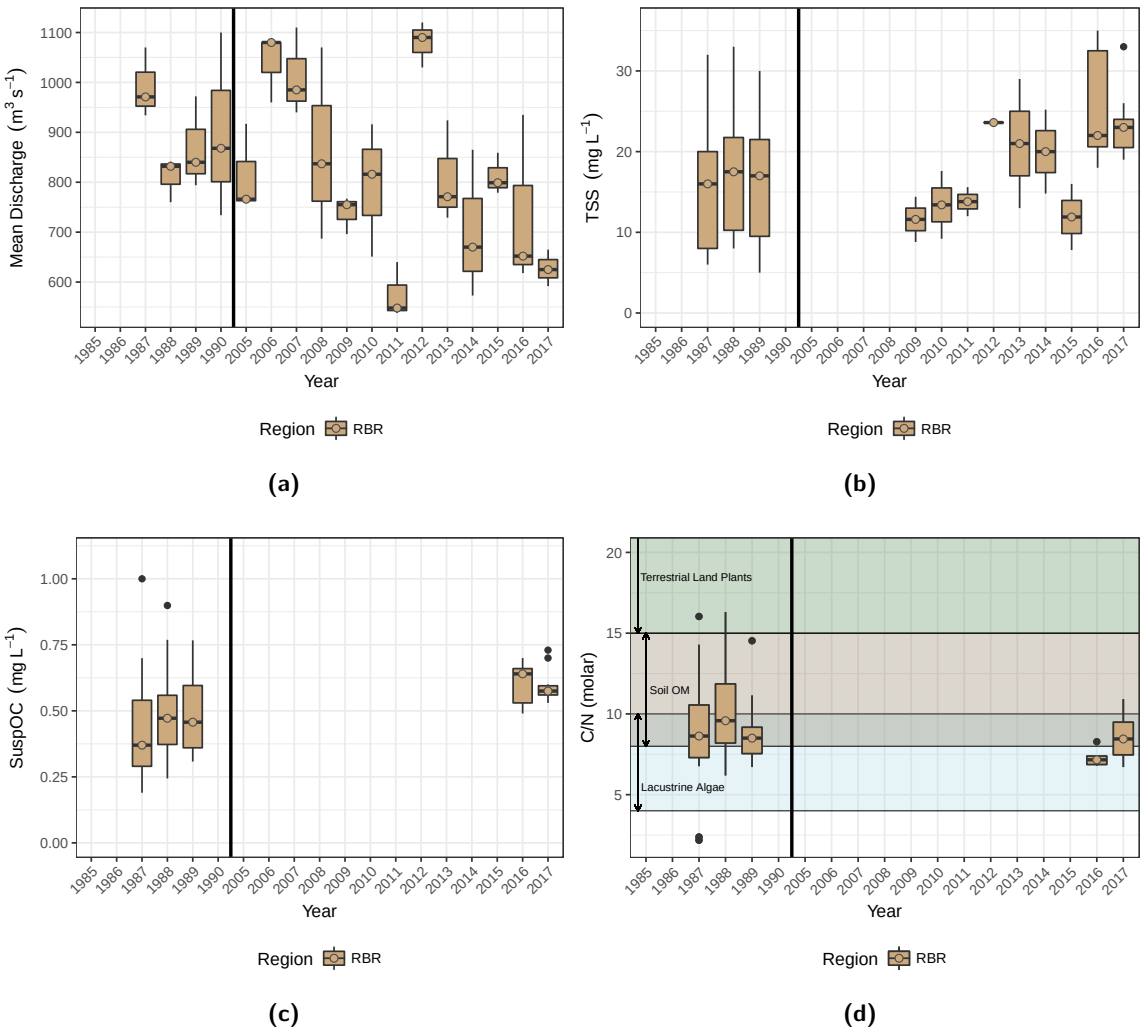

Fig. 2.17: Median and quartile boxplots summarizing water quality parameters from all sampling programs in the RBR between 1986 and 2017. Note the break in time between the late 1990s and early 2000s defined by the vertical black line. **2.17a**: Mean summer season discharge ($m^3 s^{-1}$). **2.17b**: TSS ($mg L^{-1}$). **2.17c**: SuspOC concentration ($mg L^{-1}$). **2.17d**: Molar C/N.

Statistically significant differences between time periods were observed in water quality parameters in each region (Figure 2.16 and 2.17). TSS concentration increased significantly in the RBR and LNR, whereas the proportion of SuspOC in TSS dropped in both the RBR and LNR, but rose significantly in the UNR. SuspOC concentration in the RBR increased significantly even though % SuspOC of TSS decreased between time periods. Molar C/N

ratios only saw significant differences in the UNR, where they decreased between time periods.

Median TSS concentration in the RBR was $\sim$17.0 mg L^{-1} between 1987-1989, but shows more variation between 2009-2017 with median (interquartile range) values ranging from 11.6 mg L^{-1} (10.2 mg L^{-1} to 13.0 mg L^{-1}) to 23.0 mg L^{-1} (20.5 mg L^{-1} to 24.0 mg L^{-1}) (Figure 2.17b). Figure 2.15a shows a negative relationship between discharge and TSS concentration although it is not statistically significant. An ANOVA test revealed TSS concentration is significantly higher ($f = 17.9$, $p < 0.05$, $n = 95$) in later years (2016-2017) even though discharge is generally lower. Since the same length of the RBR was sampled during both time periods, and the analytical methods used to measure TSS concentration are the same for all programs, it is reasonable to infer that median TSS concentration has in fact increased over time in the RBR in spite of an apparent decrease in annual discharge. The high concentration of suspended solids in river waters of the RBR is therefore likely linked, as previously postulated, to erosive processes that do not depend on river discharge or reservoir water level but rather to independent environmental variables such as bank slumping/sloughing/failure and permafrost degradation.

A significant ($f = 24.17$, $p < 0.05$, $n = 170$) increase in TSS concentration is observed between time periods in the LNR with median concentrations rising from 10.0 mg L^{-1} (9.0 mg L^{-1} to 12.0 mg L^{-1}) to 14.25 mg L^{-1} (11.0 mg L^{-1} to 19.6 mg L^{-1}) (Figure 2.16b). Since no significant change to TSS concentration was observed in the UNR, it stands to reason that the increase in TSS can be linked to either added input from the RBR system that has seen rising TSS concentration over time, or proximal processes in the LNR providing more particulate matter input to this region.

A significant change between climate periods in the UNR is observed in the proportion of SuspOC in TSS. A statistically significant ($f = 26.21$, $p < 0.05$, $n = 80$) rise from 6.0 %

(4.5 % to 7.2 %) to 10.1 % (9.3 % to 17.3 %) can possibly be linked to the increase in algal productivity in Lake Winnipeg as a whole during the late 1990s (McCullough et al., 2012) (Figure 2.16c). In the RBR, % SuspOC of TSS shows a statistically significant (f = 5.295, p = 0.02, n = 93) decrease from ∼3 % to less than 3 %. SuspOC concentration, however, increased between time periods (Figure 2.17c), therefore a decrease in % SuspOC of TSS indicates that TSS includes a higher proportion of mineral sediment in the later time period. In the LNR, the median % SuspOC of TSS is significantly different (f = 21.83, p <0.05, n = 109) between between climatic periods, dropping from 4.6 % (3.9 % to 5.5 %) to 2.8 % (2.4 % to 3.4 %) (Figure 2.16c). Although % SuspOC is lower during the wet/warm (2005-2017) time period, TSS concentration increased, indicating that the decrease in % SuspOC is likely linked to an addition of mineral sediment, not necessarily by a decrease in organic loading. Median SuspOC concentration in the RBR is below 0.5 mg L^{-1} in the dry/cool time period, but is higher in wet/warm time period with median values up to 0.6 mg L^{-1} (0.5 mg L^{-1} to 0.7 mg L^{-1}) (Figure 2.17c). Like TSS, Figure 2.15b shows an apparent, although not statistically significant, relationship between instantaneous SuspOC concentration and discharge. This relationship appears to occur over time in the RBR as well. An ANOVA test revealed that SuspOC concentration is significantly higher (f = 11.4, p <0.05, n = 93) in later years even though discharge is generally lower. As with TSS, the increase in SuspOC concentration could also be linked to erosive processes independent of discharge and water level that deliver terrestrial OM into river waters of the RBR.

Median molar C/N ratios in the UNR decrease significantly (f = 10.64, p <0.05, n = 80) from 8.3 (7.5 to 10.4) in 1987-1993 to 7.2 (5.5 to 8.0) in 2005-2017 (Figure 2.16d). This, paired with the increase in % SuspOC between climatic periods, indicates an increasing dominance of lacustrine algae source of particulate OM in the UNR as a result of algal productivity in Lake Winnipeg. No statistically significant difference in C/N ratios exists between time periods in the RBR and LNR indicating that sources to particulate OM in

these regions have not changed significantly over time (Figure 2.16d and 2.17d).

In summary, the UNR saw an increase in discharge between climatic periods and statistically significant changes to % SuspOC of TSS and C/N ratios. The dominant source of particulate OM in the UNR was lacustrine algae in both climate periods. This is supported by an increase in algal productivity in Lake Winnipeg in the late 1990s that lowered C/N ratios. TSS concentration did not significantly change between climate periods. A relative decrease in discharge over time coupled with an increase in TSS and SuspOC concentration, and decrease in % SuspOC of TSS over time indicates that particulate matter is likely entering the RBR system by erosive processes that occur independent of discharge and water level fluctuations. Similar observations were made during BaySys field seasons when active shoreline erosion was observed at sites BR1 and BR2 in the lower reaches of the Rat-Burntwood River (Figure 2.12). Fine-grained (fine sand to silt and clay-sized) overbank deposits are scalloped and slumping into the RBR immediately upstream of Split Lake (Figure 2.12a) and farther upstream, surficial materials capped with vegetation were observed cutting back toward the shoreline after being removed from bedrock shorelines (Figure 2.12b). Molar C/N ratios remain nearly uniform over time, indicating that the SOM source has not changed between sampling periods. Along with an increase in discharge between dry/cool and wet/warm time periods in the LNR, a significant increase in TSS concentration and decrease in % SuspOC of TSS occurred. It is tempting to relate an increase in TSS to the increase in discharge observed between time periods, but since these parameters are not directly correlated, it is likely that higher concentrations of particulate parameters are linked to higher erosion rates in both the RBR and LNR. Molar C/N ratios, on the border of both SOM and lacustrine algae sources, are similar in both climate periods indicating that source types in the LNR have not changed over time.

2.4.2.2 Implication for sediment and organic matter supply to Hudson Bay

Mean summer season fluxes were calculated at Longspruce GS in the LNR using concentrations of TSS and SuspOC. Due to the lack of new data collected in the LNR, a comparison can only be made between flux calculations in the dry/cool (1987-1993) time period from this study and other particulate fluxes calculated at the Nelson River mouth in recent years. Mean summer fluxes of TSS and SuspOC between 1987-1993 were $870\,\mathrm{Gg\,yr^{-1}}$ (n=10, se=96.6) and $39\,\mathrm{Gg\,yr^{-1}}$ (n=10, se=4.9) respectively. RSW-Environment Illimite Inc. (2014) calculated a TSS flux of $\sim$1800 $\mathrm{Gg\,yr^{-1}}$, whereas Godin (2014) reported an annual SuspOC flux of $53\,\mathrm{Gg\,yr^{-1}}$. Although it is not possible to directly compare mean summer and annual fluxes, fluxes calculated with the compiled data set can inform upon seasonal delivery of each particulate parameter. These flux rates indicate a likelihood that the bulk of SuspOC is delivered from the Nelson River to Hudson Bay during the summer months. TSS concentration, however, does not vary much between seasons indicating that although in natural systems TSS concentration would be lower during winter months, this does not appear to be the case in the Nelson River.

In the LNR, OM is derived from both lacustrine algae and SOM sources. The river delivers OM to the coastal carbon cycle in Hudson Bay that is both labile and recalcitrant, allowing for both the immediate and prolonged breakdown of terrestrial OM in the coastal zone.

2.5 Conclusions

There are different controls on the amount and composition of particulate OM contributing to the lower Nelson River from its upstream catchments.

The UNR represents a dominantly lacustrine source that has fairly low concentration of

TSS with a high proportion of SuspOC that has increased over time as a result of increased algal productivity in Lake Winnipeg. The RBR contributes dominantly mineral sediment and OM associated with soils, as exemplified by high TSS concentration in the region that have increased between sampling periods. The proportion of SuspOC in TSS is generally low in the RBR even though there are abundant lakes on the river system. In the LNR, the signals from the RBR and UNR become less distinct since the reservoirs around dams dominate the trends associated with each contributing catchment.

Although the UNR delivers 75% of the flow to the LNR, lacustrine OM sourced from this region does not persist downstream to the LNR. There are limitations to using compositional tracers such as C/N ratios because they only deliver a bulk source representation and do not account for mixed source signals. This makes it difficult to distinguish sources in the LNR, however, the increase in TSS and increase in % SuspOC of TSS in the RBR over time is represented by similar changes in the LNR. Further delineating the proportional contributions of particulate OM from each system is the goal of the second objective of this Masters thesis and will be explored further in Chapter 3.

Chapter 3

Compound-Specific Stable Isotope (CSSI) fingerprinting of particulate organic matter in the Nelson River system

3.1 Introduction

Rivers play a key role in the transport of sediment and organic matter (OM) from the continental land mass to the world's coastal zones (Battin et al., 2008; Aufdenkampe et al., 2011; Bianchi, 2011). Particulate OM in rivers is sourced from allochthonous OM (e.g. soil organic matter (SOM) and plant debris) and autochthonous in-stream OM (e.g. macrophytes, algae, and phytoplankton) (Ittekkot & Laane, 1991). It can also be produced in-situ by physico-chemical and biological processes acting on dissolved OM (Ittekkot & Laane, 1991). Carbon is a major constituent of OM and the quantity and form of organic

carbon (OC) derived from OM discharged by rivers influences its fate in coastal waters. Organic carbon can undergo burial or be mineralized to dissolved inorganic carbon in the coastal zone, which affects the pH and trophic status of coastal waters and how the coastal ocean as a whole behaves as either a sink for CO_2 or as a source of CO_2 to the atmosphere. It is prudent to study OM sources in watersheds that contribute terrestrial OC to the coastal zone as well as watershed processes that may affect the form and magnitude in which OC is delivered to the ocean because estuarine zones and continental shelves have recently been shown to be significant sources of CO_2 to the atmosphere (Cole et al., 2007; Cai, 2011).

Subarctic river basins typically sequester OC in perennially frozen soils and areas of extensive peatlands and are particularly susceptible to processes that alter delivery of OC to the coastal ocean. Increasing temperatures in subarctic drainage basins (Arctic Climate Impact Assessment, 2005) and altered hydrology due to erosion and thawing of permafrost (Romanovsky et al., 2017) could result in the mobilization of previously stored OC associated with SOM and peatlands into rivers (Guo et al., 2007; Gustafsson et al., 2011; Vonk et al., 2013; Vonk & Gustafsson, 2013), and therefore contribute more OC to the coastal carbon cycle.

The Nelson River is a subarctic river in Manitoba, Canada with a watershed exceeding $>1\,000\,000\,km^2$ and is the largest river discharging to Hudson Bay (Figure 3.1). It is a major source of terrestrial OC to the costal zone (Godin et al., 2017) and its watershed comprises physically distinct subcatchments that are all impacted by hydroelectric development as well as anthropogenic-driven climatic change. Waters in the Nelson River system flow through river channels, lake basins, and hydroelectric reservoirs, therefore, the mainstem of the river exhibits longitudinal complexity.

The Nelson River system has been studied extensively by industry, government agen-

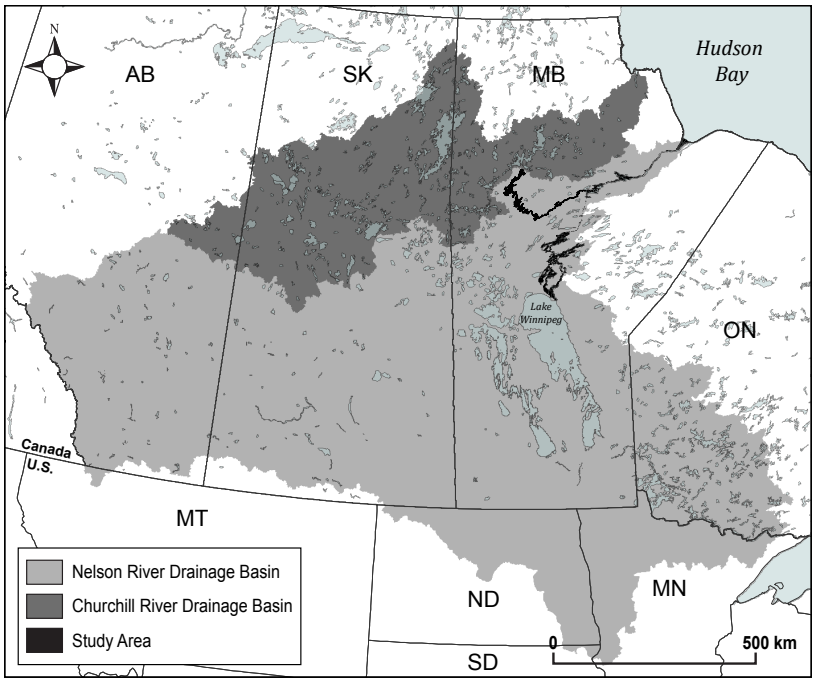

Fig. 3.1: Map showing the extent of the Nelson and Churchill River Drainage Basins in central Canada and northern United States. Study area water bodies are outlined in black.

cies, and academic institutions since the beginning of hydroelectric development in the region (Newbury et al., 1984; Newbury & McCullough, 1984; Hecky & McCullough, 1984; Strange, 1990; Green, 1990; Environment Canada and Department of Fisheries and Oceans, 1992a, 1992c, 1992b; Split Lake Cree and Manitoba Hydro, 1996; Déry et al., 2005; Kirk & St. Louis, 2009; Kuzyk et al., 2009; North/South Consultants Inc., 2012; Coordinated Aquatic Monitoring Program, 2014; RSW-Environment Illimite Inc., 2014; Manitoba Hydro, 2015; Theroux, 2017; Duboc et al., 2017; Godin et al., 2017). Although many of these programs measured parameters related to OM within the Nelson River system, and workers like Godin et al. (2017) have calculated OC flux contributions from the Nelson River to Hudson Bay, little work has been done to investigate terrestrial and in-stream OM sources using compositional, biochemical, and isotopic tracers or to determine the extent that OM sources from the watershed are transported downstream.

In this work, Compound-Specific Stable Isotope (CSSI) analysis of fatty acids is used on terrestrial and in-stream samples collected in 2016-2017 to identify and characterize OM sources and quantify their relative contributions to downstream total suspended sediment that ultimately enters into Hudson Bay. The biochemical and isotopic composition of OM in the Nelson River system shows variation between region and substrate type, and these characteristics are utilized to create Bayesian statistical unmixing model frameworks for use in MixSIAR, an open-source R package. By using CSSI fingerprinting techniques that define sources in downstream suspended sediment mixtures, and employing unmixing models to determine the dominant sources of OM to downstream suspended sediment, we can obtain insight into regions that may contribute more OM downstream to the coastal zone of Hudson Bay and help define regions for future study.

3.1.1 Study area description

The Nelson River in Manitoba is the single largest river discharging to Hudson Bay, at a mean annual rate (1987-2017) of $110\,\mathrm{km^3 yr^{-1}}$ (Environment and Climate Change Canada, 2018d, 2018e, 2018f). Its local watershed extends over $91\,000\,\mathrm{km^2}$ in north central Manitoba to the southwest of Hudson Bay, and its $>1\,000\,000\,\mathrm{km^2}$ drainage basin ranges as far as Minnesota and South Dakota in the south, the Alberta in the west, and Ontario near Lake Superior in the east (Figure 3.1).

As a result of hydrological alteration for hydroelectric power development, the lower Nelson River (LNR) between Split Lake and Hudson Bay receives water primarily from two physically distinct catchments: 1) the upper Nelson River (UNR), which is the natural upstream portion of the Nelson River and 2) the Rat-Burntwood River (RBR) system, which exhibits discharge considerably augmented from natural conditions due to cross-watershed diversion. The study area encompasses the main stem waterbodies of these

three regions, four associated tributaries, and the north basin of Lake Winnipeg (Figure 3.2). Since the inception of the Churchill River Diversion (CRD) project in the 1970s, the RBR system (from Southern Indian Lake to Split Lake) transports diverted Churchill River waters and supplies ∼25% of total flow to the LNR, an approximate 10-fold increase from pre-development levels. The remaining ∼75% of total flow to the LNR is supplied by the UNR between the outflow of Lake Winnipeg and Split Lake. These catchments differ in their physical characteristics: the RBR drains the predominantly Precambrian Shield landscape of the Churchill River basin, whereas the UNR drains the vast, agriculturally-developed prairie landscape of the Lake Winnipeg watershed. River channels in all regions are either bounded by bedrock or incised into glacial deposits. In the UNR and RBR, river channels expand to flow through several natural lakes whereas in the LNR, the largest reservoirs downstream of Split Lake (Stephens Lake and generating station forebays) occur as a result of hydroelectric development.

Four terrestrial ecozones intersect at the study area: Boreal Plain, Boreal Shield, Hudson Plain, and Taiga Shield are distinguished by different types of soil, vegetation, wetland, and permafrost. Although variation occurs between ecozones, vegetation throughout the study area primarily consists of black spruce, jack pine, aspen, sphagnum, and willows (Rosenberg et al., 2005). Permafrost in the study area underlies wetlands and upland forest with sufficient overburden and becomes more prevalent towards Hudson Bay. In the UNR, peat plateaus cover between $0.1-10\,\%$ of the land surface whereas in the RBR this range increases to between $20-30\,\%$; in the LNR peat plateaus cover between $20-80\,\%$ of the landscape whereas permafrost-dominated open permafrost bogs dominate the landscape north of the Nelson River in the LNR near the western coast of Hudson Bay (Halsey et al., 1997).

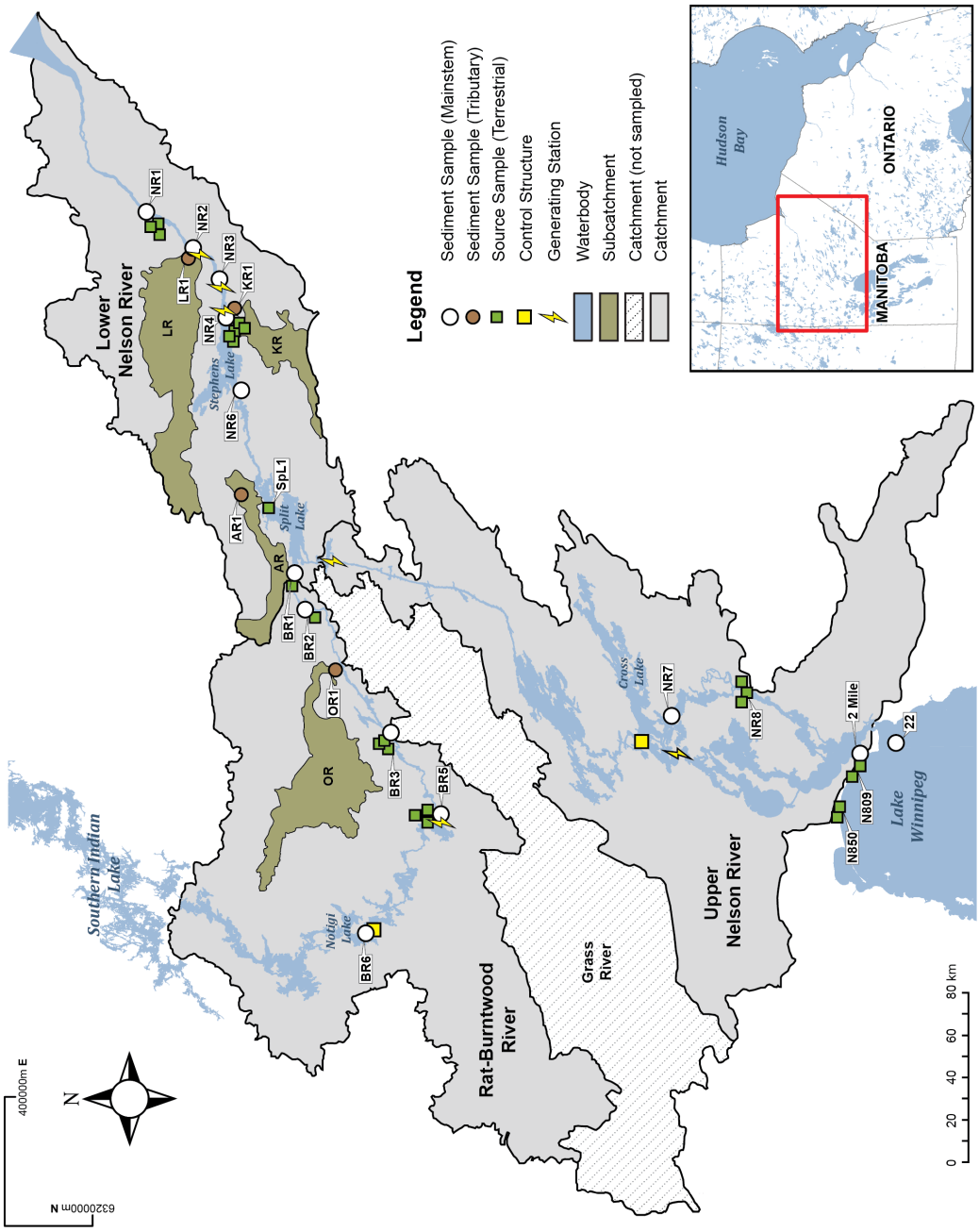

Fig. 3.2: Map showing location of CSSI sample sites visited during 2016 and 2017 field seasons in each catchment and subcatchment of the study area. OR: Odei River, AR: Assean River, KR: Kettle River, LR: Limestone River

3.2 Methods

3.2.1 Data collection

3.2.1.1 Sampling design and site characteristics

A total of 43 samples were collected from 21 sites in the study area during field work completed in late July and early August of 2016 and 2017 (Figure 3.2). A combination of terrestrial source and instream suspended sediment samples were collected at each site, described in Table 3.1. Site coordinates are listed in Table B.2. Sites were selected based on their accessibility by truck to accommodate generator-run pump and filtration equipment used in collecting bulk suspended sediment samples, and to provide maximum site density along the run of the river in each catchment. Sampling gaps exist in regions where the main river channel is not accessible by truck, especially in the lower half of the UNR, lower reaches of the LNR, and the Grass River catchment.

Previous studies involving CSSI fingerprinting typically linked potential sources of downstream suspended sediment to differences in land-use and focused on farming versus naturally vegetated areas (Alewell et al., 2016; Upadhayay et al., 2017). In this study, sources are distinguished either by geophysical differences between each catchment contributing to downstream mixtures in the LNR or by differences in substrates that are associated with types of OM or OM transformation processes. Source samples were collected from areas proximal to river channels and represent materials that could enter the system under natural hydrological or erosional conditions. This study also utilizes upstream suspended sediment samples as potential sources due to the many large lakes along the river system. Suspended sediment samples (both those used as sources and downstream mixtures) in this study are operationally defined as suspended particulate matter, $\geq$1.0 µm in size, in flowing channel waters or in lake water.

Table 3.1: CSSI fingerprinting sample site characteristics for all catchments. UNR: upper Nelson River, RBR: Rat-Burntwood River, LNR: lower Nelson River, P: peat, S: soil, Ba: river bank, Ss: suspended sediment, Be: river bed sediment and T: tributary suspended sediment, GS: Generating Station.

Catchment	Site	Sample(s)	Site Description	Vegetation
UNR	NR7	Ss	Site on north side of Nelson River under Kichi Sipi Bridge, south of the Cross Lake townsite.	Black spruce, poplar, sedge
	NR8	S	Site on west side of Nelson River at the Nelson House ferry crossing.	Black spruce, alder, sedge
	22	Ss	Site in the north basin of Lake Winnipeg, upstream of natural outflow.	NA
	2-mile	Ss	Site at outlet of 2-Mile Channel, engineered outflow of Lake Winnipeg.	NA
	N809	P, Ba	Site on north bank of Lake Winnipeg north basin, north west of 2-mile channel.	Peat
	N850	P, Ba	Site on north bank of Lake Winnipeg north basin, north west of site N809.	Peat
RBR	BR1	Ba, Ss	Site on north bank of the Burntwood River just upstream of Split Lake.	Black spruce, poplar, juniper, sphagnum moss
	BR2	Ba, Ss	Located at boat launch on north bank of Burntwood River, south of provincial road 280, downstream of confluence of Odei and Burntwood Rivers.	Poplar, grasses, alder
	BR3	S, Ba, Ss	Site on north bank of Burntwood River beneath bridge in Thompson on provincial road 391.	Black spruce, poplar, grasses, willow
	BR5	S, Ba, Ss	Located on north bank of Burntwood River downstream of Wuskwatim GS. Special permission required from Manitoba Hydro as site is accessed through private road.	Black spruce, poplar, juniper, sphagnum moss
	BR6	Ss	Site on south east shore of Notigi Lake at boat launch north west of provincial road 391.	Birch, poplar, spruce saplings, sphagnum moss, labrador tea

continued ...

. . . continued

Catchment	Site	Sample(s)	Site Description	Vegetation
	OR1	T	Located on east bank of Odei River upstream of large steel bridge on provincial road 280, upstream on confluence with Burntwood River.	Black spruce, poplar, grasses, willow
LNR	NR1	S, Ss, Be	Site on north side of Nelson River at Conawapa boat launch, 107 km from river mouth. Special permission required from Manitoba Hydro as site is accessed through Keewatinohk Converter Station work site.	Alder, willow, grasses, wildflowers
	NR2	Ss	Located on north side of Nelson River near boat launch downstream of Limestone GS	Black spruce, alder, sphagnum moss
	NR3	Ss	Site on south side of Nelson River downstream of Long Spruce GS at bridge over inflowing tributary.	Aspen, willow, alder, sapling spruce, grasses, wildflowers
	NR4	S, Ss	Located on the south shore of Stephens Lake upstream of Kettle GS, accessed via Kettle work camp.	Alder, willow, grasses
	NR6	Ss	Site on south side of Nelson River upstream of Stephens Lake, across the river from the Keeyask GS construction site.	Black spruce, poplar, alder, sphagnum moss, labrador tea
	SpL1	Be	Sediment core collection site 0.5 km southwest of the Split Lake townsite.	NA
	AR1	T	Site on east bank of Assean River directly below steel bridge on provincial road 280 upstream on confluence with Burntwood River.	Black spruce, pine saplings, sphagnum moss, labrador tea
	KR1	T	Sampled from west culvert on north side of bridge over Kettle River on provincial road 280 ∼3 km upstream of LNR.	Black spruce, larch, poplar, willow, sphagnum moss, labrador tea
	LR1	T	Located on west bank of Limestone River downstream of culvert bridge on provincial road 290 ∼1 km upstream of LNR.	Black spruce, poplar, alder, sphagnum moss

3.2.1.2 Sampling methods

Source materials collected for this study comprise peat, soils, river bank sediment, river bed sediment, and upstream suspended sediment (sediment collection methods described below). Peat, bank samples and bed sediment were collected by trowel or shovel into Whirl-Pak® bags (Figure 3.3a). Soil samples were collected by digging test pits to ensure proper separation between soil horizons and sampled by trowel or by hand into Whirl-Pak bags (Figure 3.3b). Soil test pits are described in Table B.3. All source samples were kept cold in coolers during field investigations and stored in refrigerators at the Centre for Earth Observation Science at the University of Manitoba prior to sample preparation.

Bulk suspended sediment samples were collected with generator-powered submersible pumps from <1.0 m depth. Water was then filtered using a M512 centrifuge, which collects particles ≥1.0 µm, or Pentek bag filter housings lined with 1.0 µm nominal pore size Pentair BP-420-1 filter bags (Figure 3.3c and 3.3d). Pumps were installed in river and tributary channels as far from the shoreline as allowed by safety protocols, typically between 1 m and 15 m from shore, and raised off the river bed using cinder blocks to ensure consistent sampling depth between sites. Lake Winnipeg suspended sediment samples at sites 22 and 2-mile Channel were collected by Ph.D candidate Masoud Goharrokhi in June of 2016 and 2017 aboard the MV *Namao* as a part of the Create-H_2O program.

3.2.1.3 Sample preparation

Source samples were manually cleaned of larger organic and inorganic fragments (e.g. wood, leaves, roots, and gravel-sized clasts), weighed, and frozen. Samples were then dried using a Labconco® bench top freeze dry system and weighed again to determine soil moisture percentage (Table B.4). Dried samples were hand ground by mortar and pestle, passed through a 850 µm sieve to limit maximum particle size, and transferred into

(a)

(b)

(c)

(d)

Fig. 3.3: Source and suspended sediment sampling in the Nelson River system. **3.3a:** River bank sediment at site BR1. Trowel for scale is ∼ 25 cm long. **3.3b:** Soil pit (∼65 cm deep) at site NR4 showing buried soil horizon (between 40-50 cm). **3.3c:** Submersible pump installation at site NR4. **3.3d:** Pentek bag filter housings connected to a generator-run submersible pump at site BR2.

50 mL polypropylene Falcon® tubes sealed with Parafilm to exclude moisture.

Sediment was washed from 1.0 µm Pentair BPHE filter bags with deionized water into a collection container and allowed to settle for 7-10 days. Water was incrementally siphoned to achieve a volume of sediment and water less than 500 mL and subsequently frozen and freeze dried using a Labconco bench top freeze dry system. Centrifuge sediment samples were also frozen and freeze dried. All suspended sediment samples were transferred into 50 mL polypropylene Falcon tubes and sealed with Parafilm to avoid moisture accumulation. Samples were stored frozen until shipped to the University of Northern British Columbia for analysis.

3.2.2 Laboratory analysis

Following sample preparation at the University of Manitoba, all laboratory analysis for Compound-Specific Stable Isotope fingerprinting was completed at the University of Northern British Columbia's Northern Analytical Laboratory Services (NALS) in Prince George, British Columbia by Ph.D. candidate Dominic Reiffarth.

3.2.2.1 Total organic carbon and bulk carbon isotope analysis

Freeze dried and sieved samples were pre-treated with HCl until no effervescence was observed to remove inorganic carbon, dried, measured into tin capsules, and loaded into an auto-sampler. Total percent OC and bulk carbon isotope ratios were measured using an elemental analyzer coupled to an isotope ratio mass spectrometer (EA-IRMS). The standard deviation for triplicate analyses of total OC ranged between 0.20 % and 1.71 %. Bulk stable carbon isotope ratios were expressed as δ^{13}C values in per mil relative to the Vienna Pee Dee Belemnite (VPDB) reference standard.

3.2.2.2 Fatty acid extraction and carbon isotope measurement

Laboratory methods for fatty acid (FA) extraction and carbon isotope measurement of individual FA chain lengths are outlined in detail by Reiffarth et al. (2018). A summary of these methods is given below.

Freeze dried and sieved samples were sonicated using a Misonix S-4000 sonicator to homogenize each sample. A 4:1 ratio of solvent to sample mass was used with a solvent mixture that combined dichloromethane, hexanes, and methanol in a 9:7:1 ratio (solvent A). Extraction of fatty acids using solvent A was performed using an automated Büchi E-916 pressurized solvent extractor or by soxhlet if samples were high in biofilms. A low-pressure liquid chromatography pump was used with Michel-Miller filter columns with three types of silica (basic, neutral, and acidic). Crude extracts were loaded after columns were conditioned with 60% by volume dichloromethane and hexanes (solvent B) and subsequently pumped though the system with solvent B. Fatty acids were remobilized using a mixture of 1% formic acid in solvent A with the fatty-acid-containing effluent then being evaporated to dryness. Samples were derivitized to fatty acid methyl esters (FAME) using diazomethane (CH_2N_2) as the methylating agent. Purified residue was combined in a vial with 0.5 mL to 1 mL of CH_2N_2, swirled until homogenous, allowed to sit for at least 20 minutes, and then evaporated to dryness using N_2. The level of detection and standard deviation for individual chain lengths ranged between 2.21 ppm and 31.11 ppm, and 0.74 ppm and 20.37 ppm respectively. The RSD for all chain lengths was <2 %.

Derivitized sample FAMEs were analyzed on a Varian GC-3800 with CP-8400 autosampler equipped with a flame ionization detector to detect and quantify fatty acid concentration. Samples were analyzed for carbon isotope ratios (relative to VPDB) using a Delta V Advantage continuous flow IRMS interfaced with a ConFlo IV, GCC(III) combustion unit, and Agilent 6890A with A200S autosampler. Results were evaluated using methyl

icosanoate standards purchased from Arndt Schimmelmann at Indiana University, USA as well as standards produced in-lab.

3.2.3 Data processing

Following CSSI analysis, a tracer set comprising $\delta^{13}C$ values of long-chain saturated fatty acids (C_{22}-C_{32}) was selected based on graphical/statistical tests and recommendations from previous literature (Alewell et al., 2016; Reiffarth et al., 2016; Upadhayay, Smith, et al., 2018). Bulk properties of samples in the CSSI data set was explored and used to designate source and suspended sediment sediment samples and construct mixing model frameworks for use in MixSIAR. The ability of each tracer to discriminate between sources in each model framework were explored with a series of statistical tests and biplot analysis. All statistical analysis and un-mixing modelling described in this section, as well as graphical methods used to produce plots, were undertaken using R software (version 3.3.2, R Core Team, 2016) using the following packages in the library: tidyverse (Wickham, 2017), gridextra (Auguie, 2017), klaR (Weihs, Ligges, Luebke, & Raabe, 2005), MASS (Venables & Ripley, 2002), broom (Robinson et al., 2018), ggplot2 (Wickham, 2016), and MixSIAR (Stock & Semmens, 2016). All raw data are listed in Section B.4 (Tables B.4, B.5, B.6, and B.7).

MixSIAR is a flexible Bayesian statistics-based model framework created as an open-source package for use in R software that uses mixing models and biotracer data to estimate the proportions of source contributions to a mixture (Stock et al., 2018). It was originally used by ecologists to study diet composition and animal movement (Stock & Semmens, 2016), but this "prey" and "consumer" model framework can also be applied to upstream sources (prey) to downstream suspended sediment (consumer) in watersheds by "unmixing" sources using biotracers present in the natural environment. Models are fit hierarchically in the Bayesian framework of MixSIAR using a Markov Chain Monte Carlo (MCMC) method

and can be modified to account for fixed and random effects, and uncertainty in sources such as prior information and concentration dependency of isotope ratios (Parnell et al., 2013; Stock & Semmens, 2016).

3.2.3.1 Biplot analysis

Biplots are often used in sediment fingerprinting as a preliminary visual technique to ensure that each tracer can classify mixture data within the error range of each source type. Two-dimensional scatter plots are created for each combination of tracers, and in the case of CSSI fingerprinting, δ^{13}C values of sediment samples are plotted versus the mean $\pm$ 1 standard deviation of each source group. This helps to constrain the most effective tracers in the tracer group by eliminating biotracers that do not behave conservatively and/or identifying sediments influenced by an unsampled source.

3.2.3.2 Statistical tests

Statistical tests were performed using the built-in R stats package in R software (R Core Team, 2013) to explore the ability of each tracer to differentiate between sources. Shapiro-Wilks normality tests were performed using the **shapiro.test()** fuction. Analysis of variance (ANOVA) was calculated using the **aov()** function and Tukey's HSD (Honest Significant Difference) test was performed using the **TukeyHSD()** function. Principal component analysis (PCA) was explored for each pooled model framework using the **prcomp()** function and source loadings within each PCA were calculated using the **tidy()** function from the broom package (Robinson et al., 2018).

3.3 Results

3.3.1 Compound-Specific Stable Isotope (CSSI) analysis

Prior to the construction of mixing models, biochemical compositions and isotopic characteristics of OM from all samples were visually/graphically explored based on properties of individual fatty acids (FA weight % and δ^{13}C values for tracers C_{22}-C_{32}) and bulk properties (% OC and bulk δ^{13}C) to determine major compositional differences. By investigating the properties of individual FAs for all samples on the coarsest scale, only general FA characteristics can be described. Even-numbered fatty acid chain lengths (C_{22}, C_{24}, C_{26}, C_{28}, and C_{30}) exhibit the highest weight % in each sample (Figure 3.4a), whereas the odd-numbered FA lengths individually make up <5% of all samples by weight. Individual FAs show variation in their median δ^{13}C values for all samples, but cannot be readily distinguished from each other with median δ^{13}C of ~ -35 ‰ (Figure 3.4b). More information can be gleaned from the data set by categorizing samples.

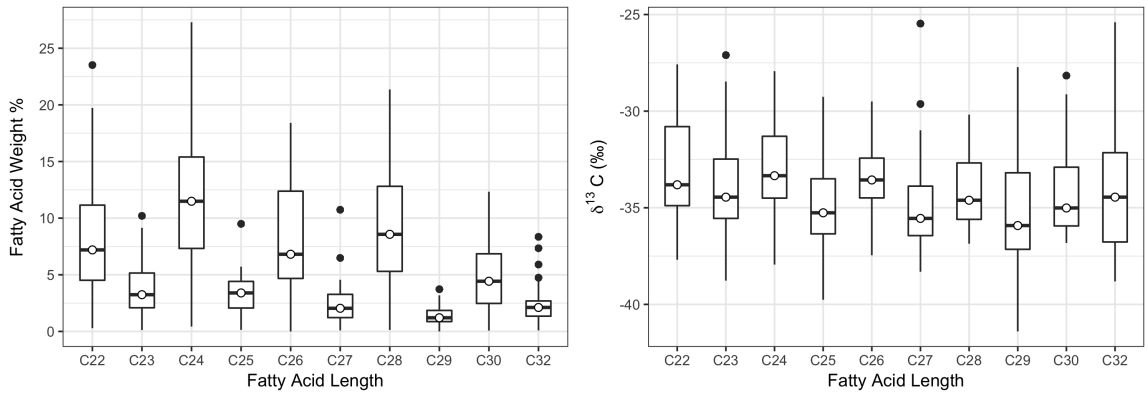

Fig. 3.4: Quantitative results from CSSI analysis on individual fatty acids from all samples. **3.4a:** Median and quartile values of fatty acid concentration (weight % in sample). **3.4b:** Median and quartile values of carbon isotope ratios (δ^{13}C (‰) relative to VPDB). Box and whisker plots show median as line and open circle, upper and lower hinges represent 75% and 25% quartile, upper and lower whiskers are ymin and ymax, and black dots are outliers.

3.3.1.1 Bulk properties and fatty acid composition

Compositional differences in both bulk properties and individual FAs are best highlighted by categorizing samples in the data set (Figure 3.5 and 3.6). To determine if there are compositional differences between the various subcatchments delivering particulate OM to downstream suspended sediment in the LNR, source samples were grouped spatially into each subcatchment (UNR, RBR, and LNR) and tributaries. To further elucidate compositional variations within each region, source samples were also grouped by substrate type that includes: peat, soil, river bank material, mainstem riverine and lacustrine suspended sediment (here on referred to as suspended sediment), river bed material, and tributary suspended sediment. Both regional and substrate categories were compared to suspended sediment samples in the lower reaches of the LNR (downstream of Stephens Lake) that represent the downstream mixture.

Examining bulk source properties, median % OC is highest in the UNR and lowest in the RBR with mid-range values seen in tributaries, the LNR, and the suspended sediment mixture (Figure 3.5a). With regard to substrate types in the whole study area, peat samples contain the highest median proportion of OC whereas remaining substrate types contain $<10\,\%$ OC with the most variation in % OC seen within soils (Figure 3.5c). Tributaries exhibit the lowest bulk δ^{13}C values with a median value of $-29.52\,‰$, whereas median bulk δ^{13}C values from samples in the UNR, RBR, LNR are all above $-28.00\,‰$ (Figure 3.5b). A distinction between substrates was also observed where suspended sediment and tributary suspended sediment show lower bulk δ^{13}C signatures than all other substrates (Figure 3.5d).

Samples from the UNR comprise peat, river bank material, soil, and suspended sediment samples and exhibit a median (interquartile range) of $5.65\,\%$ ($3.14\,\%$ to $12.61\,\%$) OC. Variation in % OC in the UNR is attributed to the characteristics of each substrate. Peat

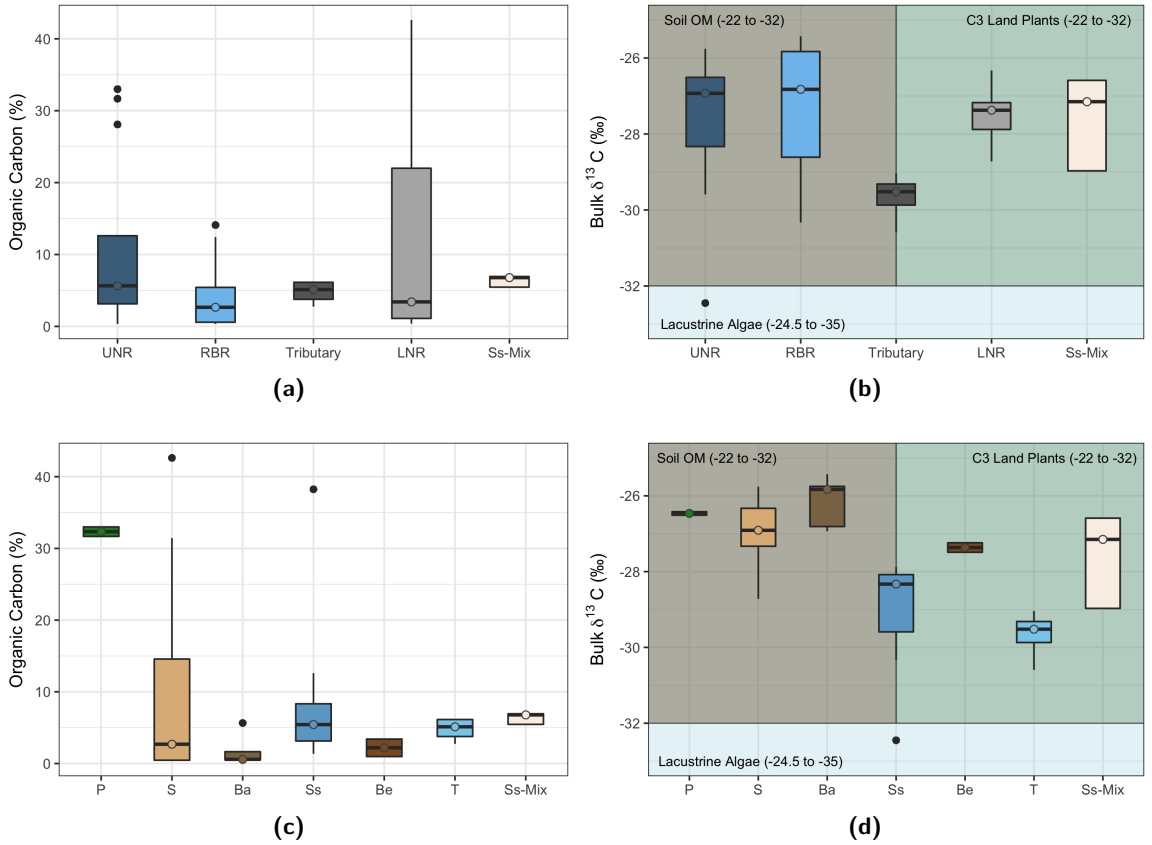

Fig. 3.5: Bulk composition of all terrestrial and suspended sediment samples grouped both spatially and by substrate. **3.5a:** % OC by spatial region. **3.5b:** Bulk δ^{13}C by spatial region. **3.5c:** % OC by substrate type. **3.5d:** Bulk δ^{13}C by substrate type. Typical bulk δ^{13}C ranges for soil OM, C3 land plants, and lacustrine algae are shown in the background of Figures 3.5b and 3.5d. Note that soil OM and C3 land plants are split in plot because these ranges overlap with one another. P: peat, S: soil, Ba: river bank, Ss: suspended sediment, Be: river bed sediment, T: tributary suspended sediment, Ss-Mix: suspended sediment downstream of Stephens Lake.

samples in the UNR contain a much higher proportion of OC (up to 33 % OC) whereas soils, bank material, and suspended sediment exhibit lower proportions (Figure 3.5c). Median bulk δ^{13}C in the UNR is −26.93 ‰ (Figure 3.5b) and most of the variation in this region is explained by suspended sediment samples that show bulk δ^{13}C as low as −32.45 ‰ (Figure 3.5d).

From the RBR region, samples comprising soil, bank material and suspended sediment contain a median (interquartile range) of 2.66 % (0.58 % to 5.43 %) OC (Figure 3.5a). Although median values are low, soil C-horizons and suspended sediment sources in this region contain up to 14.10 % and 12.43 % OC respectively (Figure 3.5c). Median bulk δ^{13}C of samples from the RBR is −26.83 ‰ (Figure 3.5b), but some samples such as suspended sediment show bulk δ^{13}C as low as −30.33 ‰ (Figure 3.5d).

Tributary suspended sediment samples have a median (interquartile range) of 5.12 % (3.77 % to 6.14 %) OC (Figure 3.5a). Suspended sediment from tributaries flowing into the LNR (Assean River, Kettle River, and Limestone River) contain a higher proportion of OC (between 4.11 % and 6.16 %) than the sole tributary sampled in the RBR system, the Odei River (4.11 %) (Figure 3.5c). Median bulk δ^{13}C in tributary samples is −29.52 ‰ (Figure 3.5b). The Limestone River exhibits the lowest bulk δ^{13}C of −30.59 ‰, however tributaries do not show as much variation as other regions (Figure 3.5b).

Samples from the LNR comprise soil, suspended sediment, and river bed material samples and have a median (interquartile range) of 3.41 % (1.11 % to 22.00 %) OC (Figure 3.5a). A large variation in % OC in the LNR is attributed to a high proportion of OC in both A and C soil horizons (between 14.57 % to 42.62 % OC) and suspended sediment (up to 38.25 % OC) (Figure 3.5c). Other soil horizons and bed material, however, contain a lower proportion of OC. Median bulk δ^{13}C of samples from the LNR is −27.38 ‰ (Figure 3.5b) and although little variation is observed in this region, soil sources exhibit slightly higher

bulk δ^{13}C (up to −28.72 ‰) (Figure 3.5d).

Suspended sediment samples assigned as the downstream mixture were collected from three sites (NR1, NR2, and NR3) in the LNR and have a median (interquartile range) of 6.78 % (5.46 % to 6.94 %) OC (Figure 3.5a and 3.5c). Median bulk δ^{13}C of mixture samples is −27.15 ‰ with an interquartile range from −28.97 ‰ to −26.59 ‰ (Figure 3.5b and 3.5d).

Individual FA lengths from all samples were also categorized by region and substrate to evaluate their proportion within samples and their isotopic composition (Figure 3.6). When grouped both by region and substrate, even chain length FAs (C_{22}, C_{24}, C_{26}, C_{28}, and C_{30}) comprise the highest proportion of sample weight.

When grouped by region, samples from the UNR contain higher concentrations of C_{22}, C_{24}, C_{26}, and C_{28} FA chain lengths (medians 6.32 wt% to 9.46 wt%) compared to other FA chain lengths, which contribute less than 5 wt% (Figure 3.6a). Median δ^{13}C of individual FAs in the UNR range from −34.90 ‰ to −33.12 ‰ except for C_{25}, C_{27}, C_{29}, and C_{32} that exhibit δ^{13}C values below −35.0 ‰ (Figure 3.6c). RBR samples also contain higher concentrations of C_{22}, C_{24}, C_{26}, and C_{28} FA chain lengths (medians 6.73 wt% to 11.04 wt%) compared to other FA chain lengths, which contribute less than 5 wt% (Figure 3.6a). Median δ^{13}C of individual FAs range from −34.92 ‰ to −33.15 ‰ except for C_{27}, C_{29}, and C_{30} that exhibit δ^{13}C values below −35.0 ‰ (Figure 3.6c). Tributary samples contain higher concentrations of C_{22}, C_{24}, C_{26}, C_{28}, and C_{30} FA chain lengths (medians 5.68 wt% to 12.70 wt%) compared to other FA chain lengths, which contribute less than 5 wt% (Figure 3.6a). Median δ^{13}C of individual FAs are lower than other source regions and range from −37.06 ‰ to −35.04 ‰ except for C_{24} and C_{26} which exhibit δ^{13}C values above −35.0 ‰ (Figure 3.6c). LNR samples also contain higher concentrations of C_{22}, C_{24}, C_{26}, C_{28}, and C_{30} FA chain lengths (medians 5.38 wt% to 13.61 wt%) compared to other FA chain lengths,

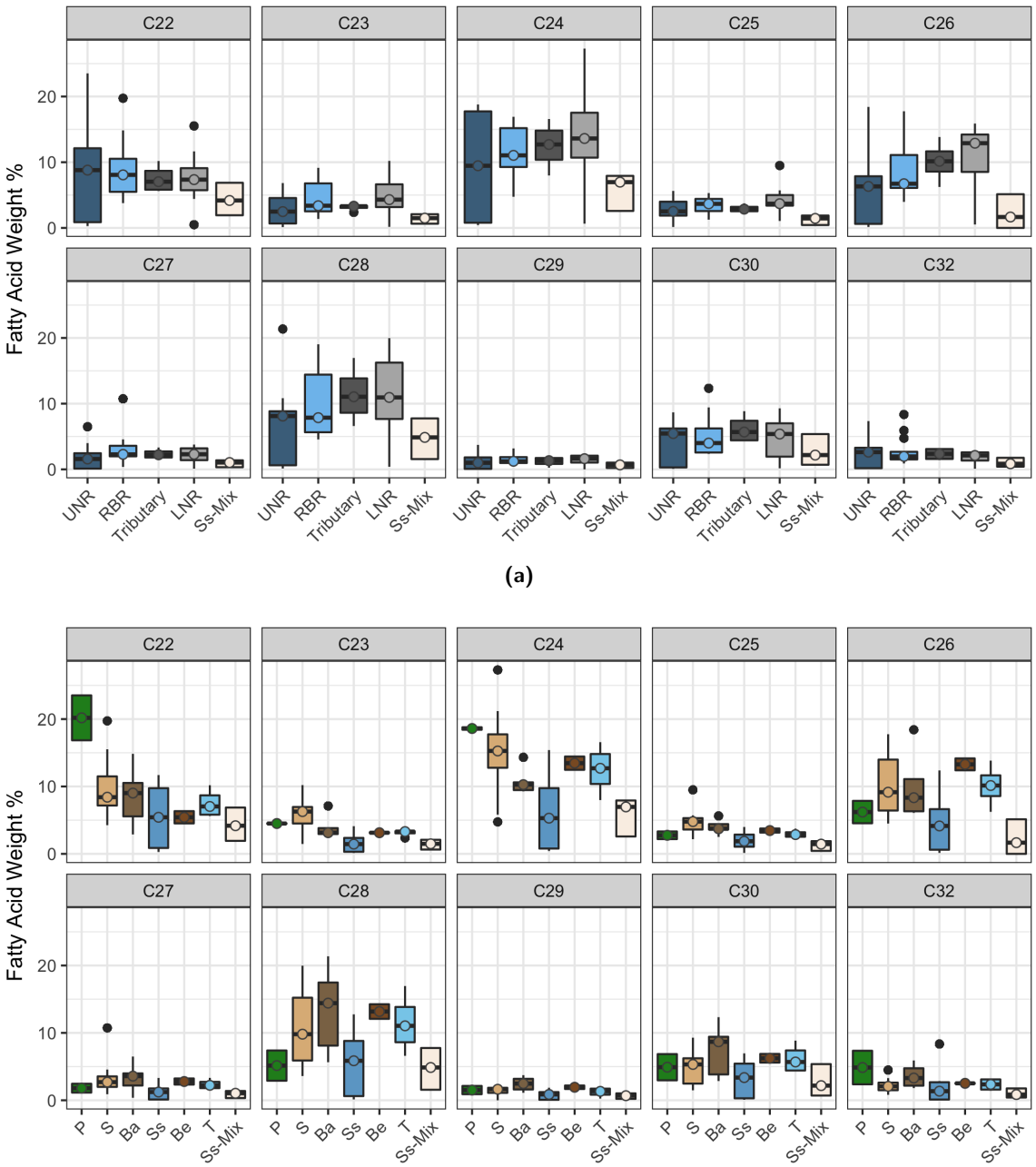

Fig. 3.6: Median and quartile values for bulk concentration and composition of terrestrial and suspended sediment samples for each fatty acid tracer grouped both spatially and by substrate. **3.6a**: Fatty acid concentration (weight % in sample) by spatial region. **3.6b**: Fatty acid concentration (weight % in sample) by substrate. **3.6c**: Carbon isotope ratios (δ^{13}C in permil) by spatial region. **3.6d**: Carbon isotope ratios (δ^{13}C in permil) by substrate. P: peat, S: soil, Ba: river bank, Ss: suspended sediment, Be: river bed sediment, T: tributary suspended sediment, SS-Mix: suspended sediment downstream of Stephens Lake.

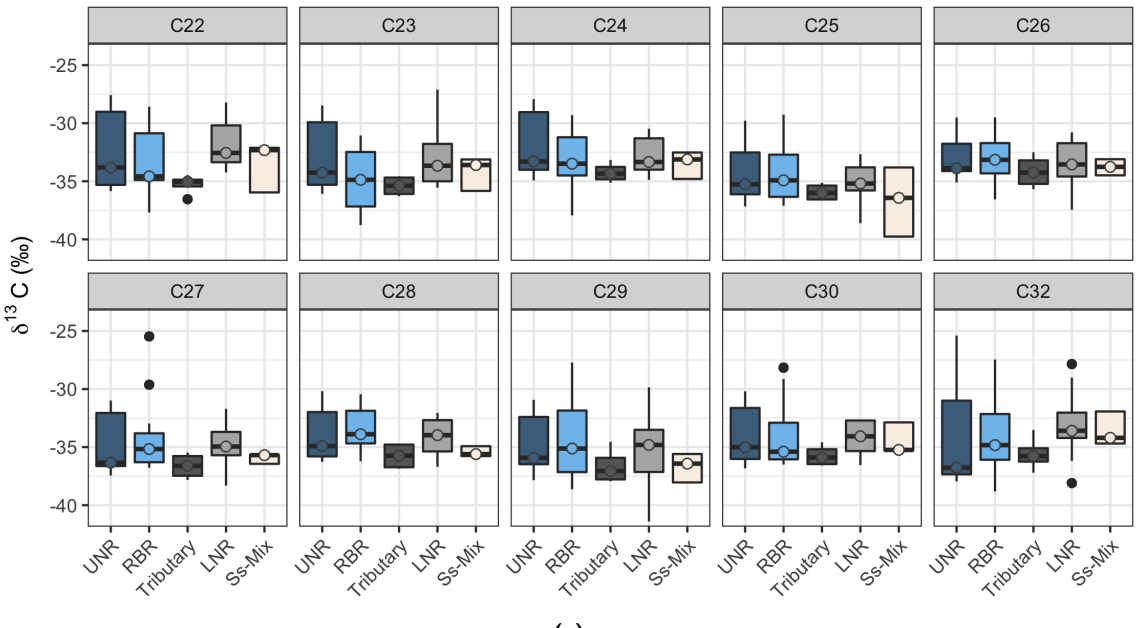

(c)

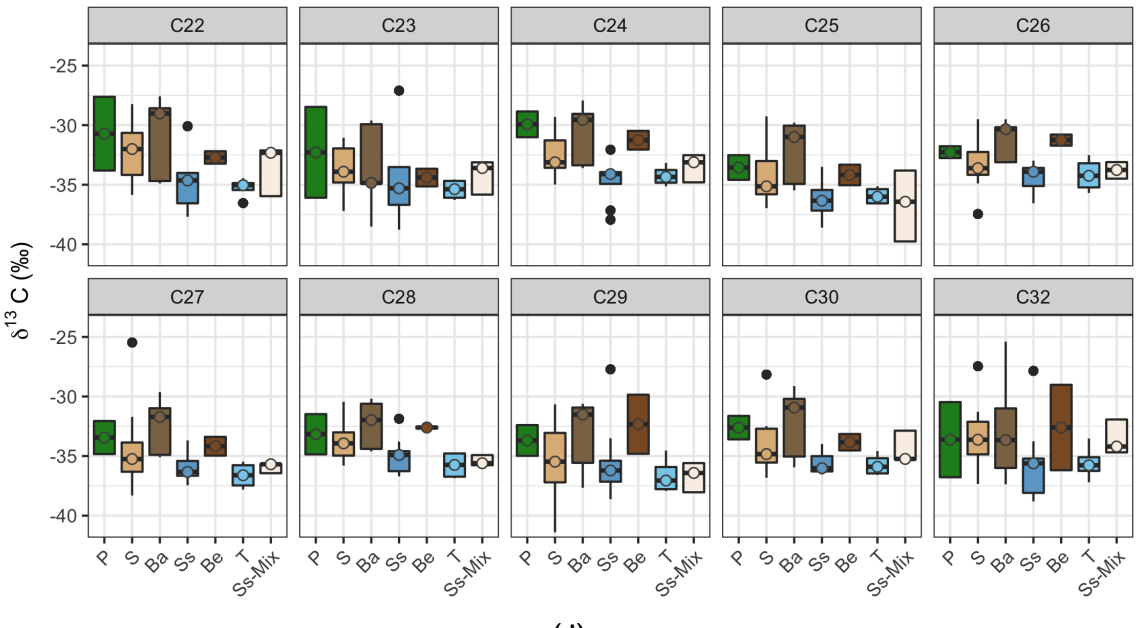

(d)

Fig. 3.6: Median and quartile values for bulk concentration and composition of terrestrial and suspended sediment samples for each fatty acid tracer grouped both spatially and by substrate. **3.6a**: Fatty acid concentration (weight % in sample) by spatial region. **3.6b**: Fatty acid concentration (weight % in sample) by substrate. **3.6c**: Carbon isotope ratios (δ^{13}C in permil) by spatial region. **3.6d**: Carbon isotope ratios (δ^{13}C in permil) by substrate. P: peat, S: soil, Ba: river bank, Ss: suspended sediment, Be: river bed sediment, T: tributary suspended sediment, SS-Mix: suspended sediment downstream of Stephens Lake.

which contribute less than 5 wt% (Figure 3.6a). Median δ^{13}C of individual FAs range from −34.95 ‰ to −32.56 ‰ except for C_{25} which exhibits δ^{13}C values below −35.0 ‰ (Figure 3.6c). Sediment mixtures contain higher concentrations of C_{22}, C_{24}, C_{28}, and C_{30} FA chain lengths (medians 2.17 wt% to 6.97 wt%) compared to other FA chain lengths, which contribute less than 2 wt% (Figure 3.6a and 3.6b). For individual FAs C_{22}, C_{23}, C_{24}, C_{26}, and C_{32}, median δ^{13}C values range from −34.20 ‰ to −32.32 ‰ and the remaining FAs exhibit δ^{13}C values below −35 ‰ with a range from −36.43 ‰ to −35.24 ‰ (Figure 3.6c and 3.6d).

When grouped by substrate, peat sources contain substantially higher concentrations of C_{22} and C_{24} FA chain lengths (medians 20.19 wt% and 18.60 wt% respectively) compared to other FA chain lengths, which contribute less than 8 wt% (Figure 3.6b). Median δ^{13}C of individual FAs range from −33.69 ‰ to −30.72 ‰ except for C_{24} that exhibits a median δ^{13}C value of −29.93 ‰ (Figure 3.6d). Soils contain a higher proportion of C_{22}, C_{24}, C_{26}, and C_{28} FA chain lengths (medians 8.41 wt% to 15.27 wt%) compared to other FA chain lengths, which contribute less than 7 wt% (Figure 3.6b). Median δ^{13}C of individual FAs range from −34.84 ‰ to −32.01 ‰ except for C_{25}, C_{27}, and C_{29} which are lower with δ^{13}C values below −35.00 ‰ (Figure 3.6d). Bank samples contain higher proportions of C_{22}, C_{24}, C_{26}, C_{28} and C_{30} FA chain lengths (medians 8.34 wt% to 10.27 wt%) compared to other FA chain lengths, which contribute less than 4 wt% (Figure 3.6b). Median δ^{13}C of individual FAs range from −34.85 ‰ to −30.43 ‰ except for C_{22} and C_{24} with δ^{13}C values above −30.00 ‰ (Figure 3.6d). Compared to other substrates, suspended sediment samples contain lower concentrations of long chain fatty acids, but still show elevated concentrations of C_{22}, C_{24}, and C_{28} FAs (medians 5.30 wt% to 5.86 wt%) compared to other FA chain lengths, which contribute less than 5 wt% (Figure 3.6b). Median δ^{13}C of individual FAs range from −36.32 ‰ to −35.30 ‰ except for C_{22}, C_{24}, C_{26}, and C_{28} which have δ^{13}C values above −35.00 ‰ (Figure 3.6d). Bed material contains higher proportions of C_{24},

C_{26}, and C_{28} FAs (medians 13.17 wt% to 13.46 wt%) compared to other FA chain lengths, which contributed less than 7 wt% (Figure 3.6b). Median $\delta^{13}C$ of individual FAs range from -34.40 ‰ to -31.26 ‰ (Figure 3.6d). Tributary suspended sediment substrate samples are described previously in this section.

3.3.2 MixSIAR model design and setup

Mixing models were designed for this study to estimate the proportional contribution of both spatial- and substrate-based OM sources to downstream suspended sediment in the LNR. To achieve this, two different concentration-dependent MixSIAR model framework methods were used: the pooled method (Pooled-MixSIAR) and the deconvolutional method (D-MixSIAR) (Blake et al., 2018). Using the pooled method, all designated source samples from each subcatchment are pooled and unmixed against the sediment mixture node at the downstream-most point; the deconvolutional method allows for unmixing of sub-catchment-specific sources against proximal, in-catchment sediment mixture nodes, followed by the unmixing of these sub-catchment sources against the sediment mixture node at the downstream-most point (Blake et al., 2018). Mixture nodes are instream suspended sediments (ideally the combination of three or more samples) that represent a mixture in relation to all upstream sources from that point (Blake et al., 2018).

Using both of these methods, three isotope mixing model frameworks were constructed for the Nelson River watershed: 1) pooled-spatial, 2) pooled-substrate, and 3) deconvolutional-substrate (Table 3.2 and Figure 3.7). Since CSSI analysis measures $\delta^{13}C$ values of long-chain saturated FAs and their concentration in each sample, all mixing models are concentration-dependent to best quantify sediment source contributions (Upadhayay, Bodé, et al., 2018). The remaining model settings are consistent between all three models, using a no prior information, no source factors, and a residual error term, which accounts for unknown sources

of variability in the sediment mixtures (Upadhayay et al., 2017). Each model was run using a chain length of 300,000 and a burn-in of 200,000 ("long" setting). Mixing model convergence was evaluated using the Gelman-Rubin and Geweke diagnostics (Stock & Semmens, 2016).

Pooled-spatial model In this model framework, to distinguish spatially defined OM source contributions from each catchment and associated tributaries to downstream sediment at mixture node M_3, source and upstream sediment samples were pooled into four categories: upper Nelson River (UNR), Rat-Burntwood River (RBR), lower Nelson River (LNR), and tributaries (Figure 3.7a and Table 3.2). Pooled categories incorporate all sample types from each catchment to represent a complete package of organic signatures from the spatially distinct UNR, RBR, and LNR. Tributary sources are pooled suspended sediment samples from the Odei River, Assean River, Kettle River and Limestone River.

Pooled-substrate model To determine the proportional contributions of various source substrates in all catchments to downstream sediment and mixture node M_3, source samples in the substrate-based model framework were pooled into six categories: peat (P), soil (S), river bank material (Ba), river bed sediment (Be), tributary suspended sediment (T), and suspended sediment (Ss) (Figure 3.7a and Table 3.2). Source apportionment in this model is determined solely by source substate type, independent of location within the study area.

Deconvolutional-substrate model A deconvolutional MixSIAR model framework was created to allow for the unmixing of subcatchment source substrates against mixture nodes M_1 and M_2 in the UNR and RBR respectively (Figure 3.7b). Substrate sources contributing to M_1 in the UNR comprise peat (P_1), soil (S_1), river bank material (Ba_1), and suspended

Table 3.2: Mixture samples and sources used in each MixSIAR model framework. Mixture nodes are defined by grouping suspended sediment samples in each region. Sources for all model designs are abbreviated where UNR: upper Nelson River, RBR: Rat-Burntwood River, LNR: lower Nelson River, Trib: tributary, P: peat, S: soil, Ba: river bank, Ss: suspended sediment, Be: river bed sediment and T: tributary suspended sediment. Sample sites listed in footnote are described in Table 3.1

Model Framework	Mixture Node	Source(s)
Pooled-Spatial	$\mathbf{M}_3$[a]	UNR, RBR, LNR, Tributary
Pooled-Substrate	$\mathbf{M}_3$[a]	P, S, Ba, Ss, Be, T
Deconvolutional-Substrate	$\mathbf{M}_1$[b]	P_1, S_1, Ba_1, Ss_1
	$\mathbf{M}_2$[c]	S_2, Ba_2, Ss_2
	$\mathbf{M}_3$[a]	M_1[d] M_2[d] S_3, Ss_3, Be_3, T_3

[a] Suspended sediment samples from sites NR1, NR2, and NR3
[b] Suspended sediment samples from sites 22 and NR7
[c] Suspended sediment samples from sites BR1 and BR2
[d] Results from M_1 and M_2 mixing models act as sources to M_3 in partial deconvolutional model

sediment (Ss_1)[1]. In the RBR, sources to M_2 consist of soils (S_2), river bank material (Ba_2), and upstream suspended sediment (Ss_2)[2]. The proportional contributions of sources are determined against each subcatchment's mixture node. A merge node function developed by Blake et al. (2018) (Listing B.2) is used to incorporate the mixture nodes from each upstream subcatchment as sources against mixture node M_3 alongside local sources comprising soils (S_3), river bed sediment (Be_3), upstream suspended sediment (Ss_3), and tributary suspended sediment (T_3) in the LNR. A complete description of the deconvolutional MixSIAR method is outlined in Blake et al. (2018). Source, sediment and discrimination data, as well as R code, are shown in Appendix B (Table B.11 and Listing B.1 respectively).

[1]Note that due to a low number of samples, suspended sediment samples in the UNR were used as both upstream sources (Ss_1) and sediment mixtures (M_1).

[2](Ss_2) include upstream suspended sediment samples from the mainstem RBR and a tributary suspended sediment sample from the Odei River.

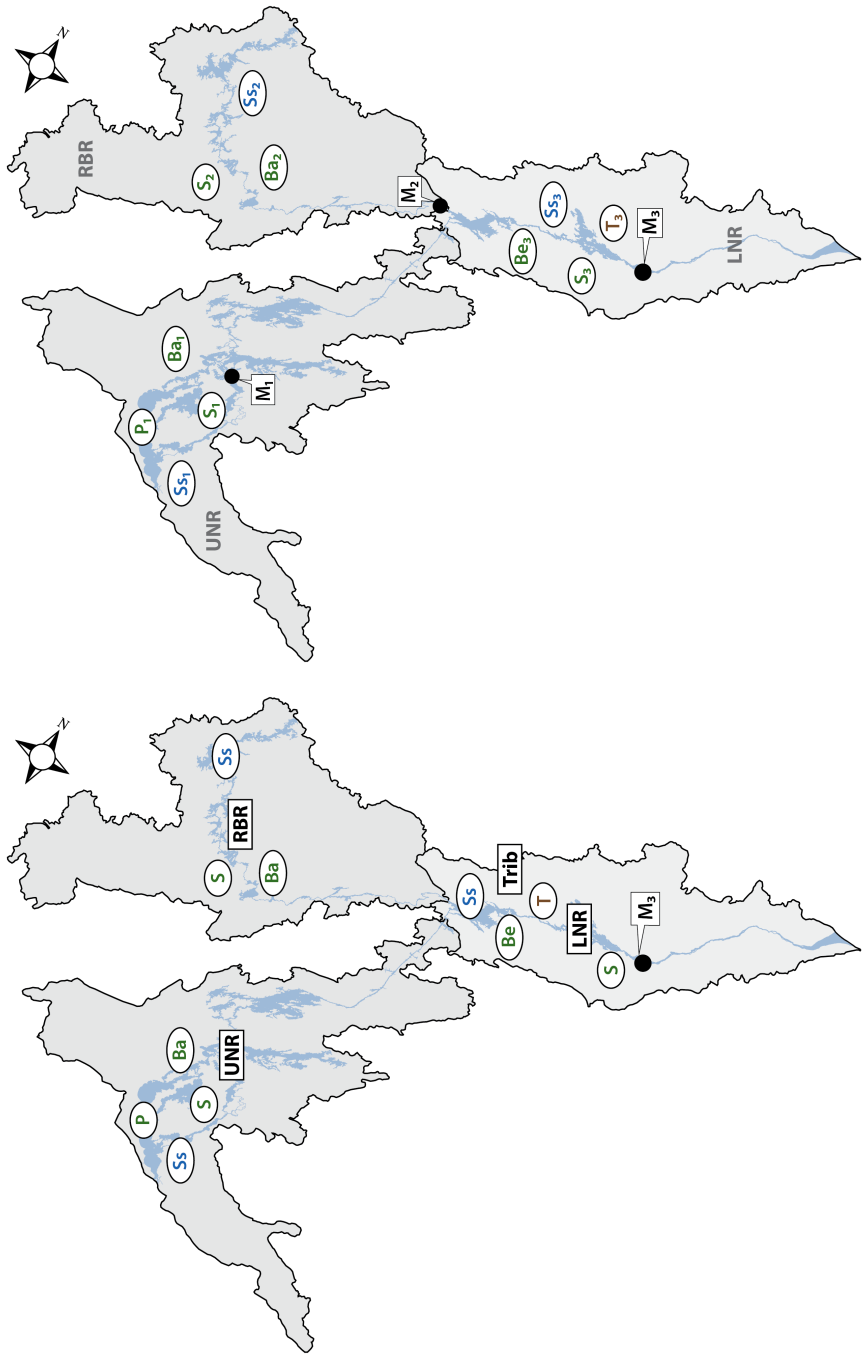

Fig. 3.7: Conceptual mixing model design schematics. **3.7a:** Pooled MixSIAR model schematic where rectangular labels represent sources for the spatial catchment-based pooled model and oval labels represent sources for the substrate-based pooled model. **3.7b:** Deconvolutional MixSIAR model schematic. Sources for all model designs are abbreviated where UNR: upper Nelson River, RBR: Rat-Burntwood River, LNR: lower Nelson River, Trib: tributary, P: peat, S: soil, Ba: bank, Ss: suspended sediment, Be: bed sediment and T: tributary suspended sediment. Mixture nodes (M_n) are indicated by black circles for all models. Labels do not represent precise sample locations.

3.3.3 Source discrimination

Tracers for source discrimination were selected initially based on literature review and previous studies, but then evaluated to determine appropriate tracer properties to include in the mixing models. Graphical/visual and statistical tests were performed for each model to assess the ability of each tracer to differentiate between sediment sources. Biplot analysis, Shapiro-Wilk, ANOVA, and TukeyHSD tests were completed on all models, but principal component analysis was only done on the pooled models due to an insufficient number of samples in each subcatchment of the deconvolutional model. Results of Shapiro-Wilk, ANOVA, and TukeyHSD statistical tests are listed in Tables B.8, B.9, and B.10 respectively.

3.3.3.1 Biplot analysis

Biplot analysis was used for each model framework as a visual test to ensure each FA tracer could classify mixture node samples within the range (mean $\pm$ 1 standard deviation) of each source's isotopic composition. This method was used to compare every combination of tracers, but due to the large number of tracers used in this study, only a subset of biplots are shown in this section. For all models, biplot analysis helped to constrain FA tracers used by eliminating short chain fatty acids (C_{16}-C_{21}) since they were not able to classify sediment mixtures within their isotopic compositional range.

Pooled mixing model frameworks used the same source and mixture samples, but varied in the classification of sources (Table 3.2 and Figure 3.7a). In the pooled-spatial mixing model framework, all tracers effectively classify the downstream mixtures within source group ranges except for C_{23} and C_{27}. For these FA tracers, $\delta^{13}C$ values of sediment from site NR2 are much more lower (nearing $-40.00\,‰$) than the remaining samples comprising mixture node M_3 (Figure 3.8a). The same results occur in the pooled-Substrate model

framework (Figure 3.8b) with the addition of FA tracer C_{30}, which for sediment from site NR2 also lies just outside source ranges.

In the deconvolutional-substrate mixing model framework, biplots were constructed for all subcatchments (Table 3.2 and Figure 3.7b) and their respective sources and mixture nodes (Figure 3.9). For mixture node M_1, all tracers effectively classify downstream mixtures within one standard deviation of the mean (Figure 3.9a). For mixture node M_2, sediment mixture BR1 fall within source ranges for all FA tracers except for C_{27} and C_{29} (Figure 3.9b). Sediment sample BR2 however is not effectively classified by many of the FA tracers, falling outside of the source range. For mixture node M_3, each tracer effectively classifies all sediment mixtures except for NR2 which does not fall within the range of source composition for FA lengths C_{23}, C_{27}, and C_{30} (Figure 3.9c).

3.3.3.2 Statistical tests

Shapiro-Wilk, ANOVA and TukeyHSD tests were performed using R software to determine whether the FA tracer data are normally distributed, whether there are statistical differences between each source type in all models, and how effective each tracer is at differentiating between sources in each model framework. A principal component analysis (PCA) was also completed for each pooled mixing model framework.

Shapiro-Wilk tests were used to test for normality of individual tracers for all model frameworks. Tracers C_{23}, C_{24}, C_{26}, C_{28}, and C_{29} show high p-values ($p > 0.05$, $n = 39$); therefore not all fatty acid chain lengths selected as tracers display normal distributions.

Using an ANOVA test, all FA tracers fail to distinguish a statistical difference between source means in the pooled-spatial model. In the pooled-substrate model, all FA lengths show statistical distinction between source means ($p < 0.05$, $n = 39$) except C_{23}, C_{29}, and

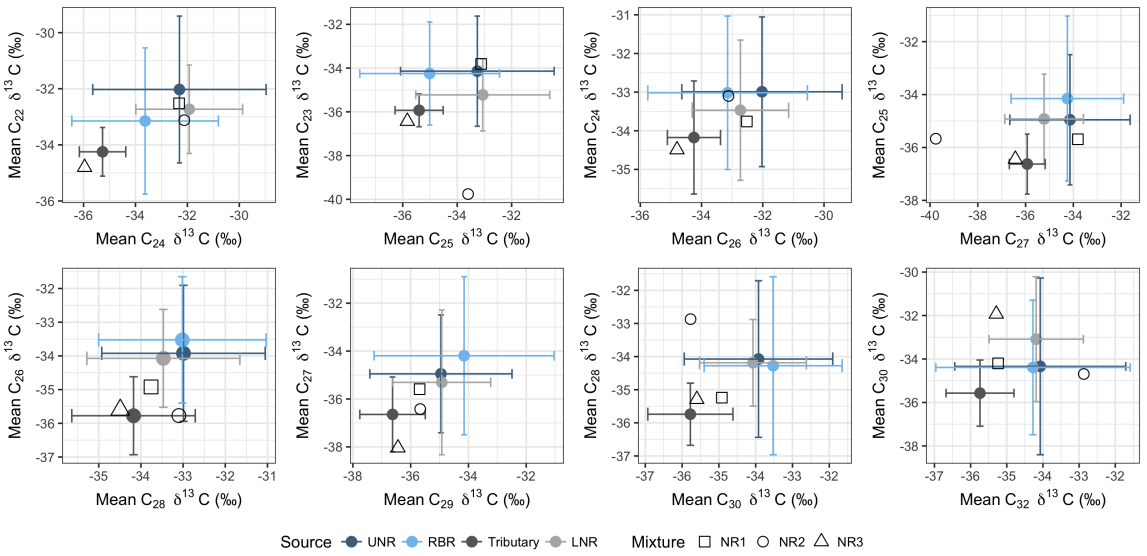

(a)

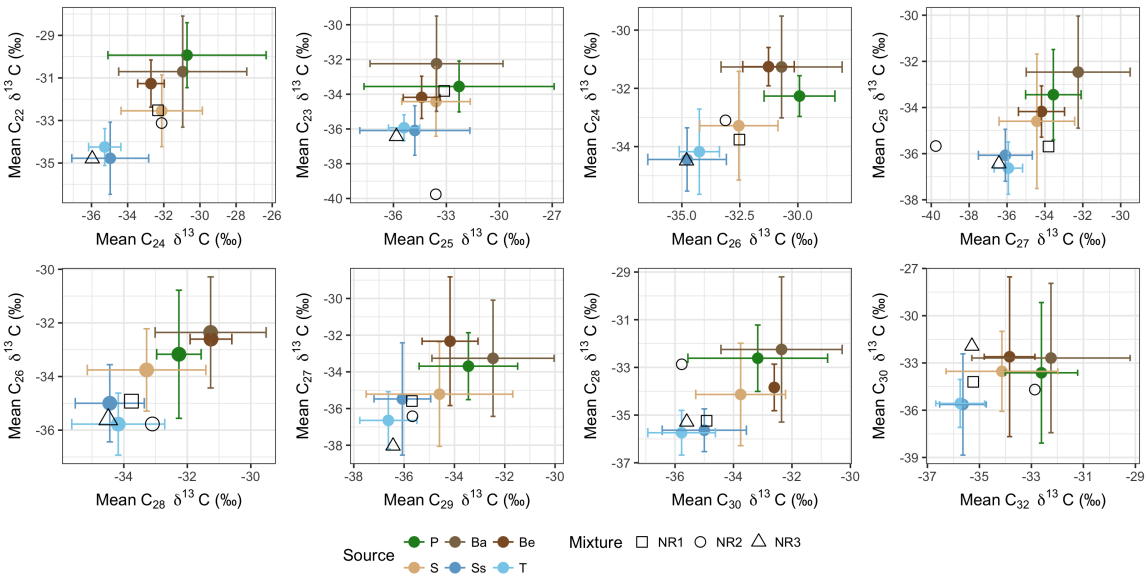

(b)

Fig. 3.8: Mixing polygons for pooled mixing models. (error bars represent ±1 standard deviation) **3.8a:** Pooled-spatial model. **3.8b:** Pooled-substrate model.

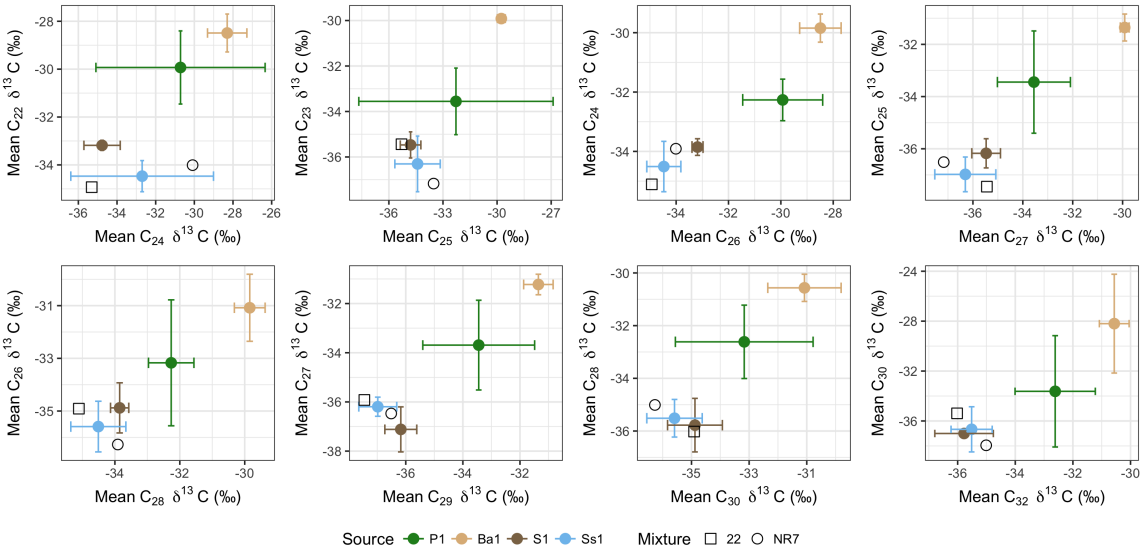

(a)

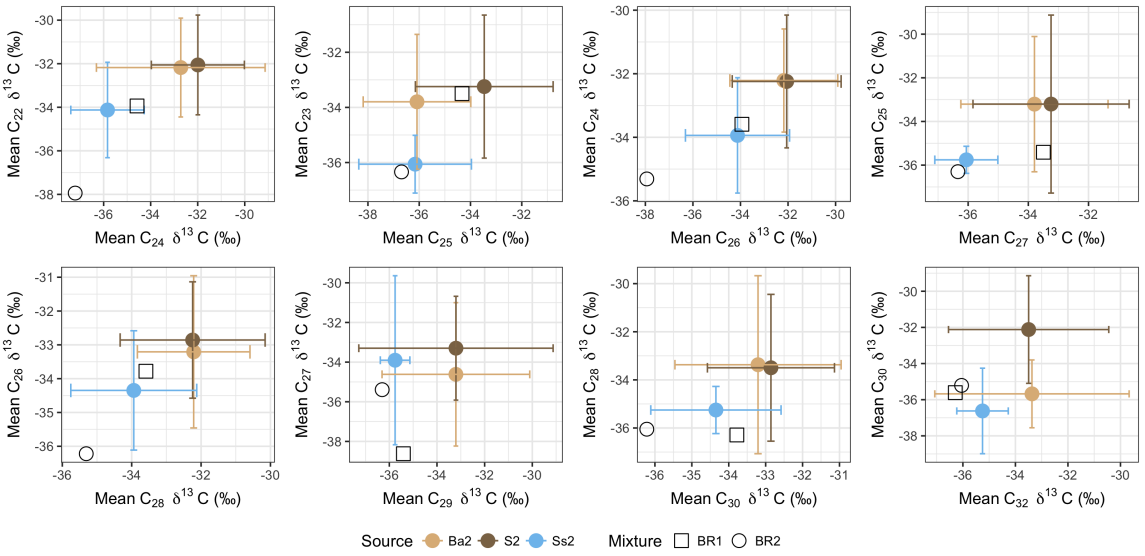

(b)

Fig. 3.9: Mixing polygons for deconvolutional mixing model. (error bars represent ±1 standard deviation) **3.9a:** Sources to mixture node M1. **3.9b:** Sources to mixture node M2. **3.9c:** Sources to mixture node M3.

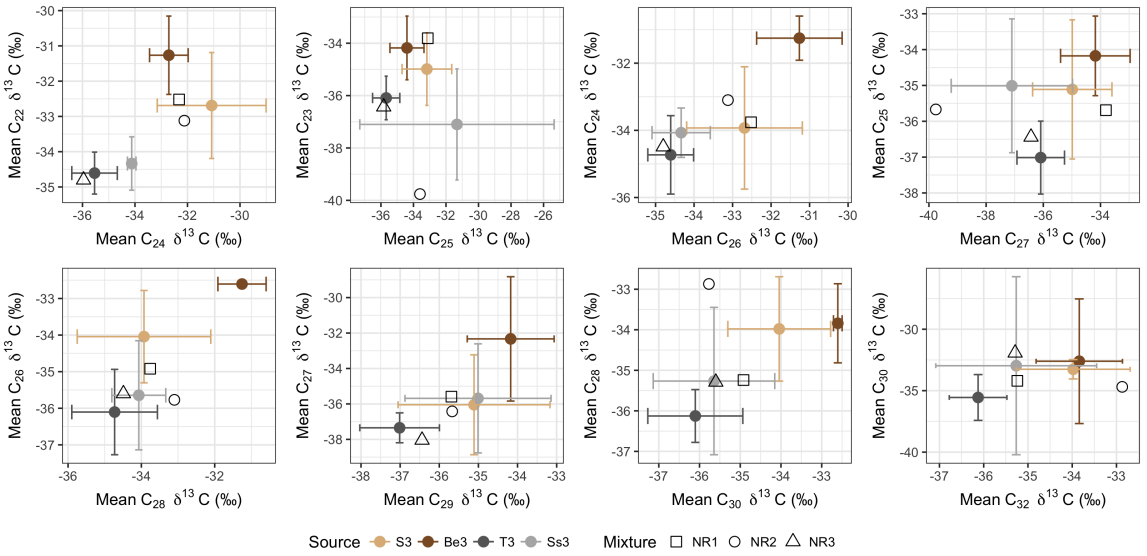

(c)

Fig. 3.9: Mixing polygons for deconvolutional mixing model. (error bars represent ±1 standard deviation) **3.9a:** Sources to mixture node M1. **3.9b:** Sources to mixture node M2. **3.9c:** Sources to mixture node M3.

C_{32}. In the deconvolutional model, source subsets to each mixture node were tested separately. Source means to mixture node M_1 are statistically different ($p < 0.05$, $n = 9$) for all FA tracers except for C_{22} and C_{23}. For mixture node M_2, no FA tracers show a statistical difference in source means ($p < 0.05$, $n = 13$), although C_{22} and C_{32} yield p-values < 0.1. Proximal sources to mixture node M_3 are only distinguished by FA tracers C_{22}, C_{24}, and C_{28} ($p < 0.05$, $n = 14$).

Whereas ANOVAs will determine if there are significant differences between source groups, Tukey HSD tests aim to show where exactly the differences in means exist and pinpoint the source combinations that are significantly different from each other. For the pooled-spatial model, all source combinations have high p-values ($p > 0.05$, $n = 39$) with a minimum p-value of 0.127 , which indicates that there is no statistically significant difference between means of each source type. In the pooled-substrate model, some FA tracers distinguish statistical differences ($p < 0.05$, $n = 39$) between certain source combinations.

For C_{24}, suspended sediment differs from peat sources, soils, and bank material; tributary suspended sediment is also distinguishable from bank material. Tracers C_{25}-C_{27} and C_{30} effectively differentiate between suspended sediment and bank material, as does C_{28} which also shows statistical significance between tributary suspended sediment and bank material. For sources to mixture node M_1, statistical differences between soil and bank material exist using FA tracers C_{24}, C_{25}, C_{26}, C_{27}, C_{29}, and C_{30}. Suspended sediment and bank material are shown to be significantly different by tracers C_{24}-C_{27} and C_{30}. FA tracers C_{24}, C_{25}, and C_{26} also shows statistical differences between respective source combinations of peat and other sources (soil and suspended sediment), bank material and peat, and peat paired with both bank material and suspended sediment. No statistical differences were observed between combinations of sources to mixture node M_2 and only FA tracers C_{22} and C_{28} shows differentiation between tributary suspended sediment and bed material of proximal sources to mixture node M_3.

Principal component analysis (PCA) was completed for each pooled model framework to determine the underlying structure and directions with the most variance, or principal components, within the data. PCA based on isotopic FA tracers shows that the two dimensions, principal component 1 (PC1) and principal component 2 (PC2) accounted for 76.06 % of the variance (PC1 = 65.09%, PC2 = 10.96%; Figure 3.10). Ellipses denoting each source group in both PCAs were calculated at 95 % confidence level. In both PCAs, isotopic tracer loadings show that all FA lengths are negatively correlated to PC1, whereas PC2 shows positive correlation with C_{22}-C_{24} and C_{32} and negative correlation with C_{25}-C_{30}. In the pooled-spatial model, most of the variance for UNR, RBR, and tributary sources is accounted for by PC1, whereas the largest variance for proximal LNR sources occurs on PC2 (Figure 3.10a). In the pooled-substrate model, bank material shows a large range of variation on both PC1 and PC2 (Figure 3.10b). Soils and suspended sediments see most variance on PC2 and tributary suspended sediments show most on PC1 (Figure 3.10b).

Since only 76.06 % of the variability is explained by these PCAs, not all sources in each model are necessarily distinguishable from one another.

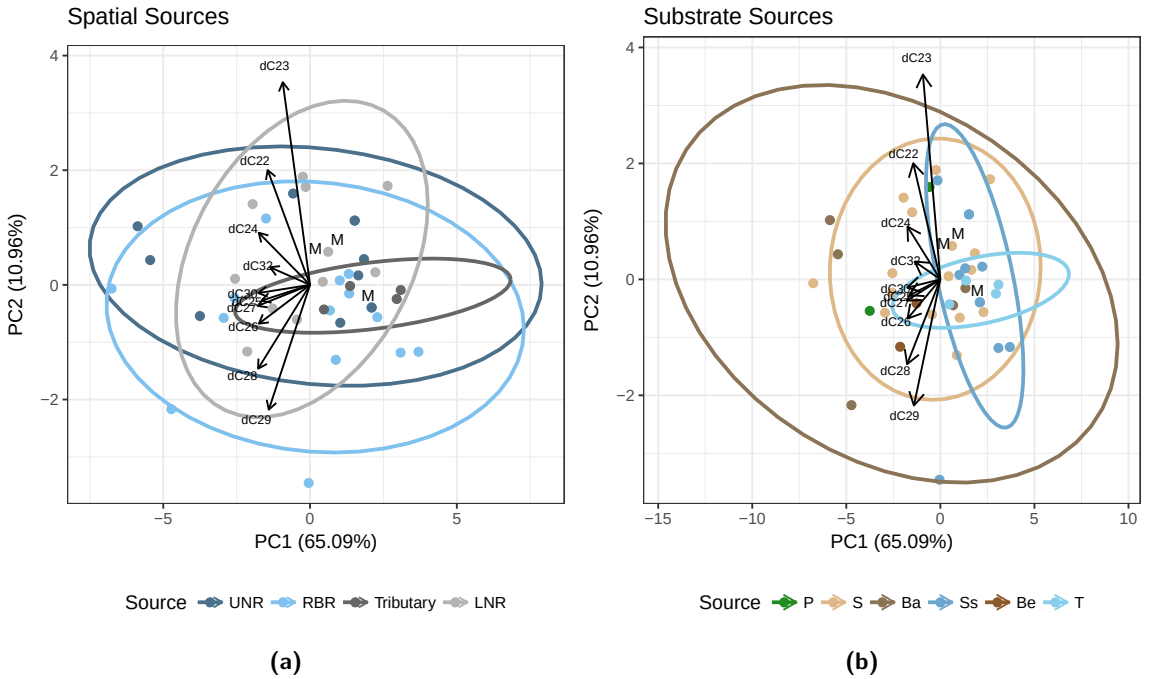

Fig. 3.10: Principal component analysis (PCA) with proportion of variance in parenthesis for Pooled mixing models. **3.10a:** Pooled-spatial model. **3.10b:** Pooled-substrate model.

MixSIAR unmixing models assume that each isotopic tracer exhibits a normal data distribution; when tested this was not the case for some tracers. Due to the limited size of the data set, no outliers were removed as this would effectively eliminate either important source material or reduce the number of sediment samples to a point where the mixing model could no longer calculate means and standard deviation. Eliminating tracers that do not show a normal distribution might also overlook unique features of sources or sediment mixtures that should be considered. As an initial investigation into using this method in the Nelson River system, it is thought to be more important to include all samples and tracers so that no potentially important sources are missed, especially if they represent material that has been proven to enter the river system through observations in the field.

3.3.4 MixSIAR modelling

Proportional source contributions to downstream suspended sediment in the lower Nelson River (mixture node M_3; Figure 3.7) were estimated by constructing three mixing model frameworks using both pooled-MixSIAR and deconvolutional-MixSIAR model styles.

Pooled models used catchment-wide source groups that are pooled to compare spatial- and substrate-based grouping of sources. The deconvolutional model accounted for sub-catchment specific sources to their respective proximal mixture nodes together with other downstream sources, before unmixing all of these sources against the final downstream-most mixture node.

3.3.4.1 Pooled MixSIAR models

Spatial sources Using fatty acid chain lengths C_{22}-C_{32} as tracers, sources in the pooled-spatial model were grouped into four regions of the study area: the UNR, the RBR, tributaries, and the LNR (Figure 3.7a). Pooled-MixSIAR results for this model are summarized in Table 3.3 (means ± SD) and Figure 3.11a (means ± SD; median and quartiles). The estimated mean relative contributions of each spatial source to sediment at mixture node M_3 indicate that dominant sources are tributaries (48.8 % ± 12.7%) and proximal LNR sources (30.1 % ± 15.0%). Both UNR and RBR sources reflect less of a contribution at 11.1 % ± 8.6% and 10.0 % ± 8.3% respectively. The proportional contribution of tributaries compared to upstream catchments are notable since the discharge of each tributary is far less than that of the RBR and UNR (<10 % and <3 % respectively).

The Gelman-Rubin Diagnostic test reported that 0 of 5 variables are above expected values of 1.05 The Geweke Diagnostic test is a standard z-score and reported only 1 variable on MCMC Chain 2 outside of the expected ± 1.96 range. Results of these diagnostic tests

Table 3.3: Proportional contributions to M_3 suspended sediment using pooled MixSIAR model frameworks. Sources for all model designs are abbreviated where UNR: upper Nelson River, RBR: Rat-Burntwood River, LNR: lower Nelson River, P: Peat, S: Soil, Ba: Bank, Be: Bed sediment, T: Tributary suspended sediment, Ss: upstream suspended sediment. Mean ± standard deviation.

Model Framework	Source	n	Contribution (%)
Pooled (Spatial)	UNR	10	11.1 ± 8.6
	RBR	14	10.0 ± 8.3
	Tributary	4	48.8 ± 12.7
	LNR	11	30.1 ± 15.0
Pooled (Substrate)	P	2	1.2 ± 1.0
	S	16	19.0 ± 10.5
	Ba	5	16.0 ± 13.6
	Be	2	15.1 ± 12.8
	T	3	32.7 ± 12.9
	Ss	8	16.0 ± 12.9

indicate that the model achieved convergence and that the estimated posterior distributions of each spatial region source type are accurate (Stock & Semmens, 2016).

Substrate sources Using FA chain lengths C_{22}-C_{32} as tracers, sources in the pooled-substrate model were grouped into six groups: peat, soil, bank material, bed sediment, tributary suspended sediment, and upstream suspended sediment (Figure 3.7a). Pooled-MixSIAR results for this model are summarized in Table 3.3 (means ± SD) and Figure 3.11b (means ± SD; median and quartiles). The estimated mean relative contributions of each source to sediment at mixture node M_3 indicate that dominant sources are tributaries (32.7 % ± 12.9%) and soils (19.0 % ± 10.5%), with near equal contributions of bank (16.0 % ± 13.6%), suspended sediment (16.0 % ± 12.9%) and bed sediment sources (15.1 % ± 12.8%). Peat sources are negligible at 1.2 % ± 1.0%.

Results of the Gelman-Rubin Diagnostic test indicate that 0 of 7 variables are above expected values of 1.05 The Geweke Diagnostic test reported only 2 variables on MCMC

Chain 3 outside of the expected ± 1.96 range. Results of these diagnostic tests indicate that the model achieved convergence and that the estimated posterior distributions of each substrate source type are accurate.

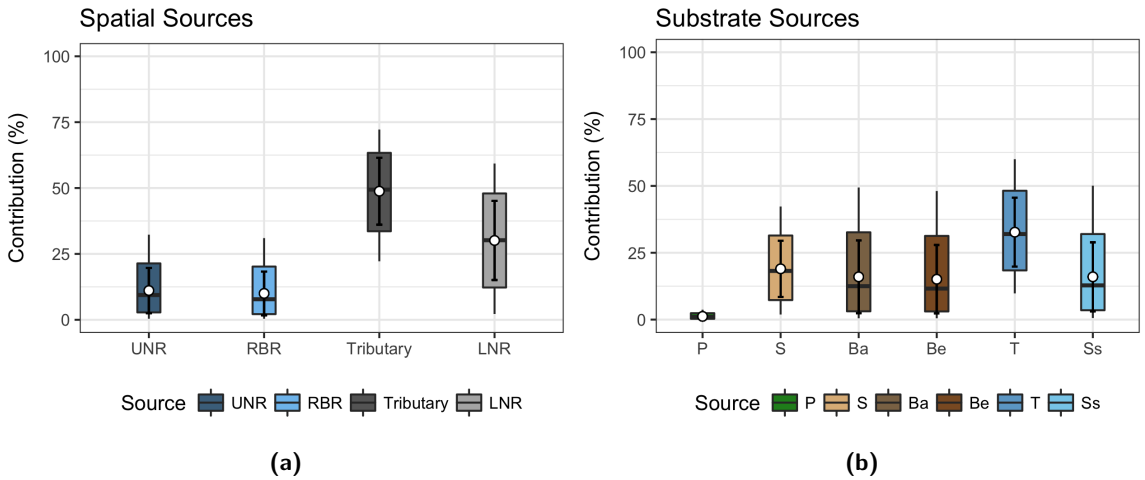

(a) **(b)**

Fig. 3.11: Proportional contributions to M_3 suspended sediment using Pooled mixing model framework. **3.11a:** Pooled spatial model. **3.11b:** Pooled substrate model. Median values shown by middle bars, upper and lower hinges represent 75th and 25th quantile, upper and lower whiskers are the y and x minimums, white circles are means ± 1 standard deviation. (UNR: upper Nelson River, RBR: Rat-Burntwood River, LNR: lower Nelson River, P: Peat, S: Soil, Ba: Bank, Be: Bed sediment, T: Tributary suspended sediment, Ss: upstream suspended sediment)

3.3.4.2 Deconvolutional MixSIAR model

Fatty acid chain lengths C_{22}-C_{32} were used as tracers in this deconvolutional MixSIAR model. Since D-MixSIAR uses a step-wise approach to unmixing in watersheds with sub-catchments, the estimated mean relative contributions to each upstream mixture node will be outlined separately prior to listing results from the final unmixing against mixture node M_3.

Sources to the M_1 mixture node are divided into four categories: peat (P_1), soil (S_1), bank material (Ba_1), and suspended sediment (Ss_1) (Figure 3.7b). D-MixSIAR results for

Table 3.4: Proportional contributions to M_3 suspended sediment using deconvolutional MixSIAR model framework. Sources for all model designs are abbreviated where P: peat, S: soil, Ba: bank, Ss: suspended sediment, Be: bed sediment and T: tributary suspended sediment. Mean ± standard deviation.

Model Framework	Mixture Node	Source	n	Contribution (%)
Deconvolutional	M_1	P_1	2	0.6 ± 0.5
		Ba_1	2	19.6 ± 15.3
		S_1	3	17.3 ± 11.7
		Ss_1	2	62.5 ± 16.1
	M_2	Ba_2	3	20.9 ± 17.0
		S_2	6	3.1 ± 2.9
		Ss_2	4	76.0 ± 16.6
	M_3	M_1	2	9.0 ± 8.0
		M_2	2	7.7 ± 6.3
		S_3	7	28.4 ± 12.3
		Be_3	2	19.1 ± 15.7
		T_3	3	15.8 ± 10.7
		Ss_3	2	20.0 ± 13.9

this model are summarized in Table 3.4 (means ± SD) and Figure 3.12 (means ± SD; median and quartiles). The estimated mean relative contributions of each source to sediment at mixture node M_1 indicate that the dominant source is upstream suspended sediment (62.5 % ± 16.1%) with near equal contributions of bank (19.6 % ± 15.3%) and soil (17.3 % ± 11.7%). Peat sources are negligible at 0.6 % ± 0.5%.

Sources to the M_2 mixture node are divided into four categories: soil (S_2), bank material (Ba_2), and suspended sediment (Ss_2) (Figure 3.7b). The estimated mean relative contributions of each source to sediment at mixture node M_2 indicate that the dominant source is upstream suspended sediment (76.0 % ± 16.6%) followed by bank (20.9 % ± 17.0%) and soil (3.1 % ± 2.9%).

Using a statistical function in R software developed by Blake et al. (2018) (Listing B.1), the results from each subcatchment are taken into account as sources to the final unmixing

against mixture node M_3. Sources to M_3 comprise M_1, M_2, as well as proximal sources in the LNR that consist of soil (S_3), bed sediment (Be_3), tributary suspended sediment (T_3), and upstream suspended sediment (Ss_3) (Figure 3.7b). The estimated mean relative contributions of each source to sediment at mixture node M_3 indicate that the dominant source is proximal soils (28.4 % ± 12.3%) followed by upstream suspended sediment in the LNR (20.0 % ± 13.9%), LNR bed sediment (19.1 % ± 15.7%), and proximal tributaries (15.8 % ± 10.7%). Sources from each subcatchment yield lower estimated contribution proportions with 9.0 % ± 8.0% (M_1) and 7.7 % ± 6.3% (M_2).

Results of the Gelman-Rubin Diagnostic test for the final unmixing against M_3 indicate that 0 of 7 variables are above expected values of 1.05 The Geweke Diagnostic test reported one variable on MCMC Chain 1 and one variable on MCMC Chain 2 outside of the ± 1.96 range. Results of these diagnostic tests indicate that the model achieved convergence and that the estimated posterior distributions of each source type are accurate (Stock & Semmens, 2016).

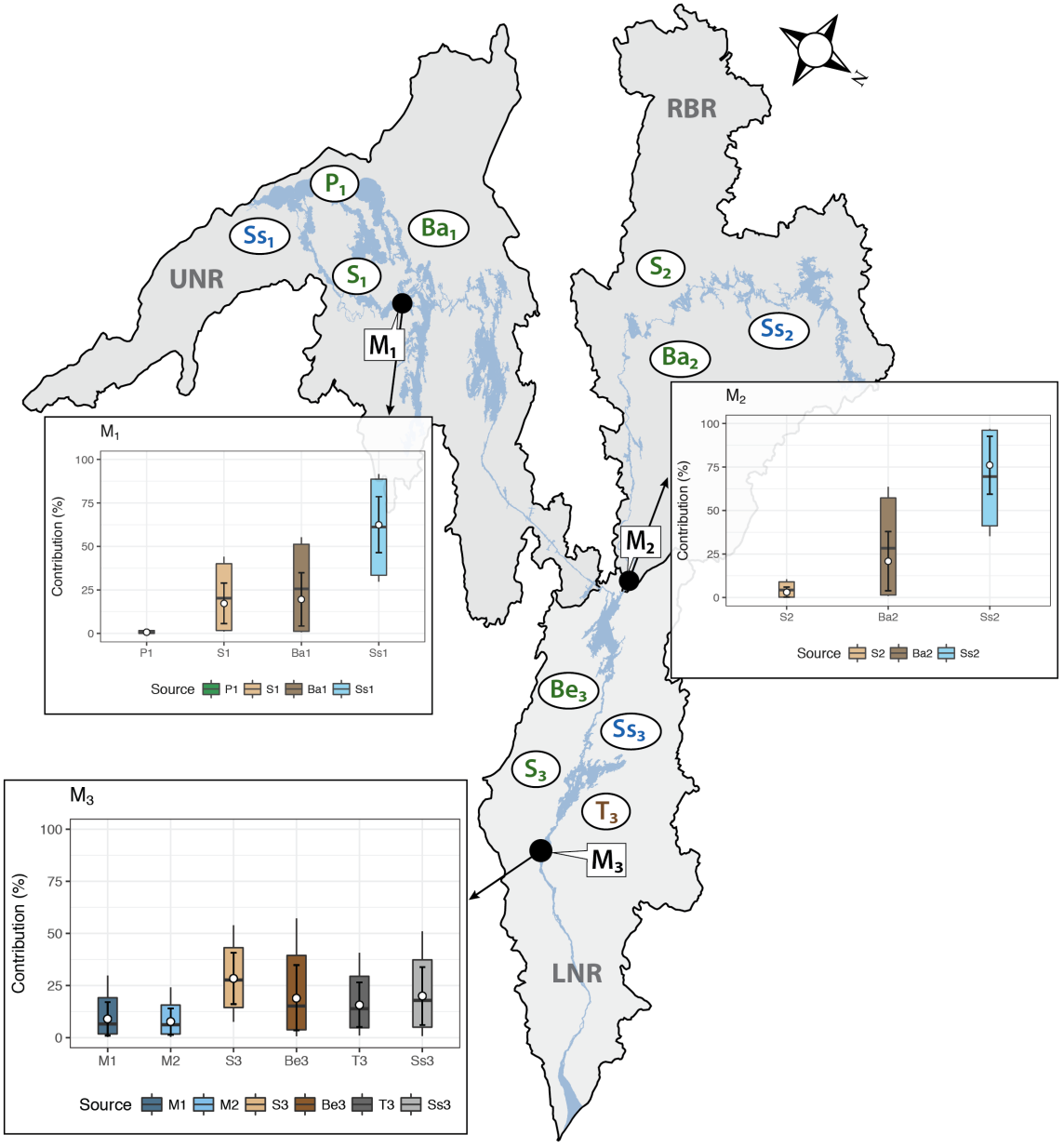

Fig. 3.12: Proportional contributions to M_3 suspended sediment using deconvolutional MixSIAR model framework. Sources for deconvolutional model design are abbreviated where P: peat, S: soil, Ba: bank, Ss: suspended sediment, Be: bed sediment and T: tributary suspended sediment. Black circles represent all mixture nodes. In inset plots, median values shown by middle bars, upper and lower hinges represent 75th and 25th quantile, upper and lower whiskers are the y and x minimums, white circles are means $\pm$ standard deviation.

3.4 Discussion

Previous work in the study area concerning OM in the Nelson River system predominantly focused on OM delivery to Hudson Bay and involved the calculation of dissolved OC exports to Hudson Bay (Kirk & St. Louis, 2009), bulk characterization of particulate OM at the river mouth (using atomic C/N ratios and bulk δ^{13}C composition) as part of carbon budgeting to Hudson Bay (Kuzyk et al., 2009), and the investigation of OM physical and chemical properties (particulate OC concentration and bulk δ^{13}C composition) alongside the calculation of particulate carbon fluxes to Hudson Bay (Godin et al., 2017). To date, work within the watershed to yield information on particulate OM has been undertaken by Manitoba Hydro (or hired consultants on their behalf) that reported bulk sediment properties such as concentration of particulate OC in water, % OC in suspended or lake sediments (Baker, 1989; Green, 1990; Strange, 1990; Environment Canada and Department of Fisheries and Oceans, 1992b; Coordinated Aquatic Monitoring Program, 2014). A gap is left by these investigations to discover the dominant sources delivering particulate OM to the Nelson River system, and the extent of their transport downstream.

The MixSIAR modelling exercise seeks to test the findings determined from bulk properties (SuspOC and C/N) concerning OM sources and their longitudinal variation within this system. This work has attempted to shed light on OM sources within the watershed through the application of CSSI analysis of particulate organic matter in the Nelson River system. This is the first study to use CSSI fingerprinting and sophisticated mixing models to estimate the relative proportion of OM sources from each major subcatchment and from proximal sources to downstream suspended sediment in the lower Nelson River. Sediment fingerprinting using unmixing models and MixSIAR applied to inorganic properties have previously been employed within the study area (Theroux, 2017). The results discussed in this section represent an initial investigation using CSSI fingerprinting methods which

have been applied in previous work to small watersheds containing both C_3 and C_4 land plants and used to differentiate between land use sources (Gibbs, 2008; Blake et al., 2012; Hancock & Revill, 2012; Alewell et al., 2016; Upadhayay, Smith, et al., 2018). Since C_3 and C_4 plants use different photosynthetic pathways, typical $\delta^{13}C$ values are readily distinguishable from one another with ranges between $-32.0\,‰$-$-22.0\,‰$ and $-16.0\,‰$-$-9.0\,‰$ respectively. This study area contains no C_4 plants, and therefore presents a challenge for the distinction of OM sources with overlapping $\delta^{13}C$ value ranges (e.g. C_3 land plants, macrophytes, SOM, and lacustrine algae). In view of the large size and complexity of the Nelson River system and the relatively uniformity of its vegetation, the results should be thought of as a preliminary evaluation of particulate OM sources to the LNR.

3.4.1 Mixing model framework evaluation and comparison

Prior to discussing the sources of particulate OM to the LNR, an evaluation and comparison of each mixing model framework must be made. Diagnostic and statistical tests are important in the assessment of each model framework, but physical and chemical processes occurring within the riverine and lacustrine environment must also be considered.

All model frameworks in this study are concentration-dependent, which accounts for the difference in relative fatty acid concentrations in each source during the unmixing process. Previous CSSI studies, such as Alewell et al. (2016) and Gibbs (2008), used concentration-independent, linear stable isotope mixing models that corrected for concentration after unmixing. More recent work recommended a concentration-dependent model that more realistically estimates source contributions (Upadhayay et al., 2017; Upadhayay, Smith, et al., 2018). Individual fatty acid chain lengths for some sources show vastly different $\delta^{13}C$ values than others and if the concentration of the respective FA is not considered, it may skew the importance of that tracer in either source or sediment samples. Concentration-

dependency also helps to put into perspective the importance of some sources that show very high concentrations of FAs in source samples. For example, UNR peat sources in the pooled-substrate model show high median concentrations of FAs C_{22} (20.19 wt%) and C_{24} (18.60 wt%) and high proportions of OC (32.34 %), but due to deposition or degredation, contribute a negligible amount to downstream sediment at mixture node M_3.

Using study area regions as source groups, the pooled-spatial model estimates that the dominant OM sources contributing to sediment at mixture node M_3 come from tributaries (48.8 % ± 12.7%) and proximal LNR sources (30.1 % ± 15.0%). Lesser input is received from the upstream UNR (11.1 % ± 8.6%) and RBR (10.0 % ± 8.3%) systems. This model was constructed as an experiment to see if each individual catchment has its own spatially distinct OM signature, but based on statistical tests, this is not the case. Neither the ANOVA nor the Tukey HSD test shows statistically significant differences between regional source types for any of the FA tracers. Principal component analysis determined that the variance of all four source groups overlap (Figure 3.10a). This model framework combines multiple source substrates to define regional source groups, which is logical to a point since it divides the two catchments flowing to the LNR that each exhibit different geophysical characteristics. However, this model does not determine the proportion of OM source substrate types that contribute the most to sediment downstream, and lacks the ability to define where within each region OM sources are derived.

In the pooled-substrate model, the highest estimated mean relative OM source contributions are from tributaries (32.7 % ± 12.9%) and soils (19.0 % ± 10.5%) whereas bank, suspended sediment, and bed sources exhibit near equal proportions of around 16.0 %. Peat sources are negligible at 1.2 % ± 1.0%. This model adheres to the conventional application of MixSIAR that pools and categorizes OM sources by substrate-type and shows statistical distinction between sources for all but three of the ten FA tracers. In this model, a Tukey HSD test reveals that tracers can only reliably differentiate between suspended sediment

and terrestrial sources. If sources are grouped as such, the combined terrestrial contribution outweighs that of suspended sediment in this model. Similar to the pooled-spatial model, principal component analysis determined that the variance of all four source groups overlaps (Figure 3.10b). Although this model accounts for all possible source substrates, it does not allow for differentiation of sources from each region of the study area, which makes interpretation of localized source contribution results more difficult and less meaningful. If the goal is to determine sources of OM that contribute most to downstream sediment, it is also just as important to determine where these sources originate.

The deconvolutional model estimates that upstream suspended sediment OM sources dominate suspended composition at both mixture nodes M_1 (62.5 % $\pm$ 16.1%) and M_2 (76.0 % $\pm$ 16.6%) and bank material in both subcatchments contributes $\sim$20.0 %. Most tracers statistically differentiate sources to M_1, whereas none do for sources to M_2. In the UNR, this is likely due to the large spectrum of distinct OM sources (e.g. algae in suspended samples from Lake Winnipeg, peat, and bank material rich in mineral sediment), but also due to the fact that key suspended sediment samples had to be used as both sources and mixtures. Tukey HSD tests distinguished between bank material and soils/suspended sediments for some FA tracers in M_1 sources, but no source combinations are statistically different for M_2 sources. The lack of statistically significant differences between sources to M_2 in the RBR could indicate homogeneity in OM composition between sources, which is seen in similar % OC, bulk δ^{13}C, and δ^{13}C of individual FA results outlined in Section 3.3.1.1. The ultimate sources of OM in the RBR, therefore, are similar regardless of their proximity to the downstream mixture node. Clay-rich banks and their associated soils and vegetation, along with wide-spread bank erosion observed in the field could explain the general homogeneity between suspended sediment and terrestrial OM sources. Total suspended solids in the RBR system are dominantly comprised of silt- to clay-sized mineral sediment, attributed by many studies to an influx of eroded bank material into the system caused by

the Churchill River Diversion (Hecky & McCullough, 1984; Newbury & McCullough, 1984; Newbury et al., 1984).

Using the newly developed deconvolutional MixSIAR function (Blake et al., 2018), the estimated mean relative contributions of each source to sediment at mixture node M_3 indicate that the dominant source is proximal soils (28.4 % ± 12.3%) followed by upstream suspended sediment in the LNR (20.0 % ± 13.9%), LNR bed sediment (19.1 % ± 15.7%), and proximal tributaries (15.8 % ± 10.7%). Sources from each upstream subcatchment show much lower proportions (<10 %). Proximal sources to M_3 were only distinguished by three FA tracers, and only a statistical distinction between tributary and bed sediment source means could be made. Shortcomings aside, based on field observations and subcatchment characteristics, this model illustrates the most intuitively reasonable breakdown of sources contributing to each mixture node and will be explained further in the next section.

Although all models achieved convergence in MixSIAR, they are all limited in some way by tracer effectiveness, non-normal distributions of some data subsets, and a lack of significant differences between some sources. Based on the above, it was determined that the deconvolutional model best estimates the sources to sediment at mixture node M_3 and therefore will be the main topic of the remaining sections. The study area size and budget of this M.Sc. project did not allow for more in-depth sampling and sample analysis. Interpretation of sources presented in subsequent sections should be read with the realization that this is an initial study of OM sources in the Nelson River system, and that more work should be done to improve upon mixing model results.

3.4.2 Sources of sediment to the lower Nelson River

As previously discussed, the dominant OM sources contributing to downstream suspended sediment (M_3) are proximally derived soils (S_3), upstream suspended sediment

(Ss_3), bed sediment (Be_3), tributary suspended sediment (T_3), and upstream subcatchment sources (M_1 and M_2).

Organic matter (and mineral sediment) from soils enter waterbodies in the LNR by natural bank or bluff erosion where rivers incise the glacial sediments in this region. This erosion is perhaps more prevalent since construction of the CRD and the reservoir impoundment upstream of Kettle GS that produced Stephens Lake. Cosford et al. (2013) reported that most of the sediment accumulating in the lake is derived from bank or bluff erosion, which delivers both mineral sediment and abundant OM from peat. Shoreline soils at Stephens Lake contain buried peat layers (Figure 3.3b) representing the pre-flooded surface and were observed at site NR4 where shorelines were scalloped and actively slumping from wave action. Bank or bluff slumping was observed at all sampling sites in the LNR and appear to be related to water level fluctuations, common in the entire hydroelectric system. This provides a likely explanation for the abundance of soil sources contributing to downstream suspended sediment.

In general, bed sediment is resuspended when water velocity increases. Altered flow regimes in LNR waterbodies and fluctuations in discharge rates due to daily fluctuations in hydroelectric power needs could explain the observed upstream bed sediment contributions to downstream suspended sediment.

Approximately 35 % of OM at M_3 was sourced from upstream (Ss_3) and tributary (T_3) suspended sediment sources indicating that suspended particulate OM from both the main stem LNR and tributaries persists in suspension as river waters flow through Stephens Lake and three hydroelectric dams (Kettle GS, Long Spruce GS, and Limestone GS), in spite of the fact that reservoirs are thought to act as sinks removing sediment from suspension (Fryirs, 2013). When bulk $\delta^{13}C$ properties of these sources are compared using typical compositional ranges of particulate OM, most source samples comprise OM signatures analogous

with SOM or C_3 terrestrial plants (Figure 3.5d).

Minor OM source signatures from the UNR (M_1) and RBR (M_2) each contribute 9 % and 7.7 % to downstream suspended sediment at M_3, respectively. This is notable because discharge from the UNR (75 %) and RBR (25 %) to the LNR vary considerably. Both the UNR and RBR mixture nodes comprise mostly upstream suspended sediment sources when unmixed against their respective in-catchment sources. In the UNR, the lack of suspended sediment source samples required samples to be grouped from different sources. If more samples were collected from each compositionally distinct source (lacustrine algae vs. SOM), more information could be gained from the relative contribution of each of these upstream suspended sediment sources to the LNR mixture.

To summarize, OM in downstream suspended sediment in the LNR is predominantly derived from sources within the LNR or associated tributaries. Although soils dominate, suspended sediment that contains OM classified within the SOM range contributes an estimated combined proportion of ∼35 %, and minor sources from subcatchments also show the same SOM compositional signature. Therefore, erosional processes in the LNR that deliver soils and OM derived from soils are important drivers of the input of OC to the LNR and downstream to Hudson Bay.

3.4.3 CSSI fingerprinting effectiveness and utility in the Nelson River system

Based on model diagnostics, the deconvolutional MixSIAR model achieved convergence and estimated posterior source distributions are accurate. However, the effectiveness of mixing model results using MixSIAR depends on the quality of data and therefore completeness of investigations in the field to yield robust results.

Although the lack of statistically significant differences between sources and lack of

normally distributed data for certain tracers are attributed mainly to the small size of the CSSI data set, another major shortcoming that may hinder the effectiveness of this fingerprinting method can be illustrated by biplot analysis. Sediment compositions in the deconvolutional model do not fall within the range of source compositions for some tracer combinations (Figure 3.9), potentially due to a missed source. Other sediment compositions are too well defined as a result of how each subcatchment's model was constructed due to sample availability. In the UNR, sediment isotopic composition falls within source ranges in M_1 because suspended sediment in the UNR was used as both a source and a downstream mixture due to lack of samples (Figure 3.9a). The lack of data in this catchment is due to the difficulty and cost of access. Since bulk properties (SuspOC and C/N) indicate a dominantly lacustrine algae signature is present in particulate OM in the UNR, it was decided that suspended organic sediment from Lake Winnipeg is likely a notable source. Since there were only two suspended sediment samples analyzed from the UNR, and the deconvolutional model requires mean values for sediment mixture input, these samples had to be grouped, yielding an overly simplistic relationship to source and sediment composition in mixing polygon biplots. In the RBR, sediment from site BR2 falls outside the source isotopic range for many tracer combinations (Figure 3.9b). This indicates that either one (or more) main sources were missed from sampling, or that not enough samples were collected from each major source type to account for variation in isotopic composition. As site BR2 is just downstream of a small tributary that drains low-lying wetlands, perhaps small tributaries contribute OM compositionally different than the larger tributary sampled in the RBR. In the LNR, a similar issue arose with sediment from site NR2 that falls outside source isotopic ranges for some tracer combinations (Figure 3.9c), indicating that either a key source was missed or duplicates of NR2 should have been collected to ensure the isotopic composition at this site was properly represented.

It is worth emphasizing that only the particulate fraction of OM was studied in the Nel-

son River system, and information is missing on sources supplied by the dissolved fraction. Also, no samples were collected from the Grass River watershed, a tributary draining into the UNR (Figure 3.2). All in all, it is possible that some significant sources were missed, the number of samples was insufficient to cover variation within source types, or sediment samples that do not fall within isotopic source ranges are anomalous. Collection of more sediment samples would help to address these issues.

3.4.4 Modelling limitations and recommendations for future work

The author recognizes that CSSI tracers yielded results on source contributions consistent with previous literature and field observations, but also realizes that these results could be improved by addressing some of the limitations of this study and implementing a number of recommendations, to be discussed in this section. The most significant limitations faced by this study were the size and remoteness of the study area, and the high cost of both fieldwork and CSSI analysis.

Waterbodies (river channels and lakes) in the study area flow over a combined length of ∼900 km through remote areas with few roads making access and equal sampling coverage in each region a significant challenge. Since all field work was completed by truck, sample collection was limited to truck-accessible sites during the summer season. The results of this study are only applicable to summer conditions, and do not describe sources in any other season. The size of the study area and length of time required to collect bulk samples (at least 3 h per site) also limited the number of sites visited during field investigations. Temporal variance in OM sources could be addressed through the collection of samples from dated sediment cores. Specifically, the use of CSSI fingerprinting on sediment cores could be used to investigate changes to OM sources in the Nelson River system before and after major hydroelectric power development projects.

Analytical costs incurred by CSSI fingerprinting are very high. The entire cost per sample, including bulk analysis (such as FA quantification, % OC and bulk δ^{13}C) and CSSI analysis, was ~$320 Considering the size of the study area, it would be difficult to fund a program that included enough samples to run a more effective model and gain more robust results.

All in all, the author's recommendations for future work include: increased site density, increased number of samples collected at each site (including sediment duplicates), sample collection in the Grass River watershed, and sample collection in regions of the upper Nelson River not covered by this study. Other possible means of sample analysis could include stable nitrogen isotope ratios (δ^{15}N) to better characterize and distinguish between terrestrial and algal sources, and ^{14}C dating of soils and bank material to determine whether comparatively "old" or "new" OC is contributed to the Nelson River system. It is also recommended, if most OM in suspended sediment mixtures in the LNR are sourced locally, that a more detailed study on proximal sources in the LNR using this CSSI tracer set could be implemented. All of the above are especially important considering planned reservoir flooding of peatlands associated with the current construction of the Keeyask GS upstream of Stephens Lake (ECOSTEM Ltd., 2011).

3.5 Conclusions

Through the use of CSSI analysis and the δ^{13}C of individual FA chain lengths as tracers, mixing models were constructed using MixSIAR, a flexible Bayesian statistics-based model framework. Although three models were tested, it is likely that the new deconvolutional MixSIAR method best estimates source proportions to downstream suspended sediment in the LNR because it accounts for the complexity of the river system by including results from nested subcatchments. Based on this model, dominant OM sources comprise soils,

upstream suspended sediment, bed sediment, and tributary suspended sediment proximally derived from the LNR region, whereas OM from subcatchments (UNR and RBR) contribute the least to downstream suspended sediment.

Though the small sample size limited the power of this method, it is apparent that proximal OM sources dominate downstream suspended sediment mixtures in the LNR. Sources contributing OM to the downstream-most reaches of the LNR visited in this study are indicators of OM sources delivered to Hudson Bay and therefore the LNR warrants further study.

This work represent the first application of CSSI fingerprinting using MixSIAR in the Nelson River system, and demonstrates its potential for more detailed study of the sources and transport of particulate OM in the Nelson River system.

Chapter 4

Final synthesis and conclusions

4.1 Summary of conclusions and research significance

The general goal of this thesis was to assess the sources of suspended sediment and particulate organic matter (OM) within the Nelson River watershed and the extent of their transport downstream. To achieve this goal, the specific research objectives were to: 1) examine historical and newly collected summer-season physical and chemical water quality data from riverine stations to identify the characteristics and distribution of particulate matter sources in the Nelson River system, and 2) use compositional and biochemical tracers, Compound-Specific Stable Isotope (CSSI) fingerprinting techniques, and Bayesian statistical unmixing models to quantify the relative source contributions to particulate OM in downstream suspended sediments.

Previous work concerning particulate matter (both OM and mineral sediment) in the Nelson River system include programs conducted by industry, provincially- and federally-funded monitoring programs, and academic institutions (Section 1.3). Although the Nelson River system has been extensively studied, and many of these programs measured param-

eters related to particulate matter, little work has been done to explore particulate matter sources and processes that may affect their downstream transport in all regions of the watershed, or to determine what OM sources ultimately contribute the highest proportions to downstream suspended sediment and ultimately to Hudson Bay.

To meet Objective 1, physical and chemical water quality data were used to characterize particulate OM sources in each region of the Nelson River system and investigate longitudinal and temporal changes to the sources of particulate matter (OM and mineral sediment) in the study area as a whole. Water quality parameters examined in this thesis include the measured concentration of total suspended solids (TSS), suspended organic carbon (SuspOC) and total suspended nitrogen (SuspN) from surface water samples, as well as calculated parameters derived from these concentrations such as % SuspOC of TSS and molar C/N ratios. Particulate water quality data for this thesis were collected from the study area via new field investigations and water sample analysis, and through the compilation of existing water quality data sets from historical and ongoing monitoring programs.

Distinct regional, longitudinal, and temporal differences in water quality parameters and particulate OM sources were observed among all three regions of the Nelson River system. Particulate matter concentration in the UNR was generally low, and included a high proportion of suspended SuspOC derived from a dominantly lacustrine source that has increased over time due to increased algal productivity in Lake Winnipeg. The RBR mainly contributes mineral sediment and OM associated with soils with generally high TSS and low SuspOC concentrations. Suspended sediment concentrations in the RBR have also increased over time. Although concentrations of particulate matter are high due to abundant erosional sites advanced by permafrost degradation, the proportion of SuspOC in TSS is low (and has decreased over time) since the bulk of bank material comprises silt-clay sized mineral sediment from glacial deposits. The LNR shows variation in water quality parameter concentrations and particulate OM derived from both lacustrine algae

and soil OM sources. Over time, TSS concentration has increased and the proportion of SuspOC has decreased, likely due to an increased input of particulate matter from the RBR or local shoreline/bank destabilization. The distinct OM compositional signatures of the LNR's upstream catchments do not persist throughout the length of the LNR as waters flow through a series of reservoirs and hydroelectric dams.

Using results from this thesis, bulk properties of OM (δ^{13}C and C/N) can be compared to average compositional ranges of particulate OM reported in the literature, and in doing so it is evident that most OM in suspended sediment samples have a soil organic matter (SOM) signature (Figure 4.1). In the UNR, OM composition consists of a mixture of lacustrine algae and SOM, whereas in the RBR, OM in suspended sediment sources is derived predominantly from SOM, but also classifies near the same composition as sphagnum. Organic matter in suspended sediment from the LNR and all tributaries is also derived from SOM. Thus, bulk OM properties demonstrate that there are weak regional differences in OM composition that relate to source differences and that SOM is a significant OM source. Particulate OM at paired sites in both the UNR (NR8 and NR7) and RBR (BR5 and BR3), show a decrease in nitrogen and increase in δ^{13}C between the lacustrine environment and the downstream river channel (Figure 4.1, inset panel). This suggests that either labile, autochthonous OM sources from lakes are broken down in the riverine system, changing the composition of OM within the watershed, or that the river is picking up material with less nitrogen from river banks or the river bottom.

To meet Objective 2 and further tease apart source contributions to downstream suspended sediment, CSSI fingerprinting using unmixing models and MixSIAR were employed to estimate the proportional contribution of OM sources to downstream suspended sediment. In addition to bulk properties (% organic carbon (OC) and bulk δ^{13}C), CSSI analysis on newly collected terrestrial and in-stream material yielded biochemical and isotopic compositions of OM based on individual fatty acid (FA) chain lengths (FA weight % and δ^{13}C values

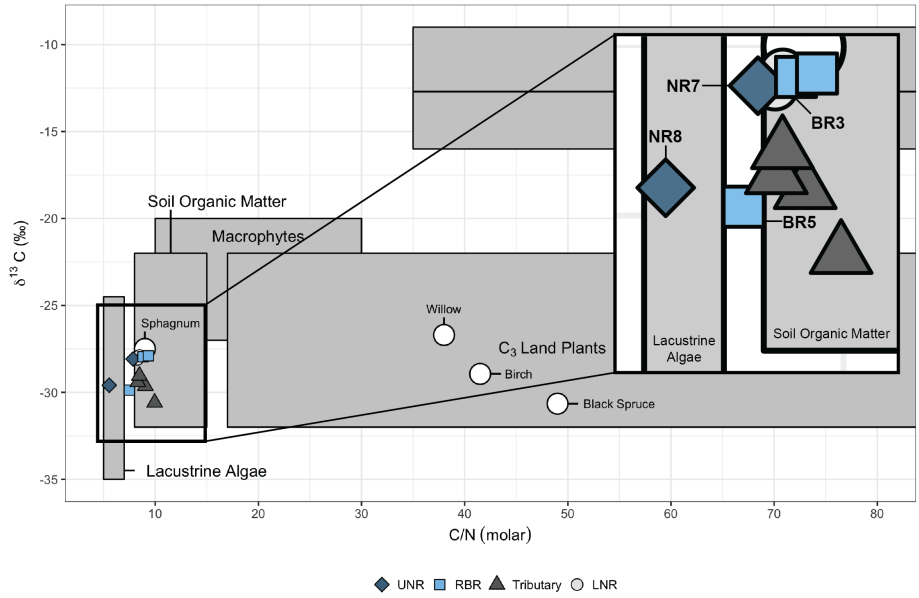

Fig. 4.1: Mean molar C/N ratios plotted versus bulk δ^{13}C ratios of suspended sediment samples collected from all regions of the study area compared to ranges of lacustrine algae, SOM, C3 plants, C4 plants, and macrophytes determined by Meyers and Ishiwatari (1993) and summarized by Kendall et al. (2001). Typical values for plants present in the study area are shown by white circles (Meyers, 1994; Meyers et al., 1995; Chikaraishi & Naraoka, 2003; Moingt et al., 2016). Inset panel shows selected sites (labeled) from the UNR and RBR where a change in the OM characteristics occurs downstream from lacustrine to soil source. Locations of labeled sites are shown in Figures 2.2 and 3.2.

for tracers C_{22}-C_{32}). These parameters were used to create spatial- and substrate-specific unmixing models.

The δ^{13}C values for FAs C_{22}-C_{32} were used as tracers in the construction of unmixing models using MixSIAR, a flexible Bayesian statistics-based model framework. The deconvolutional MixSIAR method best accounts for the complexity of the Nelson River watershed by including results from nested subcatchments (Blake et al., 2018) in the estimation of proportional source contributions to downstream suspended sediment in the LNR. Based on this model, dominant OM sources comprise soils, upstream suspended sediment, bed sediment, and tributary suspended sediment (listed in rank order) that are proximally derived from the LNR region, whereas OM from subcatchments (UNR and RBR) contributes the least to downstream suspended sediment. However, the data from two years of sampling

do not meet the needs of the deconvolutional model. Furthermore, the CSSIs of FAs were limited in their ability to differentiate regional sources.

Although OM composition and particulate concentration vary longitudinally and over time, as outlined in both Chapter 2 and 3, processes that promote river bank and shoreline erosion (e.g. permafrost degradation, water level fluctuation, current and wave action) persist in all regions of the study area. Agricultural land use dominates upstream of the UNR, but neither water quality parameters nor CSSI fingerprinting directly identify OM associated with crop vegetation in the study area. Indirect effects of agricultural activities however, such as eutrophication in Lake Winnipeg, was clearly seen using both techniques. Both the bulk properties and CSSI of FAs of suspended sediment in all regions reveal that OM is dominantly derived from SOM, via watershed processes that promote the addition of soils (and associated OM) into suspension. Proximal OM sources dominate the composition of downstream suspended sediment in the LNR and most of these sources comprise either soil material itself or upstream suspended sediment containing OM with the same bulk properties as SOM.

The Nelson River conforms to the general scheme established for dammed river systems and shows discontinuity in sediment transport (Kondolf, 1997; Syvitski et al., 2005; Fryirs, 2013) and changes to water body morphologies, hydraulic regimes, and geochemical cycles throughout the watershed (Rosenberg et al., 1997; Friedl & Wuest, 2002). The Nelson River delivers particulate OC to Hudson Bay at an estimated annual rate of $53\,\mathrm{Gg\ yr^{-1}}$ (Godin et al., 2017), and based on results from this thesis, most of this particulate OC is locally sourced from OM in the LNR. The lower reach of the LNR is underlain by extensive discontinuous or continuous permafrost, and its landscape is dominated by peat plateaus and open permafrost bogs (Halsey et al., 1997). Changes to climate and hydrological conditions in subarctic regions like the LNR makes the below-ground OC pool present in soils or shallow permafrost vulnerable to re-enter the modern carbon cycle (Tarnocai et al.,

2009; Gustafsson et al., 2011). Since particulate OC is a major component of thaw-released permafrost carbon in fluvial systems (Guo & Macdonald, 2006; Guo et al., 2007), processes in the LNR that deliver soils and OM derived from soils into suspension in river waters are important to consider with regard to the input of OC to the lower reaches of the LNR and ultimately Hudson Bay.

4.2 Focus for future research

This research was conducted as part of the Hudson Bay System Study (BaySys) project, which, in collaboration with six academic institutions and Manitoba Hydro, is investigating the relative impacts of hydroelectric activity and climate change on the freshwater-marine coupling in Hudson Bay (Barber, 2015).

Due to the expansive size of the study area and expense associated with conducting field work in the region, a number of recommendations can be made for future work in the Nelson River system. Results from this thesis represent conditions during the summer months over the course of two field seasons and only provide a snapshot in seasonality for all parameters from 2016-2017. Although the hydrograph of the Nelson River system is affected by hydroelectric power production, a multi-seasonal approach over multiple years to water and suspended sediment sampling would inform as to how these results may differ between seasons and year over year. This could be achieved by the installation of sediment traps at key sites in the study area.

Although limited by budgetary constraints, this work would have benefited from the addition of more sampling sites, especially in the lower reaches of both the UNR and LNR. No new samples were collected in these areas since they are inaccessible by road. Of particular interest in the LNR is the region between site NR1 and the river mouth (Figures 2.2 and 3.2). Annual particulate OC fluxes estimated by Godin et al. (2017) were calculated

using samples from the Nelson River mouth, ∼100 km downstream of NR1. Since OM in downstream suspended sediment is dominantly sourced from the LNR, increased sample density in this section of the LNR would be beneficial. All samples for this work were collected from the shoreline. Although nearshore samples were tested for and found to be free of bias (in one limited test), it is recommended that in future programs either mid-channel or full channel transects by boat are completed to collect suspended sediment and water samples. To investigate OM sources over time, sediment core collection in on-system waterbodies is recommended. An attempt was made to collect sediment cores for this purpose, but more work is needed to locate sampling sites with undisturbed sedimentation records that are datable as coring sites selected did not yield usable results. All in all, a more comprehensive, multidisciplinary, long term study on the Nelson River system is recommended.

In the LNR, a study investigating the relative ages of OC sources that contribute to downstream suspended sediment using radiocarbon dating would be of interest. A significant portion of the LNR was once submerged beneath waters of the Tyrrell Sea, leaving expansive glaciomarine sediment deposits. Peatlands also sequester OC over time, and therefore it would be interesting to study the relative ages of OC entering the Nelson River system to determine if long-term mechanisms of carbon storage on the landscape are being degraded and contributing ancient carbon downstream to Hudson Bay. An increasing number of studies are linking the liberation of old OC in soils and permafrost and its mobilization by rivers from the landscape to an increase in release of CO_2 to the atmosphere as it is processed by the coastal zone carbon cycle. As the largest subarctic river discharging to Hudson Bay with extensive peatlands that is undergoing permafrost degradation and exhibiting pervasive shoreline/bank erosion, the Nelson River is an ideal system in which to apply similar research.

References

Alewell, C., Birkholz, A., Meusburger, K., Schindler Wildhaber, Y., & Mabit, L. (2016). Quantitative sediment source attribution with compound-specific isotope analysis in a C3 plant-dominated catchment (central Switzerland). *Biogeosciences*, *13*(5), 1587–1596.

Arctic Climate Impact Assessment. (2005). *ACIA - Arctic climate impact assessment*. New York: Cambridge University Press.

Aufdenkampe, A. K., Mayorga, E., Raymond, P. A., Melack, J. M., Doney, S. C., Alin, S. R., ... Yoo, K. (2011). Riverine coupling of biogeochemical cycles between land, oceans, and atmosphere. *Frontiers in Ecology and the Environment*, *9*(1), 53–60.

Auguie, B. (2017). gridextra: Miscellaneous functions for "grid" graphics [Computer software manual]. Retrieved from `http://CRAN.R-project.org/package=gridExtra` (R package version 2.3)

Badeck, F. W., Tcherkez, G., Nogues, S., Piel, C., & Ghashghaie, J. (2005). Post-photosynthetic fractionation of stable carbon isotopes between plant organs - a widespread phenomenon. *Rapid Communications in Mass Spectrometry*, *19*, 1381–1391.

Baker, R. F. (1989). An environmental assessment and biological investigation of the Nelson River estuary (Tech. Rep.). Prepared for Manitoba Hydro by North/South

Consultants Inc. 160 pp.

Baker, R. F., & Davies, S. (1989). Biophysical effects of the Churchill River diversion and Lake Winnipeg regulation on aquatic ecosystems (Tech. Rep.). North/South Consultants Inc. 120 pp.

Baker, R. F., & Davies, S. (1991). Physical, chemical, and biological effects of the Churchill River diversion and Lake Winnipeg regulation on aquatic ecosystems. *Canadian Technical Report of Fisheries and Aquatic Sciences 1806*, 1–53.

Baker, R. F., Lawrence, M. J., & Schneider, F. (1993). Oceanography and mid-summer distribution and abundance of plankton and fish in the Nelson River Estuary, Hudson Bay (Report No. 4153). Prepared for Manitoba Hydro by North/South Consultants Inc. 67 pp.

Barber, D. (2015). BaySys - Contributions of climate change and hydroelectric regulation to the variability and change of freshwater-marine coupling in the Hudson Bay System (Research Proposal). Centre for Earth Observation Science, University of Manitoba.

Battin, T. J., Kaplan, L. A., Findlay, S., Hopkinson, C. S., Marti, E., Packman, A. I., ... Sabater, F. (2008). Biophysical controls on organic carbon fluxes in fluvial networks. *Nature Geoscience*, *1*(2), 95–100.

Bianchi, T. S. (2011). The role of terrestrially derived organic carbon in the coastal ocean: A changing paradigm and the priming effect. *Proceedings of the National Academy of Sciences*, *108*(49), 19473–19481.

Blake, W. H., Boeckx, P., Stock, B., Smith, H. G., Bodé, S., Upadhayay, H. R., ... Semmens, B. (2018). A deconvolutional Bayesian mixing model approach for river basin sediment source apportionment. *Scientific Reports*, *8*(1), 1–12.

Blake, W. H., Ficken, K. J., Taylor, P., Russell, M. A., & Walling, D. E. (2012). Tracing crop-specific sediment sources in agricultural catchments. *Geomorphology*, *139-140*(C), 322–329.

Cai, W. J. (2011). Estuarine and coastal ocean cabon paradox: CO2 sinks or sites of terrestrial carbon incineration? *Annual Review of Marine Science*, *3*, 123–145.

Chikaraishi, Y. (2014). 13C/12C Signatures in Plants and Algae. In H. D. Holland & K. K. Turekian (Eds.), *Treatise on Geochemistry* (2nd ed., pp. 95–123). Elsevier Science.

Chikaraishi, Y., & Naraoka, H. (2003). Compound-specific δD–δ13C analyses of n-alkanes extracted from terrestrial and aquatic plants. *Annual Review of Marine Science*, *63*(3), 361–371.

Cole, J. J., Carpenter, S. R., Kitchell, J. F., & Pace, M. L. (2002). Pathways of organic carbon utilization in small lakes: Results from a whole-lake 13C addition and coupled model. *Limnology Oceanography*, *47*(6), 1664–1675.

Cole, J. J., Prairie, Y. T., Caraco, N. F., McDowell, W. H., Tranvik, L. J., Striegl, R. G., ... Melack, J. (2007). Plumbing the global carbon cycle: Integrating inland waters into the terrestrial carbon budget. *Ecosystems*, *10*, 171–184.

Coordinated Aquatic Monitoring Program. (2014). Three year summary report (2008-2010). Report prepared for the Manitoba/Manitoba Hydro MOU Working Group. *North/South Consultants Inc.*.

Coplen, T. B. (1994). Reporting of stable hydrogen, carbon and oxygen isotopic abundances. *Pure and Applied Chemistry*, *66*(2), 273–276.

Corkery, T. M. (1996). Geology and Landforms of Manitoba. In J. Welsted, J. Everitt, & C. Stadel (Eds.), *The geography of manitoba: Its land and its people* (pp. 11–30). Winnipeg: University of Manitoba Press.

Cosford, J., Glaser, P., Penner, L., & St. Laurent, M. (2013). Characteristics of nearshore sedimentation from coring in Stephens Lake, Manitoba, a 35-year old hydroelectric reservoir (CDA 2013 Annual Conference). Canadian Dam Association.

Déry, S. J., Stieglitz, M., McKenna, E. C., & Wood, E. F. (2005). Characteristics and

trends of river discharge into Hudson, James, and Ungava Bays, 1964–2000. *Journal of Climate*, *18*(14), 2540–2557.

Duboc, Q., St-Onge, G., & Patrickl, L. (2017). Sediment records of the influence of river damming on the dynamics of the Nelson and Churchill Rivers, western Hudson Bay, Canada, during the last centuries. *The Holocene*, *27*(5), 712–725.

Dyke, L. D., & Sladen, W. E. (2010). Permafrost and peatland evolution in the northern Hudson Bay Lowland, Manitoba. *ARCTIC*, *63*(4), 429–441.

ECOSTEM Ltd. (2011). Keeyask Generation Project, Stage IV Studies - Physical Environment: Composition and Distribution of Shoreline and Inland Peatlands in the Keeyask Reservoir Area and Historical Trends in Peatland Disintegration (Manitoba Hydro File: No. 00195-11100-00152-01). Report prepared for: Hydro Power Planning Department, Power Projects Development Division, Power Supply, 1-127.

Eglinton, G., & Hamilton, R. J. (1967). Leaf epicuticular waxes. *Science*, *156*, 1322–1335.

Egré, D., & Milewski, J. C. (2002, November). The diversity of hydropower projects. *Energy Policy*, *30*(14), 1225–1230.

Environment and Climate Change Canada. (2017, February). *Canadian Climate Normals (1981-2010).* Retrieved from `http://climate.weather.gc.ca/climate_normals/`

Environment and Climate Change Canada. (2018a, August). *Canadian Historical Climate Data. Station Data: Cross Lake Jenpeg.* Retrieved from `http://climate.weather.gc.ca/historical_data/search_historic_data_e.html`

Environment and Climate Change Canada. (2018b, August). *Canadian Historical Climate Data. Station Data: Gillam A.* Retrieved from `http://climate.weather.gc.ca/historical_data/search_historic_data_e.html`

Environment and Climate Change Canada. (2018c, August). *Canadian Historical Climate Data. Station Data: Thompson A.* Retrieved from `http://climate.weather.gc.ca/historical_data/search_historic_data_e.html`

Environment and Climate Change Canada. (2018d, February). *Kelsey Annual and Monthly Mean Flow (1960-2017).* Retrieved from `https://wateroffice.ec.gc.ca/mainmenu/historical_data_index_e.html`

Environment and Climate Change Canada. (2018e, February). *Longspruce Annual and Monthly Mean Flow (1987-2017).* Retrieved from `https://wateroffice.ec.gc.ca/mainmenu/historical_data_index_e.html`

Environment and Climate Change Canada. (2018f, February). *Thompson Annual and Monthly Mean Flow (1957-2017).* Retrieved from `https://wateroffice.ec.gc.ca/mainmenu/historical_data_index_e.html`

Environment Canada and Department of Fisheries and Oceans. (1992a). Federal Ecological Monitoring Program Final Report (Volume 1). Environment Canada, Conservation and Protection Western and Northern Region, and Department of Fisheries and Oceans, Central and Arctic Region, 1-58.

Environment Canada and Department of Fisheries and Oceans. (1992b). Federal Ecological Monitoring Program Final Report (Volume 2). Environment Canada, Conservation and Protection Western and Northern Region, and Department of Fisheries and Oceans, Central and Arctic Region, 1-42.

Environment Canada and Department of Fisheries and Oceans. (1992c). Federal Ecological Monitoring Program Summary Report (Tech. Rep.). Environment Canada, Conservation and Protection Western and Northern Region, and Department of Fisheries and Oceans, Central and Arctic Region, 1-20.

Friedl, G., & Wuest, A. (2002). Disrupting biogeochemical cycles – Consequences of damming. *Aquatic Sciences*, *64*, 55–65.

Fryirs, K. (2013). (Dis)Connectivity in catchment sediment cascades: a fresh look at the sediment delivery problem. *Earth Surface Processes and Landforms*, *38*, 30–46.

Gellis, A. C., & Walling, D. E. (2011). Sediment source fingerprinting (tracing) and sediment

budgets as tools in targeting river and watershed restoration programs. In A. Simon, S. J. Bennet, & J. M. Castro (Eds.), *Stream restoration in dynamic fluvial systems: scientific approaches, analyses, and tools.* (pp. 263–291). Washington, DC, USA: Geophysical Monograph Series, American Geophysical Union.

Gibbs, M. M. (2008). Identifying source soils in contemporary estuarine sediments: a new compound-specific isotope method. *Estuaries and Coasts*, *31*(2), 344–359.

GIS Map Gallery. (2006). Surficial Geology Compilation Map Series. *Manitoba Science, Technology, Energy and Mines, Manitoba Geological Survey*. Retrieved from `http://geoapp2.gov.mb.ca/website/surficialgeo/viewer.htm`

Glaser, B. (2005). Compound-specific stable-isotope (δ13C) analysis in soil science. *Journal of Plant Nutrition and Soil Science*, *168*(5), 633–648.

Godin, P. (2014). Using Lignin Biomarkers and 14C, of both River DOC and POC, and Permafrost Soils, to Characterize the Impacts of Climate Warming and Permafrost Degradation on the Organic Carbon Budget of the Hudson Bay, Canada. (Unpublished master's thesis). *University of Manitoba*.

Godin, P., Macdonald, R. W., Kuzyk, Z. A., Goñi, M. A., & Stern, G. A. (2017). Organic matter compositions of rivers draining into Hudson Bay: Present-day trends and potential as recorders of future change. *Journal of Geophysical Research: Biogeosciences*, *122*, 1848–1869.

Goñi, M. A., Moore, E., Kurtz, A., Portier, E., Alleau, Y., & Merrell, D. (2014). Organic matter compositions and loadings in soils and sediments along the Fly River, Papua New Guinea. *Geochimica et Cosmochimica Acta*, *140*(C), 275–296.

Green, D. J. (1990). Physical an chemical water quality data collected from the Rat-Burntwood and Nelson River systems, 1985-1989 (Fisheries Branch MS report No. 90-15). Manitoba Department of Natural Resources, 1-242.

Guo, L., & Macdonald, R. W. (2006). Source and transport of terrigenous organic matter

in the upper Yukon River: Evidence from isotope (δ 13C, Δ 14C, and δ 15N) composition of dissolved, colloidal, and particulate phases. *Global Biogeochemical Cycles*, *20*(GB2011), 1–12.

Guo, L., Ping, C.-L., & Macdonald, R. W. (2007). Mobilization pathways of organic carbon from permafrost to arctic rivers in a changing climate. *Geophysical Research Letters*, *34*(13), 1–5.

Gustafsson, O., van Dongen, B. E., Vonk, J. E., Dudarev, O. V., & Semiletov, I. P. (2011). Widespread release of old carbon across the Siberian Arctic echoed by its large rivers. *Biogeosciences*, *8*, 1737–1743.

Halsey, L., Vitt, D., & Zoltai, S. (1997). Climatic and physiographic controls on wetland type and distribution in Manitoba, Canada. *WETLANDS*, *17*(2), 243–262.

Hancock, G. J., & Revill, A. T. (2012). Erosion source discrimination in a rural Australian catchment using compound-specific isotope analysis (CSIA). *Hydrological Processes*, *27*(6), 923–932.

Hecky, R. E., & McCullough, G. K. (1984). Effect of impoundment and diversion on the sediment budget and nearshore sedimentation of Southern Indian Lake. *Canadian Journal of Fisheries and Aquatic Sciences*, *41*, 567–578.

Hedges, J. I., Keil, R. G., & Benner, R. (1997). What happens to terrestrial organic matter in the ocean? *Organic Geochemistry*, *27*(5-6), 195–212.

Ittekkot, V., & Laane, R. W. P. M. (1991). Fate of Riverine Particulate Organic Matter. In E. T. Degens, S. Kempe, & J. E. Richey (Eds.), *Scope 42 - biogeochemistry of major world rivers* (pp. 1–356). Chichester: John Wiley.

J.D. Mollard and Associated (2010) Limited. (2009). Keeyask Generation Project, Stage IV Studies - Physical Environment, Nearshore Lake Bottom Sediment Coring (Manitoba Hydro File: 00195-11100-00163-01). Prepared for: Hydro Power Planning Department, Power Projects Development Division, Power Supply.

Kellerhals Engineering Services Ltd. (1987). Morphological Effects of the Churchill River Diversion Volume 1: General Assessment (Northern Flood Agreement Manitoba Ecological Report Series). Prepared for: Environment Canada, Inland Water Directorate.

Kellerhals Engineering Services Ltd. (1988). Morphological Effects of the Churchill River Diversion Volume 2: Feasibility Studies and Monitoring Recommendations (Northern Flood Agreement Manitoba Ecological Report Series). Prepared for: Environment Canada, Inland Water Directorate.

Kendall, C., Silva, S. R., & Kelly, V. J. (2001). Carbon and nitrogen isotopic compositions of particulate organic matter in four large river systems across the United States. *Hydrological Processes*, *15*(7), 1301–1346.

Kirk, J. L., & St. Louis, V. L. (2009). Multiyear total and methyl mercury exports from two major sub-arctic rivers draining into Hudson Bay, Canada. *Environmental Science and Technology*, *43*(7), 2254–2261.

Koiter, A. J., Owens, P. N., Petticrew, E. L., & Lobb, D. A. (2013). The behavioural characteristics of sediment properties and their implications for sediment fingerprinting as an approach for identifying sediment sources in river basins. *Earth-Science Reviews*, *125*, 24–42.

Kondolf, G. M. (1997). Hungry Water: Effects of Dams and Gravel Mining on River Channels. *Environmental Management*, *21*(4), 533–551.

Kuzyk, Z. A., Macdonald, R. W., Johannessen, S. C., Gobeil, C., & Stern, G. A. (2009). Towards a sediment and organic carbon budget for Hudson Bay. *Marine Geology*, *264*(3-4), 190–208.

Lake Winnipeg Stewardship Board. (2007). Reducing Nutrient Loading to Lake Winnipeg and its Watershed. Lake Winnipeg Stewardship Board Final Report to the Minister of Water Stewardship. Retrieved from `http://www.gov.mb.ca/waterstewardship/water_quality/lake_winnipeg/lwsb2007-12_final_rpt.pdf`

Mackenzie, F. T., & Lerman, A. (2006). *Carbon in the Geobiosphere.* Dordrecht, The Netherlands: Springer.

Manitoba Hydro. (1991). Churchill River Diversion, 1991 Erosion Study (Report No. 91G11). Geotechnical Department, Engineering and Construction.

Manitoba Hydro. (2015). Regional Cumulative Effects Assessment for Hydroelectric Developments on the Churchill, Burntwood and Nelson River systems: Phase II Report. Retrieved from `https://www.hydro.mb.ca/regulatory_affairs/rcea/pdf/rcea_phase2_part_i_preface_and_introduction.pdf`

Manitoba Water Stewardship. (2005, January). *Manitoba Gross Watersheds.* Manitoba Water Stewardship. Retrieved from `http://web2.gov.mb.ca/mli`

McConnachie, J. L., & Petticrew, E. L. (2006). Tracing organic matter sources in riverine suspended sediment: Implications for fine sediment transfers. *Geomorphology*, *79*(1-2), 13–26.

McCullough, G. K., Page, S. J., Hesslein, R. H., Stainton, M. P., Kling, H. J., Salki, A. G., & Barber, D. G. (2012). Hydrological forcing of a recent trophic surge in Lake Winnipeg. *Journal of Great Lakes Research*, 1–11.

Meyers, P. A. (1994). Preservation of elemental and isotopic source identification of sedimentary organic matter. *Chemical Geology*, *114*(3-4), 289–302.

Meyers, P. A., & Ishiwatari, R. (1993). Lacustrine organic geochemistry - an overview of indicators of organic matter in sources and diagenesis in lake sediments. *Organic Geochemistry*, *20*(7), 867–900.

Meyers, P. A., Leenheer, M. J., & Bourbonniere, R. A. (1995). Diagenesis of vascular plant organic matter components during burial in lake sediments. *Aquatic Geochemistry*, *1*, 35–52.

Meyers, P. A., & Teranes, J. L. (2001). Sediment organic matter. In W. M. Last & J. P. Smol (Eds.), *Tracking Environmental Change Using Lake Sediments. Volume*

2: Physical and Geochemical Methods (pp. 239–269). Dordrecht, The Netherlands: Kluwer Academic Publishers.

Moingt, M., Lucotte, M., & Paquet, S. (2016). Lignin biomarker signatures of common plants and soils of eastern Canada. *Biogeochemistry*, *129*, 133–148.

Natural Resources Canada. (2013). *Earth sciences sector integrated model, expl, 50k* (Hydro Features). Retrieved from `http://ftp.geogratis.gc.ca/pub/nrcan_rncan/vector/canvec/shp/Hydro/`

Newbury, R. W., & McCullough, G. K. (1984). Shoreline erosion and restabilization in the Southern Indian Lake reservoir. *Canadian Journal of Fisheries and Aquatic Sciences*, *41*, 558–566.

Newbury, R. W., McCullough, G. K., & Hecky, R. E. (1984). The Southern lndian Lake Impoundment and Churchill River Diversion. *Canadian Journal of Fisheries and Aquatic Sciences*, *41*, 548–557.

North/South Consultants Inc. (2012). Limestone Generating Station: Aquatic Environment Monitoring Programs: A Synthesis of Results from 1985 to 2003 (Report for Manitoba Hydro). Retrieved from `https://keeyask.com/wp-content/uploads/2013/07/Limestone-GS-Synthesis-Part-1.pdf`

Northwest Hydraulic Consultants Ltd. (1987). Assessment of Sediment Effects, Churchill River Diversion, Manitoba (Phase I Report). Prepared for: Sediment Survey, Water Survey of Canada.

Northwest Hydraulic Consultants Ltd. (1988). Assessment of Sediment Effects, Churchill River Diversion, Manitoba (Phase II Report). Prepared for: Sediment Survey, Water Survey of Canada.

O'Leary, M. H. (1988, August). Carbon Isotopes in Photosynthesis. *BioScience*, *38*(5), 328–336.

Parnell, A. C., Phillips, D. L., Bearhop, S., Semmens, B. X., Ward, E. J., Moore, J. W.,

... Inger, R. (2013). Bayesian stable isotope mixing models. *Enironmentrics*, *24*(6), 387–399.

R Core Team. (2013). R: A language and environment for statistical computing [Computer software manual]. Vienna, Austria. Retrieved from `http://www.R-project.org/`

Reiffarth, D. G., Petticrew, E. L., Owens, P. N., & Lobb, D. A. (2016). Sources of variability in fatty acid (FA) biomarkers in the application of compound-specific stable isotopes (CSSIs) to soil and sediment fingerprinting and tracing: A review. *Science of the Total Environment*, *565*, 8–27.

Reiffarth, D. G., Petticrew, E. L., Owens, P. N., Reimer, K. B., & Lobb, D. A. (2018). Development of standardized protocols for the quantitative and 13C isotope analysis of very longchain fatty acids (VLCFAs) used in compound-specific stable isotope (CSSI) soil and sediment tracing. *Catena*, *Submitted August 2018*.

Robinson, D., Hayes, A., Gomez, M., Demeshev, B., Menne, D., Nutter, B., ... Werner, K. D. (2018). *Package 'broom'.* Retrieved from `http://github.com/tidyverse/broom` (Version 0.5.0)

Romanovsky, V. E., Isaksen, K., Drozdov, D., Anisimov, O. A., Instanes, A., Leibman, M. O., ... Walker, D. (2017). Changing permafrost and its impacts. In *Snow, Water, Ice and Permafrost in the Arctic (SWIPA)* (pp. 65–102). Oslo, Norway: Arctic Monitoring and Assessment Programme (AMAP).

Rosenberg, D. M., Berkes, F., Bodaly, R. A., Hecky, R. E., Kelly, C. A., & Rudd, J. W. M. (1997). Large-scale impacts of hydroelectric development. *Environmental Reviews*, *5*(1), 27–54.

Rosenberg, D. M., Chambers, P. A., Culp, J. M., Franzin, W. G., Nelson, P. A., Salki, A. G., ... Newbury, R. W. (2005). Nelson and Churchill River Basins. In A. C. Benke & C. E. Cushing (Eds.), *Rivers of North America* (pp. 1265–1303).

RSW-Environment Illimite Inc. (2014). Conwapa Generating Station - Stage IV Studies -

Physical Environment of the Nelson River Estuary, Existing Environment Sediment Processes, Revision 2 (Manitoba Hydro File: No. 00192-11100-0066). Report prepared for: Water Resources Engineering Department, Power Planning Division, Power Supply.

Sánchez-García, L., Alling, V., Pugach, S., Vonk, J. E., van Dongen, B., Humborg, C., ... Gustafsson, O. (2007). Inventories and behaviour of particulate organic carbon in the Laptev and East Siberian seas. , *25*, 1–13.

Schlesinger, W. H., & Melack, J. M. (2016). Transport of organic carbon in the world's rivers. *Tellus*, *33*(2), 172–187.

Sella, G. F., Stein, S., Dixon, T. H., Craymer, M., James, T. S., Mazzotti, S., & Dokka, R. K. (2007). Observation of glacial isostatic adjustment in "stable" North America with GPS. *Geophysical Research Letters*, *34*(L02306), 1–6.

Sikes, E. L., Uhle, M. E., Nodder, S. D., & Howard, M. E. (2009). Sources of organic matter in a coastal marine environment: Evidence from n-alkanes and their δ13C distributions in the Hauraki Gulf, New Zealand. *Marine Chemistry*, *113*(3), 149–163.

Simon, K. M., Riva, R. E. M., Kleinherenbrink, M., & Tangdamrongsub, N. (2017). A data-driven model for constraint of present-day glacial isostatic adjustment in North America. *Earth and Planetary Science Letters*, *474*, 322–333.

Split Lake Cree and Manitoba Hydro. (1996). Analysis of change: Split Lake Cree post project environmental review, Volume One (Tech. Rep.). Split Lake Cree/Manitoba Hydro Joint Study Group, 1-96.

Stainton, M. P., Capel, M. J., & Armstrong, F. A. J. (1977). The Chemical Analysis of Fresh Water, Second Edition. *Canadian Fisheries and Marine Service Miscellaneous Special Publication*(25), 1–180.

Stein, R., & Macdonald, R. W. (2004). Organic Carbon Budget: Arctic Ocean vs. Global Ocean. In R. Stein & R. W. Macdonald (Eds.), *The organic carbon cycle in the Arctic*

Ocean (pp. 315–322). Berlin; New York: Springer.

Stock, B. C., Jackson, A. L., Ward, E. J., Parnell, A. C., Phillips, D. L., & Semmens, B. X. (2018). Analyzing mixing systems using a new generation of Bayesian tracer mixing models. *PeerJ*, *6*(e5096), 1–27.

Stock, B. C., & Semmens, B. X. (2016). *MixSIAR GUI User Manual.* Retrieved from `https://github.com/brianstock/MixSIAR` (Version 3.1) doi: 10.5281/zenodo.1209993

Strange, N. (1990). Water quality data for sites affected by Churchill River Diversion and Lake Winnipeg Regulation, northern Manitoba, 1986-89 (Tech. Rep.). North/South Consultants Inc.

Syvitski, J. P. M., & Milliman, J. D. (2007). Geology, Geography, and Humans Battle for Dominance over the Delivery of Fluvial Sediment to the Coastal Ocean. *The Journal of Geology*, *115*(1), 1–19.

Syvitski, J. P. M., Vorosmarty, C., Kettner, A. J., & Green, P. (2005). Impact of humans on the flux of terrestrial sediment to the global coastal ocean. *Science*, *308*, 376–380.

Tarnocai, C., Canadell, J. G., Schuur, E. A. G., Kuhry, P., Mazhitova, G., & Zimov, S. (2009). Soil organic carbon pools in the northern circumpolar permafrost region. *Global Biogeochemical Cycles*, *23*, 1–11.

Teller, J. T., & Yang, Z. (2015). Mapping and measuring Lake Agassiz strandlines in North Dakota and Manitoba using LiDAR DEM data: Comparing techniques, revising correlations, and interpreting anomalous isostatic rebound gradients. *The Geological Society of America Bulletin*, *127*(3-4), 608–620.

Theroux, J. (2017). Characterizing turbidity and identifying sediment sources in Norway House Cree Nation drinking water using sediment fingerprinting (Unpublished master's thesis). *University of Manitoba*.

Umbanhowar, C. J., Camill, P., Edlund, M., Geiss, C., Durham, W., Kreger, D., ...

Williams, J. (2013). Contrasting changes in surface waters and barrens over the past 60 years for a subarctic forest-tundra site in northern Manitoba based on remote sensing imagery. *Canadian Journal of Earth Science*, *50*, 967–977.

Upadhayay, H. R., Bodé, S., Griepentrog, M., Bajracharya, R., Blake, W. H., Cornelis, W., & Boeckx, P. (2018). Isotope mixing models require individual tracer content for correct quantification of sediment source contributions. *Hydrological Processes*, *32*, 981–989.

Upadhayay, H. R., Bodé, S., Griepentrog, M., Huygens, D., Bajracharya, R., Blake, W. H., ... Boeckx, P. (2017). Methodological perspectives on the application of compound-specific stable isotope fingerprinting for sediment source apportionment. *Journal of Soils and Sediments*, *17*, 1537–1553.

Upadhayay, H. R., Smith, H. G., Griepentrog, M., Bodé, S., Bajracharya, R., Blake, W. H., ... Boeckx, P. (2018). Community managed forests dominate the catchment sediment cascade in the mid-hills of Nepal: A compound-specific stable isotope analysis. *Science of the Total Environment*, *637-638*, 306–317.

Venables, W. N., & Ripley, B. D. (2002). *Modern applied statistics with s* (Fourth ed.). New York: Springer. Retrieved from `http://www.stats.ox.ac.uk/pub/MASS4` (ISBN 0-387-95457-0)

Vitt, D. H., & Halsey, L. A. (1994). The bog landforms of continental and western Canada in relation to climate and permafrost patterns. *Arctic and Alpine Research*, *26*(1), 1–13.

Vonk, J. E., & Gustafsson, O. (2013). Permafrost-carbon complexities. *Nature Geoscience*, *6*(9), 675–676.

Vonk, J. E., Mann, P. J., Davydov, S., Davydova, A., Spencer, R. G. M., Schade, J., ... Holmes, R. M. (2013). High biolability of ancient permafrost carbon upon thaw. *Geophysical Research Letters*, *40*, 2689–2693.

Vonk, J. E., van Dongen, B., & Gustafsson, O. (2008). Lipid biomarker investigation of the origin and diagenetic state of sub-arctic terrestrial organic matter presently exported into the northern Bothnian Bay. *Marine Chemistry*, *112*, 1–10.

Walling, D. E. (2013). The evolution of sediment source fingerprinting investigations in fluvial systems. *Journal of Soils and Sediments*, *13*, 1658–1675.

Weihs, C., Ligges, U., Luebke, K., & Raabe, N. (2005). klar analyzing german business cycles. In D. Baier, R. Decker, & L. Schmidt-Thieme (Eds.), *Data analysis and decision support* (p. 335-343). Berlin: Springer-Verlag.

Wickham, H. (2016). *ggplot2: Elegant graphics for data analysis*. Springer-Verlag New York. Retrieved from `http://ggplot2.org`

Wickham, H. (2017). *Package 'tidyverse'*. Retrieved from `http://tidyverse.tidyverse.org,https://github.com/tidyverse/tidyverse` (Version 1.2.1)

Appendix A

Supplementary information to Chapter 2: particulate matter in the Nelson River system

A.1 BaySys sample list and water quality data

Water samples collected as part of the BaySys program are listed in this section in Table A.1 that includes site coordinates, sample collection years, and data for all measured and calculated water quality parameters.

Table A.1: Site coordinates, sampling years, and water quality data for summer season surface water samples collected as part of BaySys program. TSS, SuspOC, and SuspN in $\mathrm{mg\,L^{-1}}$. C/N ratios calculated from molar concentrations. UNR: upper Nelson River, RBR: Rat-Burntwood River, LNR: lower Nelson River

Region	Site	UTM Zone	Easting	Northing	Year	Sample ID	TSS	SuspOC	SuspN	% OC of TSS	C/N
UNR	NR7	14 U	581189	6046758	2017	NR7-17-01	10	0.89	0.154	8.90	6.74
		14 U	581188	6046751	2017	NR7-17-01-a	8	0.77	0.102	9.63	8.8
		14 U	581187	6046706	2017	NR7-17-01-b	9	0.77	0.111	8.56	8.09
		14 U	581187	6046665	2017	NR7-17-01-c	7	0.73	0.112	10.43	7.6
		14 U	581186	6046621	2017	NR7-17-01-d	7	0.68	0.098	9.71	8.09
		14 U	581186	6046575	2017	NR7-17-01-e	8	0.73	0.109	9.13	7.81
	NR8	14 U	591973	6011540	2017	NR8-17-01	15	2.59	0.545	17.27	5.54
RBR	BR1	14 V	648649	6224492	2016	BR1-16-01	35	0.64	0.101	1.83	7.39
		14 V	648649	6224492	2017	BR1-17-01	19	0.60	0.092	3.16	7.61
	BR2	14 V	630848	6219519	2016	BR2-16-01	34	0.70	0.114	2.06	7.16
		14 V	630848	6219519	2017	BR2-17-01	19	0.73	0.106	3.84	8.03
	BR3	14 U	572723	6179289	2016	BR3-16-01	31	0.66	0.112	2.13	6.87
		14 U	572723	6179289	2017	BR3-17-01	24	0.58	0.062	2.42	10.91
		14 U	572709	6179286	2017	BR3-17-01-a	26	0.58	0.071	2.23	9.53
		14 U	572690	6179267	2017	BR3-17-01-b	23	0.56	0.088	2.43	7.42
		14 U	572672	6179250	2017	BR3-17-01-c	24	0.56	0.064	2.33	10.2
		14 U	572654	6179233	2017	BR3-17-01-d	22	0.53	0.066	2.41	9.36
		14 U	572636	6179217	2017	BR3-17-01-e	23	0.55	0.087	2.39	7.37
	BR4	14 U	532895	6155060	2016	BR4-16-01	20	0.53	0.091	2.65	6.79
		14 U	532895	6155060	2017	BR4-17-01	33	0.70	0.092	2.12	8.87
	BR5	14 U	532599	6154843	2016	BR5-16-01	18	0.49	0.069	2.72	8.28
		14 U	532599	6154843	2017	BR5-17-01	20	0.57	0.099	2.85	6.71

continued ...

. . . continued

Region	Site	UTM Zone	Easting	Northing	Year	Sample ID	TSS	SuspOC	SuspN	% OC of TSS	C/N
	BR6	14 U	478960	6191495	2016	BR6-16-01	11	0.42	0.055	3.82	8.91
		14 U	478960	6191495	2017	BR6-17-01	6	0.41	0.049	6.83	9.76
	OR1	14 U	602453	6206716	2016	OR1-16-01	32	0.88	0.128	2.75	8.02
		14 U	602453	6206716	2017	OR1-17-01	26	0.75	0.098	2.88	8.92
LNR	NR1	15 V	451094	6282833	2016	NR1-16-01	25	0.67	0.134	2.68	5.83
		15 V	451094	6282833	2017	NR1-17-01	19	0.75	0.117	3.95	7.48
	NR2	15 V	431454	6263982	2016	NR2-16-01	23	0.65	0.104	2.83	7.29
		15 V	431454	6263982	2017	NR2-17-01	19	0.71	0.112	3.74	7.39
	NR3	15 V	416536	6250951	2016	NR3-16-01	25	0.71	0.106	2.84	7.81
		15 V	416536	6250951	2017	NR3-17-01	4	0.49	0.059	12.25	9.69
	NR4	15 V	398420	6249281	2016	NR4-16-01	19	0.63	0.107	3.32	6.87
		15 V	398420	6249281	2017	NR4-17-01	44	2.17	0.228	4.93	11.1
	NR6	15 V	363173	6245225	2016	NR6-16-01	46	1.01	0.161	2.20	7.32
		15 V	363173	6245225	2017	NR6-17-01	28	0.81	0.098	2.89	9.64
	AR1	14 V	684777	6249782	2016	AR1-16-01	10	0.65	0.089	6.50	8.52
		14 V	684777	6249782	2017	AR1-17-01	8	0.73	0.105	9.13	8.11
	KR1	15 V	401151	6247112	2016	KR1-16-01	6	0.62	0.082	10.33	8.82
		15 V	401151	6247112	2017	KR1-17-01	7	0.85	0.107	12.14	9.26
	LR1	15 V	430142	6264165	2016	LR1-16-01	3	0.41	0.046	13.67	10.39
		15 V	430142	6264165	2017	LR1-17-01	4	0.70	0.086	17.50	9.49

A.2 Monitoring program water quality sample list

Table A.2: Site names and coordinates for summer season surface water samples collected during supplementary water quality monitoring programs. GS: Generating Station. Program name abbreviations described in Table 2.1.

Program	Region	Site	Waterbody	UTM Zone	Easting	Northing
CAMP	UNR	UFS017	Nelson River	14 V	654222	6212271
		UBS010	Lake Winnipeg outlet at Warren's Landing	14 U	577455	5985383
	RBR	TGS015	Burntwood River	14 V	650313	6224470
		TGS014	Apussigamasi Lake	14 U	587919	6190398
	LNR	NR-8	Nelson River	15 V	512157	6309449
		NR-7	Nelson River	15 V	491015	6309699
		NR-6	Nelson River	15 V	460068	6288792
		UHS002	Nelson River	15 V	458766	6288038
		NR-5	Nelson River	15 V	451043	6282812
		UHS003	Nelson River	15 V	437420	6266330
		NR-4	Limestone GS Forebay	15 V	431503	6262075
		UHS004	Limestone GS Forebay	15 V	431387	6261078
		NR-3	Long Spruce GS Forebay	15 V	415415	6251278
MEMP	UNR	Kelsey GS	Nelson River	14 V	653306	6213292
		Jenpeg GS	Nelson River	14 U	562863	6044419
	RBR	Thompson	Burntwood River	14 U	573195	6178782
	LNR	Kettle GS	Nelson River	15 V	399042	6250027
FEMP	UNR	UF0005	Nelson River	14 V	653185	6215650
		UB0006	Nelson River	14 U	592088	6011436
		UB0013	Jack River	14 U	570747	5976903
	RBR	TG0003	Burntwood River	14 V	645226	6224405
		TG0001	Burntwood River	14 U	572691	6179229
		TF0004	Burntwood River	14 U	509934	6170653
		TF0001	Rat River	14 U	493568	6172286
ArcticNet	LNR	B5	Nelson River	15 V	530475	6326098
		B4	Nelson River	15 V	527178	6322265
DFO	LNR	Conwapa	Nelson River	15 V	451094	6282833
		Limestone	Nelson River	15 V	431855	6263055
		Long Spruce	Nelson River	15 V	415435	6251491
		Kettle	Nelson River	15 V	399042	6250027

continued ...

. . . continued

Program	Region	Site	Waterbody	UTM Zone	Easting	Northing
Baker	LNR	4	Nelson River	15 V	517204	6311144
		3	Nelson River	15 V	511968	6309889
		2	Nelson River	15 V	512477	6309396
		1	Nelson River	15 V	505344	6307618

Appendix B

Supplementary information to Chapter 3: CSSI analysis and MixSIAR

B.1 Recent applications of CSSI analysis

Recent publications that have used CSSI fingerprinting and carbon isotope unmixing models to estimate proportional source contributions to suspended sediment are listed in Table B.1.

Table B.1: Previous applications of Compound-Specific Stable Isotope (CSSI) fingerprinting and carbon isotope unmixing models to estimate source contributions to suspended sediment. FA: fatty acid.

Publication	Catchment	Modelling Method	Results
Gibbs (2008)	Mahurangi River, New Zealand ($117\,km^2$)	$\delta^{13}C$ values of C_{10} to C_{24} FAs as tracers, IsoSource mixing model was used and scaled post-mixing to account for % carbon in soil.	Examined the proportion of urban, pasture, native forest and pine forest sources in estuarine sediment to determine soil sources to the estuary based on land use. Effectively estimated that pine forests contribute the highest proportion to estuary sediment.
Blake et al. (2012)	Furze Brook, United Kingdom ($1.45\,km^2$)	Bulk $\delta^{13}C$ isotopic composition and $\delta^{13}C$ values of C_{16} to C_{32} FAs as tracers, IsoSource mixing model with linear correction equation post-mixing to account for % carbon in soil after Gibbs (2008).	CSSI used alongside geochemical fingerprints to determine contribution of soils from different land uses (pasture, wheat, maize, trees/shrubs) to sediment load and estimated that sediment load is dominated by pasture sources.
Hancock and Revill (2012)	Logan River, Albert River and tributaries, Australia ($3860\,km^2$)	Bulk $\delta^{13}C$ isotopic composition and $\delta^{13}C$ values of C_{14} to C_{20} FAs as tracers, IsoSource mixing model with linear correction equation post-mixing to account for % carbon in soil after Gibbs (2008).	CSSI used to discriminate between forest, pasture, and cultivated land sources to a rural Australian catchment. Albert River sediment was dominated by forest soil sources whereas sediment in the Logan River comprised primarily channel bank sources.
Alewell et al. (2016)	Enziwigger River, Switzerland ($31\,km^2$)	$\delta^{13}C$ values of C_{18}, C_{22}, C_{26}, and C_{28} FAs as tracers, IsoSource mixing model with linear correction equation post-mixing after Gibbs (2008), but modified to correct for concentration sum of each respective fatty acid.	Distinguished sediment sourced from forest and agricultural soils during different flow conditions. During base flow, agricultural sources dominated whereas at high flow, forest sources contributed most to suspended sediment.
Upadhayay, Smith, et al. (2018)	Chilang Catchment, Nepal ($23\,km^2$)	Bulk $\delta^{13}C$ isotopic composition and $\delta^{13}C$ values of C_{22} to C_{32} FAs as tracers, concentration-dependent Baysian Deconvolutional MixSIAR mixing model (from Blake et al. (2018)) was used to account for source contributions from sub-catchments.	Model showed mixed forest soil sources contributed most to sediment during the pre-wet season whereas agricultural terraces contributed minimally to sediment at the catchment outlet.

B.2 CSSI fingerprinting sample list

Table B.2: Sample ID codes, substrate types, and site coordinates for terrestrial and suspended sediment samples collected for CSSI analysis and used in MixSIAR unmixing models. P: peat, S: soil, Ba: bank, Ss: suspended sediment, Be: bed sediment and T: tributary suspended sediment

Catchment	Site	Sample ID	Type	UTM Zone	Easting	Northing
UNR	NR7	NR7-06	Ss	14 U	581189	6046758
	NR8	NR8-02-02	S	14 U	591807	6011654
		NR8-02-03	S	14 U	591807	6011654
		NR8-02-04	S	14 U	591807	6011654
	22	22	Ss	14 U	568332	5941372
	2-mile	2-mile	Ss	14 U	560744	5956100
	N809	N809-P	P	14 U	559848	5956990
		N809-Ba	Ba	14 U	559848	5956990
	N850	N850-P	P	14 U	532730	5967097
		N850-Ba	Ba	14 U	532730	5967097
RBR	BR1	BR1-06	Ss	14 V	648649	6224492
		BR1-08	Ba	14 V	648649	6224492
	BR2	BR2-06	Ss	14 V	630848	6219519
		BR2-08	Ba	14 V	630924	6219577
	BR3	BR3-02-02	S	14 U	572710	6179375
		BR3-02-03	S	14 U	572710	6179375
		BR3-02-04	S	14 U	572710	6179375
		BR3-06	Ss	14 U	572723	6179289
	BR5	BR5-02-02	S	14 U	532620	6154869
		BR5-02-03	S	14 U	532620	6154869
		BR5-02-04	S	14 U	532620	6154869
		BR5-06	Ss	14 U	532599	6154843
		BR5-08	Ba	14 U	532630	6154857
	BR6	BR6-06	Ss	14 U	478960	6191495
	OR1	OR1-06	T	14 U	602453	6206716
LNR	NR1	NR1-02-02	S	15 V	451088	6282905
		NR1-02-03	S	15 V	451088	6282905
		NR1-02-04	S	15 V	451088	6282905
		NR1-06	Ss	15 V	451094	6282833
		NR1-07	Be	15 V	451138	6282910

continued . . .

. . . continued

Catchment	Site	Sample ID	Type	UTM Zone	Easting	Northing
	NR2	NR2-06	Ss	15 V	431454	6263982
	NR3	NR3-06	Ss	15 V	416536	6250951
	NR4	NR4-02-01	S	15 V	398408	6249283
		NR4-02-02	S	15 V	398408	6249283
		NR4-02-03	S	15 V	398408	6249283
		NR4-02-04	S	15 V	398408	6249283
		NR4-02-05	S	15 V	398408	6249283
		NR4-05	Ss	15 V	398420	6249281
	NR6	NR6-06	Ss	15 V	363173	6245225
	SpL1	SpL-01	Be	14 V	678487	6236828
	AR1	AR1-06	T	14 V	684777	6249782
	KR1	KR1-06	T	15 V	401151	6247112
	LR1	LR1-06	T	15 V	430142	6264165

B.3 Soil test pit descriptions

Descriptions of soil horizons from test pits sampled during field work are listed Table B.3. Site coordinates of each test pit are listed in Table B.2.

Table B.3: Test pit descriptions for soil samples used in CSSI fingerprinting and MixSIAR unmixing models. Site coordinates listed Table B.2.

Site	Horizon	Thickness	Structure	Texture	Colour	Consistency	Roots	Porosity	Physical Environment
NR1	F: NR1-02-01	55–52 cm			greyish-brown				Moderately sloping (10°) north bank of Nelson River with forested area at top of bank. Site is ∼20 m from shoreline, ∼6 m up-bank from shoreline, and faces south. Primary vegetation is grasses, alders, and willows.
	A: NR1-02-02	52–48 cm	granular, grainy	sandy clay loam	5YR 3/2	dry: loose, wet: non-sticky	abundant, fine	abundant, fine	
	B: NR1-02-03	48–22 cm	granular, grainy	silty clay loam	7.5YR 4/2	dry: friable, wet: non-sticky	few, very fine	few, fine	
	C: NR1-02-04	22–0 cm	massive	silty clay loam	7.5YR 3/2	dry: friable, wet: non-sticky	none	very few, very fine	
NR2	O: NR2-02-01	37–30 cm	peat	organic					North facing slope (∼25°) of Nelson River. Primary vegetation is black spruce with alders understory with a mossy forest floor.
	A: NR2-02-02	30–25 cm	granular, massive	loamy sand	10YR 2/2	dry: very friable, wet: non-sticky	plentiful, coarse to fine	abundant, very fine	
	B: NR2-02-03	25–13 cm	granular, massive	sand	2.5YR 4/4	dry: loose, wet: non-sticky	few, fine	abundant, very fine	
	C: NR2-02-04	13–0 cm	granular, massive with few peds	loamy sand	2.5YR 5/4	dry: loose, wet: non-sticky	few, fine	abundant, very fine	

continued . . .

...continued

Site	Horizon	Thickness	Structure	Texture	Colour	Consistency	Roots	Porosity	Physical Environment
NR3	A: NR3-02-01	126–124 cm		silty clay loam	5YR 2.5/1	moist: loose, wet: non-sticky	abundant, fine	many, medium, vesicular	North east facing partly slumped till bank on Nelson River ∼1 m from shoreline. Primary vegetation is aspen, willow, spruce, and grasses.
	C: NR3-02-02	124–108 cm		sandy clay	2.5YR 5/3	moist: very friable, wet: slightly sticky	few, fine	very few, fine, vesicular	
	Ab: NR3-02-03	108–105 cm		silty clay	7.5 YR 2.5/2	moist: very friable, wet: slightly sticky	very few, fine	few, fine, vesicular	
	Cb: NR3-02-04	105–20 cm		loamy sand to sandy clay	2.5YR 5/3	moist: very friable, wet: slightly sticky	very few, fine	very few, fine, vesicular	
	Rb: NR3-02-05	20–0 cm		sand and gravel	10 YR 5/4	moist: loose, wet: non-sticky	very few, very fine	many, very fine, vesicular	
NR4	A: NR4-02-01	66–63 cm	massive	silty clay loam	10YR 2/2	moist: very friable, wet: non-sticky	few, fine	continuous, vesicular	North facing till bank on Stephens Lake ∼1 m from shoreline. Primary vegetation is alder, willow, and grasses.
	C: NR4-02-02	63–50 cm	massive	sand	25Y 6/3	moist: loose, wet: non-sticky	few, fine	continuous, vesicular	

continued ...

...continued

Site	Horizon	Thickness	Structure	Texture	Colour	Consistency	Roots	Porosity	Physical Environment
	Abi: NR4-02-03	50–46 cm	massive	silty loam	10YR 2/1	moist: very friable, wet: non-sticky	few, fine	continuous, vesicular	
	Hb: NR4-02-04	46–40 cm	massive	silty loam	7/5YR 5/6	moist: very friable, wet: non-sticky	few, fine	continuous, vesicular	
	Abii: NR4-02-05	40–0 cm	massive	silty loam	10YR 2/1	moist: very friable, wet: non-sticky	very few, very fine	continuous, vesicular	
NR6	O: NR6-02-01	60–46 cm		organic					North facing slope (~10°) of Nelson River. Pit is ~10 m from till bank. Primary vegetation is alder, moss, and labrador tea. Proximal forest is black spruce and poplar.
	A: NR6-02-02	46–36 cm	massive, peaty	coarse organic material	light brown	organic, fibrous	abundant, fine	many, medium	
	B: NR6-02-03	36–23 cm	massive, granular	silty clay	medium brown	dry: loose, wet: sticky	few, fine	few, fine, irregular	
	C: NR6-02-04	23–0 cm	massive, granular	pebbly silt	light grey-brown	dry: loose, wet: non-sticky	none	few	

continued ...

...continued

Site	Horizon	Thickness	Structure	Texture	Colour	Consistency	Roots	Porosity	Physical Environment
NR7	O: NR7-02-01	40–30 cm		organic			abundant		South facing, north side of Nelson River. Pit is ∼100 m from partial bedrock-bound bank shoreline. Primary vegetation is black spruce, poplar, birch and moss forest floor.
	A: NR7-02-02	30–27 cm	granular, massive	sandy silt	medium-dark brown	dry: brittle, wet: non-sticky	abundant	few	
	C: NR7-02-03	27–0 cm	blocky, coarse	clayey silt	medium-light brown	dry: fissile, wet: non-sticky	few	few	
NR8	O: NR8-02-01	39–30 cm	moderate fabric	organic		moist: loose	few, fine	irregular, medium, plentiful	South facing, north side of Nelson River. Pit is ∼145 m from till bank. Primary vegetation is black spruce.
	A: NR8-02-01	30–21 cm	weak, granular	sandy loam	10YR 2/2	moist: very friable, wet: slightly sticky	plentiful, medium, very coarse	vesicular, fine, plentiful	
	B: NR8-02-01	21–9 cm	moderate, granular	loamy sand	10YR 4/4	moist: very friable, wet: sticky	few, fine	tabular, fine, plentiful	
	C: NR8-02-01	9–0 cm	massive	sandy clay	2.5YR 6/2	moist: firm, wet: sticky	very few, very fine	tabular, very fine, few	

continued ...

...continued

Site	Horizon	Thickness	Structure	Texture	Colour	Consistency	Roots	Porosity	Physical Environment
BR1	O: BR1-02-01	56–50 cm	massive	organic	dark brown		few, fine		South facing, north side of Burntwood River. Pit is ∼20 m from clay-rich bank. Primary vegetation is black spruce, poplar, juniper, and moss.
	A: BR1-02-02	50–39 cm	massive, granular	clay, colloidal, friable	medium red-brown	dry: loose	abundant, fine	abundant	
	B: BR1-02-03	39–0 cm	massive	clay	grey-brown	wet: moderately sticky	few	few, fine	
BR2	O: BR2-02-01	39–36 cm		organic					South facing, north side of Burntwood River. Pit is ∼20 m from bank. Primary vegetation is black spruce, poplar, juniper, and moss.
	A: BR2-02-02	36–33 cm	massive	loamy sand	7.5YR 2.5/2	moist: loose, wet: non-sticky	plentiful, medium	abundant, fine	
	B: BR2-02-03	33–26 cm	granular	clay loam	7.5YR 3/3	moist: loose, wet: non-sticky	plentiful, very fine	abundant, fine	
	C: BR2-02-04	26–0 cm	subangular blocky	clay	10YR 5/3	moist: friable, wet: slightly sticky	very few, very fine	few, fine	
BR3	O: BR3-02-01	52–50 cm		organic	dark brown				North east facing partly slumped till bank on Nelson River ∼1 m from shoreline. Primary vegetation is aspen, willow, spruce, and grasses.
	A: BR3-02-02	50–48 cm	massive	sandy clay	medium-dark brown	moist: friable, wet: slightly sticky	abundant, fine	abundant, inter-granular	

continued ...

...continued

Site	Horizon	Thickness	Structure	Texture	Colour	Consistency	Roots	Porosity	Physical Environment
	B: BR3-02-03	48–39 cm	granular	clay	medium brown	moist: friable, wet: slightly sticky	common, fine	abundant, intergranular	
	C: BR3-02-04	39–0 cm	massive, granular, mottled	clay	light-dark brown	moist: firm, wet: slightly sticky	few, fine	few to uncommon, fine	
BR5	O: BR5-02-01	86–78 cm		organic	medium reddish grey		abundant		South facing, north side of Burntwood River. Pit is ∼15 m from bank. Primary vegetation is black spruce, poplar, juniper, and moss.
	A: BR5-02-02	78–74 cm	massive	fine sand	dark brown	fissile		common, fine	
	B: BR5-02-03	74–50 cm	massive	silty/clayey sand	medium grey brown	fissile		common, medium	
	C: BR5-02-04	50–15 cm	massive	clay	medium grey brown	wet: very sticky		few, fine	
	C': BR5-02-05	15–0 cm	massive	clay	medium grey brown	wet: very sticky		few, fine	

continued ...

...continued

Site	Horizon	Thickness	Structure	Texture	Colour	Consistency	Roots	Porosity	Physical Environment
BR6	O: BR6-02-01	64–53 cm		organic	red-brown		common		South facing, south side of ridge above Notigi Lake. Pit is ∼200 m from shoreline. Primary vegetation is birch, poplar, alder, willow, moss, and labrador tea.
	A: BR6-02-02	53–50 cm	massive	find sand	dark brown	moist: loose	common	common, interparticle	
	B: BR6-02-03	50–44 cm	massive	pebbly fine-medium sand	medium grey	moist: loose, wet: non-sticky	common, fine-medium	common, fine	
	C: BR6-02-04	44–13 cm	massive, mottled	fine silty sand	medium brown	wet: non-sticky	few, fine	common	
	C': BR6-02-05	13–0 cm	massive, mottled	fine silty sand	light grey-brown	wet: non-sticky	few, fine	common	
AR1	O: AR1-02-01	40–28 cm	massive	organic, peat	moist: loose				South facing, north side of Assean River. Pit is ∼12 m from bank. Primary vegetation is black spruce, pine saplings, with labrador tea and moss understory.
	A: AR1-02-02	28–14 cm	massive	sand	10YR 2/1	moist: loose, wet: non-sticky	abundant, medium	common, irregular	
	C: AR1-02-03	14–0 cm	massive	clay	1-YR 4/4	moist: firm, wet: sticky	very few, very fine	few, very fine	

continued ...

...continued

Site	Horizon	Thickness	Structure	Texture	Colour	Consistency	Roots	Porosity	Physical Environment
KR1	O/A: KR1-02-01	54–44 cm	massive	organic	dark brown	moist: moderately sticky	many	few, fine to medium	South facing, west side of Kettle River. Pit is ∼20 m from bank. Primary vegetation is black spruce, tamarack, poplar, alder, and willow, with labrador tea and moss on forest floor.
	A: KR1-02-02	44–0 cm	massive, granular	clay	light grey brown	wet: very sticky	few, fine	few, very fine	
LR1	A: LR1-02-01	60–56 cm	massive	fine sand	medium brown	dry: brittle, wet: non-sticky	abundant, fine	common, medium	South facing, east side of Limestone River. Pit is ∼60 m from bank. Primary vegetation is black spruce, poplar, with moss on forest floor.
	B: LR1-02-02	56–40 cm	massive	fine-medium sand	medium reddish brown	dry: brittle, wet: non-sticky	abundant, fine	few, fine	
	C: LR1-02-03	40–12 cm	massive	gravely fine-medium sand	medium to light brown	dry: brittle, wet: non-sticky	few, fine	common, medium to coarse	
	C$^{\flat}$: LR1-02-04	12–0 cm	massive	fine-medium clayey sand	light greyish brown	dry: brittle, wet: non-sticky	none		

B.4 CSSI data

Table B.4: Bulk properties of source and suspended sediment samples collected for CSSI fingerprinting and used in MixSIAR unmixing models. P: peat, S: soil, Ba: bank, Ss: suspended sediment, Be: bed sediment and T: tributary suspended sediment.

Site	Sample ID	Type	Sample Mass (g)	% Moisture	% OC	FA Mass (µg)	Bulk $\delta^{13}C$
NR7	NR7-06	Ss	7.63		8.3	18754.56	-28.1
NR8	NR8-02-02	S	2.06	57.6	28.1	857.59	-26.8
	NR8-02-03	S	56.90	9.0	0.4	510.96	-25.9
	NR8-02-04	S	55.88	17.3	0.3	425.13	-25.8
22	22-2016	Ss	5.28		12.6	2608.87	-32.5
	22-2017	Ss	1.96		4.8	463.20	-29.6
2-mile	2-mile	Ss	9.13		3.1	3509.35	-28.3
N809	N809-P	P	3.54	66.2	33.0	408.74	-26.5
	N809-Ba	Ba	39.45	8.0	0.5	31.81	-26.8
N850	N850-P	P	4.86	50.3	31.7	532.43	-26.4
	N850-Ba	Ba	36.25	15.1	5.6	129.30	-26.9
BR1	BR1-06	Ss	2.52		5.7	708.64	-29.2
	BR1-08	Ba	66.31	19.2	0.4	371.81	-25.8
BR2	BR2-06	Ss	3.02		5.4	876.64	-30.3
	BR2-08	Ba	67.84	16.8	0.6	376.99	-25.4
BR3	BR3-02-02	S	10.87	44.4	0.5	1228.83	-28.6
	BR3-02-03	S	32.37	21.0	3.1	91.45	-27.1
	BR3-02-04	S	34.56	16.0	14.1	20.67	-26.5
	BR3-06	Ss	12.24		12.4	98.78	-28.0
BR5	BR5-02-02	S	13.18	40.3	1.6	672.34	-26.2
	BR5-02-03	S	33.52	19.2	0.4	72.44	-25.8
	BR5-02-04	S	32.56	26.8	2.7	25.45	-26.4
	BR5-06	Ss	3.11		3.0	300.38	-29.9
	BR5-08	Ba	32.30	9.0	1.7	312.29	-25.8
BR6	BR6-06	Ss	11.13		2.6	574.40	-27.9
OR1	OR1-06	T	14.63		2.7	974.00	-29.0
NR1	NR1-02-02	S	33.66	19.5	14.6	1200.01	-27.4
	NR1-02-03	S	28.43	34.4	0.5	1957.28	-27.2
	NR1-02-04	S	37.53	21.7	1.2	291.18	-27.9

continued . . .

. . . continued

Site	Sample ID	Type	Sample Mass (g)	% Moisture	% OC	FA Mass (µg)	Bulk $\delta^{13}C$
	NR1-06	Ss	10.83		5.5	606.91	-26.6
	NR1-07	Be	47.89	15.5	3.4	233.18	-27.5
NR2	NR2-06	Ss	10.33		6.9	4519.91	-27.2
NR3	NR3-06	Ss	2.19		6.8	792.24	-29.0
NR4	NR4-02-01	S	19.17	43.58	42.6	933.62	-28.7
	NR4-02-02	S	50.30	3.57	31.5	28.52	-26.9
	NR4-02-03	S	4.98	70.99	3.4	275.09	-27.1
	NR4-02-04	S	2.34	84.78	0.4	1196.01	-27.3
	NR4-02-05	S	4.96	75.42	18.9	726.13	-26.3
	NR4-05	Ss	15.75		38.3	2850.81	-28.1
NR6	NR6-06	Ss	15.22		1.4	551.35	-27.9
SpL1	SpL-01	Be	28.71	53.33	1.0	277.40	-27.2
AR1	AR1-06	T	2.46		6.2	232.32	-29.4
KR1	KR1-06	T	3.01		6.1	642.26	-29.6
LR1	LR1-06	T	24.84		4.1	724.79	-30.6

Table B.5: Fatty acid mass (µg) in source and suspended sediment samples for all chain lengths. Sample substrate types listed in Table B.2.

Sample ID	C_{16}	C_{17}	C_{18}	C_{20}	C_{21}	C_{22}	C_{23}	C_{24}	C_{25}	C_{26}	C_{27}	C_{28}	C_{29}	C_{30}	C_{32}
NR7-06	15349.69	0.00	2523.67	129.85	11.91	164.05	58.29	148.04	26.17	115.33	21.82	116.25	13.79	55.02	20.68
NR8-02-02	98.05	5.09	56.98	38.74	11.86	103.98	53.83	152.96	34.24	74.67	18.62	91.79	15.91	62.39	38.49
NR8-02-03	66.82	3.27	53.30	18.36	11.28	68.16	34.88	90.63	25.20	32.22	9.15	43.85	5.63	31.41	16.80
NR8-02-04	67.97	4.14	52.74	10.94	8.30	37.39	21.92	55.63	23.47	37.26	13.97	46.05	7.75	26.47	11.14
22-2016	2278.92	24.94	100.87	5.14	54.69	7.53	17.58	11.27	93.41	3.76	2.48	3.45	0.36	1.95	2.53
22-2017	128.97	11.53	59.26	18.76	6.58	54.16	10.97	42.63	8.68	30.25	7.31	40.97	4.64	25.24	13.23
2-mile	3185.87	28.68	168.02	10.42	2.00	19.50	4.38	21.06	20.22	18.87	3.86	13.00	2.58	4.72	6.17
N809-P	11.19	0.00	19.08	58.72	4.24	68.88	18.60	75.28	13.60	32.14	10.03	30.21	8.70	28.02	30.04
N809-Ba	8.88	0.37	6.76	0.99	0.16	1.77	0.79	3.01	0.80	2.01	1.27	2.58	0.51	1.22	0.69
N850-P	15.87	0.00	39.12	133.38	4.56	125.22	23.72	100.03	11.65	24.17	6.07	15.44	4.80	15.77	12.62
N850-Ba	9.58	0.92	7.16	1.60	1.11	3.73	4.06	13.72	7.28	23.81	8.39	27.62	4.82	11.22	4.27
BR1-06	279.87	9.66	173.99	15.26	5.42	38.47	9.71	37.54	10.03	29.36	8.66	41.54	6.16	29.66	13.31
BR1-08	48.55	0.23	38.88	13.01	5.98	39.13	14.21	38.19	13.84	31.00	13.34	53.60	9.19	35.04	17.64
BR2-06	445.96	17.72	145.99	19.11	7.30	48.14	13.58	44.92	11.05	34.76	8.90	39.89	5.12	22.35	11.83
BR2-08	42.11	1.84	33.32	10.93	5.22	34.00	11.09	34.96	13.61	41.83	1.42	65.88	12.01	46.49	22.27
BR3-02-02	57.36	3.20	36.53	53.88	18.69	110.29	83.32	187.65	65.19	218.16	43.59	233.89	21.95	21.95	18.56
BR3-02-03	12.02	1.13	6.41	3.31	1.31	6.56	5.24	11.97	4.59	11.02	4.17	13.92	2.20	5.35	2.23
BR3-02-04	6.81	0.39	4.33	0.52	0.27	0.88	0.60	0.98	0.45	0.93	2.22	1.22	0.20	0.53	0.35
BR3-06	21.59	1.07	15.67	2.81	1.69	3.73	1.43	11.67	2.91	12.23	2.01	8.46	1.20	4.05	8.25
BR5-02-02	25.35	2.28	44.18	123.57	16.15	132.67	61.49	113.71	25.62	41.63	13.35	35.65	6.17	16.63	13.89
BR5-02-03	9.83	0.51	7.84	10.36	1.72	8.33	5.74	11.00	3.47	4.68	1.72	4.02	0.86	1.71	0.65
BR5-02-04	6.78	0.28	5.48	0.80	0.13	1.43	0.64	2.44	0.65	1.63	1.03	2.09	0.42	0.99	0.56
BR5-06	94.13	3.54	49.22	8.06	4.63	19.28	8.51	29.29	8.28	29.99	6.17	22.48	3.75	10.12	2.93
BR5-08	20.58	0.00	29.70	68.58	4.80	46.36	22.18	44.75	13.79	19.01	6.84	17.64	3.47	8.92	5.67
BR6-06	93.13	3.98	68.62	12.30	7.54	55.98	23.06	88.45	22.92	40.16	19.02	73.23	10.69	39.97	15.36
OR1-06	416.1	3.11	140.01	20.13	11.17	57.30	22.99	77.74	20.15	60.76	14.42	64.27	9.91	42.01	13.91

continued ...

. . . continued

Sample ID	C_{16}	C_{17}	C_{18}	C_{20}	C_{21}	C_{22}	C_{23}	C_{24}	C_{25}	C_{26}	C_{27}	C_{28}	C_{29}	C_{30}	C_{32}
NR1-02-02	92.56	2.94	25.46	26.16	16.56	89.75	83.48	201.30	56.72	167.86	38.29	233.41	25.06	108.66	31.50
NR1-02-03	128.58	5.16	40.65	38.60	8.89	120.36	127.85	362.46	111.91	310.84	73.88	383.80	40.69	144.81	48.78
NR1-02-04	31.72	1.96	62.53	10.24	5.88	24.49	10.82	37.20	10.52	38.10	7.84	28.56	4.76	12.85	3.72
NR1-06	339.74	13.05	64.48	11.33	3.35	25.35	9.06	42.29	8.79	31.14	6.30	29.53	4.14	13.20	5.16
NR1-07	60.03	2.23	14.43	5.90	2.10	14.78	7.48	33.69	7.35	28.91	5.43	28.18	3.90	13.04	5.72
NR2-06	3400.15	13.12	502.57	50.8	80.14	87.21	28.93	116.71	19.96	75.09	14.76	70.63	9.58	31.74	18.53
NR3-06	326.09	8.03	147.32	17.65	7.42	54.44	16.56	62.77	14.95	0.00	10.92	61.45	8.14	42.54	13.95
NR4-02-01	54.15	2.20	23.47	28.50	18.27	104.11	95.27	197.79	51.11	118.61	21.12	141.61	11.20	49.66	16.56
NR4-02-02	8.01	0.34	5.90	0.79	0.55	2.06	1.35	2.09	0.99	2.61	0.41	2.52	0.00	0.49	0.39
NR4-02-03	18.96	0.98	150.18	8.75	1.91	12.15	4.03	16.01	26.13	12.87	2.48	9.90	4.44	4.08	2.23
NR4-02-04	32.18	0.00	61.96	196.04	9.74	185.58	53.88	326.42	42.28	173.31	15.51	50.85	6.38	24.01	17.86
NR4-02-05	38.48	2.17	15.8	16.24	10.28	55.70	51.81	124.93	35.2	104.18	23.77	145.04	15.56	67.43	19.55
NR4-05	2493.97	61.96	173.56	10.12	2.20	14.04	4.66	18.50	30.20	14.87	2.86	11.44	5.13	4.71	2.58
NR6-06	122.04	5.86	69.17	32.00	8.06	64.23	22.64	65.17	15.76	36.58	9.69	48.56	6.85	29.98	14.77
SpL-01	53.8	2.33	27.03	4.74	3.32	12.53	8.50	34.59	10.44	39.30	8.98	39.54	6.08	19.08	7.15
AR1-06	69.98	3.52	34.49	5.89	3.10	13.04	7.62	25.95	6.26	21.73	4.44	21.57	0.60	10.34	3.80
KR1-06	71.73	3.52	48.4	11.99	6.94	52.57	22.45	91.38	24.06	88.87	21.37	108.89	13.05	56.86	20.18
LR1-06	111.51	5.27	66.37	17.93	9.04	73.82	24.13	120.14	21.94	79.19	18.36	92.86	11.80	50.10	22.34

Table B.6: Fatty acid concentration ($\mu g\, g^{-1}$) in source and suspended sediment samples for all chain lengths. Sample substrate types listed in Table B.2.

Sample ID	C_{16}	C_{17}	C_{18}	C_{20}	C_{21}	C_{22}	C_{23}	C_{24}	C_{25}	C_{26}	C_{27}	C_{28}	C_{29}	C_{30}	C_{32}
NR7-06	2012.26	0.00	330.84	17.02	1.56	21.51	7.64	19.41	3.43	15.12	2.86	15.24	1.81	7.21	2.71
NR8-02-02	47.55	2.47	27.63	18.79	5.75	50.42	26.10	74.17	16.60	36.21	9.03	44.51	7.71	30.26	18.67
NR8-02-03	1.17	0.06	0.94	0.32	0.20	1.20	0.61	1.59	0.44	0.57	0.16	0.77	0.10	0.55	0.30
NR8-02-04	1.22	0.07	0.94	0.20	0.15	0.67	0.39	1.00	0.42	0.67	0.25	0.82	0.14	0.47	0.20
22-2016	5765.96	63.11	255.22	12.99	138.36	19.04	44.48	28.51	236.35	9.50	6.27	8.73	0.92	4.94	6.41
22-2017	65.68	5.87	30.18	9.55	3.35	27.58	5.59	21.71	4.42	15.41	3.72	20.86	2.36	12.86	6.74
2-mile	1468.35	13.22	77.44	4.80	0.92	8.99	2.02	9.71	9.32	8.70	1.78	5.99	1.19	2.18	2.84
N809-P	30.89	0.00	52.67	162.07	11.69	190.11	51.35	207.78	37.54	88.72	27.69	83.39	24.02	77.34	82.91
N809-Ba	0.22	0.01	0.17	0.03	0.00	0.04	0.02	0.08	0.02	0.05	0.03	0.07	0.01	0.03	0.02
N850-P	25.81	0.00	63.62	216.95	7.41	203.68	38.58	162.71	18.95	39.32	9.87	25.12	7.81	25.66	20.53
N850-Ba	0.26	0.03	0.20	0.04	0.03	0.10	0.11	0.38	0.20	0.66	0.23	0.76	0.13	0.31	0.12
BR1-06	110.98	3.83	68.99	6.05	2.15	15.26	3.85	14.89	3.98	11.64	3.44	16.47	2.44	11.76	5.28
BR1-08	0.73	0.00	0.59	0.20	0.09	0.59	0.21	0.58	0.21	0.47	0.20	0.81	0.14	0.53	0.27
BR2-06	147.52	5.86	48.29	6.32	2.42	15.92	4.49	14.86	3.66	11.5	2.95	13.2	1.69	7.39	3.91
BR2-08	0.62	0.03	0.49	0.16	0.08	0.50	0.16	0.52	0.20	0.62	0.02	0.97	0.18	0.69	0.33
BR3-02-02	18.17	1.01	11.58	17.07	5.92	34.94	26.40	59.46	20.65	69.12	13.81	74.11	6.96	24.26	5.88
BR3-02-03	0.37	0.04	0.20	0.10	0.04	0.20	0.16	0.37	0.14	0.34	0.13	0.43	0.07	0.17	0.07
BR3-02-04	0.20	0.01	0.13	0.01	0.01	0.03	0.02	0.03	0.01	0.03	0.06	0.04	0.01	0.02	0.01
BR3-06	1.76	0.09	1.28	0.23	0.14	0.30	0.12	0.95	0.24	1.00	0.16	0.69	0.10	0.33	0.67
BR5-02-02	17.49	1.58	30.48	85.25	11.14	91.53	42.42	78.45	17.68	28.72	9.21	24.59	4.26	11.47	9.59
BR5-02-03	0.29	0.02	0.23	0.31	0.05	0.25	0.17	0.33	0.10	0.14	0.05	0.12	0.03	0.05	0.02
BR5-02-04	0.21	0.01	0.17	0.02	0.00	0.04	0.02	0.07	0.02	0.05	0.03	0.06	0.01	0.03	0.02
BR5-06	30.27	1.14	15.83	2.59	1.49	6.20	2.74	9.42	2.66	9.65	1.99	7.23	1.21	3.25	0.94
BR5-08	0.64	0.00	0.92	2.12	0.15	1.44	0.69	1.39	0.43	0.59	0.21	0.55	0.11	0.28	0.18
BR6-06	8.37	0.36	6.17	1.11	0.68	5.03	2.07	7.95	2.06	3.61	1.71	6.58	0.96	3.59	1.38
OR1-06	28.44	0.21	9.57	1.38	0.76	3.92	1.57	5.31	1.38	4.15	0.99	4.39	0.68	2.87	0.95

continued ...

...continued

Sample ID	C_{16}	C_{17}	C_{18}	C_{20}	C_{21}	C_{22}	C_{23}	C_{24}	C_{25}	C_{26}	C_{27}	C_{28}	C_{29}	C_{30}	C_{32}
NR1-02-02	2.75	0.09	0.76	0.78	0.49	2.67	2.48	5.98	1.68	4.99	1.14	6.94	0.74	3.23	0.94
NR1-02-03	4.52	0.18	1.43	1.36	0.66	4.23	4.50	12.75	3.94	10.93	2.60	13.5	1.43	5.09	1.72
NR1-02-04	0.85	0.05	1.67	0.27	0.16	0.65	0.29	0.99	0.28	1.02	0.21	0.76	0.13	0.34	0.10
NR1-06	89.04	3.42	16.90	2.97	0.88	6.64	2.37	11.08	2.30	8.16	1.65	7.74	1.09	3.46	1.35
NR1-07	1.25	0.05	0.30	0.12	0.04	0.31	0.16	0.70	0.15	0.60	0.11	0.59	0.08	0.27	0.12
NR2-06	329.25	1.27	48.67	4.92	7.76	8.44	2.80	11.30	1.93	7.27	1.43	6.84	0.93	3.07	1.79
NR3-06	148.76	3.66	67.20	8.05	3.39	24.84	7.55	28.63	6.82	0.00	4.98	28.03	3.71	19.41	6.36
NR4-02-01	25.74	1.04	11.15	13.55	8.68	49.48	45.28	94.01	24.29	56.37	10.04	67.31	5.32	23.6	7.87
NR4-02-02	0.16	0.01	0.12	0.02	0.01	0.04	0.03	0.04	0.02	0.05	0.01	0.05	0.00	0.01	0.01
NR4-02-03	19.74	1.02	156.36	9.11	1.98	12.65	4.20	16.67	27.21	13.40	2.58	10.30	4.63	4.24	2.32
NR4-02-04	13.74	0.00	26.44	83.67	4.16	79.20	23.00	139.31	18.04	73.97	6.62	21.70	2.72	10.25	7.62
NR4-02-05	7.75	0.44	3.18	3.27	2.07	11.22	10.44	25.17	7.09	20.99	4.79	29.23	3.13	13.59	3.94
NR4-05	535.13	13.30	37.24	2.17	0.47	3.01	1.00	3.97	6.48	3.19	0.61	2.45	1.10	1.01	0.55
NR6-06	8.02	0.39	4.54	2.10	0.53	4.22	1.49	4.28	1.04	2.40	0.64	3.19	0.45	1.97	0.97
SpL-01	1.87	0.08	0.94	0.17	0.12	0.44	0.30	1.20	0.36	1.37	0.31	1.38	0.21	0.66	0.25
AR1-06	28.49	1.43	14.05	2.40	1.26	5.31	3.10	10.56	2.55	8.85	1.81	8.78	0.24	4.21	1.55
KR1-06	23.82	1.17	16.07	3.98	2.30	17.45	7.45	30.34	7.99	29.51	7.10	36.15	4.33	18.88	6.70
LR1-06	4.49	0.21	2.67	0.72	0.36	2.97	0.97	4.84	0.88	3.19	0.74	3.74	0.47	2.02	0.90

Table B.7: Carbon isotope ratios (δ^{13}C) of individual fatty acid chain lengths in source and suspended sediment samples. Sample substrate types listed in Table B.2.

Sample ID	C_{16}	C_{18}	C_{20}	C_{21}	C_{22}	C_{23}	C_{24}	C_{25}	C_{26}	C_{27}	C_{28}	C_{29}	C_{30}	C_{32}
NR7-06					-30.1	-33.5	-34.0	-37.2	-33.9	-36.5	-36.3	-36.5	-35.0	-38.0
NR8-02-02	-32.9	-30.6	-31.4	-34.2	-34.4	-34.8	-33.3	-36.1	-33.6	-36.3	-34.9	-37.9	-35.7	-37.3
NR8-02-03	-31.4	-31.8	-33.2	-34.4	-34.1	-34.3	-33.3	-35.3	-33.9	-36.6	-35.8	-37.4	-36.8	-36.9
NR8-02-04	-31.1	-31.1	-33.9	-35.8	-35.9	-35.4	-32.9	-35.0	-34.1	-35.6	-33.9	-36.1	-34.8	-36.8
22-2016														
22-2017	-31.5	-31.1	-34.0	-35.3	-35.3	-35.3	-34.9	-35.4	-35.1	-37.5	-34.9	-35.9	-36.0	-35.4
2-mile														
N809-P	-28.7	-25.1	-26.0	-29.8	-27.6	-36.1	-28.9	-32.5	-31.8	-32.1	-31.5	-32.4	-31.6	-30.5
N809-Ba	-29.3	-28.5	-27.8	-29.2	-27.6	-29.9	-27.9	-29.8	-30.2	-31.7	-32.0	-30.9	-30.2	-25.4
N850-P	-28.7	-27.4	-29.0	-24.5	-33.8	-28.5	-31.0	-34.6	-32.8	-34.8	-34.9	-35.0	-33.6	-36.8
N850-Ba	-26.8	-26.0	-27.9	-29.3	-29.0	-29.6	-29.1	-30.0	-29.5	-31.0	-30.2	-31.5	-30.9	-31.0
BR1-06	-30.9	-27.3	-32.6	-38.2	-34.6	-34.3	-33.9	-33.5	-33.6	-35.4	-33.8	-38.6	-36.3	-35.6
BR1-08	-31.1	-31.7	-33.2	-35.8	-34.9	-34.9	-33.6	-35.5	-33.2	-34.9	-34.6	-37.7	-35.9	-37.4
BR2-06			-36.7	-36.7	-37.2	-36.7	-37.9	-36.3	-35.3	-36.3	-36.2	-35.4	-36.1	-35.2
BR2-08	-31.3	-31.6	-32.9	-33.5	-34.7	-34.9	-33.4	-34.9	-33.1	-35.1	-34.4	-35.6	-35.0	-36.0
BR3-02-02	-33.9	-31.5	-32.3	-34.6	-34.4	-37.2	-35.0	-36.4	-34.3	-36.3	-35.0	-37.8	-36.4	-36.1
BR3-02-03	-29.9	-29.3	-31.1	-36.3	-34.6	-36.5	-34.5	-35.8	-34.9	-36.8	-34.0	-31.9	-35.2	-31.3
BR3-02-04	-27.2	-26.8	-26.1	-28.5	-29.9	-31.1	-29.3	-29.3	-29.5	-25.5	-30.5	-32.7	-28.2	-27.5
BR3-06	-28.3	-29.0	-40.3	-36.4	-36.6	-38.8	-34.1	-36.8	-33.0	-35.2	-31.9	-27.7	-34.4	-33.8
BR5-02-02	-28.1	-25.9	-27.5	-29.5	-30.9	-31.2	-30.2	-33.1	-32.4	-33.9	-33.7	-34.9	-35.8	-32.2
BR5-02-03	-30.7	-28.4	-29.1	-30.3	-31.5	-32.4	-32.1	-32.7	-31.7	-33.0	-32.5	-31.9	-32.5	-31.3
BR5-02-04	-29.8	-30.3	-31.6	-29.6	-30.8	-32.5	-31.2	-32.2	-30.6	-33.8	-31.4	-30.7	-32.9	-34.5
BR5-06	-31.8	-30.7	-37.1	-39.4	-37.7	-37.2	-37.2	-37.1	-36.6	-36.7	-36.1	-36.2	-35.6	-38.3
BR5-08	-27.5	-25.8	-26.1	-30.4	-28.6	-38.5	-29.6	-31.0	-30.3	-29.6	-30.6	-30.6	-29.1	-33.7
BR6-06	-31.8	-32.0	-35.7	-35.4	-34.6	-34.1	-32.1	-34.9	-33.7	-35.7	-34.7	-37.2	-36.5	-38.8
OR1-06	-34.9	-30.9	-33.3	-33.3	-34.5	-34.6	-33.2	-35.5	-32.5	-35.5	-34.8	-34.5	-34.6	-35.6

continued ...

...continued

Sample ID	C_{16}	C_{18}	C_{20}	C_{21}	C_{22}	C_{23}	C_{24}	C_{25}	C_{26}	C_{27}	C_{28}	C_{29}	C_{30}	C_{32}
NR1-02-02	-30.3	-29.9	-33.1	-32.6	-32.6	-33.6	-33.4	-35.1	-33.7	-35.7	-34.4	-37.1	-35.3	-34.2
NR1-02-03	-31.7	-29.8	-32.5	-33.2	-33.2	-34.5	-33.4	-35.2	-33.3	-34.8	-34.0	-36.7	-35.5	-33.8
NR1-02-04	-30.4	-27.8	-31.8	-30.2	-31.2	-32.0	-31.7	-32.7	-31.6	-31.7	-32.1	-33.9	-32.7	-33.7
NR1-06	-33.3	-30.6	-31.2	-32.5	-32.3	-33.1	-32.5	-33.8	-33.8	-35.7	-34.9	-35.6	-35.2	-34.2
NR1-07	-31.4	-31.0	-32.8	-33.9	-32.2	-35.1	-30.5	-35.0	-30.8	-35.0	-32.5	-29.9	-34.5	-29.0
NR2-06			-29.9	-28.4	-32.1	-33.6	-33.1	-39.8	-33.1	-35.7	-35.8	-36.4	-32.9	-34.7
NR3-06	-33.0	-31.3	-32.9	-35.3	-36.0	-35.8	-34.8	-36.4	-34.5	-36.4	-35.6	-38.0	-35.3	-31.9
NR4-02-01	-35.0	-33.2	-36.6	-38.4	-33.4	-34.3	-34.0	-35.8	-32.9	-35.0	-33.6	-33.2	-32.7	-32.4
NR4-02-02														
NR4-02-03	-29.7	-25.9	-26.5	-29.0	-28.2	-31.1	-30.6	-33.8	-34.0	-34.8	-33.2	-33.9	-32.7	-32.0
NR4-02-04	-30.7	-28.2	-28.4	-30.5	-30.2	-35.0	-34.5	-37.0	-37.5	-38.3	-35.7	-41.4	-34.9	-33.6
NR4-02-05	-28.5	-26.6	-27.7	-32.2	-28.8	-31.8	-31.3	-35.4	-34.6	-35.6	-35.4	-36.1	-34.1	-33.2
NR4-05	-32.6	-35.8	-35.6	-27.0	-34.2	-27.1	-34.9	-38.6	-34.6	-33.7	-34.6	-33.5	-34.0	-27.9
NR6-06	-31.3	-30.5	-32.4	-36.7	-34.0	-35.6	-33.8	-35.6	-33.6	-36.3	-36.7	-37.9	-36.6	-38.1
SpL-01	-31.3	-30.0	-32.9	-33.5	-33.2	-33.7	-32.1	-33.3	-31.7	-33.4	-32.7	-34.8	-33.2	-36.2
AR1-06	-32.7	-31.2	-33.2	-34.6	-35.1	-36.3	-35.1	-36.6	-35.1	-37.4	-36.7	-37.7	-36.4	-37.2
KR1-06	-31.2	-29.9	-33.1	-35.1	-35.0	-34.7	-34.0	-35.1	-33.4	-35.9	-34.8	-37.9	-35.4	-35.9
LR1-06	-32.1	-30.3	-33.9	-36.9	-36.5	-36.0	-34.7	-36.6	-35.7	-37.8	-36.9	-36.4	-36.6	-33.5

B.5 Statistical test results

Table B.8: Shapiro-Wilks test results for carbon isotope ratios (δ^{13}C) of fatty acid tracer lengths C_{22}-C_{32}. * p <0.05, ** p <0.01, *** p <0.001, statistically significant.

Analyte	Tracer	W	p-value
δ^{13}C	C_{22}	0.938	0.03 *
	C_{23}	0.957	0.14
	C_{24}	0.965	0.27
	C_{25}	0.919	0.008 **
	C_{26}	0.977	0.60
	C_{27}	0.866	0.0003 ***
	C_{28}	0.955	0.12
	C_{29}	0.967	0.31
	C_{30}	0.880	0.0006 ***
	C_{32}	0.941	0.04 *

Table B.9: ANOVA (analysis of variance) test results between sources using carbon isotope ratios (δ^{13}C) of fatty acids as tracers C_{22}-C_{32} in all unmixing model frameworks. * p <0.05, ** p <0.01, *** p <0.001, statistically significant.

Unmixing Model	Tracer	F-value	p-value
Pooled-spatial	C_{22}	2.041	0.126
	C_{23}	1.971	0.136
	C_{24}	1.055	0.381
	C_{25}	1.108	0.359
	C_{26}	0.504	0.682
	C_{27}	1.073	0.373
	C_{28}	1.723	0.180
	C_{29}	0.827	0.488
	C_{30}	0.631	0.600
	C_{32}	0.695	0.561
Pooled-substrate	C_{22}	2.900	0.03 *
	C_{23}	0.656	0.66
	C_{24}	6.149	0.0004 ***
	C_{25}	3.856	0.007 **
	C_{26}	3.895	0.007 **
	C_{27}	2.555	0.04 *
	C_{28}	3.777	0.008 **
	C_{29}	1.209	0.33

continued ...

. . . continued

Unmixing Model	Tracer	F-value	p-value
	C_{30}	3.056	0.02 *
	C_{32}	1.243	0.31
Deconvolutional-substrate: M_1	C_{22}	2.563	0.17
	C_{23}	1.896	0.25
	C_{24}	23.430	0.002 **
	C_{25}	19.580	0.003 **
	C_{26}	28.460	0.001 **
	C_{27}	13.680	0.008 **
	C_{28}	4.221	0.08
	C_{29}	15.010	0.006 **
	C_{30}	14.400	0.007 **
	C_{32}	4.629	0.07
Deconvolutional-substrate: M_2	C_{22}	3.510	0.05
	C_{23}	1.934	0.58
	C_{24}	1.122	0.86
	C_{25}	2.022	0.45
	C_{26}	1.091	0.45
	C_{27}	0.872	0.37
	C_{28}	0.798	0.18
	C_{29}	0.155	0.36
	C_{30}	0.585	0.20
	C_{32}	4.094	0.07
Deconvolutional-substrate: M_3	C_{22}	5.579	0.02 *
	C_{23}	1.649	0.24
	C_{24}	3.688	0.05
	C_{25}	2.005	0.18
	C_{26}	2.224	0.15
	C_{27}	1.325	0.32
	C_{28}	4.358	0.03 *
	C_{29}	1.490	0.28
	C_{30}	2.600	0.11
	C_{32}	0.564	0.65

Table B.10: Tukey HSD test results between source combinations using carbon isotope ratios (δ^{13}C) of fatty acids as tracers C_{22}-C_{32} in all unmixing model frameworks. * p <0.05, ** p <0.01, *** p <0.001, statistically significant. UNR: upper Nelson River, RBR: Rat-Burntwood River, LNR: lower Nelson River, P: peat, S: soil, Ba: river bank, Ss: suspended sediment, Be: river bed sediment, T: tributary suspended sediment.

Unmixing Model	Tracer	Source Combination	p-value
Pooled-spatial	C_{22}	RBR - UNR	0.63
		Tributary - UNR	0.26
		LNR - UNR	0.99
		Tributary - RBR	0.70
		LNR - RBR	0.40
		LNR - Tributary	0.16
	C_{23}	RBR - UNR	0.35
		Tributary - UNR	0.48
		LNR - UNR	0.99
		Tributary - RBR	0.99
		LNR - RBR	0.23
		LNR - Tributary	0.39
	C_{24}	RBR - UNR	0.63
		Tributary - UNR	0.35
		LNR - UNR	0.89
		Tributary - RBR	0.82
		LNR - RBR	0.97
		LNR - Tributary	0.66
	C_{25}	RBR - UNR	0.99
		Tributary - UNR	0.49
		LNR - UNR	0.65
		Tributary - RBR	0.51
		LNR - RBR	0.67
		LNR - Tributary	0.94
	C_{26}	RBR - UNR	0.99
		Tributary - UNR	0.71
		LNR - UNR	0.94
		Tributary - RBR	0.70
		LNR - RBR	0.93
		LNR - Tributary	0.92
	C_{27}	RBR - UNR	0.86
		Tributary - UNR	0.66
		LNR - UNR	0.99

continued ...

. . . continued

Unmixing Model	Tracer	Source Combination	p-value
		Tributary - RBR	0.30
		LNR - RBR	0.86
		LNR - Tributary	0.64
	C_{28}	RBR - UNR	0.95
		Tributary - UNR	0.30
		LNR - UNR	0.99
		Tributary - RBR	0.13
		LNR - RBR	0.87
		LNR - Tributary	0.36
	C_{29}	RBR - UNR	0.92
		Tributary - UNR	0.76
		LNR - UNR	0.99
		Tributary - RBR	0.45
		LNR - RBR	0.77
		LNR - Tributary	0.86
	C_{30}	RBR - UNR	0.99
		Tributary - UNR	0.57
		LNR - UNR	0.99
		Tributary - RBR	0.63
		LNR - RBR	0.99
		LNR - Tributary	0.61
	C_{32}	RBR - UNR	0.99
		Tributary - UNR	0.92
		LNR - UNR	0.81
		Tributary - RBR	0.92
		LNR - RBR	0.75
		LNR - Tributary	0.56
Pooled-substrate	C_{22}	S - P	0.97
		Ba - P	1.00
		Be - P	0.97
		Ss - P	0.37
		T - P	0.31
		Ba - S	0.94
		Be - S	1.00
		Ss - S	0.16
		T - S	0.24
		Be - Ba	0.96

continued . . .

. . . continued

Unmixing Model	Tracer	Source Combination	p-value
		Ss - Ba	0.11
		T - Ba	0.13
		Ss - Be	0.93
		T - Be	0.84
		T - Ss	0.96
	C_{23}	S - P	0.99
		Ba - P	0.99
		Be - P	0.96
		Ss - P	0.84
		T - P	0.74
		Ba - S	1.00
		Be - S	0.99
		Ss - S	0.90
		T - S	0.82
		Be - Ba	0.99
		Ss - Ba	0.97
		T - Ba	0.90
		Ss - Be	1.00
		T - Be	0.99
		T - Ss	0.99
	C_{24}	S - P	0.36
		Ba - P	0.99
		Be - P	0.97
		Ss - P	0.01 *
		T - P	0.07
		Ba - S	0.32
		Be - S	0.92
		Ss - S	0.03 *
		T - S	0.51
		Be - Ba	0.99
		Ss - Ba	0.002 **
		T - Ba	0.04 *
		Ss - Be	0.13
		T - Be	0.37
		T - Ss	0.99
	C_{25}	S - P	0.99
		Ba - P	0.96
		Be - P	0.99

continued . . .

. . . continued

Unmixing Model	Tracer	Source Combination	p-value
		Ss - P	0.44
		T - P	0.67
		Ba - S	0.21
		Be - S	1.00
		Ss - S	0.17
		T - S	0.69
		Be - Ba	0.80
		Ss - Ba	0.004 **
		T - Ba	0.05
		Ss - Be	0.71
		T - Be	0.88
		T - Ss	1.00
	C_{26}	S - P	0.95
		Ba - P	0.97
		Be - P	0.99
		Ss - P	0.49
		T - P	0.72
		Ba - S	0.15
		Be - S	0.52
		Ss - S	0.47
		T - S	0.91
		Be - Ba	1.00
		Ss - Ba	0.009 **
		T - Ba	0.09
		Ss - Be	0.12
		T - Be	0.28
		T - Ss	1.00
	C_{27}	S - P	0.98
		Ba - P	0.99
		Be - P	0.99
		Ss - P	0.64
		T - P	0.58
		Ba - S	0.45
		Be - S	1.00
		Ss - S	0.53
		T - S	0.59
		Be - Ba	0.59
		Ss - Ba	0.05

continued . . .

... continued

Unmixing Model	Tracer	Source Combination	p-value
		T - Ba	0.09
		Ss - Be	0.87
		T - Be	0.80
		T - Ss	0.99
	C_{28}	S - P	0.99
		Ba - P	0.99
		Be - P	0.99
		Ss - P	0.59
		T - P	0.40
		Ba - S	0.51
		Be - S	0.92
		Ss - S	0.25
		T - S	0.21
		Be - Ba	1.00
		Ss - Ba	0.03 **
		T - Ba	0.03 **
		Ss - Be	0.31
		T - Be	0.20
		T - Ss	0.98
	C_{29}	S - P	0.98
		Ba - P	1.00
		Be - P	0.99
		Ss - P	0.95
		T - P	0.83
		Ba - S	0.75
		Be - S	0.75
		Ss - S	1.00
		T - S	0.94
		Be - Ba	0.99
		Ss - Ba	0.66
		T - Ba	0.48
		Ss - Be	0.67
		T - Be	0.50
		T - Ss	0.97
	C_{30}	S - P	0.89
		Ba - P	1.00
		Be - P	0.99
		Ss - P	0.33

continued ...

... continued

Unmixing Model	Tracer	Source Combination	p-value
		T - P	0.41
		Ba - S	0.38
		Be - S	1.00
		Ss - S	0.38
		T - S	0.65
		Be - Ba	0.91
		Ss - Ba	0.03 **
		T - Ba	0.09
		Ss - Be	0.83
		T - Be	0.85
		T - Ss	1.00
	C_{32}	S - P	1.00
		Ba - P	0.99
		Be - P	0.99
		Ss - P	0.94
		T - P	0.98
		Ba - S	0.99
		Be - S	0.99
		Ss - S	0.43
		T - S	0.85
		Be - Ba	1.00
		Ss - Ba	0.44
		T - Ba	0.75
		Ss - Be	0.76
		T - Be	0.88
		T - Ss	1.00
Deconvolutional-substrate: M_1	C_{22}	Ba_1 - P_1	0.804
		S_1 - P_1	0.425
		Ss_1 - P_1	0.876
		S_1 - Ba_1	0.147
		Ss_1 - Ba_1	0.433
		Ss_1 - S_1	0.829
	C_{23}	Ba_1 - P_1	0.754
		S_1 - P_1	0.704
		Ss_1 - P_1	0.829
		S_1 - Ba_1	0.241
		Ss_1 - Ba_1	0.350
		Ss_1 - S_1	0.998

continued ...

. . . continued

Unmixing Model	Tracer	Source Combination	p-value
	C_{24}	Ba_1 - P_1	0.40
		S_1 - P_1	0.03 *
		Ss_1 - P_1	0.01 *
		S_1 - Ba_1	0.006 **
		Ss_1 - Ba_1	0.003 **
		Ss_1 - S_1	0.42
	C_{25}	Ba_1 - P_1	0.04 *
		S_1 - P_1	0.23
		Ss_1 - P_1	0.11
		S_1 - Ba_1	0.005 **
		Ss_1 - Ba_1	0.004 **
		Ss_1 - S_1	0.77
	C_{26}	Ba_1 - P_1	0.03 *
		S_1 - P_1	0.09
		Ss_1 - P_1	0.04 *
		S_1 - Ba_1	0.002 **
		Ss_1 - Ba_1	0.002 **
		Ss_1 - S_1	0.61
	C_{27}	Ba_1 - P_1	0.28
		S_1 - P_1	0.11
		Ss_1 - P_1	0.06
		S_1 - Ba_1	0.01 *
		Ss_1 - Ba_1	0.01 *
		Ss_1 - S_1	0.82
	C_{28}	Ba_1 - P_1	0.51
		S_1 - P_1	0.59
		Ss_1 - P_1	0.41
		S_1 - Ba_1	0.11
		Ss_1 - Ba_1	0.08
		Ss_1 - S_1	0.94
	C_{29}	Ba_1 - P_1	0.20
		S_1 - P_1	0.05
		Ss_1 - P_1	0.19
		S_1 - Ba_1	0.006 **
		Ss_1 - Ba_1	0.02 *
		Ss_1 - S_1	0.77

continued . . .

. . . continued

Unmixing Model	Tracer	Source Combination	p-value
	C_{30}	Ba_1 - P_1	0.27
		S_1 - P_1	0.06
		Ss_1 - P_1	0.11
		S_1 - Ba_1	0.008 **
		Ss_1 - Ba_1	0.01 *
		Ss_1 - S_1	0.99
	C_{32}	Ba_1 - P_1	0.32
		S_1 - P_1	0.59
		Ss_1 - P_1	0.71
		S_1 - Ba_1	0.06
		Ss_1 - Ba_1	0.09
		Ss_1 - S_1	0.99
Deconvolutional-substrate: M_2	C_{22}	S_2 - Ba_2	0.90
		Ss_2 - Ba_2	0.23
		Ss_2 - S_2	0.06
	C_{23}	S_2 - Ba_2	0.32
		Ss_2 - Ba_2	0.99
		Ss_2 - S_2	0.25
	C_{24}	S_2 - Ba_2	0.99
		Ss_2 - Ba_2	0.52
		Ss_2 - S_2	0.37
	C_{25}	S_2 - Ba_2	0.93
		Ss_2 - Ba_2	0.41
		Ss_2 - S_2	0.17
	C_{26}	S_2 - Ba_2	1.00
		Ss_2 - Ba_2	0.49
		Ss_2 - S_2	0.39
	C_{27}	S_2 - Ba_2	1.00
		Ss_2 - Ba_2	0.57
		Ss_2 - S_2	0.46
	C_{28}	S_2 - Ba_2	0.96
		Ss_2 - Ba_2	0.71
		Ss_2 - S_2	0.45
	C_{29}	S_2 - Ba_2	0.85
		Ss_2 - Ba_2	0.96

continued . . .

. . . continued

Unmixing Model	Tracer	Source Combination	p-value
		Ss_2 - S_2	0.96
	C_{30}	S_2 - Ba_2	0.99
		Ss_2 - Ba_2	0.66
		Ss_2 - S_2	0.60
	C_{32}	S_2 - Ba_2	0.18
		Ss_2 - Ba_2	0.89
		Ss_2 - S_2	0.06
Deconvolutional-substrate: M_3	C_{22}	Be_3 - S_3	0.63
		Ss_3 - S_3	0.17
		T_3 - S_3	0.01 *
		Ss_3 - Be_3	0.83
		T_3 - Be_3	0.30
		T_3 - Ss_3	0.79
	C_{23}	Be_3 - S_3	0.91
		Ss_3 - S_3	0.75
		T_3 - S_3	0.43
		Ss_3 - Be_3	0.56
		T_3 - Be_3	0.93
		T_3 - Ss_3	0.22
	C_{24}	Be_3 - S_3	0.53
		Ss_3 - S_3	0.41
		T_3 - S_3	0.19
		Ss_3 - Be_3	0.14
		T_3 - Be_3	0.07
		T_3 - Ss_3	0.99
	C_{25}	Be_3 - S_3	0.88
		Ss_3 - S_3	0.28
		T_3 - S_3	0.66
		Ss_3 - Be_3	0.21
		T_3 - Be_3	0.46
		T_3 - Ss_3	0.85
	C_{26}	Be_3 - S_3	0.20
		Ss_3 - S_3	0.99
		T_3 - S_3	0.87
		Ss_3 - Be_3	0.32
		T_3 - Be_3	0.12

continued . . .

. . . continued

Unmixing Model	Tracer	Source Combination	p-value
		T_3 - Ss_3	0.96
	C_{27}	Be_3 - S_3	0.90
		Ss_3 - S_3	1.00
		T_3 - S_3	0.42
		Ss_3 - Be_3	0.96
		T_3 - Be_3	0.32
		T_3 - Ss_3	0.60
	C_{28}	Be_3 - S_3	0.48
		Ss_3 - S_3	0.39
		T_3 - S_3	0.12
		Ss_3 - Be_3	0.12
		T_3 - Be_3	0.04 *
		T_3 - Ss_3	0.97
	C_{29}	Be_3 - S_3	0.35
		Ss_3 - S_3	0.99
		T_3 -S_3	0.89
		Ss_3 - Be_3	0.61
		T_3 - Be_3	0.23
		T_3 - Ss_3	0.90
	C_{30}	Be_3 - S_3	0.99
		Ss_3 - S_3	0.58
		T_3 - S_3	0.11
		Ss_3 -Be_3	0.66
		T_3 - Be_3	0.24
		T_3 - Ss_3	0.87
	C_{32}	Be_3 - S_3	0.99
		Ss_3 - S_3	0.99
		T_3 - S_3	0.69
		Ss_3 - Be_3	0.99
		T_3 - Be_3	0.71
		T_3 - Ss_3	0.78

B.6 Deconvolutional MixSIAR model data sets

Source, sediment and discrimination data used in the deconvolutional-substrate MixSIAR model is listed in Table B.11.

Table B.11: Source, sediment, and discrimination data sets used in deconvolutional-substrate MixSIAR model that include mean and standard deviation of carbon isotope ratios (δ^{13}C), and concentration ($\mu g\, g^{-1}$) for fatty acid tracers C_{22}-C_{32}.

M_1 Source Data

Source	n	MeandC22	MeandC23	MeandC24	MeandC25	MeandC26	MeandC27	MeandC28	MeandC29	MeandC30	MeandC32
Ba	2	-28.30	-29.77	-28.49	-29.92	-29.85	-31.36	-31.08	-31.23	-30.57	-28.20
P	2	-30.72	-32.28	-29.93	-33.56	-32.27	-33.45	-33.17	-33.69	-32.62	-33.63
S	3	-34.77	-34.80	-33.18	-35.47	-33.85	-36.17	-34.88	-37.12	-35.78	-37.00
Ss	2	-32.70	-34.41	-34.47	-36.31	-34.51	-36.98	-35.59	-36.20	-35.52	-36.67
Source	n	SDdC22	SDdC23	SDdC24	SDdC25	SDdC26	SDdC27	SDdC28	SDdC29	SDdC30	SDdC32
Ba	2	1.02	0.22	0.79	0.18	0.47	0.52	1.27	0.42	0.52	3.96
P	2	4.38	5.39	1.53	1.46	0.70	1.96	2.39	1.82	1.39	4.46
S	3	0.94	0.57	0.21	0.57	0.28	0.56	0.95	0.92	1.02	0.30
Ss	2	3.69	1.26	0.65	1.22	0.85	0.66	0.96	0.39	0.71	1.81
Source	n	ConcdC22	ConcdC23	ConcdC24	ConcdC25	ConcdC26	ConcdC27	ConcdC28	ConcdC29	ConcdC30	ConcdC32
Ba	2	0.07	0.07	0.23	0.11	0.36	0.13	0.42	0.07	0.17	0.07
P	2	196.90	44.97	185.25	28.25	64.02	18.78	54.26	15.92	51.50	51.72
S	3	7.43	9.03	25.59	5.82	12.48	3.15	15.37	2.65	10.43	6.39
Ss	2	24.55	6.62	20.56	3.93	15.27	3.29	18.05	2.09	10.04	4.73

M_2 Source Data

Source	n	MeandC22	MeandC23	MeandC24	MeandC25	MeandC26	MeandC27	MeandC28	MeandC29	MeandC30	MeandC32
Ba	3	-32.72	-36.09	-32.18	-33.80	-32.21	-33.21	-33.21	-34.62	-33.37	-35.68
S	6	-31.99	-33.46	-32.06	-33.25	-32.24	-33.20	-32.86	-33.30	-33.50	-32.12
Ss	4	-35.84	-36.16	-34.13	-36.06	-33.94	-35.76	-34.35	-33.91	-35.25	-36.62
Source	n	SDdC22	SDdC23	SDdC24	SDdC25	SDdC26	SDdC27	SDdC28	SDdC29	SDdC30	SDdC32
Ba	3	3.59	2.10	2.27	2.45	1.62	3.10	2.25	3.62	3.70	1.88
S	6	1.98	2.69	2.29	2.59	2.09	4.08	1.72	2.62	3.05	2.98
Ss	4	1.56	2.20	2.19	1.05	1.82	0.62	1.76	4.26	0.98	2.37

Source	n	ConcdC22	ConcdC23	ConcdC24	ConcdC25	ConcdC26	ConcdC27	ConcdC28	ConcdC29	ConcdC30	ConcdC32
Ba	3	0.84	0.35	0.83	0.28	0.56	0.14	0.78	0.14	0.50	0.26
S	6	21.17	11.53	23.12	6.43	16.40	3.88	16.56	1.89	6.00	2.60
Ss	4	3.86	1.63	5.91	1.59	4.60	1.21	4.72	0.74	2.51	0.99

M_3 Source Data

Source	n	MeandC22	MeandC23	MeandC24	MeandC25	MeandC26	MeandC27	MeandC28	MeandC29	MeandC30	MeandC32
Be	2	-32.71	-34.40	-31.27	-34.18	-31.26	-34.18	-32.61	-32.33	-33.84	-32.61
M_1	2	-32.70	-34.41	-34.47	-36.31	-34.51	-36.98	-35.59	-36.20	-35.52	-36.67
M_2	2	-35.90	-35.51	-35.94	-34.92	-34.45	-35.86	-35.00	-37.01	-36.17	-35.41
S	7	-31.08	-33.17	-32.69	-34.99	-33.93	-35.11	-34.04	-36.05	-33.98	-33.26
Ss	2	-34.13	-31.33	-34.34	-37.10	-34.07	-35.01	-35.65	-35.69	-35.27	-32.97
T	3	-35.54	-35.68	-34.61	-36.09	-34.73	-37.01	-36.10	-37.35	-36.13	-35.55

Source	n	SDdC22	SDdC23	SDdC24	SDdC25	SDdC26	SDdC27	SDdC28	SDdC29	SDdC30	SDdC32
Be	2	0.74	1.05	1.11	1.22	0.66	1.11	0.11	3.51	0.98	5.07
M_1	2	3.69	1.26	0.65	1.22	0.85	0.66	0.96	0.39	0.71	1.81
M_2	2	1.86	1.67	2.83	2.01	1.22	0.63	1.73	2.28	0.17	0.28
S	7	2.07	1.53	1.50	1.39	1.82	1.94	1.26	2.82	1.29	0.79
Ss	2	0.16	5.98	0.76	2.12	0.74	1.87	1.49	3.08	1.82	7.24
T	3	0.87	0.84	0.59	0.83	1.17	1.02	1.17	0.84	0.65	1.86

Source	n	ConcdC22	ConcdC23	ConcdC24	ConcdC25	ConcdC26	ConcdC27	ConcdC28	ConcdC29	ConcdC30	ConcdC32
Be	2	0.38	0.23	0.95	0.26	0.99	0.21	0.99	0.15	0.47	0.19
M_1	2	24.55	6.62	20.56	3.93	15.27	3.29	18.05	2.09	10.04	4.73
M_2	2	15.59	4.17	14.88	3.82	11.57	3.20	14.84	2.07	9.58	4.60
S	7	22.87	12.88	42.13	11.79	25.95	4.00	21.39	2.59	8.62	3.50
Ss	2	3.62	1.25	4.13	3.76	2.80	0.63	2.82	0.78	1.49	0.76
T	3	8.58	3.84	15.25	3.81	13.85	3.22	16.22	1.68	8.37	3.05

M_1 Sediment Data

Site	dC22	dC23	dC24	dC25	dC26	dC27	dC28	dC29	dC30	dC32
NR7	-30.09	-33.52	-34.01	-37.17	-33.91	-36.51	-36.27	-36.47	-35.01	-37.95
22	-35.31	-35.3	-34.93	-35.44	-35.11	-37.45	-34.91	-35.92	-36.02	-35.39

M_2 Sediment Data

Site	dC22	dC23	dC24	dC25	dC26	dC27	dC28	dC29	dC30	dC32
BR1	-34.58	-34.33	-33.94	-33.5	-33.59	-35.41	-33.78	-38.62	-36.29	-35.61
BR2	-37.21	-36.69	-37.94	-36.34	-35.31	-36.3	-36.22	-35.39	-36.05	-35.21

M_3 Sediment Data

Source	dC22	dC23	dC24	dC25	dC26	dC27	dC28	dC29	dC30	dC32
NR1	-32.32	-33.12	-32.52	-33.81	-33.76	-35.69	-34.92	-35.59	-35.24	-34.2
NR2	-32.12	-33.6	-33.12	-39.76	-33.1	-35.67	-35.77	-36.42	-32.87	-34.69
NR3	-35.96	-35.83	-34.8	-36.43	-34.49	-36.44	-35.6	-38.04	-35.29	-31.93

M_1 Discrimination Data

Source	n	MeandC22	MeandC23	MeandC24	MeandC25	MeandC26	MeandC27	MeandC28	MeandC29	MeandC30	MeandC32
Ba	2	0	0	0	0	0	0	0	0	0	0
P	2	0	0	0	0	0	0	0	0	0	0
S	3	0	0	0	0	0	0	0	0	0	0
Ss	2	0	0	0	0	0	0	0	0	0	0

Source	n	SDdC22	SDdC23	SDdC24	SDdC25	SDdC26	SDdC27	SDdC28	SDdC29	SDdC30	SDdC32
Ba	2	0	0	0	0	0	0	0	0	0	0
P	2	0	0	0	0	0	0	0	0	0	0
S	3	0	0	0	0	0	0	0	0	0	0
Ss	2	0	0	0	0	0	0	0	0	0	0

M_2 Discrimination Data

Source	n	MeandC22	MeandC23	MeandC24	MeandC25	MeandC26	MeandC27	MeandC28	MeandC29	MeandC30	MeandC32
Ba	3	0	0	0	0	0	0	0	0	0	0
S	6	0	0	0	0	0	0	0	0	0	0
Ss	4	0	0	0	0	0	0	0	0	0	0

Source	n	SDdC22	SDdC23	SDdC24	SDdC25	SDdC26	SDdC27	SDdC28	SDdC29	SDdC30	SDdC32
Ba	3	0	0	0	0	0	0	0	0	0	0
S	6	0	0	0	0	0	0	0	0	0	0
Ss	4	0	0	0	0	0	0	0	0	0	0

M_3 Discrimination Data

Source	n	MeandC22	MeandC23	MeandC24	MeandC25	MeandC26	MeandC27	MeandC28	MeandC29	MeandC30	MeandC32
Be	2	0	0	0	0	0	0	0	0	0	0
M_1	2	0	0	0	0	0	0	0	0	0	0
M_2	2	0	0	0	0	0	0	0	0	0	0
S	7	0	0	0	0	0	0	0	0	0	0
Ss	2	0	0	0	0	0	0	0	0	0	0
T	3	0	0	0	0	0	0	0	0	0	0

Source	n	SDdC22	SDdC23	SDdC24	SDdC25	SDdC26	SDdC27	SDdC28	SDdC29	SDdC30	SDdC32
Be	2	0	0	0	0	0	0	0	0	0	0
M_1	2	0	0	0	0	0	0	0	0	0	0
M_2	2	0	0	0	0	0	0	0	0	0	0
S	7	0	0	0	0	0	0	0	0	0	0
Ss	2	0	0	0	0	0	0	0	0	0	0
T	3	0	0	0	0	0	0	0	0	0	0

B.7 R code

B.7.1 Deconvolutional-substrate MixSIAR model R code

Listing B.1: R code for deconvolutional-substrate MixSIAR model.

```
library(MixSIAR)
library(dplyr)
setwd("/Users/tassiastainton/Documents/MixSIAR-master/projects/nelson_cssi/mix_model_decon")
#
# Part 1: Deconvolutional MixSIAR
# 1a. Load mixture data
mix.1 <- load_mix_data(filename="/Users/tassiastainton/Documents/MixSIAR-master/projects/nelson_cssi/mix_model_decon/data/mix.1.csv",
            iso_names=c("dC22","dC23","dC24","dC25","dC26","dC27","dC28","dC29","dC30","dC32"),
            factors= NULL, # in my model this has to be site (I think...)
            fac_random=NULL,
            fac_nested=NULL,
            cont_effects=NULL)
mix.2 <- load_mix_data(filename="/Users/tassiastainton/Documents/MixSIAR-master/projects/nelson_cssi/mix_model_decon/data/mix.2.csv",
            iso_names=c("dC22","dC23","dC24","dC25","dC26","dC27","dC28","dC29","dC30","dC32"),
            factors= NULL,
            fac_random=NULL,
            fac_nested=NULL,
            cont_effects=NULL)
mix.3 <- load_mix_data(filename="/Users/tassiastainton/Documents/MixSIAR-master/projects/nelson_cssi/mix_model_decon/data/mix.3.csv",
            iso_names=c("dC22","dC23","dC24","dC25","dC26","dC27","dC28","dC29","dC30","dC32"),
            factors= NULL,
            fac_random=NULL,
            fac_nested=NULL,
            cont_effects=NULL)

# 1b. Load source data
source.1 <- load_source_data(filename="/Users/tassiastainton/Documents/MixSIAR-master/projects/nelson_cssi/mix_model_decon/data/source.m1.csv",
            source_factors=NULL,
            conc_dep=TRUE,
            data_type="means",
            mix.1)
source.2<- load_source_data(filename="/Users/tassiastainton/Documents/MixSIAR-master/projects/nelson_cssi/mix_model_decon/data/source.m2.csv",
            source_factors=NULL,
            conc_dep=TRUE,
            data_type="means",
            mix.2)
source.3 <- load_source_data(filename="/Users/tassiastainton/Documents/MixSIAR-master/projects/nelson_cssi/mix_model_decon/data/source.m3.csv",
            source_factors=NULL,
            conc_dep=TRUE,
            data_type="means",
            mix.3)

# 1c. Load discrimination
discr.1 <- load_discr_data(filename="/Users/tassiastainton/Documents/MixSIAR-master/projects/nelson_cssi/mix_model_decon/data/discr.m1.csv", mix.1)
discr.2 <- load_discr_data(filename="/Users/tassiastainton/Documents/MixSIAR-master/projects/nelson_cssi/mix_model_decon/data/discr.m2.csv", mix.2)
discr.3 <- load_discr_data(filename="/Users/tassiastainton/Documents/MixSIAR-master/projects/nelson_cssi/mix_model_decon/data/discr.m3.csv", mix.3)

# 1d. Define model structure and write JAGS model file
m1.filename <- "MixSIAR_model_m1.txt"
```

```
m1.resid.err <- TRUE
m1.process.err <- FALSE
write_JAGS_model(m1.filename, m1.resid.err, m1.process.err, mix.1, source.1)

m2.filename <- "MixSIAR_model_m2.txt"
m2.resid.err <- TRUE
m2.process.err <- FALSE
write_JAGS_model(m2.filename, m2.resid.err, m2.process.err, mix.2, source.2)

m3.filename <- "MixSIAR_model_m3.txt"
m3.resid.err <- TRUE
m3.process.err <- FALSE
write_JAGS_model(m3.filename, m3.resid.err, m3.process.err, mix.3, source.3)

# 1e. Run the JAGS model (advice: run="test" first to check files loaded correctly, then use a longer run to reach convergence)
jags.m1 <- run_model(run="test", mix.1, source.1, discr.1, m1.filename, alpha.prior=1, m1.resid.err, m1.process.err)
jags.m2 <- run_model(run="test", mix.2, source.2, discr.2, m2.filename, alpha.prior=1, m2.resid.err, m2.process.err)
jags.m3 <- run_model(run="test", mix.3, source.3, discr.3, m3.filename, alpha.prior=1, m3.resid.err, m3.process.err)

# Runtime start 2:50pm end
jags.m1 <- run_model(run="long", mix.1, source.1, discr.1, m1.filename, alpha.prior=1, m1.resid.err, m1.process.err)
jags.m2 <- run_model(run="long", mix.2, source.2, discr.2, m2.filename, alpha.prior=1, m2.resid.err, m2.process.err)
jags.m3 <- run_model(run="long", mix.3, source.3, discr.3, m3.filename, alpha.prior=1, m3.resid.err, m3.process.err)

output_options <- list(summary_save = TRUE,
                       summary_name = "summary_statistics",
                       sup_post = FALSE,
                       plot_post_save_pdf = TRUE,
                       plot_post_name = "posterior_density",
                       sup_pairs = FALSE,
                       plot_pairs_save_pdf = TRUE,
                       plot_pairs_name = "pairs_plot",
                       sup_xy = FALSE,
                       plot_xy_save_pdf = TRUE,
                       plot_xy_name = "xy_plot",
                       gelman = TRUE,
                       heidel = FALSE,
                       geweke = TRUE,
                       diag_save = TRUE,
                       diag_name = "diagnostics",
                       indiv_effect = FALSE,
                       plot_post_save_png = TRUE,
                       plot_pairs_save_png = TRUE,
                       plot_xy_save_png = TRUE)

# 1f. Process diagnostics, summary stats, and posterior plots
output_JAGS(jags.m1, mix.1, source.1, output_options) #don't forget to add in the other plots here
output_JAGS(jags.m2, mix.2, source.2, output_options)
output_JAGS(jags.m3, mix.3, source.3, output_options)

# 1g. Combine MixSIAR objects frome each node/model into lists (must use mix=, source=, and jags=)
model1 <- list(mix=mix.1, source=source.1, jags=jags.m1)
model2 <- list(mix=mix.2, source=source.2, jags=jags.m2)
model3 <- list(mix=mix.3, source=source.3, jags=jags.m3)

# Combine models into a single list
models <- list(model1, model2, model3)
# Load merging functions: 'merge_nodes', 'plot_nodes', 'summary_nodes'
#source("/home/brian/Documents/Isotopes/Hari_soil_Nepal/data_imixsed_mixsiar/merge_nodes.R")

```

```
# Use merging functions
merged <- merge_nodes(models)
#library(dplyr)
plot_nodes(merged, save_pdf=F, save_png=T)
res.hierarch <- summary_nodes(merged, save_txt=TRUE, filename="summary_hierarchical.csv")
# Save workspace
save.image("hierarchical.RData")
#
# Merge results from mixing models run above and below river junction

# 1. Run mixing models on each subcatchment.
#      If Model X mixture (mix.X) is used downstream as a source in Model Y, include mix.X as a source in the source.Y file
# 2. Save mix, source, and jags objects for each model as a list, e.g. model1 = list(mix=mix.1,source=source.1,jags=jags.1).
# 3. Downstream mixtures can use upstream mixtures as sources, e.g. source.3 includes mix.1 and mix.2
# 4. Save all models together in one list, like: models = list(model1, model2, model3)
# Either a) no fixed/random effects or b) the same fixed/random effect at all nodes

#### This code below is repeated from the above code given in the original document ####

# combine objects from each model into lists (must use mix=, source=, and jags=)
model0 <- list(mix=mix.1,source=source.1,jags=jags.mix1)
model2 <- list(mix=mix.2,source=source.3,jags=jags.mix3)
model3 <- list(mix=mix.3,source=source.4,jags=jags.mix4)


# combine models into a single list
models1 <- list(model0,model2,model3 )

# load merging functions: 'merge_nodes', 'plot_nodes', 'summary_nodes'
#source("C:/Users/HariRam/Documents/subcatchment/Output/merge_nodes_010816.R") ### you can run the merged_node here or from separte file (function below)

# use merging functions
merged <- merge_nodes(models1)
plot_nodes(merged,save_pdf=FALSE,save_png=TRUE)
res <- summary_nodes(merged,save_txt=TRUE,filename="summary_nodes_3.csv")
```

B.7.2 Merge Nodes function

Listing B.2: R code for merge nodes function from Blake et al. (2018).

```
merge_nodes <- function(models){
  # Number of models
  n.models <- length(models)

  # # Check each model has mix, source, and jags lists
  # for(m in 1:n.models){
  #   if(!identical(names(models[[m]]),c("mix","source","jags"))){
  #     stop(paste("*** Error: model ",m," does not contain 'mix', 'source' and 'jags' ***",sep=""))}
  #   if(!identical(names(models[[m]]$mix),c("data","data_iso","n.iso","n.re","n.ce","FAC","CE","CE_orig","CE_center","CE_scale","cont_effects","MU_names","SIG_names","iso_names","N","n.fe","n.effects","factors","fac_random","fac_nested","fere"))){
  #     stop(paste("*** Error: mix object in model ",m," does not contain correct entries ***",sep=""))}
  #   if(!identical(names(models[[m]]$source),c("n.sources","source_names","S_MU","S_SIG","S_factor1","S_factor_levels","conc","MU_array","SIG2_array","n_array","SOURCE_array","n.rep","by_factor","data_type","conc_dep"))){
  #     stop(paste("*** Error: source object in model ",m," does not contain correct entries ***",sep=""))}
  #   if(!identical(class(models[[m]]$jags),"rjags")){
  #     stop(paste("*** Error: model ",m," does not contain 'mix', 'source' and 'jags' ***",sep=""))}
  # }

```

```
# Get ALL source names (incl mix/nodes), and ORIG source names (no mix/nodes)
source.names.all <- NULL
for(m in 1:n.models) source.names.all <- c(source.names.all,models[[m]]$source$source_names)
source.names.all <- unique(source.names.all)
n.sources.all <- length(source.names.all)
# remove <- paste0("mix.",1:n.models)
remove <- paste0("node",1:n.models)
source.names.orig <- setdiff(source.names.all, remove)
n.sources.orig <- length(source.names.orig)
models[[1]]$source.names <- source.names.orig

# Get indices of source.names.orig for each model
for(m in 1:n.models) models[[m]]$ind <- match(source.names.orig,models[[m]]$source$source_names)

# Get node matrix (mix as source to other mix)
node.mat <- array(NA,dim=c(n.models,n.models))
for(m in 1:n.models) node.mat[m,] <- remove %in% models[[m]]$source$source_names

# check if we have fixed/random effect or not
effect <- ifelse(models[[1]]$mix$n.effects==1,TRUE,FALSE)

if(!effect){ # if no fixed/random effect
  for(m in 1:n.models){
    # p.merged indexed same as p.global: [draws,source], but ALL sources in system
    n.draws <- dim(models[[m]]$jags$BUGSoutput$sims.list$p.global)[1]
    models[[m]]$p.merged <- array(0,dim=c(n.draws,n.sources.orig))
    for(src in 1:n.sources.orig){
      for(src.sub in 1:models[[m]]$source$n.sources){
        # do we have a mix node?
        if(length(grep("mix", models[[m]]$source$source_names[src.sub]))==1){
          node <- TRUE
          mix.no <- as.numeric(gsub("mix.", "", models[[m]]$source$source_names[src.sub]))
        } else { node <- FALSE }
        # if(length(grep("node", models[[m]]$source$source_names[src.sub]))==1){
        #   node <- TRUE
        #   mix.no <- as.numeric(gsub("node", "", models[[m]]$source$source_names[src.sub]))
        # } else { node <- FALSE }

        if(!node){
          # if(src==models[[m]]$ind[src.sub]) models[[m]]$p.merged[,src] <- models[[m]]$p.merged[,src] +
              models[[m]]$jags$BUGSoutput$sims.list$p.global[,models[[m]]$ind[src]]
          if(!is.na(models[[m]]$ind[src])) {if(src.sub==models[[m]]$ind[src]) models[[m]]$p.merged[,src]
              <- models[[m]]$p.merged[,src] + models[[m]]$jags$BUGSoutput$sims.list$p.global[,src.sub]}
        }
        if(node){
          # tmp <- models[[m]]$jags$BUGSoutput$sims.list$p.global[,src.sub] * models[[mix.no]]$jags$
              BUGSoutput$sims.list$p.global[,models[[mix.no]]$ind[src]]
          # models[[m]]$p.merged[,src] <- models[[m]]$p.merged[,src] + tmp
          tmp <- models[[m]]$jags$BUGSoutput$sims.list$p.global[,src.sub] * models[[mix.no]]$p.merged[,
              src]
          models[[m]]$p.merged[,src] <- models[[m]]$p.merged[,src] + tmp
        }
      }
    }
  }
}

if(effect){
  # ASSUMES same fixed effects for ALL nodes, with same levels for all
  # need to write test for this...

  # # test the fixed effect is the same for nodes 1 and 2
  # if(!identical(mix.1$factors,mix.2$factors)){
  #   stop(paste("*** Error: Factors from node 1 and node 2 are not the same ***",sep=""))}

  # # confirm the indices for each FE/RE level are the same for nodes 1 and 2 (e.g. season = EW, LW, MW)
  # if(identical(mix.1$FAC[[1]]$labels,mix.2$FAC[[1]]$labels)){
```

```
80      #   seasons <- mix.1$FAC[[1]]$labels
81      #   n.seasons <- length(seasons)
82      #   } else {
83      #   stop(paste("*** ERROR: fixed/random effect levels not the same for nodes 1 and 2 ***",sep=""))
84      # }
85
86      models[[1]]$seasons <- models[[1]]$mix$FAC[[1]]$labels
87      n.seasons <- length(models[[1]]$seasons)
88      for(m in 1:n.models){
89        # p.merged indexed same as p.fac1: [draws,season,source], but ALL sources in system
90        n.draws <- dim(models[[m]]$jags$BUGSoutput$sims.list$p.fac1)[1]
91        models[[m]]$p.merged <- array(0,dim=c(n.draws,n.seasons,n.sources.orig))
92        for(i in 1:n.seasons){
93          for(src in 1:n.sources.orig){
94            for(src.sub in 1:models[[m]]$source$n.sources){
95              # do we have a mix node?
96              if(length(grep("mix", models[[m]]$source$source_names[src.sub]))==1){
97                node <- TRUE
98                mix.no <- as.numeric(gsub("mix.", "", models[[m]]$source$source_names[src.sub]))
99              } else { node <- FALSE }
100             #if(length(grep("node", models[[m]]$source$source_names[src.sub]))==1){
101             # node <- TRUE
102             # mix.no <- as.numeric(gsub("node", "", models[[m]]$source$source_names[src.sub]))
103             #} else { node <- FALSE }
104
105             if(!node){
106               if(!is.na(models[[m]]$ind[src])) {if(src.sub==models[[m]]$ind[src]) models[[m]]$p.merged[,i,
                      src] <- models[[m]]$p.merged[,i,src] + models[[m]]$jags$BUGSoutput$sims.list$p.fac1[,i,
                      src.sub]}
107             }
108             if(node){
109               # tmp <- models[[m]]$jags$BUGSoutput$sims.list$p.fac1[,i,src.sub] * models[[mix.no]]$jags$
                      BUGSoutput$sims.list$p.fac1[,i,models[[mix.no]]$ind[src]]
110               tmp <- models[[m]]$jags$BUGSoutput$sims.list$p.fac1[,i,src.sub] * models[[mix.no]]$p.merged[,
                      i,src]
111               models[[m]]$p.merged[,i,src] <- models[[m]]$p.merged[,i,src] + tmp
112             }
113           }
114         }
115       } # end season
116     } # end models
117   } # end if(effect)
118
119   return(models)
120 }
121
122 # 'merged' is result of 'merge_nodes' function
123 plot_nodes <- function(merged,save_pdf=FALSE,save_png=TRUE){
124   n.models <- length(merged)
125   effect <- ifelse(merged[[1]]$mix$n.effects==1,TRUE,FALSE)
126
127   if(!effect){ # if no fixed/random effect
128     n.sources <- dim(merged[[1]]$p.merged)[2]
129     n.draws <- dim(merged[[1]]$p.merged)[1]
130     col=RColorBrewer::brewer.pal(n.sources,"Set1")
131     for(m in 1:n.models){
132       dev.new()
133       df <- data.frame(sources=rep(NA,n.draws*n.sources), x=rep(NA,n.draws*n.sources))  # create empty data
              frame
134       for(src in 1:n.sources){
135         df$x[seq(1+n.draws*(src-1),src*n.draws)] <- as.matrix(merged[[m]]$p.merged[,src]) # fill in the p.
              global values
136         df$sources[seq(1+n.draws*(src-1),src*n.draws)] <- rep(merged[[1]]$source.names[src],n.draws)  #
              fill in the source names
137       }
138
139       # handle case where a source is not present in this node
```

```
      df[df == 0] <- NA
      y <- df %>% group_by(sources) %>% summarize(mean=mean(x)) %>% mutate(n=1:n.sources) %>% filter(mean
           >0) %>% select(n)

      my.title <- paste0("Node ",m)
      print(ggplot2::ggplot(df, ggplot2::aes(x=x, fill=sources, colour=sources)) +
              ggplot2::geom_density(alpha=.3, ggplot2::aes(y=..scaled..)) +
              ggplot2::xlim(0,1) +
              ggplot2::theme_bw() +
              ggplot2::xlab("Proportion of Diet") +
              ggplot2::ylab("Scaled Posterior Density") +
              ggplot2::labs(title = my.title) +
              ggplot2::scale_fill_manual(values=col[y$n]) +
              ggplot2::scale_colour_manual(values=col[y$n]) +
              ggplot2::theme(legend.position=c(1,1), legend.justification=c(1,1), legend.title=ggplot2::
                   element_blank()))

      # Save plot as PDF
      if(save_pdf){
        mypath <- paste0("p.node",m,".pdf")  # svalue(plot_post_name), factor1_names
        dev.copy2pdf(file=mypath)
      }

      # Save plot as PNG
      if(save_png){
        mypath <- paste0("p.node",m,".png") # svalue(plot_post_name), factor1_names
        dev.copy(png,mypath)
      }
    } # end loop over nodes/models
  } # end p.global posterior plots

  if(effect){ # if we have a fixed/random effect
    n.seasons <- dim(merged[[1]]$p.merged)[2]
    n.sources <- dim(merged[[1]]$p.merged)[3]
    n.draws <- dim(merged[[1]]$p.merged)[1]

    # get colors in advance to keep consistent even when a source is not present for a given node
    col=RColorBrewer::brewer.pal(n.sources,"Set1")

    for(m in 1:n.models){
      for(f1 in 1:n.seasons){
        dev.new()
        df <- data.frame(sources=rep(NA,n.draws*n.sources), x=rep(NA,n.draws*n.sources))  # create empty
             data frame
        for(src in 1:n.sources){
          df$x[seq(1+n.draws*(src-1),src*n.draws)] <- as.matrix(merged[[m]]$p.merged[,f1,src]) # fill in
               the p.fac1[f1] values
          df$sources[seq(1+n.draws*(src-1),src*n.draws)] <- rep(merged[[1]]$source.names[src],n.draws)  #
               fill in the source names
        }

        # handle case where a source is not present in this node
        df[df == 0] <- NA
        y <- df %>% group_by(sources) %>% summarize(mean=mean(x)) %>% mutate(n=1:n.sources) %>% filter(mean
             >0) %>% select(n)

        my.title <- paste0("Node ",m,": ",merged[[1]]$seasons[f1])  # formerly factor1_names
        print(ggplot2::ggplot(df, ggplot2::aes(x=x, fill=sources, colour=sources)) +
                ggplot2::geom_density(alpha=.3, ggplot2::aes(y=..scaled..)) +
                ggplot2::xlim(0,1) +
                ggplot2::theme_bw() +
                ggplot2::xlab("Proportion of Diet") +
                ggplot2::ylab("Scaled Posterior Density") +
                ggplot2::labs(title = my.title) +
                ggplot2::scale_fill_manual(values=col[y$n]) +
                ggplot2::scale_colour_manual(values=col[y$n]) +
```

```
200                ggplot2::theme(legend.position=c(1,1), legend.justification=c(1,1), legend.title=ggplot2::
                       element_blank()))
201
202          # Save plot as PDF
203          if(save_pdf){
204            mypath <- paste0("p.node",m,".",merged[[1]]$seasons[f1],".pdf")  # svalue(plot_post_name),
                   factor1_names
205            dev.copy2pdf(file=mypath)
206          }
207
208          # Save plot as PNG
209          if(save_png){
210            mypath <- paste0("p.node",m,".",merged[[1]]$seasons[f1],".png")  # svalue(plot_post_name),
                   factor1_names
211            dev.copy(png,mypath)
212          }
213        } # end p.fac1 posterior plots
214      } # end loop over models
215    }
216  }
217
218  # 'merged' is result of 'merge_nodes' function
219  summary_nodes <- function(merged,save_txt=TRUE,filename="summary_nodes.txt"){
220    n.models <- length(merged)
221    res <- vector("list",n.models)
222    effect <- ifelse(merged[[1]]$mix$n.effects==1,TRUE,FALSE)
223
224    # open file
225    cat("
226        Summary Statistics
227        ",sep="", file=filename, append=FALSE)
228
229    if(!effect){
230      for(m in 1:n.models){
231        # calculate stats
232        res[[m]]$quantiles <- round(apply(merged[[m]]$p.merged,2,function(x) quantile(x,c(.025,.05,.95,.975))
               ),3)
233        res[[m]]$medians <- round(apply(merged[[m]]$p.merged,2,median),3)
234        res[[m]]$means <- round(apply(merged[[m]]$p.merged,2,mean),3)
235        res[[m]]$sds <- round(apply(merged[[m]]$p.merged,2,sd),3)
236
237        # combine stats
238        res[[m]]$stats <- rbind(res[[m]]$quantiles,res[[m]]$medians,res[[m]]$means,res[[m]]$sd)
239        rownames(res[[m]]$stats) <- c(0.025,0.05,0.95,0.975,"median","mean","SD")
240        colnames(res[[m]]$stats) <- merged[[1]]$source.names
241        out <- capture.output(res[[m]]$stats)
242
243        # print to screen
244        cat("
245            # ------------------------------------------------------------------
246            # Node ",m,"
247            # ------------------------------------------------------------------
248            ",sep="")
249        cat(out,sep="\n")
250
251        # print to file
252        cat("
253            # ------------------------------------------------------------------
254            # Node ",m,"
255            # ------------------------------------------------------------------
256            ",sep="",file=filename, append=TRUE)
257        cat(out,sep="\n",file=filename, append=TRUE)
258      } # end model
259    } # end if no effect
260
261    if(effect){
262      n.seasons <- dim(merged[[1]]$p.merged)[2]
```

```
263     for(m in 1:n.models){
264       for(i in 1:n.seasons){
265         # calculate stats
266         res[[m]]$quantiles[[merged[[1]]$seasons[i]]] <- round(apply(merged[[m]]$p.merged[,i,],2,function(x)
                quantile(x,c(.025,.05,.95,.975))),3)
267         res[[m]]$medians[[merged[[1]]$seasons[i]]] <- round(apply(merged[[m]]$p.merged[,i,],2,median),3)
268         res[[m]]$means[[merged[[1]]$seasons[i]]] <- round(apply(merged[[m]]$p.merged[,i,],2,mean),3)
269         res[[m]]$sds[[merged[[1]]$seasons[i]]] <- round(apply(merged[[m]]$p.merged[,i,],2,sd),3)
270
271         # combine stats
272         res[[m]]$stats[[merged[[1]]$seasons[i]]] <- rbind(res[[m]]$quantiles[[i]],res[[m]]$medians[[i]],res
              [[m]]$means[[i]],res[[m]]$sd[[i]])
273         rownames(res[[m]]$stats[[i]]) <- c(0.025,0.05,0.95,0.975,"median","mean","SD")
274         colnames(res[[m]]$stats[[i]]) <- merged[[1]]$source.names
275         out <- capture.output(res[[m]]$stats[[i]])
276
277         # print to screen
278         cat("
279             # ------------------------------------------------------------------
280             # Node ",m,": ",merged[[1]]$seasons[i],"
281             # ------------------------------------------------------------------
282             ",sep="")
283         cat(out,sep="\n")
284
285         # print to file
286         cat("
287             # ------------------------------------------------------------------
288             # Node ",m,": ",merged[[1]]$seasons[i],"
289             # ------------------------------------------------------------------
290             ",sep="",file=filename, append=TRUE)
291         cat(out,sep="\n",file=filename, append=TRUE)
292       } # end season
293     } # end model
294     } # end if(effect)
295   return(res)
296     }
```